Effect of TBBPA on arterial contractile regulation and possible implications for the development of hypertensive diseases

Joana Rita Oliveira Feiteiro

Tese para obtenção do Grau de Doutor em
Biomedicina
(3º ciclo de estudos)

Orientadora: Professora Doutora Maria Elisa Cairrão Rodrigues Oliveira
Co-orientador: Professor Doutor Cláudio Jorge Maia Baptista

Júri:
Professor Doutor Ilídio Joaquim Sobreira Correia
Professora Doutora Marta Sofia Soares Craveiro Alves Monteiro
Professor Doutor Luís Miguel dos Santos Russo Vieira
Professora Doutora Ana Cristina Monteiro Ramalhinho Tavares Patrício
Professora Doutora Maria Elisa Cairrão Rodrigues

1 de fevereiro de 2023

Declaração de Integridade

Eu, Joana Rita Oliveira Feiteiro, que abaixo assino, estudante com o número de inscrição D1756 de/o Biomedicina da Faculdade Ciências da Saúde, declaro ter desenvolvido o presente trabalho e elaborado o presente texto em total consonância com o **Código de Integridades da Universidade da Beira Interior**.

Mais concretamente afirmo não ter incorrido em qualquer das variedades de Fraude Académica, e que aqui declaro conhecer, que em particular atendi à exigida referenciação de frases, extratos, imagens e outras formas de trabalho intelectual, e assumindo assim na íntegra as responsabilidades da autoria.

Universidade da Beira Interior, Covilhã 23 /02 /2023

Assinado por: **JOANA RITA OLIVEIRA FEITEIRO**
Num. de Identificação: 13241198
Data: 2023.02.23 15:38:27+00'00'

Ao pilar do Céu
E aos pilares da Terra!

Agradecimentos

No culminar deste percurso, quero agradecer a todos os que de alguma forma contribuíram e me apoiaram na concretização desta etapa. Foi uma etapa longa, desafiante, escorregadia e com muitos percalços, mas tive a sorte de estar rodeada das pessoas certas que me deram força para nunca desistir dos meus objetivos e da minha meta final.

Agradeço à minha orientadora Professora Doutora Elisa Cairrão por todo o apoio, orientação e conhecimentos que me foram transmitidos. Agradeço também a disponibilidade, paciência e amabilidade ao longo destes anos que tornaram possível chegar a este dia.

Ao Professor Doutor Cláudio Maia queria agradecer pela aceitação da coorientação deste projeto, pelas opiniões relevantes que me transmitiu, por se mostrar sempre prestável e disponível, bem como as palavras de apoio manifestadas durante a realização desta tese.

A todas as pessoas do Centro de Investigação em Ciências da Saúde (CICS-UBI). À Sofia Duarte e à Margarida Carrilho pela disponibilidade que sempre demonstraram. À Catarina Ferreira, à Ana Raquel Costa, à Mafalda Martins Dinis pela ajuda na aquisição de imagens de microscopia. A vocês o meu obrigada.

Aos meus colegas de laboratório agradeço toda a ajuda e partilha de conhecimentos.

O meu sincero obrigada a todas as mães dadoras e a toda a equipa do Bloco de Obstetrícia e Ginecologia do Centro Hospitalar da Cova da Beira e da Unidade Local de Saúde da Guarda pela sua colaboração, sem a qual este estudo não poderia ser realizado.

À Eduarda e à Maria Inês agradeço a grande amizade construída ao longo destes anos. Que apesar da distância, as palavras de apoio, as palavras de motivação chegam sempre nos momentos certos. Obrigada por nunca me deixarem sozinha. Gosto muito de vocês! *"Como se chama uma pessoa com o mesmo nome que eu? Joana!!! Não homónima"*!

Agradeço a amizade especial da Melissa Mariana, Sandra Rocha, Daniela Talhada, Fátima Santos, Tânia Albuquerque, as "amigas CICS". Obrigada por todos os momentos e alegrias partilhados ao longo de toda a caminhada, por me suportarem e encorajarem naqueles momentos tempestuosos e por me impulsionarem sempre para lutar! Gosto muito de vocês!

À minha família, que sempre me acompanhou, à minha cunhada e aos meus sogros. Obrigada por tudo!

O Amor é uma construção inteligente de duas pessoas que decidem ser amigos, companheiros e bons amantes. Que apesar das dificuldades/problemas/obstáculos (que nunca falham), todas as manhãs decidem caminhar juntos pela vida. É fácil?? Não, é muito difícil, mas enquanto se tenta, a vida acontece mais Feliz! Por tudo isso, agradeço ao Flávio, o meu marido, que esteve sempre ao meu lado, agradeço por todo o amor, todo o apoio e por todo o companheirismo nestes últimos anos. Obrigada por me ouvires, por nunca me deixares cair, e por nunca teres desistido de mim. Contigo tudo foi mais fácil. Agradeço-te com uma pitadinha de amor e outra bem generosa de gratidão. Obrigada por ser quem és. Amo-te muito!

Á minha mãe, que é a melhor mãe, a melhor avó, a melhor tia, a melhor sogra, a melhor cunhada, a melhor madrinha, a melhor nora, a melhor filha, a melhor irmã, a melhor esposa, a melhor amiga.... És a melhor pessoa que conheço, tens uma bondade e um coração gigante. Obrigada por tudo, mas sobretudo por seres minha Mãe, minha Amiga, minha Companheira, minha Cúmplice. Obrigada por nunca teres desistido de mim. Amo-te muito!

À minha irmã Marta pelo significado que tem na minha vida, que longe ou perto esteve sempre comigo, com a palavra certa de força e amizade. Ao meu cunhado Marco por ser a pessoa otimista que é. Aos meus sobrinhos Henrique e Manuel por me transmitirem a sua energia e alegria. Amo-vos!

Ao meu Pai, o super-herói da minha vida, agradeço por cuidar sempre por mim. A ti devo a pessoa que sou hoje, aplico orgulhosamente todos valores que me ensinaste em tudo o que faço. Quero que um dia venhas a estar orgulhoso de mim assim como eu sempre tive orgulho em ti. Pai, estás e sempre estarás no meu coração. Nunca te irei esquecer.

Funding

This project was financed by the Portuguese Foundation for Science and Technology (FCT) through a doctoral fellowship (SFRH/BD/131665/2017 and COVID/BD/151940/2021), by Health Sciences Research Centre (CICS-UBI) through National Funds by FCT (UID/Multi/00709/2019) and (UID/Multi/00709/2019), and by FEDER funds through the POCI—COMPETE 2020—Operational Programme Competitiveness and Internationalisation in Axis I—Strengthening research, technological development and innovation Project (POCI-01-0145-FEDER-007491).

Resumo Alargado

Disruptores endócrinos (EDCs) são substâncias exógenas ao corpo humano que podem interferir na síntese, secreção, transporte, metabolismo ou eliminação das diferentes hormonas, que são responsáveis pela manutenção da homeostase corporal, reprodução, desenvolvimento ou comportamento. Os EDC são um grupo muito heterogéneo de compostos, que vão desde químicos sintéticos a alguns produtos constituintes naturais de algumas plantas. A avaliação do seu impacto na saúde é extremamente difícil, assim a constante exposição humana a EDCs tem suscitado algumas preocupações. Sabe-se atualmente que existem diversas patologias em que estas substâncias podem ter um papel determinante como causadoras ou amplificadoras das suas manifestações, uma vez que esses compostos afetam a função endócrina interferindo nas vias hormonais (por exemplo: estrogénio, androgénio ou hormonas tiroidianas).

Os retardadores de chama bromados (BFRs) são produtos químicos omnipresentes usados amplamente pela indústria. Estes compostos são frequentemente usados em eletrónica, veículos motorizados, brinquedos, plásticos e têxteis para reduzir a inflamabilidade. Os BFRs são lipofílicos e persistentes, e infelizmente muitas destas substâncias químicas não permanecem fixas no produto que as contém, sendo lentamente libertadas para o ar, para as partículas de pó e água, e terminam entrando nos alimentos e no nosso organismo. Os efeitos nocivos para a saúde destes produtos químicos podem estar relacionados à sua persistência e bioacumulação em humanos. As principais vias de exposição são fontes alimentares, inalação e ingestão através de pó, como por exemplo o pó doméstico.

Dos retardadores de chama o TBBPA (Tetrabromobisphenol A) é o composto mais estudado devido à sua toxicidade e deteção em diversos meios ambientes e no ser humano. A sua incidência e/ou prevalência de problemas de saúde associados à perturbação endócrina tem aumentado ao longo dos anos. Estudos recentes têm sugerido que o TBBPA contribui para uma série de problemas de saúde, que envolvem não só, doenças como o cancro da mama ou dos rins, mas também incluem doenças metabólicas, como a obesidade. Adicionalmente foram reportados efeitos a nível do desenvolvimento e reprodução humana, assim como a nível da tiroide, sistema cardiovascular e sistema neuro-endócrino. O TBBPA foi identificado em amostras abióticas, como água, ar e poeira, solo, sedimentos e polímeros plásticos, e em amostras bióticas, como soro humano, plasma, urina e leite materno. Além disso, o TBBPA também foi detetado no cordão umbilical de grávidas, comprovando uma exposição pré-natal a este composto. Este resultado sugere que o TBBPA pode atravessar a placenta humana. Então, os efeitos da

disrupção endócrina resultantes da exposição ao TBBPA podem ser detetados em gerações futuras? Estudos em embriões e larvas de peixes-zebra, evidenciaram que o TBBPA pode causar toxicidade no sistema cardíaco comprometendo o seu desenvolvimento, resultado do stress oxidativo e consequentemente apoptose celular provocado por este composto. Foi também demonstrado que o TBBPA pode induzir hiperemia e pericardite (edema pericárdico) em embriões e larvas de peixes-zebra. Assim, estes resultados mostraram que há uma relação dose-resposta significativa entre os parâmetros de toxicidade (taxa de eclosão, taxa de sobrevivência, taxa de malformação e taxa de crescimento) e a concentração do TBBPA, nas gerações futuras.

A nível vascular, não existem dados publicados relativamente aos efeitos do TBBPA, nem sobre o seu possível papel no desenvolvimento de desordens vasculares. Neste sentido, o trabalho desenvolvido nesta tese de doutoramento teve como principal objetivo o estudo dos efeitos do TBBPA a nível da contratilidade arterial e a análise dos possíveis mecanismos envolvidos nesses efeitos, para futuramente se estudar se o efeito do TBBPA pode ou não estar associado ao desenvolvimento de patologias vasculares, de forma a minimizar o impacto da exposição ao TBBPA nas gerações futuras. Esta análise foi realizada em dois modelos de estudo diferentes, nomeadamente em artérias umbilicais humana (HUA) e em aortas de rato.

A HUA é facilmente obtida a partir do cordão umbilical, está implicada na circulação feto-placentária e é uma excelente fonte de células musculares lisas vasculares (VSMC). Mecanismos endócrinos e parácrinos que regulam o estado contrátil das VSMC na HUA são muito importantes para permitir as trocas gasosas e de nutrientes entre o feto e a placenta, uma vez que os vasos sanguíneos do cordão umbilical não são inervados. Estas características torna a HUA um bom modelo para analisar os efeitos dos EDCs no sistema vascular e compreender possíveis implicações vasculares da exposição a esses compostos na gravidez. Em relação à aorta de rato, é um modelo que tem sido utilizado ao longo dos anos devido a uma boa extrapolação dos resultados para o humano.

Para além do objetivo principal, anteriormente mencionado, no primeiro trabalho apresentado nesta tese, analisou-se a compartimentação do cGMP (cyclic Guanosine 3,5'-Monophosphate) a nível vascular através da ativação dos CNG (cyclic nucleotide gated channels) sensíveis a cGMP e a possível implicação das fosfodiesterases (PDE). A técnica patch clamp na configuração whole cell foi usada para medir o sinal de ativação dos canais de CNG. As células musculares lisas da artéria umbilical humana (HUASMC) foram infetadas com o adenovírus WT-CNGA2. Os compostos utilizados foram: peptídeo natriurético atrial (ANP), nitroprussiato de sódio (SNP), 3-isobutil-1-metilxantina (IBMX) (inibidor não seletivo das PDE), To-156 (inibidor específico da PDE5), ciloestamida (inibidor específico da PDE3) e Sp-8 (análogo da molécula cGMP). Analisando os

resultados obtidos, observa-se que o ANP e o SNP induzem um diferente aumento da I_{CNG}. O sinal do cGMP induzido pelo ANP parece ser controlado pela PDE5 e pela PDE3. Contudo, a administração do SNP parece criar dois efeitos separados, um mais localizado junto à membrana plasmática que é controlado pela PDE3 e pela PDE5, e o outro efeito localizado no interior das células que é regulado apenas pela PDE3. Em suma, a distribuição temporal e espacial diferente do cGMP pode contribuir para efeitos específicos do ANP e de dadores de oxido nítrico (NO) na função vascular, confirmando que a regulação e a síntese do cGMP são compartimentadas nas HUASMC.

No segundo trabalho apresentado foram avaliados os efeitos diretos e os efeitos após 24h de exposição ao TBBPA na HUA e analisado o seu possível modo de ação (MOA). O ensaio de MTT foi usado para analisar viabilidade celular das células musculares lisas da artéria umbilical humana (HUASMC), estas células foram expostas a diferentes concentrações de TBBPA, e observou-se uma diminuição da viabilidade celular nas concentrações maiores (500 e 1000 μM). Usando a técnica de banho de órgãos, anéis HUA sem endotélio foram contraídos com serotonina (5-HT), histamina (His) e cloreto de potássio (KCl) e, em seguida, os efeitos diretos do TBBPA (0,01-100 μM) foram analisados. Após 24 horas de exposição ao TBBPA (1, 10 e 50 μM) foram avaliadas as respostas contráteis da HUA à aplicação dos agentes contráteis, 5-HT His e KCl. Para investigar mais detalhadamente o modo de ação vascular do TBBPA, através do qual ele prejudica a homeostase vascular do HUA. Além disso, o mecanismo de ação vascular do TBBPA foi estudado através da análise da atividade dos nucleótidos cíclicos e dos canais de cálcio (Ca^{2+}), vias envolvidas respetivamente, no relaxamento e na contração da HUA. Os resultados obtidos demonstraram que os efeitos diretos do TBBPA induzem um vasorelaxamento da HUA e que a exposição de 24 horas ao TBBPA altera o padrão de resposta vasoconstritora de 5-HT, His e KCl e o padrão de resposta vasorelaxante do SNP e da nifedipina (Nif). Este efeito é devido ao envolvimento do TBBPA com a via NO/sGC/cGMP/PKG e com a interferência no influxo de Ca^{2+}. Além disso, usando a reação em cadeia da polimerase quantitativa em tempo real (qPCR), observou-se que o TBBPA modifica a expressão dos canais de Ca^{2+} tipo L, das subunidades α- e β_1 dos canais de potássio ativados por cálcio (BK_{Ca}), da guanilato ciclase solúvel (sGC) e da proteína cinase G (PKG). Assim, estes resultados apontam para alterações na homeostase vascular da HUA provocadas pela exposição ao TBBPA.

No terceiro trabalho apresentado foi analisado o efeito do TBBPA no músculo liso da aorta de ratos, para investigar a sua via de sinalização. Para atingir este objetivo, começamos também com a análise da viabilidade celular das células A7r5, usando o ensaio de MTT. As células A7r5 foram expostas durante 24 horas a diferentes concentrações de TBBPA, e os resultados obtidos mostraram que as maiores concentrações de TBBPA (500

e 1000 μM) diminuíram a viabilidade celular. Em seguida, pela técnica do banho de órgãos, os anéis de aorta de rato sem endotélio foram contraídos com Fenilefrina (Phenyl), Noradrenalina (NA) e com uma solução KCl isosmótico para avaliar o efeito vascular do TBBPA (0,01–100 μM). Para além disso, o mecanismo de ação do TBBPA foi estudado através de inibidores específicos, nomeadamente, a Nif, um inibidor de canais de cálcio dependentes de voltagem tipo L, o tetraetilamonio (TEA), um inibidor de canais de potássio dependentes de cálcio (BK_{Ca}), a 4-aminopiridina (4-AP), um inibidor de canais de potássio dependentes de voltagem (K_v) e a glibenclamida (Gly), um inibidor de canais de potássio dependentes de ATP (K_{ATP}). Os resultados mostraram que estes inibidores reduziram o efeito vasorelaxante do TBBPA, sugerindo que os efeitos vasculares do TBBPA envolvem os canais de Ca^{2+} e de K^+. Para avaliar a atividade dos canais de cálcio dependentes de voltagem (VGCC) tipo L em células A7r5, aplicou-se a técnica *patch clamp* na configuração de *whole cell, e* observou-se uma diminuição da corrente de Ca^{2+}. Estes resultados suportam a ideia que os efeitos do TBBPA induzem vasorelaxamento na aorta de ratos, devido à inibição dos canais de Ca^{2+} e ativação dos canais de K^+. Também, por qPCR, observou-se que o TBBPA modula a expressão dos canais de Ca^{2+} tipo L, das subunidades α- e β_1 dos BK_{Ca}, da sGC e da PKG.

Em suma, os resultados obtidos nesta tese, durante o desenvolvimento deste projeto, confirmaram as ações cruciais do TBBPA no músculo liso vascular. Estes resultados demonstram que o TBBPA induz um relaxamento do músculo liso agindo através de um mecanismo independente do endotélio. Este mecanismo de ação do TBBPA envolve ativação de sGC, o aumento os níveis intracelulares de cGMP, uma inibição dos VGCC tipo L e uma ativação dos canais de K^+. Outro resultado inovador da presente tese foi a identificação da existência de compartimentação de cGMP em células musculares lisas vasculares humanas.

Devido à alteração da homeostase vascular induzida por TBBPA, este composto pode ser um possível indutor de doenças hipertensivas. Nesta linha de investigação, os resultados obtidos parecem muito promissores, neste sentido estudos adicionais são necessários para conhecer melhor o mecanismo de ação do TBBPA a nível vascular e compreender a sua complexidade na exposição humana e ambiental, de forma a minimizar o risco em gerações futuras.

Palavras-chave

TBBPA; Retardante de chama; Disruptores endócrinos; Artéria umbilical humana; Células musculares lisas; Vasoconstrição; Vasorelaxamento; Canais de potássio; Canais de cálcio; Dadores de óxido nítrico; Nucleótidos cíclicos; Compartimentação.

Abstract

The endocrine disruptor (EDCs) is a compound that has been defined as “an exogenous agent that interferes with the production, release, transport, metabolism, binding, action or elimination of natural hormones in the body responsible for the maintenance of homeostasis and the regulation of developmental processes.” This compound can affect the endocrine function via interference with hormone pathways (e.g., oestrogen, androgen, or thyroid hormone). The constant human exposure to endocrine disruptors has raised some concerns. Some of these components are suspected of being harmful to human health.

Brominated flame retardants (BFRs) are chemicals widely used in consumer products, including electronics, vehicles, plastics, and textiles, to reduce flammability. These compounds can interfere with hormone homeostasis, so they are considered endocrine disruptors. Tetrabromobisphenol A (TBBPA) is the most studied BFRs due to its toxicity and presence in a variety of environmental media and the human being. The exposure to this compound is associated with several health risks: thyroid disorders, diabetes, reproductive health, cancer, and neurobehavioral development disorders. In addition, TBBPA exposure can be correlated with some cardiovascular disorders, such as diabetes and obesity. This compound has also been detected in biological samples such as human serum, urine, and breast milk. Moreover, TBBPA has also been detected in the umbilical cord of Japanese pregnant women, proving a prenatal exposure to this compound. This observation suggests that TBBPA can cross the human placenta. In this scenario, it is important to understand how the TBBPA exposure effects the vascular tonus and if the endocrine disrupting effects from that exposure can be detected in future generations.

In this project, organ bath and patch clamp techniques were developed and applied to achieve the main goal of this doctoral thesis: to study the effect of TBBPA on arterial contractility and analyse the mode of action of TBBPA as a human EDCs and understand its involvement in vascular disorders. This study was performed in two different study models: in the human umbilical artery (HUA) and in the rat aorta.

Additionally, the cGMP compartmentation in human vascular smooth muscle was also analysed. Therefore, in the first research work presented, we infected smooth muscle cells with adenovirus containing mutants of the rat olfactory cyclic nucleotide-gated (CNG) channel-subunit to understand how the cGMP conveys different information and we recorded the associated cGMP-gated current (I_{CNG}). The whole cell configuration of the patch clamp technique was used to measure the I_{CNG} and the potassium current (I_K) in

human umbilical artery smooth muscle cells (HUASMC). Atrial Natriuretic Peptide (ANP) induced an activation of basal I_{CNG}, whereas sodium nitroprusside (SNP) had a slight effect. IBMX (nonselective PDE inhibitor), T0-156 (PDE5 inhibitor), and cilostamide (PDE3 inhibitor) all had a small effect on the basal I_{CNG} current. Concerning potassium channels, we observed that ANP and testosterone induced activation of I_K and this effect is bigger than that induced by SNP, cilostamide and T0-156. Cilostamide and T0-156 decreased the I_{CNG} stimulation induced by ANP and testosterone, suggesting that the pGC pool is controlled by PDE3 and PDE5. Thus, the effects of SNP show the presence of two separated pools, one next to the plasma membrane and controlled by the PDE5 and PDE3, and a second pool in the cytosol of the cells that is regulated mainly by PDE3. These findings show the existence of cGMP compartmentalization in human vascular smooth muscle cells, and this phenomenon is controlled by PDE3 and PDE5.

The second research work evaluated the direct effects and the 24 h exposure of TBBPA on the HUA and also its mode of action (MOA). The viability of HUASMC was analysed using MTT assay and the cells exposed to high concentrations of TBBPA (500 and 1000 μM) showed a decrease in cell viability. Using the organ bath technique, endothelium-denuded HUA rings were contracted with serotonin (5-HT), histamine (His), and potassium chloride (KCl), and then the direct effects of TBBPA (0.01- 100 μM) were analysed. The effects of 24 hours TBBPA exposure (1, 10, and 50 μM) were also analysed on contractile responses of HUA to 5-HT, His, and KCl. Furthermore, the vascular MOA of TBBPA was studied through the analysis of cGMP and calcium (Ca^{2+}) channels activity, these pathways are involved in the relaxation and contraction of HUA, respectively. Our results demonstrated that the direct effects of TBBPA induce a vasorelaxation of HUA. The 24h TBBPA exposure changed the vasoconstrictor response pattern of 5-HT, His and KCl and the vasorelaxant response pattern of SNP and nifedipine. This effect is due to the involvement of TBBPA with the NO/sGC/cGMP/PKG pathway and the interference in Ca^{2+} influx. Furthermore, using the real-time quantitative polymerase chain reaction (RT-qPCR), TBBPA clearly modulates L-type Ca^{2+} and large-conductance Ca^{2+} 1.1 α- and β_1 subunit channels, and soluble guanylyl cyclase (sGC) and protein Kinase G. In this sense, our data demonstrated that TBBPA induces changes in the vascular homeostasis of HUA.

In the last part of this work, the effect of TBBPA in rat aortic smooth muscle and the possible mechanisms involved were investigated and to achieve these goals, we started with the analysis of A7r5 cells viability. These cells were exposed to different TBBPA concentrations, and the results showed that the high concentrations of TBBPA (500 and 1000 μM) decreased the viability of the A7r5 cells. Then, using the organ bath technique, rat aorta rings without endothelium were contracted with Phenylephrine, Noradrenaline, and isosmotic KCl solution to evaluate the vascular effect of TBBPA (0.01–100 μM).

Furthermore, MOA of TBBPA was studied through Nifedipine (specific blocker of L-type VGCC), tetraethylammonium (TEA), 4-aminopyridine (4-AP), and glybenclamide (Gly) (K^+ channel inhibitors). Our results suggest that the direct effects of TBBPA induced vasorelaxation of rat aorta, involving the inhibition of Ca^{2+} channels and activation of potassium channels. Moreover, through RT-qPCR, it was demonstrated that TBBPA clearly modulates L-type Ca^{2+} and large-conductance Ca^{2+} 1.1 α- and β_1 subunit channels, and sGC and protein Kinase G. Overall, it was shown that TBBPA exposure also interferes with vascular homeostasis of rat aorta through Ca^{2+} and K^+ channels.

In conclusion, the main findings of this thesis confirmed the crucial actions of TBBPA in vascular smooth muscle. These effects demonstrate that TBBPA induces smooth muscle relaxation through an endothelium-independent MOA. Due to sGC activation that increases the cGMP intracellular levels, inhibition of L-Type VGCC and activation of K^+ channels were verified. Another innovative result of the present thesis was the identification of cGMP compartmentalization in human vascular smooth muscle cells. Further understanding and targeting of these results might be exploited in future studies to acknowledge the effects of TBBPA at the vascular level and its complexity in environmental and human exposure.

Keywords

TBBPA, Flame Retardants, Endocrine Disruptors, Human Umbilical Artery; Smooth muscle cells; Vasoconstriction, Vasorelaxation, Potassium Channels, Calcium Channels, Nitric oxide donors, Cyclic Nucleotides, Compartmentation.

Thesis Overview

This doctoral thesis is divided into seven chapters.

The first and second chapters enclose the literature review that supports the theme under study. The first chapter presents the general characteristics of vascular smooth muscle, the different elements of vascular smooth muscle cells that participate in the performance and control of their essential function and regulation of vascular tone. Additionally, the physiological description of the human umbilical cord and the human umbilical artery, as well as the importance of human umbilical smooth muscle cells at the vascular level in preeclampsia and hypertension in pregnancy are also summarized. The second chapter contains the review developed in the scope of this thesis, regarding the toxicity of TBBPA and how this compound affects the environment and health.

The third chapter presents the global aims of this thesis, as well as the intermediate aims established for the implementation and development of this project.

The fourth, fifth and sixth chapters includes the original research papers developed during this PhD project, and are organized as follows:

- Fourth chapter (research work 1): Cyclic guanosine monophosphate compartmentation in human vascular smooth muscle cells.
- Fifth chapter (research work 2): Pathways involved in the human vascular Tetrabromobisphenol A response: calcium and potassium channels and nitric oxide donors.
- Sixth chapter (research work 3): Vascular response of tetrabromobisphenol A in rat aorta: Calcium channels inhibition and potassium channels activation.

Finally, the seventh chapter contains the concluding remarks highlighting the advances obtained during this research work and discusses the future directions in the implications of the TBBPA for in the development of cardiovascular diseases (such as hypertensive disorders in pregnancy), and to identify its molecular pathways that can be targeted for the prevention and treatment of these disorders.

Table of Contents

List of Figures

Chapter 1

Chapter 2

Chapter 4

Chapter 5

Chapter 6

List of Tables

Chapter 1

Chapter 2

Chapter 5

Chapter 6

List of Abbreviations

5-HT	Serotonin or 5-Hydroxytryptamine
AC	Adenylyl Cyclase
AKAP	A-Kinase Anchoring Protein
4-AP	4-Aminopyridine
ANP	Atrial Natriuretic Peptide
ATP	Adenosine Triphosphate
ATPase	Adenosine Triphosphatase
BFRs	Bromo Flame Retardants
BK_{Ca}	Large Conductance Calcium-activated Potassium Channels
MaxiK	High conductance calcium-activated potassium
BNP	Brain Natriuretic Peptide
Ca^{2+}	Calcium
Ca/CaM	Calcium-Calmodulin Complex
CaM	Calmodulin
CaMKII	Ca^{2+}/calmodulin-dependent protein Kinase II
$[Ca^{2+}]_i$	Intracellular Ca^{2+} concentrations
CCC	Criterion Continuous Concentration
Cl^-	Chlorum
cAMP	Cyclic Adenosine 3,5'- Monophosphate
cGMP	Cyclic Guanosine 3,5'- Monophosphate
cIMP	Inosine 3´, 5´- Cyclic Monophosphate
CNG	Cyclic Nucleotide Gated Channels
CNP	C-type Natriuretic Peptide
CO_2	Carbon dioxide
ER	Endoplasmic Reticulum
EC	Endothelial Cell
EDCs	Endocrine disrupting compounds
EDI	Estimated Daily Intake
ELISA	Enzyme-linked immunoassays
EPAC	Exchange Protein Activated by cAMP
FRET	Fluorescence Resonance Energy Transfer
GC	Guanylyl cyclase
GDP	Guanosine Diphosphate
GEFs	Guanine Nucleotide-Exchange Factors
αGi	αSubunit of the inhibitory
Gly	Glybenclamide
GTP	Binding Protein or G protein
GPCR	G Protein-Coupled Receptors
GTP	Guanosine Triphosphate
HCN	Hyperpolarization-Activated Cyclic Nucleotide-Gated Channels
His	Histamine
HUA	Human Umbilical Artery

HUC	Human Umbilical Cord
HUASMC	Human Umbilical Artery Smooth Muscle Cells
IBMX	3-isobutyl-1-methylxanthine
IL-1β	Interleukin 1 beta
IFNγ	Interferon gamma
IP3	Inositol-1,4,5-Tri
K^+	Potassium
K_{ATP}	ATP –Sensitive Potassium Channels
K_{Ca}	Calcium-Activated Potassium Channels
K_{HD}	Kinase Homology Domain
K_{IR}	Inwardly Rectifying Potassium Channels
K_V	Voltage-Gated Potassium Channels
LC50	Lethal Concentration
MAPK	Mitogen-Activated Protein Kinase
Mg^{2+}	Magnesium
MHC	Myosin Heavy Chain
MLC_{17}	Myosin Essential Light Chains
MLC_{20}	Myosin Regulatory Light Chains
MLCK	Myosin-Light-Chain Kinase
MLCP	Myosin-Light-Chain Phosphatase
MOA	Mode of Action
MRP4	Multidrug Resistance-associated Protein 4
MYPT1	Myosin Phosphatase Target Protein-1
Na^+	Sodium
NCX	Na^+/Ca^{2+} Exchanger
Nif	Nifedipine
NMDA receptor	N-methyl-D-aspartate receptor
NO	Nitric Oxide
NA	Noradrenaline
NOS	Nitric Oxide Synthase
NP	Natriuretic Peptide
NPR	Natriuretic Peptides Receptors
O_2	Oxygen
PBC	Printed Circuit Board
PDE	Phosphodiesterases
pGC	Particulate Guanylyl Cyclase
$PGF_{2\alpha}$	Prostaglandin F2α
Phenyl	Phenylephrine
PIP2	Phosphatidylinositol 4,5-Bisphosphate
PKA	Protein Kinase A or Cyclic AMP-dependent Protein Kinase
PKC	Protein Kinase C
PKG	Protein Kinase G or Cyclic GMP-dependent Protein Kinase
PLA	Phospholipase A
PLC	Phospholipase C
PMCA	Plasma Membrane Ca^{2+} ATPases
POPDC	Popeye Domain-Containing Proteins

PPi	Pyrophosphate
RAPGEF3	Rap Guanine Nucleotide Exchange Factor 3
ROC	Receptor-Operated Channels
ROCK	Rho-kinase
SAC	Stretch-activated ion channels
SERCA	Sarco-/Endoplasmic Reticulum Ca^{2+} ATPases
sGC	Soluble Guanylyl Cyclase
SICM	Scanning Ion Conductance Microscopy)
SM	Smooth Muscle
SMC	Smooth Muscle Cells
SNP	Sodium Nitroprusside
SR	Sarcoplasmic Reticulum
TBBPA	Tetrabromobisphenol A
TDI	Tolerable Daily Intake
TEA	Tetraethylammonium
TNF-α	Fator de Necrose Tumoral alfa
TRP	Transient receptor potential
VGCC	Voltage Gated Calcium Channel
VSM	Vascular Smooth Muscle
VSMC	Vascular Smooth Muscle Cells

List of Scientific Publications

Papers related to this doctoral thesis

I. **Vascular response of tetrabromobisphenol A in rat aorta: Calcium channels inhibition and potassium channels activation.**
Joana Feiteiro, Sandra M Rocha, Melissa Mariana, Cláudio J Maia, Elisa Cairrão.
Manuscript submitted in *Toxics journal*.

II. **Pathways involved in the human vascular Tetrabromobisphenol A response: calcium and potassium channels and nitric oxide donors.**
Joana Feiteiro, Sandra M Rocha, Melissa Mariana, Cláudio J Maia, Elisa Cairrão. Toxicology. Volume 470, 30 March 2022, 153158.
(DOI: 10.1016/j.tox.2022.153158)

III. **Health toxicity effects of Brominated Flame Retardants: From environmental to human exposure.**
Joana Feiteiro, Melissa Mariana, Elisa Cairrão (2021). Environmental Pollution. Volume 285, 15 September 2021, 117475.
(DOI: 10.1016/j.envpol.2021.117475)

IV. **Cyclic guanosine monophosphate compartmentation in human vascular smooth muscle cells.**
Joana Feiteiro, Ignacio Verde, Elisa Cairrão (2016). Cellular Signalling. Volume 28, Issue 3, March 2016, Pages 109-116.
(DOI: 10.1016/j.cellsig.2015.12.004)

Papers unrelated to this doctoral thesis

I. **Triiodothyronine modulates neuronal plasticity mechanisms to enhance functional outcome after stroke.**
Talhada D, Feiteiro J, Costa AR, Talhada T, Cairrão E, Wieloch T, Englund E, Santos CR, Gonçalves I, Ruscher K. Acta Neuropathol Commun. 2019 Dec 21;7(1):216.
(DOI: 10.1186/s40478-019-0866-4)

II. **Tributyltin role on the serotonin and histamine receptors in human umbilical artery.**
Glória S, Marques J, Feiteiro J, Marcelino H, Verde I, Cairrão. Toxicol In Vitro. 2018 Aug; 50:210-216.
(DOI: 10.1016/j.tiv.2018.03.006)

III. **Assessment of Tributyltin effects on rat vascular contractility.**
Joana Feiteiro, Melissa Mariana, Ignacio Verde, Elisa Cairrão. March 2018. International Journal of Environmental Research. 2018 March; 12(16–17):1-7. (DOI: 10.1007/s41742-018-0085-z).

IV. **How is the human umbilical artery regulated?**
Margarida Lorigo, Melissa Mariana, Joana Feiteiro, Elisa Cairrao. J Obstet Gynaecol Res. 2018 Jul;44(7):1193-1201.
(DOI: 10.1111/jog.13667).

V. **Inhibition of L-type Calcium Channels by Bisphenol A in rat aorta smooth muscle.**
Feiteiro J, Mariana M, Gloria S, Cairrao E. Journal of toxicology Sciences. 2018;43(10):579-586.
(DOI: 10.2131/jts.43.579).

VI. **Cardiovascular Response of Rat Aorta to Di-(2-ethylhexyl) Phthalate (DEHP) Exposure**
Mariana M, Feiteiro J, Cairrao E. Cardiovasc Toxicol. 2017 Dec 8.
(DOI: 10.1007/s12012-017-9439-6).

VII. **Genomic and non-genomic effects of Mifepristone at the cardiovascular level: A Review.**
Feiteiro J, Mariana M, Cairrao E, Verde I. Reproductive Sciences. 2016 Sep 27. pii: 1933719116671002.
(DOI: 10.1177/1933719116671002).

VIII. **The effects of phthalates in the cardiovascular and reproductive systems: A review.**
Mariana M, Feiteiro J, Verde I, Cairrao E. Environment International. 2016 July
(DOI: 10.1016/j.envint.2016.07.004).

IX. Mifepristone is a Vasodilator Due to the Inhibition of Smooth Muscle Cells L-Type Ca^{2+} Channels.

Mariana M, Feiteiro J, Cairrao E, Verde I. Reprod Sci. 2016 Jun; 23(6):723-30. (DOI: 10.1177/1933719115612926).

l

Chapter 1

Introduction- Part A- The Vascular Smooth Muscle

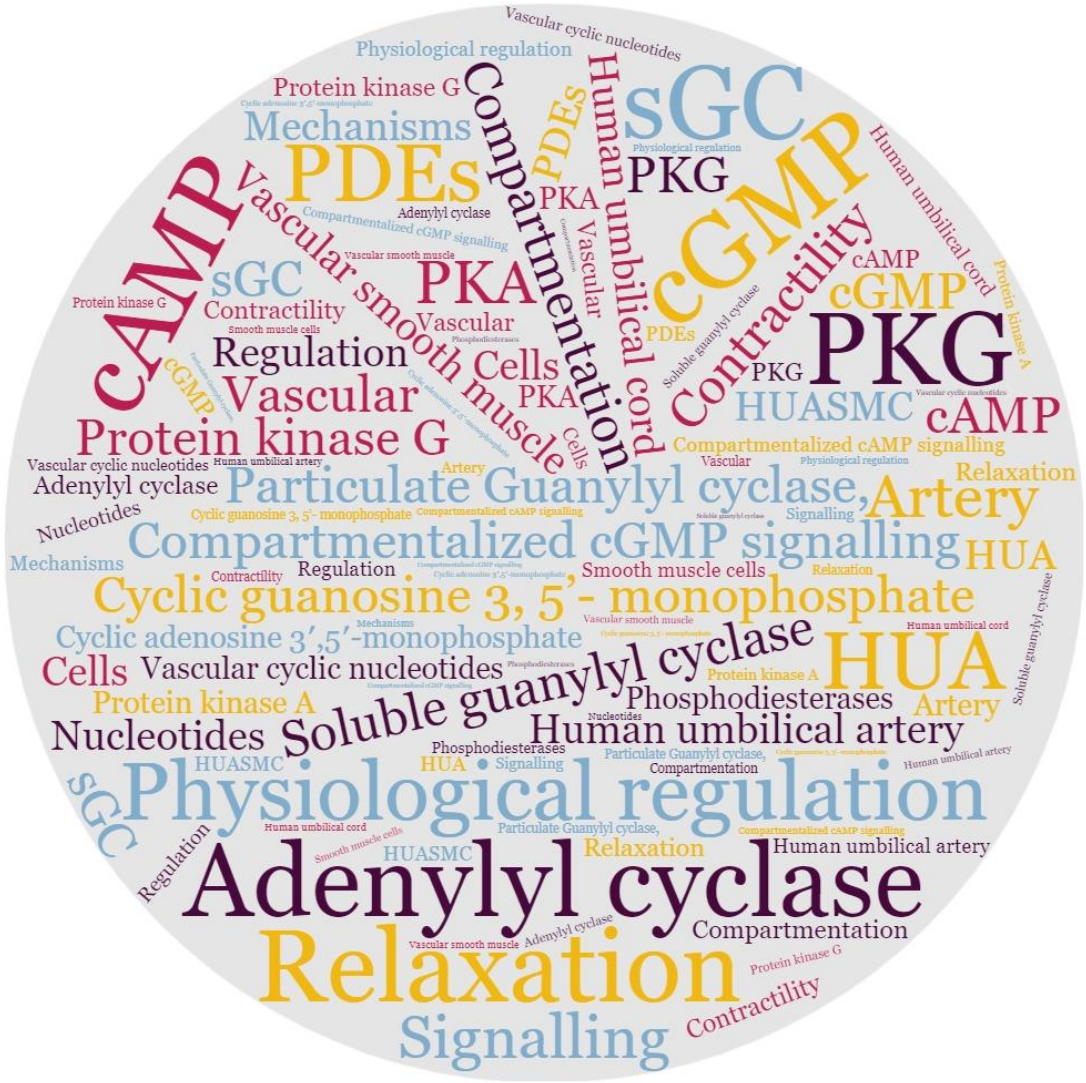

1. Vascular Smooth Muscle

1.1. General aspects of vascular smooth muscle

Smooth muscle (SM) activity is regulated by several mechanical and chemical stimuli. Usually, it is possible to distinguish the smooth muscle cells (SMC) of the different organs according to characteristics, such as physical dimensions, organization, functions, and regulation of their physiological activity, because each organ has a specific type of SM [1]. These differences suggest the existence of a high degree of specialization of the SM of the different organs that are associated with the regulation of the functions of these organs. This muscle is a highly specialized tissue present in different structures of the human body, and it has a significant role in regulating the function of a variety of hollow organ systems including the: vasculature, airways, gastrointestinal tract, uterus and reproductive tract, bladder, and urethra [2].

SM is present in arteries, which are structurally composed of three morphologically distinct layers: the tunica intima, tunica media and tunica adventitia (Figure 1.1) [1,3]. The tunica intima (also referred to as tunica interna) is the innermost layer, and it is comprised of a sheet of endothelial cells (EC) along with a basal membrane and collagen fibrils. The main function of the endothelial layer or endothelium is the regulation of vascular tone and the control of vascular permeability. The endothelium functions as a sensor of hemodynamic changes and chemical signals or stimuli in the bloodstream, subsequently transmitting them to the vascular smooth muscle cells (VSMC) [3,4]. The tunica media (middle layer) is located between the tunica intima and tunica adventitia. It is primarily composed of VSMC and elastic fibres. The VSMC have a single central core and they are commonly long (20-500 μm), thicker in the centre (2-5 μm) and tapered at the ends. These cells are responsible for arterial contractility, and they are critical to maintaining the integrity of the arterial wall [1,3]. The last and outermost layer is the tunica adventitia (also referred to as tunica externa), containing largely connective tissue, fibroblasts, and elastic fibres. In bigger vessels, there are also small blood vessels supplying the vascular wall, which are called *vasa vasorum*. In addition, the tunica adventitia anchors blood vessels to the adjacent tissues [1,3].

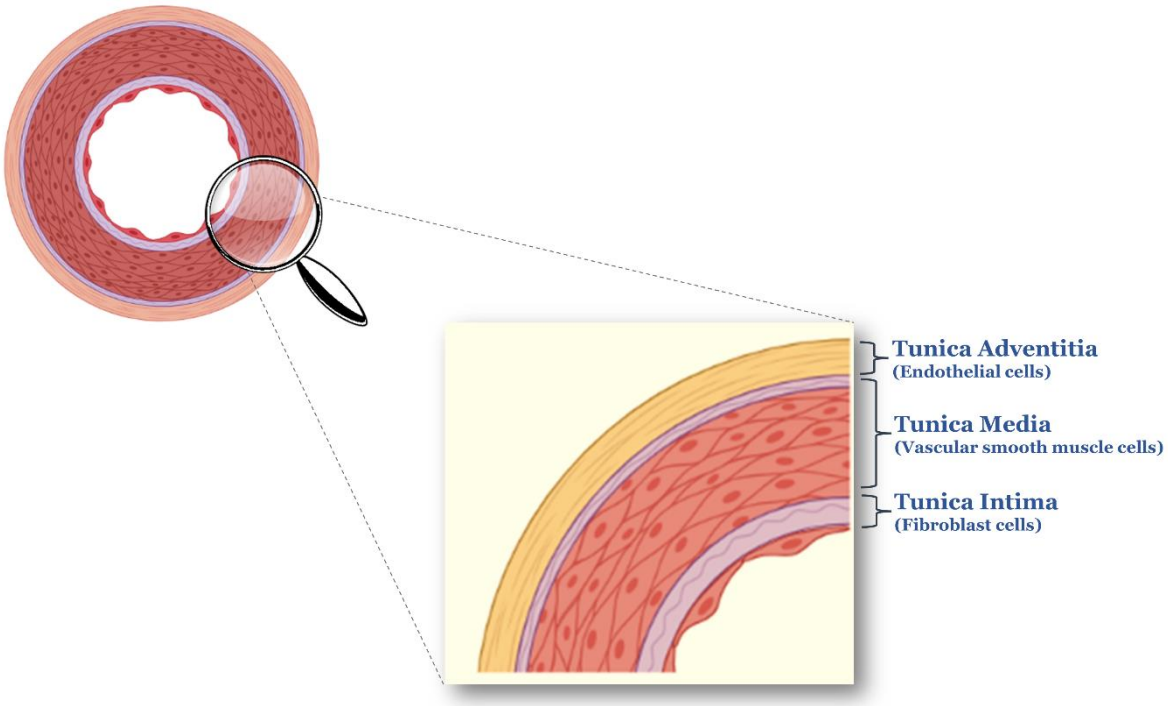

Figure 1.1. Schematic representation of the arterial structural organisation.

Anatomically, the walls of arteries are stronger than those of other blood vessels, which implies that arteries are less distensible than veins. In arteries and veins, the tunica adventitia is similar. However, in veins, the tunica media is usually thinner, due to the lower blood pressure in the venous bed, and the tunica intima in some veins contains valves to keep blood flowing in a single direction. The smallest blood vessels (capillaries) lack the three classical layers of a blood vessel wall. These vessels consist only of a fine tubular structure built of EC, which are surrounded by pericytes and phenotypically similar to VSMC [5,6]. The arterial system has large calibre (1-2.5 cm), medium calibre (0.1-1 cm) and smaller calibre (arterioles, 0.1 cm) arteries. As a result, the importance and complexity of intima, media, and adventitia layers will depend on the type of artery [3,6]. The arteries of large calibre, such as the aorta, have thicker walls with a large number of elastic fibres. Depending on the phases of the cardiac cycle, the elasticity of these arteries allows them to expand or dilate, in order to store and transmit blood to the peripheral circulation during systole and diastole, respectively [7]. The blood flow of different organs of the human body is carried by arteries and the diameter change of the arteries induces an increase or decrease in blood flow [6].

VSMC have classically been envisaged as fusiform cells, on average 200 μm long × 5 μm in diameter, with a large central nucleus surrounded by an abundant array of endoplasmic reticulum and Golgi apparatus, with the cytosol and plasma membrane tapering toward the poles (Figure 1.2) [8]. VSMC play important roles in the physiological functioning of blood vessels and in the pathological changes that occur in them. In healthy blood vessels of an adult organism, VSMC ensure that the blood vessels contract and relax, and in this way, they make a marked contribution to the regulation of blood circulation. These cells express a variety of contractile proteins [5,9],

several types of ionic channels, enzymes, and membrane receptors, allowing them to regulate the contractile function, becoming them into highly specialized cells [2].

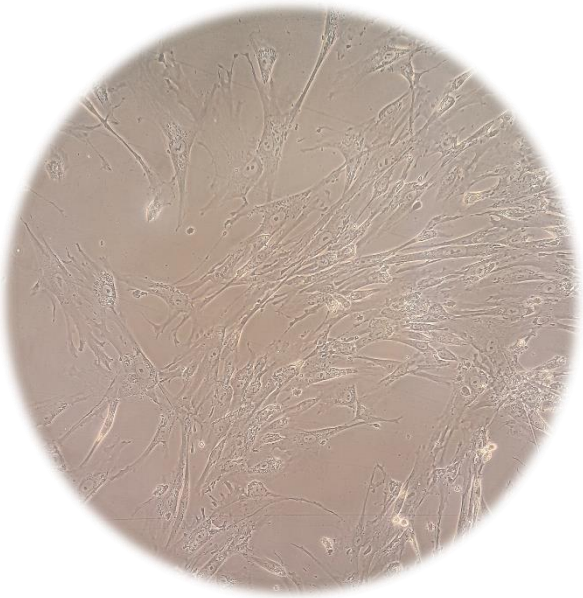

Figure 1.2. Photograph of VSMC culture after 10 days of growth.

The different vascular functions of VSMC are the result of a multiplicity of phenotypes, ranging from the contractile to the synthetic one (Figure 1.3). Contractile and synthetic VSMC, which represent the two ends of a spectrum of VSMC with intermediate phenotypes, have different morphologies [9,10]. Under pathological conditions accompanying the onset and development of vascular diseases, these cells undergo a process referred to as phenotypic modulation. VSMC switch from the contractile phenotype to the synthetic phenotype, characterized by a loss of contractile filaments and associated molecules, and by increased formation of organelles associated with proteosynthesis [2,3,11]. In VSMC *in vitro* culture, the presence of growth factors in the culture media leads to an increase in cells with synthetic phenotype. Cells with a synthetic phenotype have a high proliferative and migratory capacity, and a high activity in the synthesis of extracellular matrix components [12]. In contrast, the contractile phenotype is characterized by abundant contractile fibres containing VSMC-specific contractile proteins, such as α-isoform of actin and the SM-1 and SM-2 myosin heavy chain (MHC) isoforms, and other specific proteins (ion channels and enzymes) associated with the regulation of vascular contraction [5,10]. VSMC of synthetic phenotype are active in migration and growth. This can lead to intimal thickening, formation of atherosclerotic plaques, thickening of the blood vessel wall during hypertension, and finally to stenosis or full obliteration of the vascular lumen [5,13]. However, in healthy adult blood vessels, VSMC are in a quiescent nonproliferative phenotype, referred to as contractile phenotype [2].

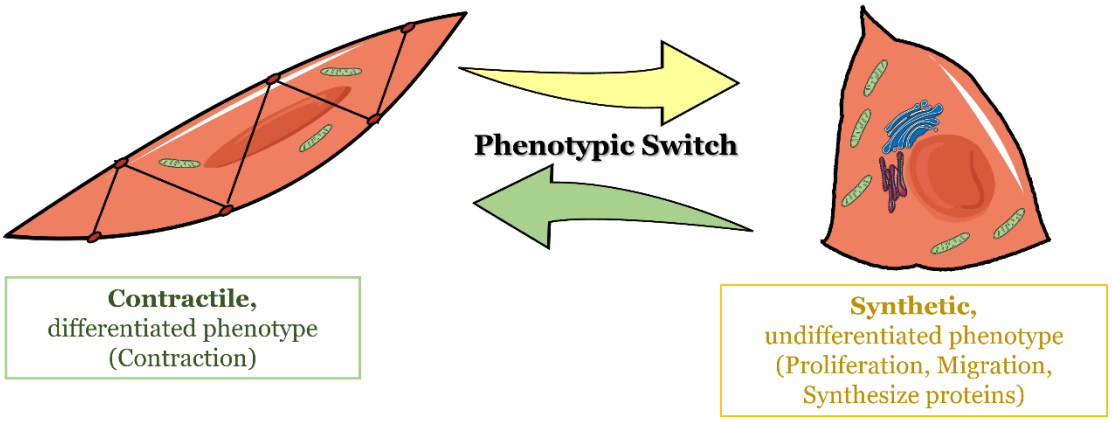

Figure 1.3. Transition between the contractile and synthetic phenotype in VSMC.

1.2. Vascular cyclic nucleotide

Numerous cellular functions are regulated by cyclic nucleotides, such as cyclic adenosine 3, 5'- monophosphate (cAMP) and cyclic guanosine 3, 5'- monophosphate (cGMP). cAMP and cGMP are the main intracellular messengers associated with SMC vasodilation and the increase of their intracellular concentrations represents a useful approach for eliciting a variety of beneficial pharmacological effects on several cardiovascular pathological conditions [14]. The intracellular levels of cAMP and cGMP are the result of the balance between the rate of their synthesis and degradation [15,16]. Synthesis of cAMP occurs after adenylyl cyclase (AC) activation and is usually stimulated by G protein-coupled receptors (GPCR) linked to stimulatory G proteins (Gs), then adenosine triphosphate (ATP) is dephosphorylated, and cAMP and pyrophosphate (PPi) are produced [17] Concerning cGMP synthesis, this happens through the stimulation of particulate (membrane) guanylyl cyclase (pGC) or soluble (cytosolic) guanylyl cyclase (sGC). The pGC can be stimulated by natriuretic peptides (NP), whereas sGC is stimulated by nitric oxide (NO) or NO donors. After stimulation of pGC and sGC, guanosine triphosphate (GTP) is dephosphorylated, and cGMP and PPi are produced [18,19]. The metabolic inactivation of these cyclic nucleotides is catalysed by phosphodiesterases (PDE) [15,20].

1.2.1. Cyclic adenosine 3, 5'- monophosphate (cAMP)

The cAMP was discovered as a signalling molecule in the 1950s during studies on hormonal regulation of mammalian metabolism [21]. This cyclic nucleotide is generated in response to the activation of a wide range of membrane receptors belonging to the GPCR superfamily. After binding a ligand, a G-protein is activated and promotes the activation of the AC that generates cAMP from ATP [16]. The cAMP signalling pathway is a highly conserved regulatory mechanism that plays a pivotal role in a wide range of physiological and pathological processes in a different system, including the cardiovascular system. This action mechanism is achieved by activating the

so-called cAMP effectors, such as cAMP-dependent protein kinase (protein kinase A, PKA), exchange protein activated by cAMP (EPAC), cyclic nucleotide-gated (CNG) ion channels, and the Popeye domain-containing proteins (POPDC) that was recently discovered [22,23]. Cellular levels of cAMP are controlled through its synthesis by AC and its degradation by PDE [17]. Figure 1.4 represents a schematic illustration of cAMP signalling pathway in vascular smooth muscle.

Adenylyl cyclase

The AC are 12 transmembrane proteins which are activated by an external signal (neurotransmitter, hormone, or drug) that, in turn, binds to GPCR [24]. Despite the profound differences in the structures and domain organization, the six AC classes are functionally remarkably similar, catalysing the conversion of a molecule of ATP into cAMP in the presence of magnesium (Mg^{2+}) [24,25]. Depending on the properties and on the relative levels of the isoforms expressed in a done tissue or a cell type, extracellular signals received through the receptors can be differentially integrated.

All mammalian AC are class III enzymes, with nine membrane-integral isoforms participating in the GPCR and G protein-mediated signalling pathway (AC1-9), and one soluble AC (AC10 or sAC) that is not directly linked to the GPCR signalling [26,27]. All membrane isoforms have a single peptide chain that consists of an N-terminal cytosolic domain of varying length [17], two membrane-spanning domains (TM1, TM2), each with two cytosolic domains C1 and C2 subdivided into catalytic (C1a, C2a) and regulatory (C1b, C2b) subdomains and six transmembrane α- helices [17,26]. Isoforms with the catalytic domain C1a are regulated by Gi, while Gs regulate those with the catalytic domain C2a. Gi is thought to cause a rotation of the C1a regions in the opposite direction to Gs, and it is this type of rotation that decreases the enzymatic activity of the AC [17,28]. In addition to their ability to respond to Gs α-subunit and to forskolin (FSK), the different isoforms can receive signals from a variety of sources, including other G proteins, e.g., Gαi and Gβγ, protein kinases A (PKA), C (PKC) and Ca^{2+}/calmodulin-dependent protein kinase II (CaMKII), phosphatases (calcineurin), calcium, and calcium-calmodulin complex (Ca/CaM), and these isoforms can support and integrate differential regulatory pathways through cross-talk with other signal transduction systems [17,25].

In VSMC, the AC2, AC3, AC5, AC6 isoforms and AC8 have been described, but the quiescent VSMC expressed mainly the AC3, AC5, and AC6 and the dedifferentiated cultured VSMC express mainly AC2 and AC8 [17,23]. The regulation of these AC isoforms occurs by phosphorylation through the activation of protein kinases such as CaMKII, PKA and PKC [29]. Thus, AC2, AC3, and AC5 can be stimulated by PKC, and the activity of AC6 is inhibited. The activities of AC 5, 6, and 8 are inhibited by PKA phosphorylation. Nevertheless, the Ca^{2+} is the main regulatory mechanism, which following binding to calmodulin (CaM), lead to a stimulation of AC1 and AC8, and CaM-independently inhibition of AC5 and AC6 as well as the inhibition of AC3 by CaMKII phosphorylation [17,27,30].

Protein kinase A

In eukaryotic cells, the cAMP actions result from the activation of PKA [31]. This includes, at the first level, the stimulation of receptors coupled to heterotrimeric G proteins which through stimulation of AC forms the second messenger cAMP [32,33]. In the phenotypic modulation of the VSMC, PKA may also play an important function that mainly depend on intracellular ATP concentrations [34].

Structurally, PKA is a heterotrimeric serine/threonine protein kinase formed by two catalytic C subunits and a dimer regulatory (R) subunit, where cAMP binds [35,36]. The three isoforms of the C subunit (α, β, γ) have virtually identical kinetic and physicochemical properties, while the four regulatory subunits RIα, RIIα, Riβ and RIIβ) exhibit distinct binding affinities for cAMP and are differentially located within cells [36,37]. There are two types of PKA: (1) PKA Type I are PKA holoenzymes containing the RI subunits (RIα and RIβ) and are predominantly in the cytoplasm; (2) PKA Type II are PKA holoenzymes containing type II subunits (RIIα and RIIβ) which appear to be associated with cellular structures and organelles [31,32,37]. This difference is due to the anchoring of A-kinase anchoring proteins (AKAP) with a greater affinity for the RII subunits. However, some studies demonstrated that there are AKAP with specificity for both RI and RII subunits and AKAP that only bind to the RI subunits [32,37]. This study suggested that both PKA type I and II may be anchored in subcellular compartments within the cells [32], and therefore, the PKA signalling specificity is achieved by binding to AKAP [38,39]. In general, AKAP directs holoenzymes PKA to different subcellular sites near neighbouring proteins, optimizing signal transduction and allowing events responsive to local cAMP to occur within specific compartments of the cell, leading to compartmentation of cAMP signalling [39,40]. So, instability in the expression or activity of some of the PKA subunits or anchoring by AKAP can lead to the progress of cardiovascular diseases [14,40,41]. In the absence of cAMP, PKA is inactive, thus developing a tetrameric complex (R2C2) with the regulatory (R) and catalytic (C) subunits. There are two binding sites (A and B) in each regulatory subunit which cooperatively bind during activation cAMP [37]. The inactivation of the PKA holoenzyme exposes the available B site for cAMP binding. When occupied, the increase of the binding of cAMP to site A induces a change of intramolecular conformational, whereby the regulatory subunits dissociate from the R2C2 complex and generate two active C subunits, which causes the phosphorylation of their substrates in the nucleus and the cytosol. Importantly, only the C subunit is in the nucleus [32,37,39]. This is, the binding of the C subunit to the inhibitory sites of the respective R subunit becomes the kinase inactive, while the cAMP allosteric binding to two C-terminal tandem cAMP binding domains (CNB-A and CNB-B) of the R subunits generates the catalytic activity of the holoenzyme [25,42]. Nevertheless, it has been proposed that cAMP can also activate PKA without releasing the catalytic subunits C and there are intact and active holoenzymes within the cytoplasm in the presence of cAMP [17,31,36].

The EPAC proteins (1 and 2) are another important downstream effector of cAMP. These proteins act as guanine nucleotide exchange factors (GEFs) for small Ras-like GTPases (Rap1 and Rap2), and, for this reason, they are also called cAMP-GEF proteins. In the human vasculature, the Rap Guanine Nucleotide Exchange Factor 3 (RAPGEF3) gene encodes the EPAC1 [43,44]. EPAC

and PKA act independently, but they can also act together in the same biological process in which they regulate synergistic or opposite effects. EPAC modulates different systems, such as cardiovascular system, which has an important function, and it induces a vasorelaxation of vascular SMC through inhibition of RhoA/ROCK signalling [44]. The cAMP-mediated activation of EPAC/Rap1 releases the inhibitory effect of RhoA/ROCK on the MLCP, leading to dephosphorylation of MLC and consequent vasorelaxation of SMC [44].

Additionally, other effectors of cAMP are CNG channels and POPDC. CNG channels are expressed in VSMC and EC. These channels are nonselective cationic channels that open in response to the direct binding of cAMP and cGMP modulating the vascular tone [45,46]. Regarding POPDC, they are expressed in VSMC colocalized with α-smooth muscle actin and may be involved in the mechanisms of vasculogenesis [22]. However, in VSMC its function as a cAMP effector is still poorly understood.

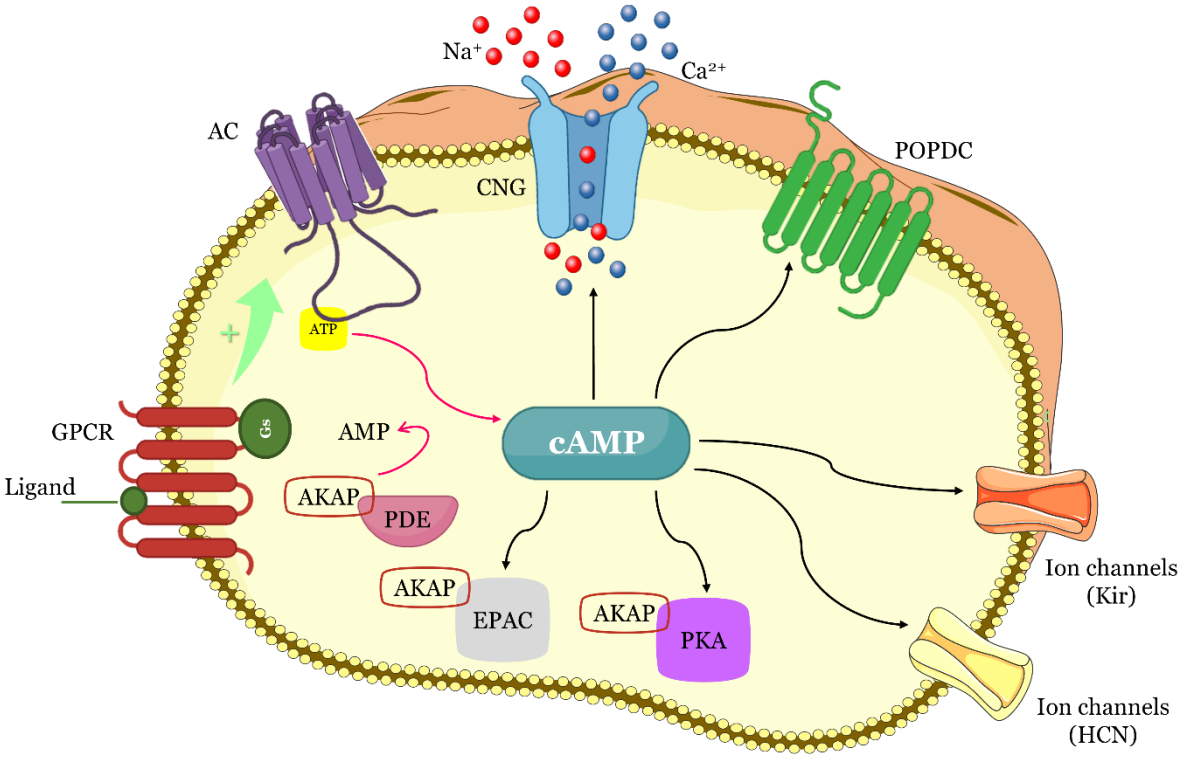

Figure 1.4. Schematic illustration of cAMP signalling pathway in VSMC. cAMP is produced by adenylyl cyclase (AC) stimulated by G protein-coupled receptors (GPCR) coupled to stimulatory G protein (Gs). cAMP activates the following substrates: cyclic nucleotide-gated channels (CNG); protein kinase A (PKA); the exchange protein activated by cAMP (EPAC); hyperpolarization activated cyclic nucleotide-gated (HCN) channels and inward rectifier K^+ channels (Kir); and phosphodiesterases (PDE) that hydrolyse cAMP to AMP.

1.2.2. Cyclic guanosine 3, 5'- monophosphate (cGMP)

The cGMP is the second messenger molecule central to a broad array of intracellular functions. However, the classical and significant physiological effect of an increase in the intracellular concentrations of cGMP in VSMC is vasodilation [47]. In addition, cGMP levels are essential for the maintenance of cardiovascular homeostasis in various cells [33,48].

In VSMC, the cGMP is synthesized by types of guanylate cyclases, which differ in their cellular location and their activation by a specific compound: (1) pGC, present in the plasma membrane, which is activated by NP such as atrial (ANP), brain (BNP), and C-type natriuretic peptide (CNP) [49]; and (2) a sGC that can be activated by NO and by NO donors. These are two ways to convert GTP into cGMP in the presence of magnesium (Mg^{2+}). The nitric oxide-soluble guanylate cyclase-cyclic guanosine monophosphate (NO-sGC-cGMP) axis belongs to the key signal transduction pathways involved in regulating the cardiovascular system [18,50]. As mentioned above, the pathway of cGMP begins with the activation by one ligand (NO, ANP, BNP, and CNP) to GC, either pGC or sGC which causes the increase of intracellular cGMP levels, and, may activate three classes of cGMP effector proteins, such as protein kinase G (PKG), CNG channels and PDE [23,40,51]. Figure 1.5 represents the cGMP signalling pathway in vascular smooth muscle.

Particulate Guanylyl cyclase

The pGC is a single-chain glycoprotein consisting of the N-terminal extracellular domain (ECD), the transmembrane domain (TMD), the intracellular kinase-homology domain (KHD) and the catalytic GC domain (GCD). In its active form, pGC forms a homodimer/tetramer [49,52]. The KHD and GCD are connected by the sequence called a hinge region. The ECD serves as a hormone receptor or a sensor for various extracellular signals. The KHD has a sequence similar to the protein kinase but lacks the sequence necessary for interaction with ATP, phosphate transfer to target proteins or interaction with a metal, all of which are necessary for kinase activity [53]. The KHD serves as a mediator for information transfer to the GCD for its catalytic activity. The C-terminal GCD has a sequence common to pGC and a sequence similar to the catalytic centre of sGC [31]. At least seven pGC (pGC-A to pGC-G) have been identified in mammals [54,55]. In VSMC, three isoforms of pGC (pGC-A, pGC-B and pGC-C) have been identified, in which binding of is NP activated. These proteins are also referred to as NP receptors (NPR): pGC-A or NPR-A, pGC-B or NPR-B, and the clearance receptor or NPR-C (Figure 1.6). The binding of these hormones activates intracellular GCD to produce cGMP from GTP (guanosine triphosphate) [49,55,56]. NPR-C receptor is the most abundant isoform, and in the cardiovascular system is mainly expressed in the atrium, vascular smooth muscle (VSM) and endothelium. Although, in VSMC, the NPR-A and NPR-B are also highly expressed [31,57]. The NP family comprises three members in mammals, ANP and BNP produced in the heart [58] and C-natriuretic peptide (CNP) synthesized in the brain and other tissues [59]. In contrast to ANP, BNP is expressed significantly in the ventricle, so BNP is suggested to be a ventricular hormone for cardiac protection [60]. Regarding affinity for NP, the ANP and BNP can bind to NPR-A and NPR-C, and CNP can bind to NPR- B and NPR-C. [31,49].

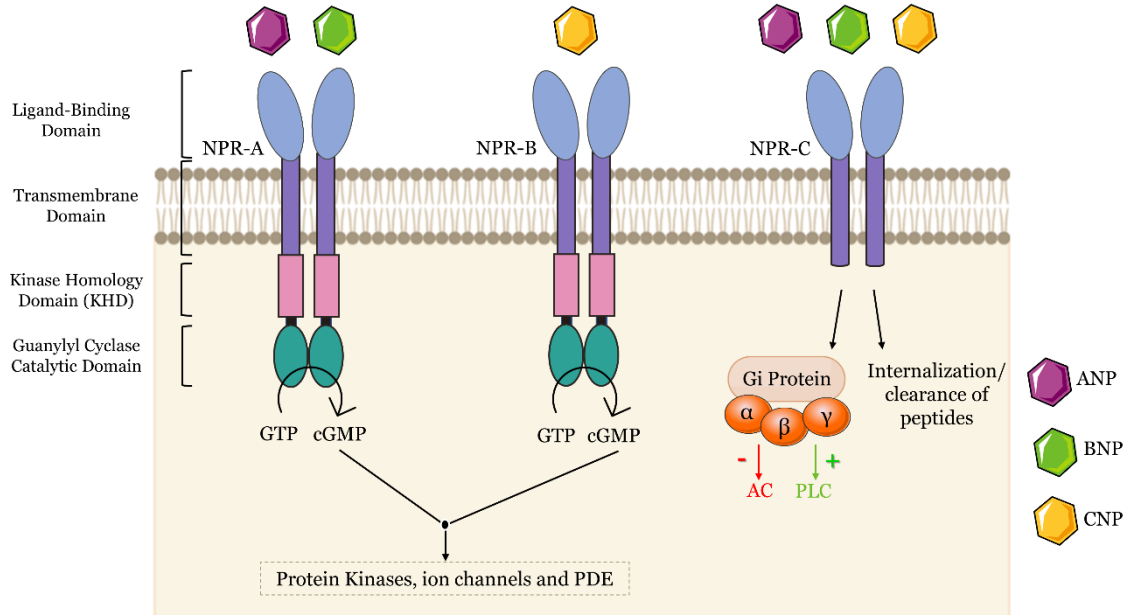

Figure 1.5. Schematic illustration of the structure of the three types of natriuretic peptide receptors (NPR). The NPR type A (NPR-A) and NPR type B (NPR-B) receptors have a analogous structure, which contains of the extracellular N-terminal domain (ligand-binding domain), the transmembrane domain, the kinase homology domain (KHD), the domain responsible for dimerization, and the guanylyl cyclase catalytic domain, which contains the C-terminal region. The NPR type C (NPR-C) receptor has extracellular N-terminal and transmembrane domains but lacks the guanylyl cyclase catalytic domain. Adapted from [61].

Soluble guanylyl cyclase

The sGC is a heterodimeric heme protein consisting of α and β subunits. Two isoforms (α1/ α2 and β1/ β2) exist for each subunit, and the heterodimer is formed by different combinations in different tissues and is involved in diverse functions in addition to vasodilation [18,62]. Each sGC subunit contains three common domains that make up its structure and function: (1) an N-terminal heme-binding (H-NOX) domain; (2) a dimerization domain; and (3) a C-terminal catalytic domain. The catalytic domain is the most highly conserved region between the subunits and is responsible for the conversion of GTP to cGMP [62]. A heme protein containing Fe(II) is linked to the N-terminal region of the β subunit, to which its activator NO binds. The carbon monoxide (CO, another gasotransmitter) also binds to the heme but with lower affinity and less ability to potentiate the catalytic activity of sGC [18,63]. Recently, the molecular structure of the sGC was elucidated by cryo-electron microscopy (cryo-EM) [64,65] allowing us to discover that the central domains are the mediators of protein-protein interactions, while enzymatic activity occurs at the C-terminal catalytic domain. The N-terminal H-NOX domain, since it has a heme group, facilitates the high-affinity binding of NO [64,65]. NO was first identified as an endothelium-derived relaxing factor that acts on the VSM for relaxation. NO is synthesized by a class of enzymes called nitric oxide synthases (NOS), which release NO through the oxidation of L-arginine to L-citrulline [18,66,67]. According to its distribution, NOS has 3 different types, neuronal NOS/NOS1, inducible NOS/ NOS2 and endothelial NOS/NOS3 [68,69]. The catalytic domain is located in the C-terminal region of each subunit, and it converts Mg^{2+}GTP to Mg^{2+}, cGMP and PPi. NO can also be generated

by the reduction of $NO^{-}2$ that, in hypoxia, is facilitated [69,70]. NO signalling is initiated by the activation of NO synthase in the donor cell to produce NO molecules. NO then readily crosses target cell membranes and binds to its sGC, which, in turn, boosts the activity of sGC several hundred-fold to produce intracellular cGMP [69-71].

Protein kinase G

In eukaryotic cells, the cGMP actions result from the activation of PKG, and this protein is considered the most important target of cGMP in the cardiovascular system [47,72]. PKG isozymes belong to the family of serine/threonine kinases and are homologous to PKA in primary sequence and domain organization.

In mammals, two PKG genes called PRKG1 and PRKG2, that encode PKG1 and PKG2, respectively, have been identified [72-74]. Regarding cardiovascular system, the membrane PKG2 is not expressed. On the other hand, cytosolic PKG 1 has two different splice variants, PKG 1α and PKG 1β, (which differ only in the first~100 amino acids). Nevertheless, in VSMC, the most expressed is PKG 1β [74,75]. The expression of PKG is dependent on the cell density in culture, this is, the low density induces a decrease in PKG expression. In addition, the increase of PKG expression causes changes in the contractile phenotypic of cultured VSMC, and the inhibition of PKG expression during cultured growth in vitro may facilitate the modulation to a more synthetic, dedifferentiated phenotype [74]. In 2016, the crystal structure of PKG1 was identified and this protein consists of a homodimer divided into a regulatory (R) and a catalytic (C) region [76,77]. The R-regulatory region is composed of four functional domains, leucine zipper, auto-inhibitory site and two tandem cGMP binding domains (CNB-A and CNB-B) [74,76,78]. The C-terminal catalytic region is composed of two domains, the kinase domain (where the Mg^{2+}/ATP binds) and the AGC-kinase C-terminal domain (where substrate/downstream proteins bind, and phosphorylation occurs) [78].

The CNG channels are nonselective cationic channels that open in response to the direct binding of cAMP and cGMP modulating the vascular tone [46,79]. These channels are more sensitive to cGMP than to cAMP. In physiological conditions, CNG channels carry inward sodium (Na^{+}) and Ca^{2+} currents [80]. Even if the divalent cations can permeate the channel, higher concentrations induce these cations to bind to specific sites within the channel pore and block further ion flow. However, in olfactory and visual systems the knowledge of CNG channels is greater while in other areas is less. Despite that, the CNG channels are used in patch-clamp experiments to observe cyclic nucleotide changes [46,81].

At last, the cGMP level can also be regulated by the PDE activity. In addition, there are crosstalk mechanisms between both cAMP/cGMP pathways induced by PDE [82,83].

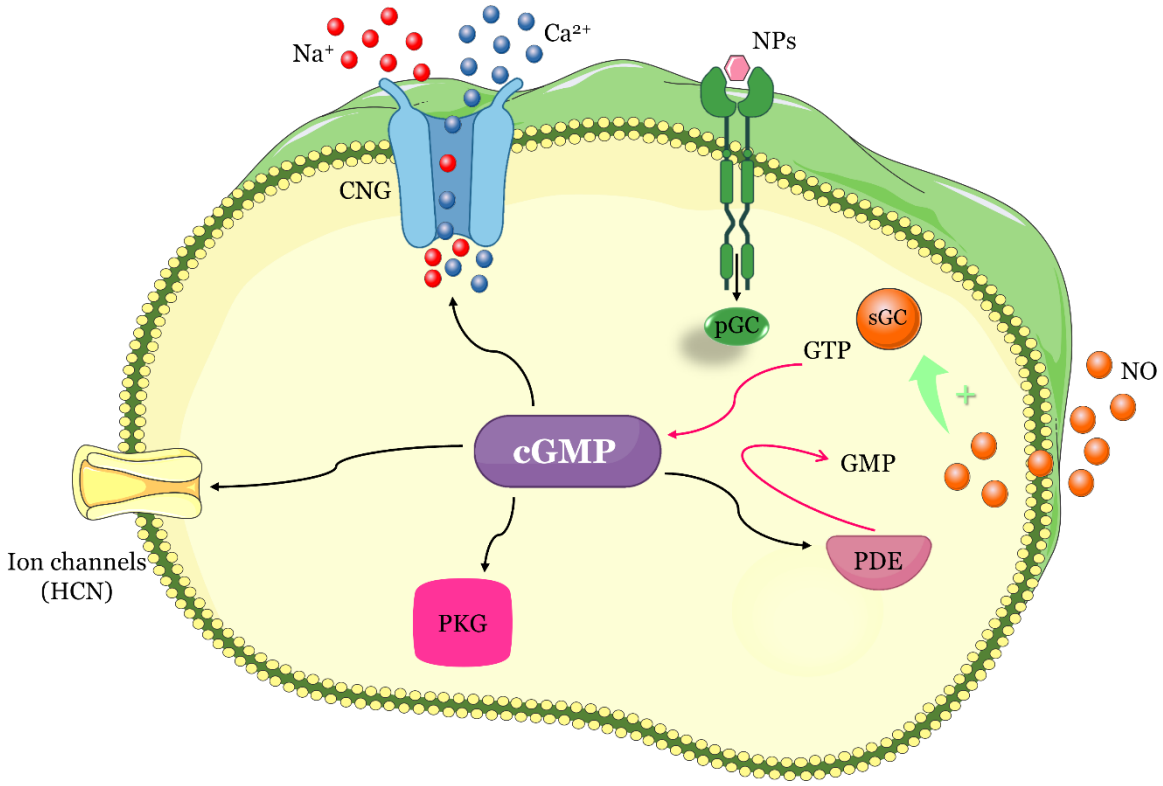

Figure 1.6. Schematic illustration of cGMP signalling pathway in VSMC. cGMP also activated CNG. cGMP is produced either by membrane-bound particulate guanylyl cyclases (pGC), which are the receptors of natriuretic peptides (NPs), or by soluble GC (sGC) that are activated by the nitric oxide (NO). Other cGMP targets are protein kinase G (PKG), hyperpolarization activated cyclic nucleotide gated (HCN) channels, and PDE, the latter degrading cGMP to GMP.

1.2.3. Phosphodiesterases

Relaxation and contraction of vascular smooth muscle and cardiac myocytes are key physiological events in the cardiovascular system. These events are regulated by second messengers, cAMP and cGMP, in response to extracellular stimulants. The intensity of signal transduction is controlled by intracellular cyclic nucleotide levels, which are determined by a balance in the production and degradation of cAMP and cGMP. Degradation of cyclic nucleotides is catalysed PDE, and therefore, the regulation of PDE hydrolytic activity is important for modulation of cellular functions [15,82,84,85]. PDE produce the inactive metabolites cAMP and cGMP limiting the activity of these molecules on their substrates, such as PKA and PKG [14,82]. However, as mentioned above, PKA and PKG are not exclusive effectors; cAMP also acts by EPAC and POPDC. Both cyclic nucleotides activate CNG channels and modulate specific PDE. In vascular tissues, the concentration of cAMP is usually about five times higher than cGMP, although levels can have significant variability [23]. The varied subcellular localization of PDE is key for the spatiotemporal regulation of cyclic nucleotide-dependent signalling. This signalling has revealed that the signal for each physiological event is independently regulated by compartmentation of certain signalling molecules [85,86]. The importance of each PDE functions is variable and depends on some factors: the species, the vascular bed, and the status of the cells [23,82]. Thus, the PDE have a fundamental role in the generation of specific physiological responses, namely in the modulation of signal

transduction in the blood vessel by crosstalk between NO and cyclic nucleotide phosphodiesterases [23].

PDE are classified into I, II, and III classes. Mammalian PDE are composed of 21 genes and are categorized into 11 families based on sequence homology, enzymatic properties, and sensitivity to inhibitors [87,88]. Mammalian PDE belong to class I PDE and have an HD domain (Pfam accession no. PF0966) [89,90] in the C-terminal half and show a high affinity for cAMP and/or cGMP [85]. The domains of proteins involved in the regulation of PDE enzymatic activity and subcellular localization are mainly present in the N-terminal half. Some PDE have phosphorylation sites targeted by protein kinases and lipid modification sites [91,92]. The PDE genes have been identified in humans, rats, and mice. They are categorized into 11 different families based on structural similarities, such as sequence homology, protein domains, and enzymatic properties (i.e., substrate specificity, kinetic properties, and sensitivity to endogenous regulators and inhibitors) [82,87,88]. Thus, the PDE isoforms are classified according to a common nomenclature: each PDE isoform has its family number (1-11); each PDE is represented by an uppercase letter indicating the gene (A-D), and a final number corresponding to the splice variant [82,84,85,93]. Moreover, the 11 PDE families can be grouped into three classes according to their selectivity [14,51]: the cAMP-specific (PDE4, 7, and 8), the cGMP-specific (PDE5, 6, and 9), and the dual hydrolytic for cAMP and cGMP (PDE1, 2, 3, 10, and 11) (Table 1.1).

In VSMC, PDE1, 3, 4, and 5 are described as the main functional PDE families, and their expression pattern depends on the cell phenotype [40]. Indeed, in vitro during cell culture, VSMC undergo a phenotype switch from contractile to synthetic phenotype [94], as well as in vivo during the pathological remodelling of the vascular wall [9]. Moreover, in these cells the main PDE that hydrolyse cAMP are PDE3 and PDE4 isoforms, while PDE1, PDE3, and PDE5 hydrolyse cGMP [14,95,96].

PDE1 is encoded by three genes (PDE1A to -C) that give rise to several isoforms and are activated by the binding of the Ca/CaM complex [97]. In humans, PDE1A shows a high affinity for cGMP. The two connection sites for the Ca/CaM complex are in the N-terminal domain. Through CaM-dependent kinase-II, the PKA and PDE1B can phosphorylate PDE1A, leading to a decrease in activation capacity caused by CaM [85,95]. Activation of PDE1C can be reduced by PKA [19,84]. Moreover, in arterial SMC, higher intracellular Ca^{2+} levels induce the inhibition of AC3 and the activation of PDE1C [98]. PDE1 is present in a wide variety of VSMC, such as human arteries [82,99]. At the vascular level, PDE1C is highly expressed in primary VSMC cultures, but in contractile phenotype the PDE is not expressed in human VSMC, suggesting that the use of this PDE as a marker of human SMC proliferation. PDE1C, in the human vasculature, is associated with functions in the development of human VSMC during normal vascular development and pathological vascular remodelling [100]. Since this PDE is only present in synthetic SMC under pathological conditions, suggests that PDE1C inhibitors may be correlated with disease development, not interfering with normal vascular function. This corroborates with a study performed with patients with pulmonary hypertension which demonstrated that an increase in activity of PDE1C induces decreased cAMP and increased proliferation of pulmonary artery SMC [101,102]. Regarding the PDE1A and PDE1B, both are expressed in human SMC with the contractile

phenotype, but in the synthetic phenotype only is present the PDE1A [84]. The total PDE1 activation occurs only after Ca^{2+} and CaM binding. Some vasoactive agents, such as norepinephrine, angiotensin II (Ang II), and endothelin-1, increase intracellular Ca^{2+} concentration causing PDE1 activation [103]. In this process, due to a decrease in the cGMP levels, the vasoconstrictor effect is increased [95,103]. This suggest that PDE1 isoforms may be helpful therapeutic targets for the disease. PDE1 selective inhibitors appear to be particularly attractive as novel therapeutics to attenuate the pathophysiological abnormalities that occur in pulmonary hypertension [101]. Furthermore, a recent study in coronary arteries proposes that inosine 3´, 5´-cyclic monophosphate (cIMP) concentrations are regulated by PDE1 and PDE5, whose inhibition at a certain level induced an increase of cIMP levels that may enhance hypoxic constriction [104].

PDE2A hydrolyses both cGMP and cAMP with similar maximal levels and relatively high K_m values. PDE2A is allosterically stimulated by cGMP binding to its GAF domain, which facilitates mutual regulation of both cAMP and cGMP signalling [105]. In mammals, the PDE2 gene encodes 3 N-terminal splice variants containing 2 GAF domains originating three splice variants (PDE2A-A3) [84,105,106]. PDE2A1 is present in the cytosol, while PDE2A2 and PDE2A3 are situated in the plasma membrane. PDE2A3, which is a human variant, is membrane associated probably because of its unique N-terminal sequence [88]. PDE2A3 transcripts are rich in the brain and normal in the heart. Immunoreactive PDE2A protein is rich in the neocortex and low in other tissues, and its signals are also localized in capillary, venous, and microvessel EC but not in arterial EC of intact tissues. However, in cultured EC, the PDE2 shows activity [88]. Curiously, the PDE2 is expressed in pulmonary artery SMC, but only in patients with pulmonary hypertension [101], pulmonary arterial hypertension and in pulmonary arteries from rats with hypoxia pulmonary hypertension [107]. Nevertheless, in the physiological conditions, the presence of this PDE is still poorly understood.

PDE3A and PDE3B are the subfamily genes of PDE3, which show a high affinity for both cAMP and cGMP. A low V_{max} value for cGMP in relation to that for cAMP allows the cGMP to act as a competitive inhibitor for cAMP hydrolysis, thus creating the so-called positive cGMP-to-cAMP crosstalk [108]. Hence, PDE3 are called cGMP-inhibited cAMP PDE. The presence of a 44-aa insert in the catalytic domain is a unique characteristic of the PDE3 family. Another special aspect is the presence of 2 N-terminal hydrophobic membrane association domains (NHRs, NHR1 and NHR2) [108]. In the cardiovascular system, mainly in the vascular SM, PDE3A is the predominant isoform found. However, PDE3B is more highly expressed in cells involved in the regulation of glucose and lipid metabolism [109]. In cardiac myocytes, PDE3A1 expression is low, but PDE3A2 expression is high in both cardiac and vascular myocytes [110,111]. The expression of PDE3A is detected in the heart, vascular and placental smooth muscle, corpus cavernosum smooth muscle, and platelets [108]. In contractile phenotype, the PDE3 activity is especially important and is activated by PKA and PKB, but in synthetic phenotype, its activity is decreased [112,113]. Furthermore, PDE3 isoforms are crucial in several cardiovascular physiological mechanisms, namely such as blood pressure regulation and vascular smooth muscle reactivity [114]. More recently, Ercu *et al.* demonstrated that a mutated PDE3A gene induces mechanisms increasing the peripheral vascular resistance leading to hypertension. These observations suggest a gain of function mutation related to hypertension associated with brachydactyly [115].

The PDE4 family consists of four highly similar subfamily genes, PDE4A to -D, which encode cAMP-specific rolipram-sensitive PDE. The PDE4 family includes several splice variants categorized into three N-terminal variant groups ("long form", "short form", and "super-short form") based on the presence or lack of N-terminal upstream conserved regions (UCR) [116,117]. The long-form variants include UCR1, linker region (LR) 1, UCR2, LR2, and the catalytic domain. The short form and the super-short form variants have LR1-UCR2-LR2 and UCR2 (truncated)-LR2 in the N-terminal region, respectively. UCR1, which includes one phosphorylation site of PKA, is coupled to UCR2 by LR1. UCR2 has a hydrophilic N-terminal region, which intramolecularly interacts with the hydrophobic C-terminal portion of UCR1 [85,116]. The PDE4 enzymatic regulation involves the UCR1 and UCR2 [85,118] through UCR2 interaction with the catalytic domain and has also been reported to participate in PDE4 dimerization [118]. Although the PDE4 catalytic site binds to the competitive inhibitor rolipram, the affinity of this site for rolipram can change markedly depending on the conformation of the enzyme. This can result in the so-called high-affinity rolipram-binding site (HARBS) [85]. At vascular smooth muscle level, the PDE4 expression was found in the aortas of bovine [82], pig [119] and rat [120], in rat mesenteric [121], human pulmonary [122] and human umbilical artery (HUA) [96,123]. The inhibition of PDE4 induces vasorelaxation at the vascular level. Moreover, some authors consider that PDE4 is the most important PDE in the regulation of vasodilation associated with cAMP, mainly, in the canine basilar artery and the HUA [96,123,124]. Concerning VSMC, the expression of PDE4A, PDE4B, and PDE4D, has been observed [125]. Moreover, PDE4D is the prevalent cAMP-degrading isoform in cultured VSMC; the prolonged cAMP elevation increases PDE4D activity, and the phenotype stage of the cell is modulated by variants of PDE4D [14,85,126].

The PDE5 family is featured by cGMP-specific hydrolysis encoded by just one gene (PDE5A). The PDE have N-terminal variants, PDE5A1 to -5A3, which show similar K_m values (e.g., ≈ 6 mol/L) have been identified in humans [51]. The PDE5 is a multidomain protein [85] and structurally is constituted by a catalytic domain, which is located at the C-terminus of the protein, and two regulatory GAF domains (GAF A and GAF B) in the N-terminal half, specifically hydrolyses cGMP [51,127]. The N-terminal GAF A domain has been reported to be responsible for this enzyme allosteric binding to cGMP [127,128] and therefore PDE5 is termed cGMP-binding cGMP-specific PDE. One PKG- and PKA-dependent phosphorylation site in the N-terminal region is related to the activation of the PDE5A enzyme [51]. cGMP binding to PDE5A GAF A domain promotes phosphorylation, which not only activates the catalytic function but also increases cGMP binding affinity [129,130]. In humans, PDE5A transcripts are found in various tissues, such as smooth muscle tissues, and platelets [85]. PDE5A1 and PDE5A2 transcripts are also widely distributed [51,104]. In contrast, specific expression of PDE5A3 in smooth and/or cardiac muscle has been suggested. In summary, in vascular SMC the PDE5 is the most abundant and active cGMP-PDE [84], and the two vascular SMC phenotypes (contractile and synthetic) have the same PDE5 expression [131]. PDE5 is the key PDE in the regulation of vasodilation associated with cGMP in arteries [96,132] and in regulating cGMP pools in both contractile and synthetic phenotypes [40].

PDE6 is highly concentrated in the retina [82]. It is most abundant in the internal membranes of retinal photoreceptors, where it reduces cytoplasmic levels of cGMP in rod and cone outer segments in response to light [133,134]. The rod PDE6 holoenzyme is a tetramer consisting of α and β catalytic subunits and two identical inhibitory γ subunits [135]. Each catalytic subunit contains three distinct globular domains corresponding to the catalytic domain and two GAF domains (responsible for allosteric cGMP binding). The PDE6 catalytic subunits resemble PDE5 in amino-acid sequence as well as in the three-dimensional structure of the catalytic dimer; preference for cGMP over cyclic cAMP as a substrate; and the ability to bind cGMP at the regulatory GAF domains [133,134,136]. Most PDE5 inhibitors inhibit PDE6 with similar potency. Turunen *et al.* demonstrated that PDE6 is regulated by Ca^{2+}, contrary to the common view that PDE1 is the unique PDE class whose activity is modulated by intracellular Ca^{2+} [137].

PDE7A and PDE7B are the subfamily of PDE7 that encode rolipram-insensitive high-affinity cAMP-specific PDE (K_m value, ≈0.2 μmol/L) [138]. A PKA pseudosubstrate site is present in the N terminus of the PDE7A subfamily. Dipyridamole nonselective inhibits PDE7 activity. Three variant forms have been reported in the human PDE7 subfamily. PDE7A1 and PDE7A2 are N-terminal variants, and PDE7A3 is a C-terminal variant of PDE7A1 [139]. The expression of PDE7 was found in several cultured vascular SMC [140], the expression of PDE7A being dominant in smooth muscle cells of adult rat aorta [138]. Furthermore, an increase in PDE7B expression in the high-density culture (contractile phenotype) of rat aortic SMC (RASMC) was recently observed [94]. However, its activity was little understood. In humans' pulmonary arteries activity of PDE7A was demonstrated [82]. Another study showed that the isoform PDE7A1 (but not PDE7A2) is present in human VSMC [141].

PDE8A and PDE8B are the subfamily genes of PDE8. PDE8 are high-affinity cAMP-specific PDE insensitive to rolipram and 3-isobutyl-1-methylxanthine (IBMX) and contain REC and PAS domains in the N-terminal portion. These PDE do not hydrolyse cGMP, nor are regulated by cGMP [142]. In humans, 5 PDE8A splice variants, PDE8A1 to -8A5, have been identified. The longest form, PDE8A1, contains REC and PAS domains. PDE8A transcripts are expressed in various tissues and are abundant in the testis, ovary, small intestine, and colon. Usually, the expression of PDE8A1 is dominant when compared with other PDE8A variants [142]. In rats, PDE8A expression is high in the liver and testis [143]. Moreover, in humans, PDE8B transcripts are predominant in the thyroid gland and are low in most brain areas except the cerebellum. However, in rats, the PDE8B transcripts are not confined to the thyroid gland, and they are abundant in the brain and are detectable in neuronal cells of several brain regions other than the cerebellum [14,143].

The PDE9 specifically hydrolyses cGMP with high affinity (K_m = 0.07–0.17 μM) [144]. PDE9A is the only gene, however, more than 20 variants have been observed suggesting that this gene may have complex expression regulation [82,145]. For a long time, there was no report on the regulation of PDE9A activity or the presence of endogenous PDE9A activity in either tissue or cell extracts [85]. Although, it is expressed at the mRNA level in confluent cultured rat pulmonary and systemic coronary SMC [140]. More recently, results have shown that this PDE may be involved in vascular compartmentation [40].

Regarding the PDE10 family, they hydrolyse both cAMP and cGMP. This PDE has only a single gene, PDE10A, which encodes this PDE10. Two major N-terminal variants, PDE10A1 and PDE10A2 and several minor variants have been identified in humans [146,147]. A PKA phosphorylation site in PDE10A2 is the most striking difference between PDE10A2 and PDE10A1. In most human tissues, PDE10A2 expression is higher than that of PDE10A1. The PDE10A GAF-B domain is the only one modulated by cAMP [148]. Moreover, some studies performed in SMC of the pulmonary artery showed the PDE10A expression (layers and cells in contractile phenotype). In addition, the same authors suggested that this PDE has a central function in progressive pulmonary vascular remodelling and suggested the use of an inhibitor of PDE10A as a novel therapeutic approach to PAH treatment [40,87,149].

PDE11 is the latest isoform of the phosphodiesterase family to be identified. Recently, the interest in PDE11 has increased because tadalafil, an oral phosphodiesterase 5 inhibitor, cross-reacts with PDE11 [150,151]. However, the function of this PDE remains largely unknown, but some studies evidence a possible role in male reproduction [152]. PDE11 has only a single gene, PDE11A, with four slicing variants PDE11A1, PDE11A2, PDE11A3, and PDE11A4 that encodes the longest protein including two GAF domains and two N-terminal phosphorylation sites for PKA and PKG [153]. This appears to be the case in all mammalian species studied (human, rat, and mouse) [85,150,154]. PDE11A acts in both cAMP and cGMP, this is, PDE is capable of degrading both substrates with similar affinities (K_m). Initial studies found evidence for PDE11 expression in skeletal muscle, prostate, testis, and salivary glands [150,154,155]. However, the tissue distribution of PDE11A remains a topic of active study and some controversy [156], since the interpretation of these studies is rendered difficult because of differences in the species (human, rat or mice) and isoforms (PDE11A1, PDE11A2, PDE11A3 or PDE11A4) studied. So, there are studies that have supported, and some contradicted these findings, making PDE11 expression and function known [85,150,154].

Table 1.1. Cyclic nucleotide phosphodiesterase isozyme families: characteristics and tissue distribution.

PDE family (no. of genes)	Substrate	Specificities	Primary Tissue Expression
PDE1 (3)	cAMP/ cGMP	Ca/CaM stimulated	Heart, brain, lung, smooth muscle
PDE2 (2)	cAMP/ cGMP	cGMP-stimulated	Adrenal gland, heart, lung, liver, platelets
PDE3 (1)	cAMP/ cGMP	cGMP-inhibited, cAMP-selective	Heart, lung, liver, platelets, adipose tissue, immunocytes, smooth muscle
PDE4 (4)	cAMP	cAMP-specific, cGMP-insensitive	Sertoli cells, kidney, brain, liver, lung, immunocytes, smooth muscle
PDE5 (1)	cGMP	cGMP-specific	Smooth muscle, platelets, Purkinje cells, gastrointestinal epithelium, pulmonary endothelium, smooth muscle

Table 1.1. Cyclic nucleotide phosphodiesterase isozyme families: characteristics and tissue distribution (continued).

PDE family (no. of genes)	Substrate	Specificities	Primary Tissue Expression
PDE6 (3)	cGMP	cGMP-specific, transducin activated	Retinal photoreceptors
PDE7 (2)	cAMP	cAMP-specific, high-affinity, rolipram-insensitive	Skeletal muscle, heart, kidney, brain, pancreas, T lymphocytes
PDE8 (2)	cAMP	cAMP-selective, IBMX insensitive, rolipram-insensitive	Testes, eye, liver, skeletal muscle, heart, kidney, ovary, brain, T lymphocytes
PDE9 (1)	cGMP	cAMP-selective, IBMX insensitive	Kidney, liver, lung, brain
PDE10 (1)	cAMP/ cGMP	cGMP-sensitive, cAMP-selective	Testes, brain
PDE11 (1)	cAMP/ cGMP	cGMP-sensitive, dual specificity	Skeletal muscle, prostate, testes, corpus cavernosum, heart

1.2.4. Compartmentation of vascular smooth muscle cells

The accuracy of a variety of cellular responses depends upon how an extracellular action mobilizes a correct orchestra of cellular messengers and effector proteins spatially and temporally. This concept, named compartmentalization of cellular signalling, is now known to form the molecular basis of various characteristics of cellular behaviour in health and disease. Cyclic nucleotide signalling compartmentation requires multiple receptor stimuli leading to several intracellular effects caused by producing just a few second messengers of cAMP and cGMP. These cyclic nucleotides are ubiquitous cellular messengers that can be compartmentalized in three ways: (I) by their physical containment; (II) by the formation of multiple protein signalling complexes; (III) by their selective depletion. Thus, compartmentation involves the mechanisms by which multiple spatially segregated cAMP/PKA and cGMP/PKG signalling pathways exert differently, or even opposite, functional effects on distinct subcellular microdomains of the same cell [40,83,157,158]. The compartmentation of cyclic nucleotide signalling is a fundamental response among all cell types. In order to understand how vascular cyclic nucleotide signalling becomes important to cellular behaviour, it is crucial to know how it is executed in cells to regulate physiological responses and, also, how its execution or dysregulation can lead to a pathophysiological condition [40,83,157-159].

Several years ago, it was demonstrated that PDE, the enzymes degrading cyclic nucleotides, participate in its compartmentalization [86,96,158-163]. PDE control the compartmentation of the cyclic nucleotides by their local hydrolytic degradation and also by creating different concentrations of cAMP and/or cGMP within a defined microenvironment (colocalized) [20,86,159]. Moreover,

other proteins appear to be involved in cyclic nucleotide compartmentation, such as GPCR [164], AC and GC [71,165], scaffold proteins (AKAP and Caveolin-3) [92,166-168] and, physical barriers formed by nucleus, sarcoplasmic reticulum and mitochondria [169]. Furthermore, there is multidrug resistance-associated protein 4 (MRP4), which is a transmembrane protein involved in the active transport of substrates out of cells, which pumps cyclic nucleotides and controls multiple cardiovascular processes, such as the endothelial barrier function, the proliferation and vasodilation of VSMC [170]. The MRP4 acts as a regulator of SMC proliferation in vascular smooth muscle [171]. In human coronary artery SMC, these energy-dependent efflux pumps are modulators of signal transduction mediated by cAMP and cGMP. The MRP4 inhibition changed the intracellular content of cyclic nucleotides and markedly enhanced their antiproliferative effect [172,173]. It is known that PDE activity does not influence the effects caused by MRP4 inhibition, but it is unclear how the MRP4 inhibition modulates the PDE expression and/or activity. In addition, the inhibition of MRP4 alone seems to be sufficient to modulate intracellular levels of cAMP and cGMP and signal transduction [171-173]. Thus, MRP4 may be an alternative or complement to PDE, ensuring intracellular cyclic nucleotide homeostasis. The inhibition of MRP4 may have therapeutic implications in vasculoproliferative disorders and protect from pulmonary hypertension [170,173]. Nevertheless, in VSMC the MRP4 role in the cyclic nucleotides' compartmentation is still uncertain.

Over the years, a large number of research is done on cAMP and cGMP signalling. Thus, the development of techniques to measure the concentrations and study the compartmentation of these cyclic nucleotides in living cells and tissues has become essential. Up to now, several techniques to study the compartmentation of cAMP and cGMP have been developed and applied in numerous studies [83,174,175]. Traditional biochemical methods such as enzyme-linked immunoassays (ELISA), radioimmunoassay [176], and immunohistochemistry [177], and electrophysiological approaches (patch-clamp technique) [158,178] are quite sensitive and specific methods to analyse cyclic nucleotide compartmentation. However, these methods represent the cell-destructive type of assays that can only measure total cAMP and cGMP levels with a low spatial resolution instead of physiologically relevant free cAMP and cGMP localized in subcellular microdomains [179]. Consequently, the development of innovative techniques, such as fluorescent energy transfer resonance (FRET) [180-182], cell transfection with CNG channels [158,178,183], the development of genetically encoded fluorescent biosensors for cGMP and even the combination of FRET and SICM (scanning ion conductance microscopy) techniques [179,184,185], have enabled studies of cyclic nucleotide dynamics and compartmentation in living cells with high temporal and spatial resolution in real time.

1.2.4.1. Compartmentalized cAMP signalling

The compartmentation of cAMP is related to the formation of specific subcellular compartments (pools) of cAMP signalosomes (Figure 1.7). These signalosomes are large supramolecular protein complexes that undergo clustering and they are key regulators in cAMP signalling, in particular: (I) a cAMP effector, principally PKA, (II) PDE, enzymes responsible for the

degradation of cAMP, (III) scaffold proteins, specifically, AKAP responsible for anchoring the whole complex to a specific subcellular location, and (IV) GPCR linked to stimulatory G (Gs) proteins, mainly β-AR (β-adrenergic receptors) situated in several membrane structures, which interact with distinct scaffolds and subsets of PDE [186-189]. In this context, compartmentalized signalling is a result of the ability that GPCR gives rise to spatially different pools of cAMP and consequently, these pools activate defined subsets of localized PKA (which are linked to anchoring proteins, AKAP) [174]. The AKAP-mediated signalling organizes within the same macromolecular complex several molecules (GPCR, AC, PDE, PKA and its targets, and phosphatases). This way, it ensures the selective phosphorylation and very strict local regulation of the duration of the cAMP signals [190-192].

In the literature, more than 50 genes encoding distinct AKAP have been found in the arterial SMC system with the most important being an AKAP that anchors PKA to L-type voltage-gated calcium channels (L-type VGCCs) at the membrane regulating vascular function [190,193]. More recently, Nystoriak et al. showed that AKAP5, (named AKAP150 in rodents and AKAP79 in humans) is anchored to PKA phosphorylates 1C in Ser1928 of L-Type VGCCs, leading to vasoconstriction in diabetes and response to the raised concentration of extracellular glucose [194]. Furthermore, AKAP5 is essential for the myogenic tone regulation and Ca^{2+} sparklets, blood pressure, and the development of hypertension provoked by Ang II [195].

In compartmentalized cAMP signalling, the PDE also have an essential function since they are the only way in which cAMP can be degraded in the cell [196-198]. PDE establish boundaries to cAMP diffusion and generates cAMP pools that are confined within subcellular compartments. Thus, the localization of specific subcellular PDE is essential for the local regulation of the magnitude, duration, and specificity of cAMP signalling. PDE4 is the one that stands out the most in compartmentation of cAMP [189,199,200]. Richter *et al.* also showed that distinct isoforms of this PDE4 are related to specific positions of β-AR (1 and 2), encouraging not only the compartmentation of cAMP but the presence of other functional effects induced by β-AR isoforms [189,201]. Concerning the pathway of AR/cAMP/PDE signalling, in a study performed with RASMC, it was also observed that cell confluency has a vital modulatory role [94]. The study performed by Belacel-Ouari *et al.* proposes that low cell density is related to loss of β1-AR membrane expression, less cAMP/PDE activity, and a baseline increase in intracellular cAMP level [94]. However, Dunkerley *et al.* detected no changes in the expression of PDE4 between the two SMC phenotypes (contractile and synthetic) [112]. Though, decreases in PDE3A activity and increased expression of PDE1C were related to a synthetic SMC phenotype [202]. Moreover, in RASMC, Zhang *et al.* showed that PDE1 has a small function in controlling cAMP pools. Nevertheless, it was observed that the function of PDE1 is increased under high intracellular Ca^{2+} concentrations ($[Ca^{2+}]_i$), since in the presence of Ang II they obtained a growth in the PDE1 activity in cAMP signals induced by the stimulation of β-AR [40]. In cultured RASMC, it was possible to demonstrated that Ang II (vasoconstrictive agent) induced the increase $[Ca^{2+}]_i$, allowing for PDE1 stimulation [203]. Although compartmentation of cAMP signalling is currently accepted, and the local subcellular organization and regulation of individual signalosomes are known, the role of PKA activation in compartmentalized cAMP remains to be explained. Under normal conditions,

localized PDE holds cAMP levels below their activation limits leading to the inactivation of PKA. When there is hormonal stimulation, the AMP production increases so much that it exceeds the ratio of degradation by PDE, which is present adjacent to PKA in the nanodomain, thus leading to a transient activation of PKA. PKA degradation of PDE stimulates the hydrolytic activity of cAMP, which leads to a return to baseline levels of cAMP [204]. So, when the PDE locally degrades cAMP establishes if the PKA present in a specific multiprotein complex is activated or inactivated and, consequently, determines which signalosome is implicated in signalling [86,197]. However, the way PDE can maintain the levels of cAMP below the PKA activation threshold considering specific parameters such as their K_m and V_{max} and the PKA activation constant determined *in vitro* at baseline concentrations it is uncertain. In the same way, it is questionable how PDE control the cAMP signalling compartmentation in situation of hormonal stimulation when concentrations of cAMP increases greatly [205]. In this sense, Koschinski *et al.* showed that the threshold for PKA activation in intact cells needs higher cAMP levels when compared to *in vitro* [204]. These authors demonstrated how PDE can maintain the concentrations of cAMP below the threshold for activation of PKA even at basal cAMP levels and promote the cAMP response compartmentation to hormonal stimulation when cAMP levels significantly increase [204]. Lastly, the different subcellular localization of PKA holoenzymes, mainly PKA regulatory subunits, seems to have an important function in the compartmentation of cAMP. Briefly, when the two catalytic subunits are released from the PKA holoenzyme, PKA-RI can become mainly cytosolic, and the PKA-RII can relate to particulate fraction [186]. Thus, it seems that depending on the ligand to which the PKA holoenzymes are bound to, it may be that the catalytic subunits are unable to diffuse within the cell but become constrained by spatial boundaries that cause the activation of local PKA substrates. Though, the catalytically active PKA holoenzymes can remain intact within the cytoplasm, indicating that the cAMP compartmentation is poorly understood [189,206].

In summary, all studies show the existence of subcellular cyclic nucleotide compartments in VSMC, demonstrating that PDE have a vital role in the compartmentation of cAMP, mostly the PDE4. Compartmentalized cAMP signalling needs coupling specific AC to GPCR isoforms that synthesize cAMP at different domains in the cell and bind to other effectors that together form signalosomes. AKAP are also involved in compartmentation of cAMP since they interact with proteins, such as GPCR, AC, PKA, PDE [40,157,175,188,199,207].

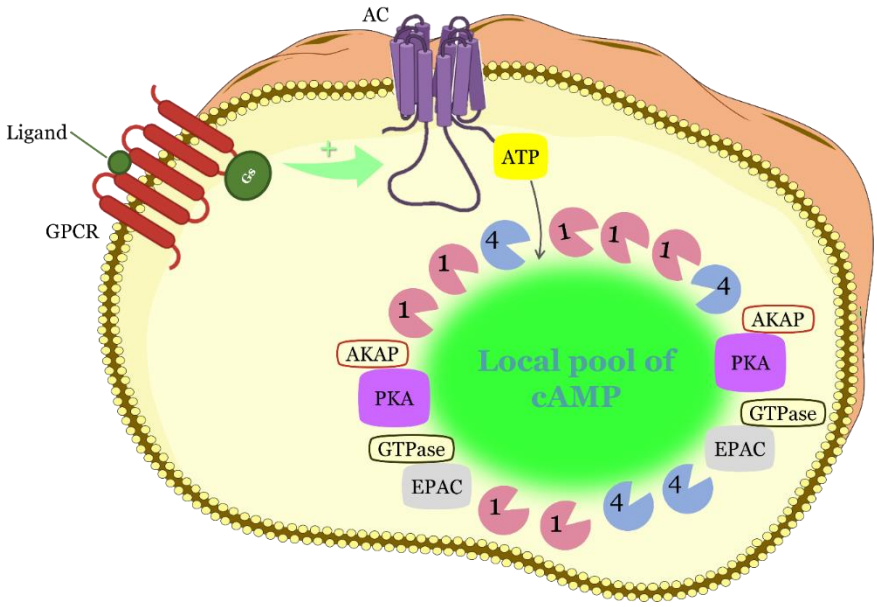

Figure 1.7. Schematic illustration of compartmentation of cAMP signalling in VSMC in a synthetic phenotype. Cyclic adenosine 3', 5'-monophosphate (cAMP) is produced from ATP by adenylyl cyclase (AC) upon activation of Gs-protein coupled receptors. The local concentration and distribution of cAMP gradients is controlled by phosphodiesterases (PDE) mainly PDE1 which generate localized pools of cAMP throughout the cell. Adapted from [14].

1.2.4.2. Compartmentalized cGMP signalling

cGMP signalling is involved in several cellular processes such as cell proliferation, differentiation, and contractility of vascular SMC [40,83]. In this sense, it is important to know the compartmentation of cGMP in VSM. One of the first indications of cGMP compartmentation was observed in the early 1990s in frog ventricular myocytes when cGMP from NO was found to be in both the soluble and the particulate fraction, while cGMP from the pGC was present only in the particulate fraction [208]. The data support the hypothesis that increase in cGMP induced by NP and NO donors can occur in different subcellular compartments [83,158,160,209]. Piggott *et al.* showed the cGMP compartmentation at the vascular level, and that PDE is not the only one involved in this phenomenon, demonstrating that actions of ANP and NO are also responsible for the functional compartmentation of cGMP signals. These authors observed that the relative increase in cGMP with NO-sGC stimulation is bigger than with NP-pGC [210]. In 2007, Cawley *et al.* using rat aorta SMC showed that NO donors caused transient increases in the concentration of GMP, and these results depend on the activity of sGC and PDE5 [211]. Nausch *et al.* performed studies using the cGMP-biosensor FincGs and showed the existence of subcellular cGMP compartments in rat aorta SMC, suggesting that the effects of NP and NO donors are differentially regulated by PDE5 [212].

As mentioned in section 1.2.3 (Phosphodiesterases), PDE3 hydrolyses both cAMP and cGMP. Nevertheless, the affinity is higher for cGMP hydrolysis, allowing that cGMP to act as a competitive inhibitor of cAMP hydrolysis [82]. In contrast, PDE5 is highly specific for cGMP [95,96]. Furthermore, Cairrao *et al.* performed studies with human umbilical artery smooth muscle cells

(HUASMC) using a whole-cell configuration of the patch-clamp technique and observed that ANP and testosterone stimulate potassium (K^+) current (I_K). This effect involves the large-conductance Ca^{2+}-activated K^+ channels (BK_{Ca}) and voltage-gated K^+ channels (K_V) activation through increasing cGMP levels and PKG activation. On the other hand, this study also demonstrated that activation of sGC with NO does not cause a stimulation of the I_K current, suggesting the existence of subcellular cGMP compartmentation in HUASMC [213]. Later, the same research group using CNG channels as cGMP biosensors demonstrated for the first time that cGMP is compartmentalized in human vascular muscle, and this compartmentation of cGMP is controlled by PDE3 and PDE5 [158]. Briefly, these data show differences in the spatiotemporal distribution of intracellular cGMP which depends on the activation of two cyclases (sGC and pGC) differently localized: 1) when pGC is activated by ANP, cGMP rises near the membrane; 2) when sGC is activated by NO donors (SNP), cGMP increases in the cytosol and also near the membrane. These suggest that when a cyclase is activated, besides its hydrosolubility, intracellular cGMP is not uniformly distributed within the cell and it is probably clustered in specific sites and found that PDE play a key role in this compartmentalization, because different PDE subtypes (PDE3 and PDE5) regulate particulate and cytosolic cGMP pools. In addition, PDE5 appears to control the particulate but not the soluble pool and the soluble cGMP pool is under the exclusive control of PDE3 [158].

In 2017, others research groups studied cGMP compartmentation in the vascular cells [40,214]. The results of Wilson *et al.* corroborate those observed by Feiteiro *et al.*, who demonstrated that the cGMP compartmentation was due to PDE5 and PDE3 [158,214]. In addition, this study also showed the existence of distinct pools of PDE5A in HUASMC that are believed to be able to control different events dependent on cGMP. Specifically, these authors observed that PDE5A is associated with an inositol-1,4,5-triphosfate (IP3) receptor complex that controls Ca^{2+} transients and that, in the cytosol, PDE5A can regulate cGMP-mediated inhibition of PDE3A [214]. In contrast, Liang Zhang *et al.* showed the cGMP compartmentation in cultured RASMC using the FRET-based cGMP sensor cGi-500 and they studied the short-and long-term modulation of the cGMP/PDE pathway in controlling vascular cell proliferation [40]. Pertaining to the short-term experiments, the basal activity of PDE1 did not influence on the intracellular concentration of cAMP but selectively controlled the intracellular concentration of cGMP produced by CNP. Ang II activates the PDE1 becoming active in the β-adrenoceptor-dependent cAMP pool and the NO-dependent cGMP pool. As a result, the PDE5 controls the cGMP levels independently of the activated GC isoform. Moreover, the authors demonstrate that the PDE9 has a key role at the vascular level and regulates the cGMP pool induced by NO. The long-term experiments show that: (I) the inhibition of PDE1 and PDE9 causes little but significant reductions in the proliferative effect of fetal bovine serum (FBS) in the absence of exogenous cGMP manipulation and (II) PDE5 controls the proliferation stimulated by FBS after cGMP stimuli. Hence, in VSMC the authors demonstrate that the cGMP pools from different origins differentially regulate cell proliferation [40].

In summary, all studies show the existence of subcellular cyclic nucleotide compartments in VSMC, thus demonstrating that PDE have a vital role in the compartmentation of cGMP, mainly the PDE1, PDE3, PDE5 and PDE9 [14,40,215]. In VSMC, the compartmentation cGMP signalling

appears to exist within two different compartments, one next to the membrane (pGC/cGMP controlled by PDE5 and PDE3) and the other in the inner of the cell (sGC/cGMP mainly controlled by PDE3) [158]. Moreover, cGMP compartmentalization may be regulated by the spatial location of PKG, PKA, and IP3 receptor complex. However, the role of other proteins such as myosin, NPR1, and tropomyosin that can act as PKG scaffolding proteins is not yet fully understood [199]. Figure 1.8 represents a schematic model of cGMP compartmentation in the vascular smooth muscle cells. However, the mechanism that causes the formation of these cGMP compartments in VSMC continues to be under intensive investigation.

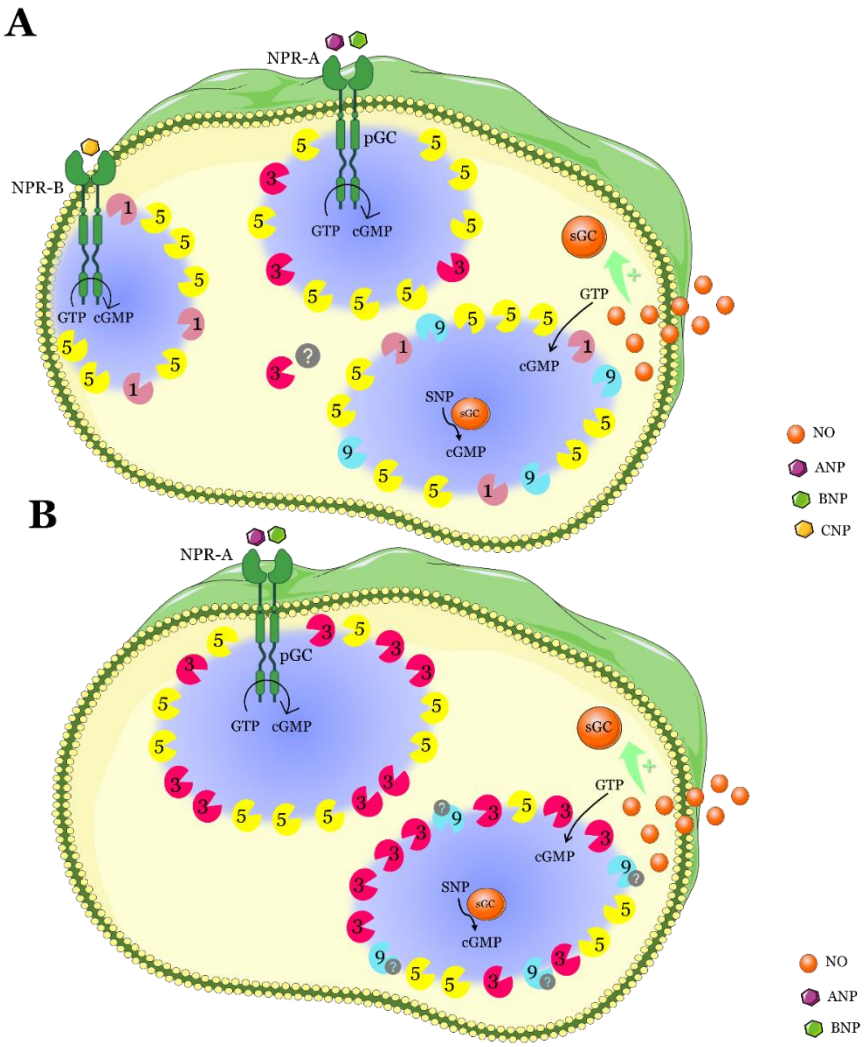

Figure 1.8. Schematic illustration of compartmentation of cGMP signalling in VSMC. **(A)** In a synthetic phenotype, activating natriuretic peptude receptors A and B leads to a pool of pGC/cGMP mainly controlled by PDE5. Moreover, activation of soluble guanylyl cyclases (sGC) by NO leads to a formation of cGMP in the intracelular medium also mainly controlled by PDE5. **(B)** In a contractile phenotype, activating natriuretic peptude receptors A leads a pool of pGC/cGMP controlled by PDE3 and PDE5. Activation of soluble guanylyl cyclases (sGC) by NO leads to a formation of cGMP in the intracelular medium also mainly controlled by PDE3. Adapted from [14].

1.3. Physiological regulation of vascular smooth muscle contractility and relaxation

Several extracellular signals, including neural, humoral, ionic, and mechanical forces induce contraction or relaxation of vascular smooth muscle (VSM). The main function of VSM is to maintain vascular tone by a balance between the cellular signalling pathways that mediate the generation of force (vasoconstriction) and the release of force (vasorelaxation), thereby regulating blood pressure and flow [2]. The signalling pathways that activate contraction include Ca^{2+}-dependent myosin light chain phosphorylation, whereas the signalling events that mediate relaxation include the removal of a contractile agonist (passive relaxation) and activation of cyclic nucleotide-dependent signalling pathways in the continued presence of a contractile agonist (active relaxation) [1].

1.3.1. Contraction of vascular smooth muscle

The contractile characteristics and the mechanisms that cause contraction of VSM are different from cardiac muscle. The contractions of VSM are slow, sustained and tonic while cardiac muscle contractions are rapid and short duration. VSM does not have the regulatory protein troponin (as it is found in the heart) but it contains actin and myosin [216,217]. Moreover, the organisation of actin and myosin in VSM is not arranged into distinct bands as it occurs in cardiac muscle. The VSM contractile proteins are highly organized and well-suited for their function in maintaining tonic contractions and reducing lumen diameter. VSMC contractile state is regulated by the autonomic nervous system, the hormonal system and local mediators of paracrine action. The contraction of VSMC can be initiated by mechanical, electrical, and chemical stimuli [1,218]. Myogenic response of VSM is related to the passive stretching of VSM that induces a contraction which is originated from the smooth muscle itself. The contraction induced by electrical depolarization of the VSM cell membrane involves the opening voltage-dependent calcium channels (L-type calcium channels), which causes an increase in the $[Ca^{2+}]_i$ [217,219-221]. Finally, several chemical stimuli (vasoactive substances, vasoconstrictors) such as histamine (His), serotonin (5-HT), norepinephrine, angiotensin II, vasopressin, endothelin-1, and thromboxane A_2 can cause contraction. Each of these substances binds to specific receptors on the VSMC (or to receptors on the endothelium adjacent to the VSM), which then leads to VSM contraction. The mechanism of contraction involves different signal transduction pathways [1,218].

1.3.1.1. Calcium-dependent pathway

VSMC contraction occurs via two interlinked pathways (calcium-dependent and -independent pathways) that contribute synergistically to the contractile properties of VSMC (Figure 1.9). Sidney Ringer, in 1882, was the first to recognize the relevance of calcium ion (Ca^{2+}). Sidney Ringer *et al.* discovered the necessity of Ca^{2+} for heart contraction and described its role during development of fertilized eggs and cell adhesion. These experiments showed, for the first time, the

role of Ca^{2+} in cell physiology [222-226]. This ion is the fifth most abundant element in the Earth's crust, and it is one of the most abundant ions in the human body. As an essential signalling molecule in cells, Ca^{2+} participates in regulating numerous important physiological activities in the human body, including the nervous system excitability, the contraction of muscles, the intestinal microbial activity, the activity of enzymes, and the biological clock [227-229]. The main factors that regulate Ca^{2+} signalling are the: cell type, cellular environment, stage of development, and cellular pathological changes. Under resting conditions, the concentration of Ca^{2+} in the cytoplasm and the extracellular medium is approximately 10^{-7} and 10^{-3} M, respectively [221]. The concentration of Ca^{2+} inside the cell is simultaneously regulated by multiple processes which can be divided into mechanisms that control its increase or mechanisms that control its decrease [11].

The calcium-dependent pathway is associated with increasing cytoplasmic calcium levels to induce phasic contraction. Increased intracellular Ca^{2+} can be triggered by mechanical, electrical, and chemical stimuli, either by Ca^{2+} influx from channels located on the plasma membrane or by the release of Ca^{2+} from the sarcoplasmic reticulum (SR) (Figure 1.9) [1,218]. Ca^{2+} entry from the extracellular space usually occurs via voltage gated calcium channels (VGCC) or non-selective cation channels. Among VSMC, the subtype of L-type, P/Q-type, and T-type VGCC are found, which are activated via plasma membrane depolarization [230,231]. Furthermore, non-selective cation channels, found to be mainly members of the transient receptor potential (TRP) ion channels, allowing for Na^{+} and Ca^{2+} influx upon receptor occupancy or capacitive Ca^{2+} entry [1,231]. The release of Ca^{2+} from the SR is primarily mediated by the activation of GPCRs (i.e., the Angiotensin II type 1 (AT1) receptors) coupled to the Gq [232,233]. The Gq protein, when in its GTP-bound state, induces activation of phospholipase C that hydrolyses phosphatidylinositol 4,5-bisphosphate (PIP2) into IP3 and diacylglycerol [234]. In turn, IP3 binds to the IP3 receptors present on the sarcolemma, which causes the opening of the calcium channels and consequent depletion of calcium intracellular store [1,231,235].

As already mentioned, instead of tropine, the smooth muscle has a high expression of CaM, another regulatory protein [236]. After an increase of cytoplasmic Ca^{2+} concentration has been established, CaM becomes bound by Ca^{2+} ions, causing a conformational change [236]. The resulting Ca^{2+}-calmodulin (Ca/CaM) complex interacts with and activates myosin light chain kinase (MLCK) [236]. Then, MLCK phosphorylates MLC-20 (also known as the myosin regulatory light chains) on the serine-19 and threonine-18 residues. The phosphorylation of serine-19 causes a resulting increase in the activity of the Mg^{2+}-ATPase and this effect is further enhanced by the phosphorylation of the threonine-18 residue [218,236]. This leads to the cross-bridge cycling to be initiated and the myosin head can actively pull on the thin filament of the actin to induce contraction of the smooth muscle [1,230].

1.3.1.2. Calcium-independent pathway

The MLC-20 light chain remains phosphorylated at a low level in the absence of external contractile stimuli, which leads to a slower tonic form of contraction that regulates the vascular tone. A calcium-independent pathway that involves Rho/Rho-associated protein kinase (ROCK)

signalling regulates VSMC tonic contractions (Figure 1.9) [230,237]. This pathway is involved in SMC contraction and cell migration, proliferation, and apoptosis. RhoA, part of the Ras superfamily (Ras homolog family member A) is a GTPase that can act as a molecular switch between a GTP/GDP-bound state [238,239]. Under resting conditions, the Rho GDP-dissociation inhibitor targets GDP-Rho for binding, as a means to localise the GTPase from the membrane to the cytosol. Though, the activation of GPCR receptors, in specific Gα12/13 subtypes, can catalyse GTP for GDP exchange in RhoA by binding to p115 Rho GTPase guanine nucleotide exchange factors [1,230]. One of the target proteins activated by RhoA is Rho-associated protein kinase (ROCK). This kinase belongs to the A, G and C (PKA/PKG/PKC) family of serine-threonine specific protein kinases. Two isoforms ROCK 1 and 2 are expressed in VSMC, and its structure is composed of an N-terminal kinase domain, a central coiled-coil domain and a C-terminal pleckstrin (PLEK) homology domain that associates with the Rho GTPase [240,241].

In VSMC, ROCK has several effects and affects actomyosin activity by two main pathways. Firstly, ROCK prevents actin filament depolymerisation through the active regulation of the cytoskeletal organisation. Secondly, ROCK inhibits MLCP., which is structurally composed of three subunits: a 37 kDa catalytic subunit; a variable subunit and a myosin-binding subunit [241-243]. The myosin-binding site is the key for MLCP regulation, and this protein is phosphorylated, specifically at residues: threonine-695/697 (major site); serine-849/854 and threonine-850/855 [244,245]. Phosphorylation prevents MLCP from regulating the MLC phosphorylation state and increases the basal phosphorylated MLC level, which leads to stimulation of VSMC contraction and increased vascular tone [1,243].

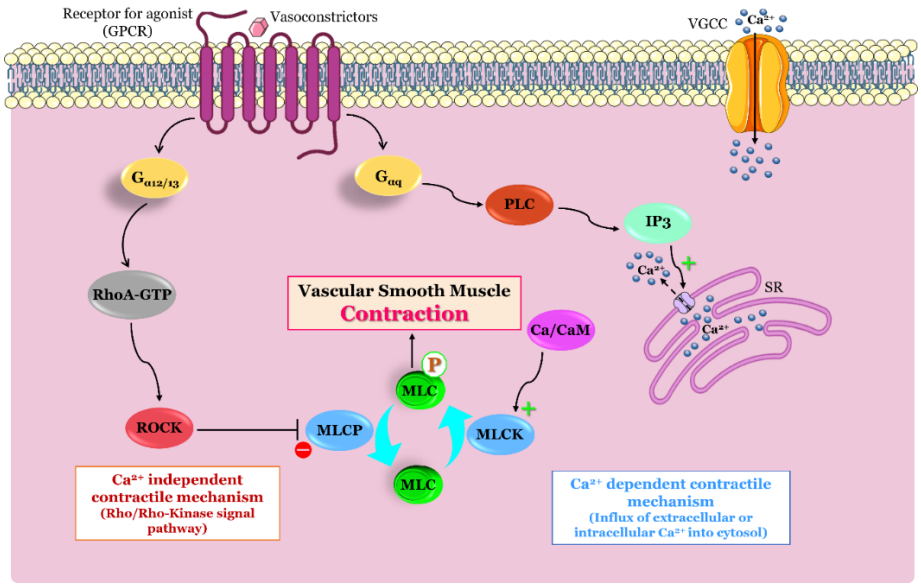

Figure 1.9. Schematic representation of calcium dependent and independent regulation of VSMC contraction. The two pathways work synergistically. Contractile activity in smooth muscle is determined primarily by the phosphorylation state of myosin light chain (MLC). Vasoconstrictors (such as norepinephrine, serotonin) bind to G protein-coupled receptors (GPCR) activating RhoA (RhoA-GTP) and phospholipase C (PLC) leading to lead to inositol 1,4,5 triphosphate (IP3) production. **Calcium-dependent contraction:** IP3 binding to its receptor in the sarcoplasmic reticulum (SR) leads to release of Ca^{2+}, increasing the cytosolic Ca^{2+} and Ca^{2+} entry from extracellular space via voltage-gated calcium channels (VGCC). Ca^{2+}/calmodulin (Ca/CaM) binds to and activates MLCK, which in turn phosphorylates MLC. **Calcium-independent contraction:** Activated RhoA binds to and activates ROCK, leading to phosphorylation and inhibition of MLCP, inhibiting MLC dephosphorylation.

1.3.2. Relaxation of vascular smooth muscle

Smooth muscle relaxation occurs due to the removal of the contractile stimulus or the direct action of a substance that stimulates inhibition of the contractile mechanisms (e.g., the atrial natriuretic factor is a vasodilator) [231,246]. Regardless, the mechanism of relaxation involves a decreased intracellular Ca^{2+} levels and increased activity of MLC phosphatase. The mechanisms that sequester or remove intracellular Ca^{2+} and/or increase MLC phosphatase activity may become altered, leading to abnormal responsiveness of smooth muscle (Figure 1.10) [218,247,248].

A decrease in the intracellular concentration of activator Ca^{2+} induces SMC relaxation. Several mechanisms are implicated in the removal of cytosolic Ca^{2+} and involve the SR and the plasma membrane [231]. In the SR, the uptake of Ca^{2+} is dependent on ATP hydrolysis. This SR Ca^{2+}, Mg-ATPase, when phosphorylated, binds two Ca^{2+} ions which are then translocated to the luminal side of the SR and released. Mg^{2+} is necessary for the activity of the enzyme; it binds to the catalytic site of the ATPase to mediate the reaction [249,250]. The plasma membrane also contains Ca^{2+} and Mg-ATPases, requiring another mechanism for reducing the level of activator Ca^{2+} in the cell. This enzyme is different from the sarcoplasmic reticular protein because it has an autoinhibitory domain that can be bound by CaM, inducing the plasma membrane Ca^{2+} pump stimulation. Na^{+}/Ca^{2+} exchangers (NCX) are also located on the plasma membrane and cause the decrease of intracellular Ca^{2+} [251-253].

Furthermore, several endogenous and exogenous compounds can also induce SM relaxation. Usually, the exogenous compounds reduce smooth muscle tone by several pathways, including blocking receptors that, when activated, cause contraction of smooth muscle and inhibit or activate enzymes or channels that are involved in contractility. Regarding endogenous compounds, there are agonists that activate receptors and generate intracellular messengers (i.e., cyclic nucleotides) that stimulate molecular mechanisms inducing arterial relaxation [218,231,254]. The main intracellular messengers involved in smooth muscle relaxation are the cyclic nucleotides, cAMP and cGMP. Under physiological conditions, the increase in intracellular concentration of cAMP and/or cGMP in vascular SMC is considered the main mechanism in the modulation of vasodilation. The increase of cGMP is performed through endogenous vasodilators, such as NO and NP, which have an especially important function in the control of vascular tone regulation [246,255,256]. In relation to the increase of cAMP, it is achieved by activation of GPCR coupled to a Gs protein or by inhibition of a receptor coupled to a Gi/o protein. Both cyclic nucleotides may still have their levels increased by inhibition of the PDE, which are enzymes that hydrolyse these nucleotides, so when these enzymes are activated the cAMP and cGMP levels decreased. This molecular mechanism is one of the fundamental areas of pharmacological study in the search for efficient vasodilators for use in pathologies such as hypertension [85,231,257]. The increase of cGMP and cAMP levels leads to the activation of the PKG and PKA, respectively, which in turn, decreases the intracellular Ca^{2+} concentrations and the sensitization of the myofilaments to Ca^{2+} in SMC, leading to relaxation. Currently, several mechanisms have already been proposed to explain how PKG and PKA induces vasodilation [75,248,256,258-261]:

1. Activation of Ca^{2+} uptake by the SERCA activation and by phosphorylation of phospholamban (PLB, is a phosphorylatable protein component of smooth muscle SR that reversibly inhibits the activity of the SERCA and SR Ca^{2+} transport).
2. Increased efflux of Ca^{2+}, through PMCA and NCX exchanger stimulation.
3. Inhibition of Ca^{2+} release from SR, through PKG-mediated phosphorylation of IP3 receptor and/or inhibition of IP3 synthesis.
4. Hyperpolarization of the smooth muscle cell membrane potential through direct or indirect activation of K^+ channels (such as K_v, BK_{Ca} or MaxiK, ATP-sensitive K^+ channels (K_{ATP}) and inward rectifier K^+ channels (K_{ir})).
5. Direct inhibition of VGCC, due to its dephosphorylation, through protein phosphatase 2A.
6. The reduction in the sensitivity of the contractile mechanism by decreasing the Ca^{2+} concentrations sensitivity of MLC20 phosphorylation due to a decrease of the myosin light-chain kinase activity and/or an increase of the MLCP activity.
7. Phosphorylation of MLC20, decreasing the affinity for the Ca/CaM complex
8. The PLC inhibition.

Normally, cGMP activates PKG, and cAMP activates PKA, but it can occur "cross-activation", a phenomenon whereby cAMP can activate PKG, and cGMP can activate PKA. Nevertheless, this phenomenon seems to have little relevance [248,256].

Changes in the activity of K^+ channels play the most prominent role in regulating the membrane potential and hence, vascular tone. Specifically, the activation of K^+ channels results in plasmalemmal K^+ efflux, membrane hyperpolarization, and reduced Ca^{2+} influx through VGCC, leading to vasorelaxation [231,262]. On the other hand, the activity of several types of K^+ channels, can be changed by different physiological factors, such as intracellular Ca^{2+}, cyclic nucleotides and different signal transduction mechanisms. Thus, the activation of K^+ channels can also be due to some vasoactive substances such as NO, NP and prostacyclins that promote the activation of kinase proteins [231,262]. These channels also seem to play a significant role in the variation of vascular tone observed in some pathologies, such as hypertension and heart failure [263,264].

The membrane potential is determined by membrane permeability to several ions, including chlorine ions (Cl^-). Cl^- channels can also regulate cytosolic Ca^{2+} levels in vascular SMC. Its inhibition causes a membrane hyperpolarization inducing the close of the VGCC and leads to VSMC vasorelaxation. However, the role of Cl^- channels in modulating membrane potential is low, due to the high density of K_{Ca} and its high conductance [219,221,264].

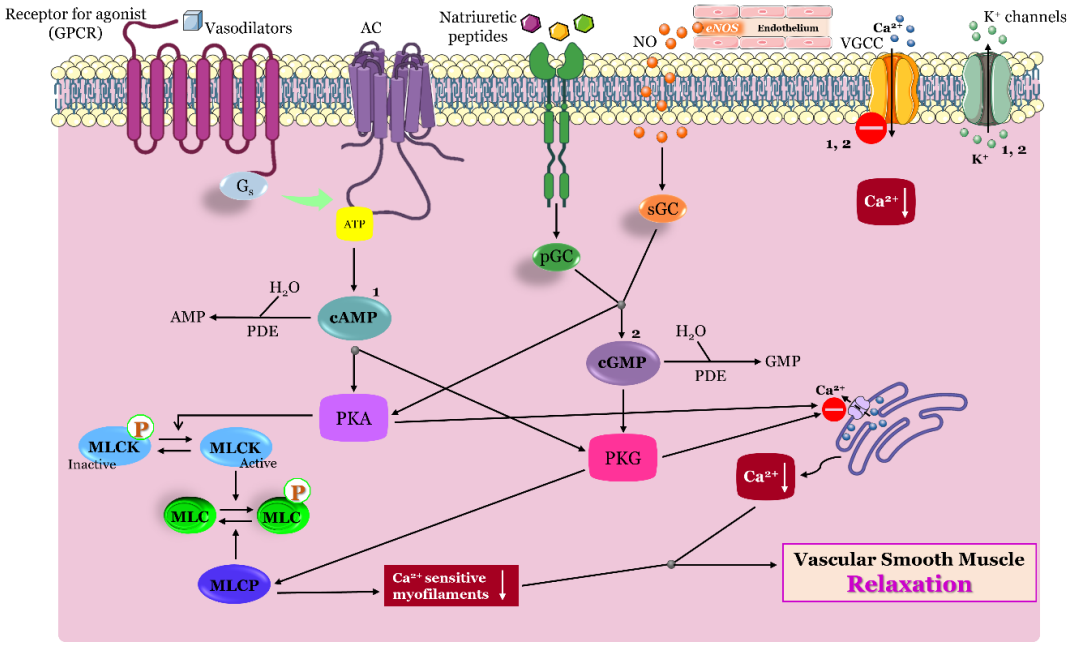

Figure 1.10. Schematic representation of VSMC relaxation. The process of relaxation requires a decreased intracellular calcium (Ca^{2+}) concentration and increased myosin light chain (MLC) phosphatase activity. The increase of cGMP is performed through endogenous vasodilators, such as nitric oxide (NO) and natriuretic peptide (NP). The increase of cAMP is achieved by activation of G protein-coupled receptors (GPCR) coupled to a Gs protein and adenylyl cyclase (Ac) activation. The increase of cGMP and cAMP levels activates the protein kinase G (PKG) and protein kinase A (PKA), respectively, leading to a decreased inhibition of Ca^{2+} release from the sarcoplasmic reticulum (SR), thus decreasing the intracellular Ca^{2+} concentrations and the sensitization of the myofilaments to Ca^{2+}. Both cyclic nucleotides have their levels increased by inhibition of the phosphodiesterases (PDE). During relaxation, voltage gated Ca^{2+} channels (VGCC) in plasma membrane close resulting in a reduced Ca^{2+} entry into the cell and the potassium (K^+) channels are activated.

1.4. Human Umbilical Cord

1.4.1. General characteristics of the human umbilical cord

The human umbilical cord (HUC), a vital organ to the growth and well-being of the foetus, besides, it is the most important structure of the fetoplacental unit, performing a primary role in determining how extrauterine life will begin. HUC is developed from the yolk sac and allantois, allowing communication between the developing embryo and the placenta, is 50-60 cm at term gestation and it is three blood vessels [265-267]. However, it may be larger or smaller. Too short umbilical cords may lead to a premature separation of the placenta from the uterus wall before or during delivery, while exceptionally long ones tend to prolapse and curl around the foetus forming knots [268,269]. Then, it is crucial to carry out a rigorous monitoring to avoid possible foetal hypoxia or anoxia [270]. Moreover, HUC is an extremely useful biological sample as a source of VSMC [271].

The HUC presents a helical shape (Figure 1.11), due to the typical spiral winding of your blood vessels [267,272,273]. These umbilical vessels are structurally and functionally different from the main vessels of the human body [272,273], and since the vessels are longer than the cord itself,

their twisting or flexing may happen [270,272]. HUC is very flexible and generally presents a whitish and shiny appearance, since it is enclosed by a simple epithelium derived from the amnion [265,274]. This embryonic attachment is mainly composed of a mucosal connective tissue, called Wharton's jelly, responsible for its gelatinous appearance [275]. The Wharton's jelly is composed of connective tissue cells dispersed in an amorphous surface matrix of glycosaminoglycans (hyaluronic acid and chondroitin sulphate) and distinct collagen types, presenting the peculiarity of not having *vasa vasorum* or *nervi vasorum*. This jelly also contains macrophages, fibroblasts dispersed, laminin and a fibrillar collagen network [276-278]. Moreover, this gelatinous substance surrounds the umbilical vessels, assuming the protective function and giving them flexibility. Due to its fibrous and porous content made from collagen and elastin fibres, the Wharton's jelly gives a certain firmness to the umbilical cord [266,279].

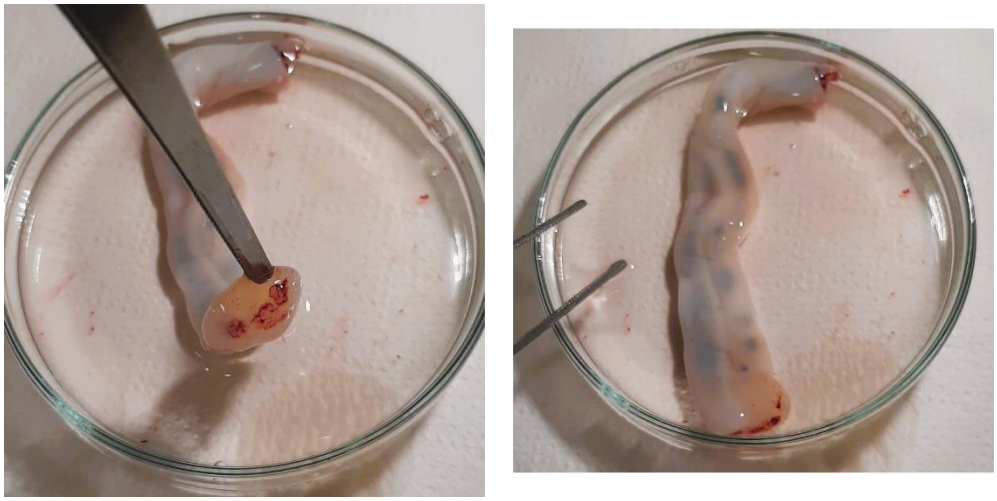

Figure 1.11. Representative photograph of the human umbilical cord (HUC).

Typically, the HUC has two arteries and a single vein, which are surrounded by Wharton's jelly and a single outer cell layer of amnion (Figure 1.11 and 1.12). However, HUC with only one artery have been observed and are usually associated with vascular complications for new-borns [280-282]. In fetoplacental circulation, the umbilical vein is the largest vessel responsible for transporting oxygen-rich blood to the foetus, while umbilical arteries are responsible for transporting oxygen-poor blood from the foetus to the placenta [267,274]. Usually, foetal blood does not mix with maternal blood, but lesser amounts of fetal blood may enter the maternal circulation through small defects that can form in the placental membrane. The HUA and vein have a similar structure, but the veins walls are thinner than the arterial walls. In addition, umbilical arteries are more easily identifiable, as their calibre is smaller (3 mm, Figure 1.13) in relation to veins (6 mm, Figure 1.14) [279,283].

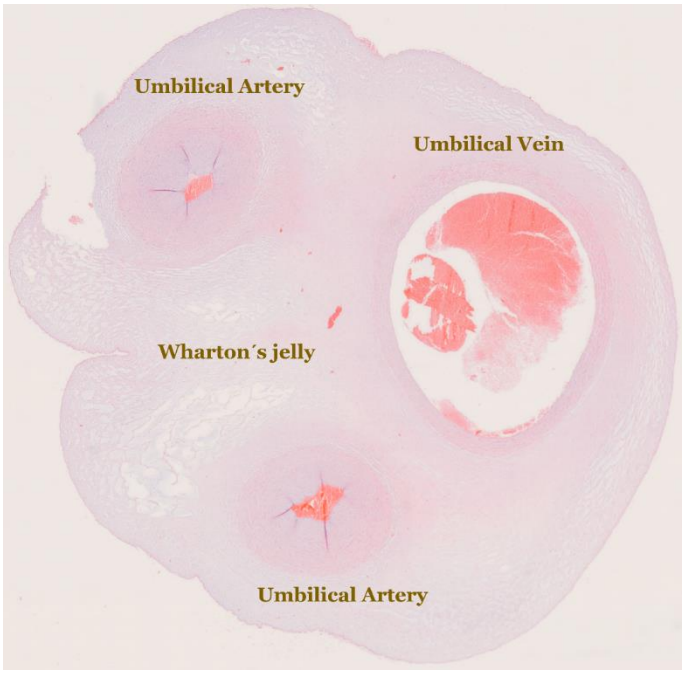

Figure 1.12. Transversal section of HUC. Two human umbilical arteries and one umbilical vein can be observed.

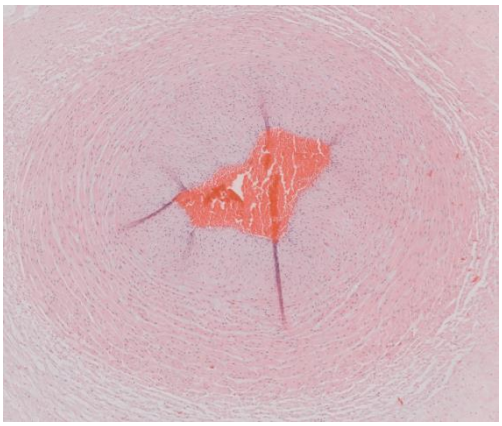

Figure 1.13. Transversal section of HUA with endothelium.

Figure 1.14. Transversal section of human umbilical vein.

1.4.2. Human Umbilical Artery (HUA)

The HUA is involved in fetoplacental circulation, and it is one of the vessels found in the human umbilical cord [282]. Through the HUA, this artery is easy to access. At present, the HUA is of foremost importance, since it is an exclusive and very useful source for several human vascular studies [158,284-286]. Physiologically, the HUA is a medium-calibre muscular artery (1 to 10 mm) whose walls are mostly made up of muscle fibres (Figure 1.13). This artery consists of three morphologically distinct tunics, which are (from the inside to the outside: the intima, media and adventitia) [267,282]. The tunica intima, or endothelium, is formed by a single layer of EC. The endothelial layer is a simple layer of endothelium that has no sub-endothelial layers or adjacent internal elastic lamina, leaving the endothelium in direct contact with the muscular layer [287,288]. Since the HUA does not have an internal elastic membrane, this artery has much less elasticity than other arteries. This layer has as main functions the regulation of vascular tone and the control of vascular permeability. The endothelium functions as a sensor of hemodynamic changes and signals or chemical stimuli from the bloodstream, and then transmits them to VSMC [4,274,288]. Regarding the tunica media, it has two layers of smooth muscle cells (an outer and an inner layer), fibres and proteoglycans. The outermost media layer is less defined than the innermost layer, and has a typical structure characterized by a circular arrangement, conferred by the SMC that are disposed of circularly. This layer responsible for arterial contractility leading to the physiological closure of the umbilical arteries [265,282,287]. In the innermost middle layer, most smooth muscle cells are disposed linearly or longitudinally (in relation to the artery axis) and dispersed (disordered) in an amorphous fundamental substance poor in elasticity but high in terms of plastic fibres [288]. This plasticity seems to be the mode of cooperation between the two layers, where the process of closing the umbilical arteries can be completed: the contraction of the muscle cells, arranged circularly, pushes the amorphous substance into the lumen of the artery, occluding it. Therefore, this plasticity of the innermost muscle layer seems to be responsible for the physiological occlusion of HUA in the postpartum period [282,287]. The major morphological difference between the smooth muscle cells of the two layers is that the cells of the outermost layer, unlike those of the innermost layer, are extraordinarily rich in myofilaments. These myofilaments are fibres that when grouped form the myofibril, which are composed by actin and myosin [12,282 ,288]. Lastly, the tunica adventitia (external tunica) is made up of fibroblasts and collagen and elastic fibres. In this tunic, the *vasa vasorum*, small muscular-type vessels that nourish it, and the *nervi vasorum*, which are nerve terminals, may also be present. The adventitia tunica does not have an internal limiting membrane, nor an external limiting membrane, becoming continuous in adjacent connective tissue, the Wharton's jelly [272,282].

HUA is involved in the fetoplacental circulation. Since HUA blood vessels are not innervated, the endocrine and paracrine mechanisms, which regulate the contractility phenotype of smooth muscle cells in the HUA, are essential for good gas and nutrient exchange between the foetus and placenta [12,267,272,282]. Thus, it is important to characterize the mechanisms that regulate vascular tone and to determine which factors regulate blood flow in the umbilical circulation [289-291]. In HUA, the vascular tonus is controlled by vasoactive substances, that can be locally released

or present in the circulation, such as prostaglandins, serotonin and histamine, or by substances transported by the blood stream and some ions such as Ca^{2+} and K^{+} [292-295].

1.4.3. Clinical and medical applications of human umbilical artery smooth muscle cells (HUASMC)

The HUASMC are isolated from HUC and are the most important structural component of this embryonic attachment [271]. HUASMC plays key role in the control of fetoplacental blood flow. Even though HUASMC are different from SMC in other systemic arteries, these cells are very particularly useful to study cellular mechanisms involved in the HUA tonus regulation. Vascular studies performed on HUASMC are crucial for the explanation of several signalling mechanisms involved in human vascular tonus control, such as Ca^{2+} metabolism and different pathways involved in modulating vascular reactivity. In addition, HUASMC are considered a useful model to study human cardiovascular endocrine disruption [158,284,286,291,296].

Gestational hypertension and pre-eclampsia are two of the main pathologies associated with pregnancy, affecting approximately 5-10% of pregnancies [297-301]. Nowadays, hypertensive disorders in pregnancy remain an important cause of maternofoetal morbidity and mortality worldwide [302,303]. Thus, it is crucial to know the mechanisms involved in the regulation of fetoplacental circulation in order to understand these pathologies [2,286,291]. As mentioned before, the HUA is devoid of nerve endings, then its regulation is achieved through local mediators (such as 5-HT and His) [292]. Some research suggested that receptors of 5-HT may be involved in contractile responses in preeclampsia and hypertension in pregnancy [304-306]. The levels of 5-HT in the placenta and plasma of women with preeclampsia were shown to be higher than in normal pregnant women, proposing the involvement of 5-HT in preeclampsia [305,307]. Additionally, the His increase is also involved in the development of hypertensive diseases, leading to an increase in the sensitivity/reactivity of the HUA to 5-HT and His, and consequently, to an increase in vascular resistance [307-309]. Other contractile agents, such as thromboxane or prostaglandin F2α (PGF2α) have also been associated with preeclampsia and gestational hypertension [310-312].

Increased HUA contractile activity can lead to decreased maternofoetal blood flow, which is a major cause of high intrauterine mortality. On the other hand, endothelial dysfunction may also be responsible for this decrease [313,314]. The increased release of vasodilator agents, such as NO has been associated with increased vascular resistance in some pathologies, such as preeclampsia and intrauterine growth restriction [315-318]. In fact, HUA has a low sensitivity to NO and, when NO levels increase, HUA cannot compensate for the pathological increase in vascular tone [317,319]. In addition, in pregnant women with preeclampsia and gestational hypertension, the HUA shows changes in the composition and metabolism [265,267,270,320]. Junek *et al.* described an increase in thickness of media and intima layers of HUA from hypertensive pregnant women [321]. In opposition, in a comparative study between normal pregnant women and those with chronic hypertension, it was observed a reduction of the luminal areas and the thickness of the walls of arteries and veins from the HUC [322]. Although these divisive studies, both suggested that

gestational hypertension is associated with a change in the structure and composition of umbilical cord blood vessels [321-324].

Ionic channels also play a crucial role in contractile regulation of SMC, and consequently for the vascular tonus control. Thus, due to its importance, it is crucial to understand its molecular composition, activity and expression. This concern is important when talking about hypertensive disorders in pregnancy, since alterations in the expression and function of HUASMC ion channels, mainly Ca^{2+} channels, which have already been described [295,325]. The activity of Ca^{2+} channels has been associated with hypertension and other cardiovascular diseases. Some studies demonstrated that VGCC L-type expression increased in hypertensive rats when compared to normotensive rats. In addition, the authors showed that this increased VGCC expression was related to an increase in Ca^{2+} currents [325-328]. Furthermore, in animals with hypertension, the increase of Ca^{2+} channels was associated with the number of open functional Ca^{2+} channels and not the possibility that the channel properties are changed is not posed [327,328]. In hypertensive VSMC, changes in the properties and functions of K^+ channels were also observed [295,329-331]. Regarding the K_v, it has been observed that changes in the function of these channels lead to vasoconstriction that, through modifications in cellular mechanisms, can lead to hypertension. Using the mesenteric arteries of hypertensive animals, studies have demonstrated that the expression of α-subunit gene and protein of these channels were increased [331-333]. In addition, in hypertensive VSMC, it was found that the K_v currents were smaller than in BK_{Ca} [327,332], and this decrease in K_v currents was mainly regulated by the intracellular Ca^{2+} (Cox 2005). Electrophysiological studies have shown that this ion may lead to a decrease in the regulation of Kv channels during hypertension, since an increase in the protein expression was associated with a decrease in their functionality [295,327,332]. The BK_{Ca} channels are important in the control of vascular tone and blood pressure. These channels mediate membrane hyperpolarization in response to elevations of intracellular Ca^{2+} and thus counteract the contractility of smooth muscle [334]. So, the expression of the BK_{Ca} channels during hypertension is also increased [329]. Studies performed on cerebral arteries of hypertensive rats have shown that there is a decrease in the activity of these channels when the expression of BK_{Ca} β_1-subunit is decreased. Though, changes in the α-subunit were not observed. These studies suggest that, although α-subunit can function separately, it is the β_1-subunit that causes the α-subunit to be more sensitive to intracellular Ca^{2+} [335-337]. A deletion of BK_{Ca} β_1-subunit leads to a decrease in Ca^{2+} sensitization, causing the channel to stop responding to Ca^{2+} sparks [337,338]. Consequently, this process induces membrane depolarization and an increase in intracellular Ca^{2+}, followed by vasoconstriction and increased blood pressure, leading to hypertension [260]. Eichhorn *et al.* showed an increase in Ca^{2+} flux and BK_{Ca} activity in SMC of different hypertensive animals. However, these authors achieved different results from other authors as they observed increased expression for both subunits (α and β) of BK_{Ca} [339]. In addition, the authors observed that inhibition of these channels by specific inhibitors caused membrane depolarization and consequent vasoconstriction [339]. On the other hand, it has also been suggested that changes in the channel conformation or sensitization to Ca^{2+} may lead them to act as pure K_V [260]. Similarly, to K_v, the mechanism responsible for the currents of BK_{Ca} channels during hypertension also appears to occur as negative feedback: the protein expression of

the channels seems to increase in response to an increase in the vascular tonus [219,327]. Furthermore, the expression or function of KIR channels is decreased in hypertension [329].

Although most studies find that contractile agents (His and 5-HT) and ion channels (Ca^{2+} and K^{+}) are the main key to the development of hypertensive disorders in pregnancy, there are also other crucial factors in the progress of these pathologies, such as Mg^{2+}. Mg^{2+} is also particularly important for the HUASMC regulation. Variations in the extracellular Mg^{2+} levels can influence the membrane transport of various ions, such as Ca^{2+}, Na^{+} and K^{+}, acting as a modulator of SMC proliferation and fibrosis, which are characteristics of hypertension [340-342]. On the other hand, in preeclampsia, a decrease in the vascular relaxation of HUA smooth muscle, associated with low levels of cAMP in HUASMC, was observed. Moreover, a reduced number of β-adrenergic receptors was also observed, suggesting that HUA may be less responsive to several drugs, which can be responsible, in part, for the development of preeclampsia [343]. Furthermore, sGC protein also appears to be involved in preeclampsia and gestational hypertension. This protein may play a function in the pathogenesis of hypertension, particularly in the expression of its β2-subunit [18,62,344-346]. Ruetten *et al*. have observed that sGC mRNA levels and protein expression in aorta of hypertensive mice are lower when compared to normotensive rats [347]. In addition, both α_1- and β_1-subunit expression were decreased in hypertensive rats, suggesting that the low levels of sGC may contribute to the development of hypertension [347,348].

In HUASMC regulation, ROCK plays an important function. In studies performed in hypertensives and normotensive rats, the ROCK inhibitor, Y27, significantly decreased blood pressure in hypertensive rats, but in normotensive rats only a small decrease was observed, suggesting that Rho/ROCK pathway is involved in the regulation of blood pressure *in vivo* and, therefore, may be a good pharmacological target for the treatment of hypertension [349,350]. Other authors also observed that RhoA mRNA is downregulated in total HUA vessels from women with preeclampsia when compared to pregnant women without hypertensive diseases [351-353].

Taken together, this observation suggested that the knowledge of the exact mechanisms that regulate the contractile state or vascular tone of HUA is fundamental to detect potential targets for the treatment of pathologies during pregnancy, such as preeclampsia and gestational hypertension [284,298,355,356]. These pathologies are multifactorial disorders, being a part of the main risk factors for cardiovascular complications. In addition, these disorders threaten not only the health of the mother but also of the foetus [286,291].

1.5. References

1. Ahmed, S.; Warren, D.T. Vascular smooth muscle cell contractile function and mechanotransduction. *Vessel Plus* **2018**, *2*, 36.

2. Worssam, M.D.; Jorgensen, H.F. Mechanisms of vascular smooth muscle cell investment and phenotypic diversification in vascular diseases. *Biochem Soc Trans* **2021**, *49*, 2101-2111.

3. Lucie Bacakova, M.T., Elena Filova, Roman Matějka, Jana Stepanovska, Jana Musilkova, Jana Zarubova and Martin Molitor. The Role of Vascular Smooth Muscle Cells in the Physiology and Pathophysiology of Blood Vessels. In *Muscle Cell and Tissue*, Sakuma, K., Ed.; October 10th, 2018: 2018; p. 370.

4. Feletou, M. The Endothelium: Multiple Functions of the Endothelial Cells—Focus on Endothelium-Derived Vasoactive Mediators. In *The Endothelium: Part 1: Multiple Functions of the Endothelial Cells-Focus on Endothelium-Derived Vasoactive Mediators*; Integrated Systems Physiology: from Molecule to Function to Disease; San Rafael (CA), 2011.

5. Wang, G.; Jacquet, L.; Karamariti, E.; Xu, Q. Origin and differentiation of vascular smooth muscle cells. *J Physiol* **2015**, *593*, 3013-3030.

6. Mahajan, W.D.T.Y.A.K. *Anatomy, Blood Vessels*; StatPearls Publishing: Treasure Island (FL), 2022.

7. Tsamis, A.; Krawiec, J.T.; Vorp, D.A. Elastin and collagen fibre microstructure of the human aorta in ageing and disease: a review. *J R Soc Interface* **2013**, *10*, 20121004.

8. Wilson, D.P. *Mechanisms of Vascular Disease: A Reference Book for Vascular Specialists*; Robert Fitridge, M.T., Ed.; BARR SMITH PRESS: The University of Adelaide, 2011.

9. Rensen, S.S.; Doevendans, P.A.; van Eys, G.J. Regulation and characteristics of vascular smooth muscle cell phenotypic diversity. *Neth Heart J* **2007**, *15*, 100-108.

10. Trillhaase, A.; Maertens, M.; Aherrahrou, Z.; Erdmann, J. Induced Pluripotent Stem Cells (iPSCs) in Vascular Research: from Two- to Three-Dimensional Organoids. *Stem Cell Rev Rep* **2021**, *17*, 1741-1753.

11. Touyz, R.M.; Alves-Lopes, R.; Rios, F.J.; Camargo, L.L.; Anagnostopoulou, A.; Arner, A.; Montezano, A.C. Vascular smooth muscle contraction in hypertension. *Cardiovasc Res* **2018**, *114*, 529-539.

12. Fisher, S.A. Vascular smooth muscle phenotypic diversity and function. *Physiol Genomics* **2010**, *42A*, 169-187.

13. Saleh Al-Shehabi, T.; Iratni, R.; Eid, A.H. Anti-atherosclerotic plants which modulate the phenotype of vascular smooth muscle cells. *Phytomedicine* **2016**, *23*, 1068-1081.

14. Lorigo, M.; Oliveira, N.; Cairrao, E. PDE-Mediated Cyclic Nucleotide Compartmentation in Vascular Smooth Muscle Cells: From Basic to a Clinical Perspective. *J Cardiovasc Dev Dis* **2021**, *9*.

15. Essayan, D.M. Cyclic nucleotide phosphodiesterases. *J Allergy Clin Immunol* **2001**, *108*, 671-680.

16. Holland, N.A.; Francisco, J.T.; Johnson, S.C.; Morgan, J.S.; Dennis, T.J.; Gadireddy, N.R.; Tulis, D.A. Cyclic Nucleotide-Directed Protein Kinases in Cardiovascular Inflammation and Growth. *J Cardiovasc Dev Dis* **2018**, *5*.

17. Khannpnavar, B.; Mehta, V.; Qi, C.; Korkhov, V. Structure and function of adenylyl cyclases, key enzymes in cellular signaling. *Curr Opin Struct Biol* **2020**, *63*, 34-41.

18. Krumenacker, J.S.; Hanafy, K.A.; Murad, F. Regulation of nitric oxide and soluble guanylyl cyclase. *Brain Research Bulletin* **2004**, *62*, 505-515.

19. Zhou, Z.; Martin, E.; Sharina, I.; Esposito, I.; Szabo, C.; Bucci, M.; Cirino, G.; Papapetropoulos, A. Regulation of soluble guanylyl cyclase redox state by hydrogen sulfide. *Pharmacol Res* **2016**, *111*, 556-562.

20. Calamera, G.; Moltzau, L.R.; Levy, F.O.; Andressen, K.W. Phosphodiesterases and Compartmentation of cAMP and cGMP Signaling in Regulation of Cardiac Contractility in Normal and Failing Hearts. *Int J Mol Sci* **2022**, *23*.

21. Sutherland, E.W.; Rall, T.W. Fractionation and characterization of a cyclic adenine ribonucleotide formed by tissue particles. *J Biol Chem* **1958**, *232*, 1077-1091.

22. Amunjela, J.N.; Swan, A.H.; Brand, T. The Role of the Popeye Domain Containing Gene Family in Organ Homeostasis. *Cells* **2019**, *8*.

23. Manoury, B.; Idres, S.; Leblais, V.; Fischmeister, R. Ion channels as effectors of cyclic nucleotide pathways: Functional relevance for arterial tone regulation. *Pharmacol Ther* **2020**, *209*, 107499.

24. Jaggupilli, A.; Dhanaraj, P.; Pritchard, A.; Sorensen, J.L.; Dakshinamurti, S.; Chelikani, P. Study of adenylyl cyclase-GalphaS interactions and identification of novel AC ligands. *Mol Cell Biochem* **2018**, *446*, 63-72.

25. Steegborn, C. Structure, mechanism, and regulation of soluble adenylyl cyclases - similarities and differences to transmembrane adenylyl cyclases. *Biochim Biophys Acta* **2014**, *1842*, 2535-2547.

26. Dessauer, C.W.; Watts, V.J.; Ostrom, R.S.; Conti, M.; Dove, S.; Seifert, R. International Union of Basic and Clinical Pharmacology. CI. Structures and Small Molecule Modulators of Mammalian Adenylyl Cyclases. *Pharmacol Rev* **2017**, *69*, 93-139.

27. Dove, S. Mammalian Nucleotidyl Cyclases and Their Nucleotide Binding Sites. *Handb Exp Pharmacol* **2017**, *238*, 49-66.

28. Halls, M.L.; Cooper, D.M.F. Adenylyl cyclase signalling complexes - Pharmacological challenges and opportunities. *Pharmacol Ther* **2017**, *172*, 171-180.

29. Marganski, W.A.; Gangopadhyay, S.S.; Je, H.D.; Gallant, C.; Morgan, K.G. Targeting of a novel Ca+2/calmodulin-dependent protein kinase II is essential for extracellular signal-regulated kinase-mediated signaling in differentiated smooth muscle cells. *Circ Res* **2005**, *97*, 541-549.

30. Bassler, J.; Schultz, J.E.; Lupas, A.N. Adenylate cyclases: Receivers, transducers, and generators of signals. *Cell Signal* **2018**, *46*, 135-144.

31. Takei, Y. Evolution of the membrane/particulate guanylyl cyclase: From physicochemical sensors to hormone receptors. *Gen Comp Endocrinol* **2022**, *315*, 113797.

32. Soberg, K.; Skalhegg, B.S. The Molecular Basis for Specificity at the Level of the Protein Kinase a Catalytic Subunit. *Front Endocrinol (Lausanne)* **2018**, *9*, 538.

33. Kim, C.; Sharma, R. Cyclic nucleotide selectivity of protein kinase G isozymes. *Protein Sci* **2021**, *30*, 316-327.

34. Hogarth, D.K.; Sandbo, N.; Taurin, S.; Kolenko, V.; Miano, J.M.; Dulin, N.O. Dual role of PKA in phenotypic modulation of vascular smooth muscle cells by extracellular ATP. *Am J Physiol Cell Physiol* **2004**, *287*, C449-456.

35. Yan, Y.; Zhou, X.E.; Xu, H.E.; Melcher, K. Structure and Physiological Regulation of AMPK. *Int J Mol Sci* **2018**, *19*.

36. Dyla, M.; Kjaergaard, M. Intrinsic disorder in protein kinase A anchoring proteins signaling complexes. *Prog Mol Biol Transl Sci* **2021**, *183*, 271-294.

37. Soberg, K.; Jahnsen, T.; Rognes, T.; Skalhegg, B.S.; Laerdahl, J.K. Evolutionary paths of the cAMP-dependent protein kinase (PKA) catalytic subunits. *PLoS One* **2013**, *8*, e60935.

38. Raslan, Z.; Aburima, A.; Naseem, K.M. The Spatiotemporal Regulation of cAMP Signaling in Blood Platelets-Old Friends and New Players. *Front Pharmacol* **2015**, *6*, 266.

39. Turnham, R.E.; Scott, J.D. Protein kinase A catalytic subunit isoform PRKACA; History, function and physiology. *Gene* **2016**, *577*, 101-108.

40. Zhang, L.; Bouadjel, K.; Manoury, B.; Vandecasteele, G.; Fischmeister, R.; Leblais, V. Cyclic nucleotide signalling compartmentation by PDEs in cultured vascular smooth muscle cells. *Br J Pharmacol* **2019**, *176*, 1780-1792.

41. Beuschlein, F.; Fassnacht, M.; Assie, G.; Calebiro, D.; Stratakis, C.A.; Osswald, A.; Ronchi, C.L.; Wieland, T.; Sbiera, S.; Faucz, F.R.; et al. Constitutive activation of PKA catalytic subunit in adrenal Cushing's syndrome. *N Engl J Med* **2014**, *370*, 1019-1028.

42. Lackey, B.R.; Gray, S.L. Identification of kinases, phosphatases, and phosphorylation sites in human and porcine spermatozoa. *Syst Biol Reprod Med* **2015**, *61*, 345-352.

43. Metrich, M.; Berthouze, M.; Morel, E.; Crozatier, B.; Gomez, A.M.; Lezoualc'h, F. Role of the cAMP-binding protein Epac in cardiovascular physiology and pathophysiology. *Pflugers Arch* **2010**, *459*, 535-546.

44. Wehbe, N.; Nasser, S.A.; Al-Dhaheri, Y.; Iratni, R.; Bitto, A.; El-Yazbi, A.F.; Badran, A.; Kobeissy, F.; Baydoun, E.; Eid, A.H. EPAC in Vascular Smooth Muscle Cells. *Int J Mol Sci* **2020**, *21*.

45. Leung, Y.K.; Du, J.; Huang, Y.; Yao, X. Cyclic nucleotide-gated channels contribute to thromboxane A2-induced contraction of rat small mesenteric arteries. *PLoS One* **2010**, *5*, e11098.

46. Biel, M., Michalakis, S. Cyclic Nucleotide-Regulated Cation Channels. In *Handbook of Cell Signaling* Munich Center for Integrated Protein Science CIPSM and Department of Pharmacy, Center for Drug Research, Ludwig-Maximilians-Universität München, Munich, Germany, 2010; Volume Second Edition, pp. 1519-1523.

47. Desch, M.; Schinner, E.; Kees, F.; Hofmann, F.; Seifert, R.; Schlossmann, J. Cyclic cytidine 3',5'-monophosphate (cCMP) signals via cGMP kinase I. *FEBS Lett* **2010**, *584*, 3979-3984.

48. Tulis, D.A. Novel therapies for cyclic GMP control of vascular smooth muscle growth. *Am J Ther* **2008**, *15*, 551-564.

49. Potter, L.R. Natriuretic peptide metabolism, clearance and degradation. *FEBS J* **2011**, *278*, 1808-1817.

50. Evgenov, O.V.; Pacher, P.; Schmidt, P.M.; Hasko, G.; Schmidt, H.H.; Stasch, J.P. NO-independent stimulators and activators of soluble guanylate cyclase: discovery and therapeutic potential. *Nat Rev Drug Discov* **2006**, *5*, 755-768.

51. Ahmed, W.S.; Geethakumari, A.M.; Biswas, K.H. Phosphodiesterase 5 (PDE5): Structure-function regulation and therapeutic applications of inhibitors. *Biomed Pharmacother* **2021**, *134*, 111128.

52. Ruhr, I.M.; Takei, Y.; Grosell, M. The role of the rectum in osmoregulation and the potential effect of renoguanylin on SLC26a6 transport activity in the Gulf toadfish (Opsanus beta). *Am J Physiol Regul Integr Comp Physiol* **2016**, *311*, R179-191.

53. Mishra, V.; Goel, R.; Visweswariah, S.S. The regulatory role of the kinase-homology domain in receptor guanylyl cyclases: nothing 'pseudo' about it! *Biochem Soc Trans* **2018**, *46*, 1729-1742.

54. Kobialka, M.; Gorczyca, W.A. Particulate guanylyl cyclases: multiple mechanisms of activation. *Acta Biochim Pol* **2000**, *47*, 517-528.

55. Chen, Y.; Burnett, J.C. Particulate Guanylyl Cyclase A/cGMP Signaling Pathway in the Kidney: Physiologic and Therapeutic Indications. *Int J Mol Sci* **2018**, *19*.

56. Kuhn, M. Molecular Physiology of Membrane Guanylyl Cyclase Receptors. *Physiol Rev* **2016**, *96*, 751-804.

57. Rahmutula, D.; Nakayama, T.; Soma, M.; Kosuge, K.; Aoi, N.; Izumi, Y.; Kanmatsuse, K.; Ozawa, Y. Structure and polymorphisms of the human natriuretic peptide receptor C gene. *Endocrine* **2002**, *17*, 85-90.

58. Goetze, J.P.; Bruneau, B.G.; Ramos, H.R.; Ogawa, T.; de Bold, M.K.; de Bold, A.J. Cardiac natriuretic peptides. *Nat Rev Cardiol* **2020**, *17*, 698-717.

59. Sellitti, D.F.; Koles, N.; Mendonca, M.C. Regulation of C-type natriuretic peptide expression. *Peptides* **2011**, *32*, 1964-1971.

60. Yamamoto, K.; Burnett, J.C., Jr.; Jougasaki, M.; Nishimura, R.A.; Bailey, K.R.; Saito, Y.; Nakao, K.; Redfield, M.M. Superiority of brain natriuretic peptide as a hormonal marker of ventricular systolic and diastolic dysfunction and ventricular hypertrophy. *Hypertension* **1996**, *28*, 988-994.

61. Meyer, T.; Herrmann-Lingen, C. Natriuretic Peptides in Anxiety and Panic Disorder. *Vitam Horm* **2017**, *103*, 131-145.

62. Derbyshire, E.R.; Marletta, M.A. Structure and regulation of soluble guanylate cyclase. *Annu Rev Biochem* **2012**, *81*, 533-559.

63. Boon, E.M.; Marletta, M.A. Ligand discrimination in soluble guanylate cyclase and the H-NOX family of heme sensor proteins. *Curr Opin Chem Biol* **2005**, *9*, 441-446.

64. Horst, B.G.; Yokom, A.L.; Rosenberg, D.J.; Morris, K.L.; Hammel, M.; Hurley, J.H.; Marletta, M.A. Allosteric activation of the nitric oxide receptor soluble guanylate cyclase mapped by cryo-electron microscopy. *Elife* **2019**, *8*.

65. Kang, Y.; Liu, R.; Wu, J.X.; Chen, L. Structural insights into the mechanism of human soluble guanylate cyclase. *Nature* **2019**, *574*, 206-210.

66. Montfort, W.R.; Wales, J.A.; Weichsel, A. Structure and Activation of Soluble Guanylyl Cyclase, the Nitric Oxide Sensor. *Antioxid Redox Signal* **2017**, *26*, 107-121.

67. Liu, R.; Kang, Y.; Chen, L. Activation mechanism of human soluble guanylate cyclase by stimulators and activators. *Nat Commun* **2021**, *12*, 5492.

68. Daff, S. NO synthase: structures and mechanisms. *Nitric Oxide* **2010**, *23*, 1-11.

69. Infante, T.; Costa, D.; Napoli, C. Novel Insights Regarding Nitric Oxide and Cardiovascular Diseases. *Angiology* **2021**, *72*, 411-425.

70. Farah, C.; Michel, L.Y.M.; Balligand, J.L. Nitric oxide signalling in cardiovascular health and disease. *Nat Rev Cardiol* **2018**, *15*, 292-316.

71. Horst, B.G.; Marletta, M.A. Physiological activation and deactivation of soluble guanylate cyclase. *Nitric Oxide* **2018**, *77*, 65-74.

72. Lincoln, T.M.; Dey, N.; Sellak, H. Invited review: cGMP-dependent protein kinase signaling mechanisms in smooth muscle: from the regulation of tone to gene expression. *J Appl Physiol (1985)* **2001**, *91*, 1421-1430.

73. Hofmann, F. The biology of cyclic GMP-dependent protein kinases. *J Biol Chem* **2005**, *280*, 1-4.

74. Hofmann, F.; Feil, R.; Kleppisch, T.; Schlossmann, J. Function of cGMP-dependent protein kinases as revealed by gene deletion. *Physiol Rev* **2006**, *86*, 1-23.

75. Feil, R.; Lohmann, S.M.; de Jonge, H.; Walter, U.; Hofmann, F. Cyclic GMP-dependent protein kinases and the cardiovascular system: insights from genetically modified mice. *Circ Res* **2003**, *93*, 907-916.

76. Kim, J.J.; Lorenz, R.; Arold, S.T.; Reger, A.S.; Sankaran, B.; Casteel, D.E.; Herberg, F.W.; Kim, C. Crystal Structure of PKG I:cGMP Complex Reveals a cGMP-Mediated Dimeric Interface that Facilitates cGMP-Induced Activation. *Structure* **2016**, *24*, 710-720.

77. Baker, D.A.; Drought, L.G.; Flueck, C.; Nofal, S.D.; Patel, A.; Penzo, M.; Walker, E.M. Cyclic nucleotide signalling in malaria parasites. *Open Biol* **2017**, *7*.

78. Maryam, A.; Khalid, R.R.; Vedithi, S.C.; Ece, A.; Cinaroglu, S.S.; Siddiqi, A.R.; Blundell, T.L. Exploring the structural basis of conformational heterogeneity and autoinhibition of human cGMP-specific protein kinase Ialpha through computational modelling and molecular dynamics simulations. *Comput Struct Biotechnol J* **2020**, *18*, 1625-1638.

79. Cheng, K.T.; Chan, F.L.; Huang, Y.; Chan, W.Y.; Yao, X. Expression of olfactory-type cyclic nucleotide-gated channel (CNGA2) in vascular tissues. *Histochem Cell Biol* **2003**, *120*, 475-481.

80. Podda, M.V.; Grassi, C. New perspectives in cyclic nucleotide-mediated functions in the CNS: the emerging role of cyclic nucleotide-gated (CNG) channels. *Pflugers Arch* **2014**, *466*, 1241-1257.

81. Feil, R.; Lehners, M.; Stehle, D.; Feil, S. Visualising and understanding cGMP signals in the cardiovascular system. *Br J Pharmacol* **2022**, *179*, 2394-2412.

82. Lugnier, C. Cyclic nucleotide phosphodiesterase (PDE) superfamily: a new target for the development of specific therapeutic agents. *Pharmacol Ther* **2006**, *109*, 366-398.

83. Bork, N.I.; Nikolaev, V.O. cGMP Signaling in the Cardiovascular System-The Role of Compartmentation and Its Live Cell Imaging. *Int J Mol Sci* **2018**, *19*.

84. Rybalkin, S.D.; Yan, C.; Bornfeldt, K.E.; Beavo, J.A. Cyclic GMP phosphodiesterases and regulation of smooth muscle function. *Circ Res* **2003**, *93*, 280-291.

85. Omori, K.; Kotera, J. Overview of PDEs and their regulation. *Circ Res* **2007**, *100*, 309-327.

86. Maurice, D.H.; Ke, H.; Ahmad, F.; Wang, Y.; Chung, J.; Manganiello, V.C. Advances in targeting cyclic nucleotide phosphodiesterases. *Nat Rev Drug Discov* **2014**, *13*, 290-314.

87. Francis, S.H.; Turko, I.V.; Corbin, J.D. Cyclic nucleotide phosphodiesterases: relating structure and function. *Prog Nucleic Acid Res Mol Biol* **2001**, *65*, 1-52.

88. Bender, A.T.; Beavo, J.A. Cyclic nucleotide phosphodiesterases: molecular regulation to clinical use. *Pharmacol Rev* **2006**, *58*, 488-520.

89. Aravind, L.; Koonin, E.V. The HD domain defines a new superfamily of metal-dependent phosphohydrolases. *Trends Biochem Sci* **1998**, *23*, 469-472.

90. Finn, R.D.; Tate, J.; Mistry, J.; Coggill, P.C.; Sammut, S.J.; Hotz, H.R.; Ceric, G.; Forslund, K.; Eddy, S.R.; Sonnhammer, E.L.; et al. The Pfam protein families database. *Nucleic Acids Res* **2008**, *36*, D281-288.

91. McConnachie, G.; Langeberg, L.K.; Scott, J.D. AKAP signaling complexes: getting to the heart of the matter. *Trends Mol Med* **2006**, *12*, 317-323.

92. Ercu, M.; Klussmann, E. Roles of A-Kinase Anchoring Proteins and Phosphodiesterases in the Cardiovascular System. *J Cardiovasc Dev Dis* **2018**, *5*.

93. Beavo, J.A. Cyclic nucleotide phosphodiesterases: functional implications of multiple isoforms. *Physiol Rev* **1995**, *75*, 725-748.

94. Belacel-Ouari, M.; Zhang, L.; Hubert, F.; Assaly, R.; Gerbier, R.; Jockers, R.; Dauphin, F.; Lechene, P.; Fischmeister, R.; Manoury, B.; et al. Influence of cell confluence on the cAMP signalling pathway in vascular smooth muscle cells. *Cell Signal* **2017**, *35*, 118-128.

95. Matsumoto, T.; Kobayashi, T.; Kamata, K. Phosphodiesterases in the vascular system. *J Smooth Muscle Res* **2003**, *39*, 67-86.

96. Santos-Silva, A.J.; Cairrao, E.; Morgado, M.; Alvarez, E.; Verde, I. PDE4 and PDE5 regulate cyclic nucleotides relaxing effects in human umbilical arteries. *Eur J Pharmacol* **2008**, *582*, 102-109.

97. Wennogle, L.P.; Hoxie, H.; Peng, Y.; Hendrick, J.P. Phosphodiesterase 1: A Unique Drug Target for Degenerative Diseases and Cognitive Dysfunction. *Adv Neurobiol* **2017**, *17*, 349-384.

98. Kasuya, J.; Goko, H.; Fujita-Yamaguchi, Y. Multiple transcripts for the human cardiac form of the cGMP-inhibited cAMP phosphodiesterase. *J Biol Chem* **1995**, *270*, 14305-14312.

99. Viguerie, N.; Clement, K.; Barbe, P.; Courtine, M.; Benis, A.; Larrouy, D.; Hanczar, B.; Pelloux, V.; Poitou, C.; Khalfallah, Y.; et al. In vivo epinephrine-mediated regulation of gene expression in human skeletal muscle. *J Clin Endocrinol Metab* **2004**, *89*, 2000-2014.

100. Ding, B.; Abe, J.I.; Wei, H.; Huang, Q.; Walsh, R.A.; Molina, C.A.; Zhao, A.; Sadoshima, J.; Blaxall, B.C.; Berk, B.C.; et al. Functional role of phosphodiesterase 3 in cardiomyocyte apoptosis: implication in heart failure. *Circulation* **2005**, *111*, 2469-2476.

101. Murray, F.; Patel, H.H.; Suda, R.Y.; Zhang, S.; Thistlethwaite, P.A.; Yuan, J.X.; Insel, P.A. Expression and activity of cAMP phosphodiesterase isoforms in pulmonary artery smooth muscle cells from patients with pulmonary hypertension: role for PDE1. *Am J Physiol Lung Cell Mol Physiol* **2007**, *292*, L294-303.

102. Chan, S.; Yan, C. PDE1 isozymes, key regulators of pathological vascular remodeling. *Curr Opin Pharmacol* **2011**, *11*, 720-724.

103. Mergia, E.; Stegbauer, J. Role of Phosphodiesterase 5 and Cyclic GMP in Hypertension. *Curr Hypertens Rep* **2016**, *18*, 39.

104. Nan, Y.; Zeng, X.; Jin, Z.; Li, N.; Chen, Z.; Chen, J.; Wang, D.; Wang, Y.; Lin, Z.; Ying, L. PDE1 or PDE5 inhibition augments NO-dependent hypoxic constriction of porcine coronary artery via elevating inosine 3',5'-cyclic monophosphate level. *J Cell Mol Med* **2020**, *24*, 14514-14524.

105. Martinez, S.E.; Wu, A.Y.; Glavas, N.A.; Tang, X.B.; Turley, S.; Hol, W.G.; Beavo, J.A. The two GAF domains in phosphodiesterase 2A have distinct roles in dimerization and in cGMP binding. *Proc Natl Acad Sci U S A* **2002**, *99*, 13260-13265.

106. Ho, Y.S.; Burden, L.M.; Hurley, J.H. Structure of the GAF domain, a ubiquitous signaling motif and a new class of cyclic GMP receptor. *EMBO J* **2000**, *19*, 5288-5299.

107. Bubb, K.J.; Trinder, S.L.; Baliga, R.S.; Patel, J.; Clapp, L.H.; MacAllister, R.J.; Hobbs, A.J. Inhibition of phosphodiesterase 2 augments cGMP and cAMP signaling to ameliorate pulmonary hypertension. *Circulation* **2014**, *130*, 496-507.

108. Murata, T.; Shimizu, K.; Hiramoto, K.; Tagawa, T. Phosphodiesterase 3 (PDE3): structure, localization and function. *Cardiovasc Hematol Agents Med Chem* **2009**, *7*, 206-211.

109. Murray, F.; MacLean, M.R.; Pyne, N.J. Increased expression of the cGMP-inhibited cAMP-specific (PDE3) and cGMP binding cGMP-specific (PDE5) phosphodiesterases in models of pulmonary hypertension. *Br J Pharmacol* **2002**, *137*, 1187-1194.

110. Wechsler, J.; Choi, Y.H.; Krall, J.; Ahmad, F.; Manganiello, V.C.; Movsesian, M.A. Isoforms of cyclic nucleotide phosphodiesterase PDE3A in cardiac myocytes. *J Biol Chem* **2002**, *277*, 38072-38078.

111. Hanna, R.; Nour-Eldine, W.; Saliba, Y.; Dagher-Hamalian, C.; Hachem, P.; Abou-Khalil, P.; Mika, D.; Varin, A.; El Hayek, M.S.; Pereira, L.; et al. Cardiac Phosphodiesterases Are Differentially Increased in Diabetic Cardiomyopathy. *Life Sci* **2021**, *283*, 119857.

112. Dunkerley, H.A.; Tilley, D.G.; Palmer, D.; Liu, H.; Jimmo, S.L.; Maurice, D.H. Reduced phosphodiesterase 3 activity and phosphodiesterase 3A level in synthetic vascular smooth muscle cells: implications for use of phosphodiesterase 3 inhibitors in cardiovascular tissues. *Mol Pharmacol* **2002**, *61*, 1033-1040.

113. Hubert, F.; Belacel-Ouari, M.; Manoury, B.; Zhai, K.; Domergue-Dupont, V.; Mateo, P.; Joubert, F.; Fischmeister, R.; Leblais, V. Alteration of vascular reactivity in heart failure: role of phosphodiesterases 3 and 4. *Br J Pharmacol* **2014**, *171*, 5361-5375.

114. Movsesian, M. Novel approaches to targeting PDE3 in cardiovascular disease. *Pharmacol Ther* **2016**, *163*, 74-81.

115. Ercu, M.; Marko, L.; Schachterle, C.; Tsvetkov, D.; Cui, Y.; Maghsodi, S.; Bartolomaeus, T.U.P.; Maass, P.G.; Zuhlke, K.; Gregersen, N.; et al. Phosphodiesterase 3A and Arterial Hypertension. *Circulation* **2020**, *142*, 133-149.

116. Beard, M.B.; Olsen, A.E.; Jones, R.E.; Erdogan, S.; Houslay, M.D.; Bolger, G.B. UCR1 and UCR2 domains unique to the cAMP-specific phosphodiesterase family form a discrete module via electrostatic interactions. *J Biol Chem* **2000**, *275*, 10349-10358.

117. Houslay, M.D. PDE4 cAMP-specific phosphodiesterases. *Prog Nucleic Acid Res Mol Biol* **2001**, *69*, 249-315.

118. Grange, M.; Sette, C.; Cuomo, M.; Conti, M.; Lagarde, M.; Prigent, A.F.; Nemoz, G. The cAMP-specific phosphodiesterase PDE4D3 is regulated by phosphatidic acid binding. Consequences for cAMP signaling pathway and characterization of a phosphatidic acid binding site. *J Biol Chem* **2000**, *275*, 33379-33387.

119. Saeki, T.; Saito, I. Isolation of cyclic nucleotide phosphodiesterase isozymes from pig aorta. *Biochem Pharmacol* **1993**, *46*, 833-839.

120. Lugnier, C.; Schoeffter, P.; Le Bec, A.; Strouthou, E.; Stoclet, J.C. Selective inhibition of cyclic nucleotide phosphodiesterases of human, bovine and rat aorta. *Biochem Pharmacol* **1986**, *35*, 1743-1751.

121. Komas, N.; Lugnier, C.; Andriantsitohaina, R.; Stoclet, J.C. Characterisation of cyclic nucleotide phosphodiesterases from rat mesenteric artery. *Eur J Pharmacol* **1991**, *208*, 85-87.

122. Rabe, K.F.; Tenor, H.; Dent, G.; Schudt, C.; Nakashima, M.; Magnussen, H. Identification of PDE isozymes in human pulmonary artery and effect of selective PDE inhibitors. *Am J Physiol* **1994**, *266*, L536-543.

123. Favot, L.; Keravis, T.; Holl, V.; Le Bec, A.; Lugnier, C. VEGF-induced HUVEC migration and proliferation are decreased by PDE2 and PDE4 inhibitors. *Thromb Haemost* **2003**, *90*, 334-343.

124. Willette, R.N.; Shiloh, A.O.; Sauermelch, C.F.; Sulpizio, A.; Michell, M.P.; Cieslinski, L.B.; Torphy, T.J.; Ohlstein, E.H. Identification, characterization, and functional role of phosphodiesterase type IV in cerebral vessels: effects of selective phosphodiesterase inhibitors. *J Cereb Blood Flow Metab* **1997**, *17*, 210-219.

125. Houslay, M.D.; Baillie, G.S.; Maurice, D.H. cAMP-Specific phosphodiesterase-4 enzymes in the cardiovascular system: a molecular toolbox for generating compartmentalized cAMP signaling. *Circ Res* **2007**, *100*, 950-966.

126. Tilley, D.G.; Maurice, D.H. Vascular smooth muscle cell phenotype-dependent phosphodiesterase 4D short form expression: role of differential histone acetylation on cAMP-regulated function. *Mol Pharmacol* **2005**, *68*, 596-605.

127. Biswas, K.H.; Sopory, S.; Visweswariah, S.S. The GAF domain of the cGMP-binding, cGMP-specific phosphodiesterase (PDE5) is a sensor and a sink for cGMP. *Biochemistry* **2008**, *47*, 3534-3543.

128. Liu, L.; Underwood, T.; Li, H.; Pamukcu, R.; Thompson, W.J. Specific cGMP binding by the cGMP binding domains of cGMP-binding cGMP specific phosphodiesterase. *Cell Signal* **2002**, *14*, 45-51.

129. Corbin, J.D.; Turko, I.V.; Beasley, A.; Francis, S.H. Phosphorylation of phosphodiesterase-5 by cyclic nucleotide-dependent protein kinase alters its catalytic and allosteric cGMP-binding activities. *Eur J Biochem* **2000**, *267*, 2760-2767.

130. Zoraghi, R.; Bessay, E.P.; Corbin, J.D.; Francis, S.H. Structural and functional features in human PDE5A1 regulatory domain that provide for allosteric cGMP binding, dimerization, and regulation. *J Biol Chem* **2005**, *280*, 12051-12063.

131. Maurice, D.H. Cardiovascular implications in the use of PDE5 inhibitor therapy. *Int J Impot Res* **2004**, *16 Suppl 1*, S20-23.

132. Larre, A.B.; Parisotto, A.; Rockenbach, B.F.; Pasin, D.M.; Capellari, C.; Escouto, D.C.; Pinheiro da Costa, B.E.; Poli-de-Figueiredo, C.E. Phosphodiesterases and preeclampsia. *Med Hypotheses* **2017**, *108*, 94-100.

133. Gulati, S.; Palczewski, K. New focus on regulation of the rod photoreceptor phosphodiesterase. *Curr Opin Struct Biol* **2021**, *69*, 99-107.

134. Cote, R.H.; Gupta, R.; Irwin, M.J.; Wang, X. Photoreceptor Phosphodiesterase (PDE6): Structure, Regulatory Mechanisms, and Implications for Treatment of Retinal Diseases. *Adv Exp Med Biol* **2022**, *1371*, 33-59.

135. Goc, A.; Chami, M.; Lodowski, D.T.; Bosshart, P.; Moiseenkova-Bell, V.; Baehr, W.; Engel, A.; Palczewski, K. Structural characterization of the rod cGMP phosphodiesterase 6. *J Mol Biol* **2010**, *401*, 363-373.

136. Mou, H.; Cote, R.H. The catalytic and GAF domains of the rod cGMP phosphodiesterase (PDE6) heterodimer are regulated by distinct regions of its inhibitory gamma subunit. *J Biol Chem* **2001**, *276*, 27527-27534.

137. Turunen, T.; Koskelainen, A. Functional modulation of phosphodiesterase-6 by calcium in mouse rod photoreceptors. *Sci Rep* **2021**, *11*, 8938.

138. Zhai, K.; Hubert, F.; Nicolas, V.; Ji, G.; Fischmeister, R.; Leblais, V. beta-Adrenergic cAMP signals are predominantly regulated by phosphodiesterase type 4 in cultured adult rat aortic smooth muscle cells. *PLoS One* **2012**, *7*, e47826.

139. Glavas, N.A.; Ostenson, C.; Schaefer, J.B.; Vasta, V.; Beavo, J.A. T cell activation up-regulates cyclic nucleotide phosphodiesterases 8A1 and 7A3. *Proc Natl Acad Sci U S A* **2001**, *98*, 6319-6324.

140. Phillips, P.G.; Long, L.; Wilkins, M.R.; Morrell, N.W. cAMP phosphodiesterase inhibitors potentiate effects of prostacyclin analogs in hypoxic pulmonary vascular remodeling. *Am J Physiol Lung Cell Mol Physiol* **2005**, *288*, L103-115.

141. Smith, S.J.; Brookes-Fazakerley, S.; Donnelly, L.E.; Barnes, P.J.; Barnette, M.S.; Giembycz, M.A. Ubiquitous expression of phosphodiesterase 7A in human proinflammatory and immune cells. *Am J Physiol Lung Cell Mol Physiol* **2003**, *284*, L279-289.

142. Wang, P.; Wu, P.; Egan, R.W.; Billah, M.M. Human phosphodiesterase 8A splice variants: cloning, gene organization, and tissue distribution. *Gene* **2001**, *280*, 183-194.

143. Kobayashi, T.; Gamanuma, M.; Sasaki, T.; Yamashita, Y.; Yuasa, K.; Kotera, J.; Omori, K. Molecular comparison of rat cyclic nucleotide phosphodiesterase 8 family: unique expression of PDE8B in rat brain. *Gene* **2003**, *319*, 21-31.

144. Wunder, F.; Tersteegen, A.; Rebmann, A.; Erb, C.; Fahrig, T.; Hendrix, M. Characterization of the first potent and selective PDE9 inhibitor using a cGMP reporter cell line. *Mol Pharmacol* **2005**, *68*, 1775-1781.

145. Rentero, C.; Monfort, A.; Puigdomenech, P. Identification and distribution of different mRNA variants produced by differential splicing in the human phosphodiesterase 9A gene. *Biochem Biophys Res Commun* **2003**, *301*, 686-692.

146. Fujishige, K.; Kotera, J.; Yuasa, K.; Omori, K. The human phosphodiesterase PDE10A gene genomic organization and evolutionary relatedness with other PDEs containing GAF domains. *Eur J Biochem* **2000**, *267*, 5943-5951.

147. Azevedo, M.F.; Faucz, F.R.; Bimpaki, E.; Horvath, A.; Levy, I.; de Alexandre, R.B.; Ahmad, F.; Manganiello, V.; Stratakis, C.A. Clinical and molecular genetics of the phosphodiesterases (PDEs). *Endocr Rev* **2014**, *35*, 195-233.

148. Gross-Langenhoff, M.; Hofbauer, K.; Weber, J.; Schultz, A.; Schultz, J.E. cAMP is a ligand for the tandem GAF domain of human phosphodiesterase 10 and cGMP for the tandem GAF domain of phosphodiesterase 11. *J Biol Chem* **2006**, *281*, 2841-2846.

149. Tian, X.; Vroom, C.; Ghofrani, H.A.; Weissmann, N.; Bieniek, E.; Grimminger, F.; Seeger, W.; Schermuly, R.T.; Pullamsetti, S.S. Phosphodiesterase 10A upregulation contributes to pulmonary vascular remodeling. *PLoS One* **2011**, *6*, e18136.

150. Makhlouf, A.; Kshirsagar, A.; Niederberger, C. Phosphodiesterase 11: a brief review of structure, expression and function. *Int J Impot Res* **2006**, *18*, 501-509.

151. Kayik, G.; Tuzun, N.S.; Durdagi, S. Investigation of PDE5/PDE6 and PDE5/PDE11 selective potent tadalafil-like PDE5 inhibitors using combination of molecular modeling approaches, molecular fingerprint-based virtual screening protocols and structure-based pharmacophore development. *J Enzyme Inhib Med Chem* **2017**, *32*, 311-330.

152. Francis, S.H. Phosphodiesterase 11 (PDE11): is it a player in human testicular function? *Int J Impot Res* **2005**, *17*, 467-468.

153. Weeks, J.L., 2nd; Zoraghi, R.; Francis, S.H.; Corbin, J.D. N-Terminal domain of phosphodiesterase-11A4 (PDE11A4) decreases affinity of the catalytic site for substrates and tadalafil, and is involved in oligomerization. *Biochemistry* **2007**, *46*, 10353-10364.

154. Loughney, K.; Taylor, J.; Florio, V.A. 3',5'-cyclic nucleotide phosphodiesterase 11A: localization in human tissues. *Int J Impot Res* **2005**, *17*, 320-325.

155. Fawcett, L.; Baxendale, R.; Stacey, P.; McGrouther, C.; Harrow, I.; Soderling, S.; Hetman, J.; Beavo, J.A.; Phillips, S.C. Molecular cloning and characterization of a distinct human phosphodiesterase gene family: PDE11A. *Proc Natl Acad Sci U S A* **2000**, *97*, 3702-3707.

156. D'Andrea, M.R.; Qiu, Y.; Haynes-Johnson, D.; Bhattacharjee, S.; Kraft, P.; Lundeen, S. Expression of PDE11A in normal and malignant human tissues. *J Histochem Cytochem* **2005**, *53*, 895-903.

157. Arora, K.; Sinha, C.; Zhang, W.; Ren, A.; Moon, C.S.; Yarlagadda, S.; Naren, A.P. Compartmentalization of cyclic nucleotide signaling: a question of when, where, and why? *Pflugers Arch* **2013**, *465*, 1397-1407.

158. Feiteiro, J.; Verde, I.; Cairrao, E. Cyclic guanosine monophosphate compartmentation in human vascular smooth muscle cells. *Cell Signal* **2016**, *28*, 109-116.

159. Fischmeister, R.; Castro, L.R.; Abi-Gerges, A.; Rochais, F.; Jurevicius, J.; Leroy, J.; Vandecasteele, G. Compartmentation of cyclic nucleotide signaling in the heart: the role of cyclic nucleotide phosphodiesterases. *Circ Res* **2006**, *99*, 816-828.

160. Castro, L.R.; Verde, I.; Cooper, D.M.; Fischmeister, R. Cyclic guanosine monophosphate compartmentation in rat cardiac myocytes. *Circulation* **2006**, *113*, 2221-2228.

161. Conti, M.; Beavo, J. Biochemistry and physiology of cyclic nucleotide phosphodiesterases: essential components in cyclic nucleotide signaling. *Annu Rev Biochem* **2007**, *76*, 481-511.

162. Dodge-Kafka, K.L.; Langeberg, L.; Scott, J.D. Compartmentation of cyclic nucleotide signaling in the heart: the role of A-kinase anchoring proteins. *Circ Res* **2006**, *98*, 993-1001.

163. Lissandron, V.; Zaccolo, M. Compartmentalized cAMP/PKA signalling regulates cardiac excitation-contraction coupling. *J Muscle Res Cell Motil* **2006**, *27*, 399-403.

164. Pani, B.; Singh, B.B. Lipid rafts/caveolae as microdomains of calcium signaling. *Cell Calcium* **2009**, *45*, 625-633.

165. Guellich, A.; Mehel, H.; Fischmeister, R. Cyclic AMP synthesis and hydrolysis in the normal and failing heart. *Pflugers Arch* **2014**, *466*, 1163-1175.

166. Francis, S.H.; Blount, M.A.; Corbin, J.D. Mammalian cyclic nucleotide phosphodiesterases: molecular mechanisms and physiological functions. *Physiol Rev* **2011**, *91*, 651-690.

167. Schrade, K.; Klussmann, E. Pharmacological Approaches for Delineating Functions of AKAP-Based Signalling Complexes and Finding Therapeutic Targets. In *Microdomains in the Cardiovascular System*, Nikolaev, V., Zaccolo, M., Eds.; Springer International Publishing: Cham, 2017; pp. 59-83.

168. Ghigo, A.; Pirozzi, F.; Li, M.; Hirsch, E. Chatting Second Messengers: PIP3 and cAMP. In *Microdomains in the Cardiovascular System*, Nikolaev, V., Zaccolo, M., Eds.; Springer International Publishing: Cham, 2017; pp. 85-95.

169. Lefkimmiatis, K.; Zaccolo, M. cAMP signaling in subcellular compartments. *Pharmacol Ther* **2014**, *143*, 295-304.

170. Belleville-Rolland, T.; Sassi, Y.; Decouture, B.; Dreano, E.; Hulot, J.S.; Gaussem, P.; Bachelot-Loza, C. MRP4 (ABCC4) as a potential pharmacologic target for cardiovascular disease. *Pharmacol Res* **2016**, *107*, 381-389.

171. Sassi, Y.; Lipskaia, L.; Vandecasteele, G.; Nikolaev, V.O.; Hatem, S.N.; Cohen Aubart, F.; Russel, F.G.; Mougenot, N.; Vrignaud, C.; Lechat, P.; et al. Multidrug resistance-associated protein 4 regulates cAMP-dependent signaling pathways and controls human and rat SMC proliferation. *J Clin Invest* **2008**, *118*, 2747-2757.

172. Wielinga, P.R.; van der Heijden, I.; Reid, G.; Beijnen, J.H.; Wijnholds, J.; Borst, P. Characterization of the MRP4- and MRP5-mediated transport of cyclic nucleotides from intact cells. *J Biol Chem* **2003**, *278*, 17664-17671.

173. Guarino, M.L.; Massimi, I.; Alemanno, L.; Conti, L.; Angiolillo, D.J.; Pulcinelli, F.M. MRP4 over-expression has a role on both reducing nitric oxide-dependent antiplatelet effect and enhancing ADP induced platelet activation. *J Thromb Thrombolysis* **2021**, *51*, 625-632.

174. Beavo, J.A.; Brunton, L.L. Cyclic nucleotide research -- still expanding after half a century. *Nat Rev Mol Cell Biol* **2002**, *3*, 710-718.

175. Lomas, O.; Zaccolo, M. Phosphodiesterases maintain signaling fidelity via compartmentalization of cyclic nucleotides. *Physiology (Bethesda)* **2014**, *29*, 141-149.

176. Williams, C. cAMP detection methods in HTS: selecting the best from the rest. *Nat Rev Drug Discov* **2004**, *3*, 125-135.

177. Barsony, J.; Marx, S.J. Immunocytology on microwave-fixed cells reveals rapid and agonist-specific changes in subcellular accumulation patterns for cAMP or cGMP. *Proc Natl Acad Sci U S A* **1990**, *87*, 1188-1192.

178. Castro, L.R.; Schittl, J.; Fischmeister, R. Feedback control through cGMP-dependent protein kinase contributes to differential regulation and compartmentation of cGMP in rat cardiac myocytes. *Circ Res* **2010**, *107*, 1232-1240.

179. Sprenger, J.U.; Nikolaev, V.O. Biophysical techniques for detection of cAMP and cGMP in living cells. *Int J Mol Sci* **2013**, *14*, 8025-8046.

180. Niino, Y.; Hotta, K.; Oka, K. Simultaneous live cell imaging using dual FRET sensors with a single excitation light. *PLoS One* **2009**, *4*, e6036.

181. Shrestha, D.; Jenei, A.; Nagy, P.; Vereb, G.; Szollosi, J. Understanding FRET as a research tool for cellular studies. *Int J Mol Sci* **2015**, *16*, 6718-6756.

182. Kraft, A.E.; Nikolaev, V.O. FRET Microscopy for Real-Time Visualization of Second Messengers in Living Cells. *Methods Mol Biol* **2017**, *1563*, 85-90.

183. Trivedi, B.; Kramer, R.H. Real-time patch-cram detection of intracellular cGMP reveals long-term suppression of responses to NO and muscarinic agonists. *Neuron* **1998**, *21*, 895-906.

184. Thunemann, M.; Fomin, N.; Krawutschke, C.; Russwurm, M.; Feil, R. Visualization of cGMP with cGi biosensors. *Methods Mol Biol* **2013**, *1020*, 89-120.

185. Berisha, F.; Nikolaev, V.O. Cyclic nucleotide imaging and cardiovascular disease. *Pharmacol Ther* **2017**, *175*, 107-115.

186. Wong, W.; Scott, J.D. AKAP signalling complexes: focal points in space and time. *Nat Rev Mol Cell Biol* **2004**, *5*, 959-970.

187. Negro, A.; Dodge-Kafka, K.; Kapiloff, M.S. Signalosomes as Therapeutic Targets. *Prog Pediatr Cardiol* **2008**, *25*, 51-56.

188. Torres-Quesada, O.; Mayrhofer, J.E.; Stefan, E. The many faces of compartmentalized PKA signalosomes. *Cell Signal* **2017**, *37*, 1-11.

189. Colombe, A.S.; Pidoux, G. Cardiac cAMP-PKA Signaling Compartmentalization in Myocardial Infarction. *Cells* **2021**, *10*.

190. Perino, A.; Ghigo, A.; Scott, J.D.; Hirsch, E. Anchoring proteins as regulators of signaling pathways. *Circ Res* **2012**, *111*, 482-492.

191. Scott, J.D.; Dessauer, C.W.; Tasken, K. Creating order from chaos: cellular regulation by kinase anchoring. *Annu Rev Pharmacol Toxicol* **2013**, *53*, 187-210.

192. Walker-Gray, R.; Pallien, T.; Miller, D.C.; Oder, A.; Neuenschwander, M.; von Kries, J.P.; Diecke, S.; Klussmann, E. Disruptors of AKAP-Dependent Protein-Protein Interactions. *Methods Mol Biol* **2022**, *2483*, 117-139.

193. Pidoux, G.; Tasken, K. Specificity and spatial dynamics of protein kinase A signaling organized by A-kinase-anchoring proteins. *J Mol Endocrinol* **2010**, *44*, 271-284.

194. Nystoriak, M.A.; Nieves-Cintron, M.; Patriarchi, T.; Buonarati, O.R.; Prada, M.P.; Morotti, S.; Grandi, E.; Fernandes, J.D.; Forbush, K.; Hofmann, F.; et al. Ser1928 phosphorylation by

PKA stimulates the L-type Ca^{2+} channel Cav1.2 and vasoconstriction during acute hyperglycemia and diabetes. *Sci Signal* **2017**, *10*.

195. Navedo, M.F.; Nieves-Cintron, M.; Amberg, G.C.; Yuan, C.; Votaw, V.S.; Lederer, W.J.; McKnight, G.S.; Santana, L.F. AKAP150 is required for stuttering persistent Ca^{2+} sparklets and angiotensin II-induced hypertension. *Circ Res* **2008**, *102*, e1-e11.

196. Zaccolo, M.; Di Benedetto, G.; Lissandron, V.; Mancuso, L.; Terrin, A.; Zamparo, I. Restricted diffusion of a freely diffusible second messenger: mechanisms underlying compartmentalized cAMP signalling. *Biochem Soc Trans* **2006**, *34*, 495-497.

197. McCormick, K.; Baillie, G.S. Compartmentalisation of second messenger signalling pathways. *Curr Opin Genet Dev* **2014**, *27*, 20-25.

198. Tibbo, A.J.; Mika, D.; Dobi, S.; Ling, J.; McFall, A.; Tejeda, G.S.; Blair, C.; MacLeod, R.; MacQuaide, N.; Gok, C.; et al. Phosphodiesterase type 4 anchoring regulates cAMP signaling to Popeye domain-containing proteins. *J Mol Cell Cardiol* **2022**, *165*, 86-102.

199. Brescia, M.; Zaccolo, M. Modulation of Compartmentalised Cyclic Nucleotide Signalling via Local Inhibition of Phosphodiesterase Activity. *Int J Mol Sci* **2016**, *17*.

200. Peng, T.; Qi, B.; He, J.; Ke, H.; Shi, J. Advances in the Development of Phosphodiesterase-4 Inhibitors. *J Med Chem* **2020**, *63*, 10594-10617.

201. Richter, W.; Day, P.; Agrawal, R.; Bruss, M.D.; Granier, S.; Wang, Y.L.; Rasmussen, S.G.; Horner, K.; Wang, P.; Lei, T.; et al. Signaling from beta1- and beta2-adrenergic receptors is defined by differential interactions with PDE4. *EMBO J* **2008**, *27*, 384-393.

202. Cai, Y.; Nagel, D.J.; Zhou, Q.; Cygnar, K.D.; Zhao, H.; Li, F.; Pi, X.; Knight, P.A.; Yan, C. Role of cAMP-phosphodiesterase 1C signaling in regulating growth factor receptor stability, vascular smooth muscle cell growth, migration, and neointimal hyperplasia. *Circ Res* **2015**, *116*, 1120-1132.

203. Kim, D.; Rybalkin, S.D.; Pi, X.; Wang, Y.; Zhang, C.; Munzel, T.; Beavo, J.A.; Berk, B.C.; Yan, C. Upregulation of phosphodiesterase 1A1 expression is associated with the development of nitrate tolerance. *Circulation* **2001**, *104*, 2338-2343.

204. Koschinski, A.; Zaccolo, M. Activation of PKA in cell requires higher concentration of cAMP than in vitro: implications for compartmentalization of cAMP signalling. *Sci Rep* **2017**, *7*, 14090.

205. Rich, T.C.; Xin, W.; Mehats, C.; Hassell, K.A.; Piggott, L.A.; Le, X.; Karpen, J.W.; Conti, M. Cellular mechanisms underlying prostaglandin-induced transient cAMP signals near the plasma membrane of HEK-293 cells. *Am J Physiol Cell Physiol* **2007**, *292*, C319-331.

206. Smith, F.D.; Esseltine, J.L.; Nygren, P.J.; Veesler, D.; Byrne, D.P.; Vonderach, M.; Strashnov, I.; Eyers, C.E.; Eyers, P.A.; Langeberg, L.K.; et al. Local protein kinase A action proceeds through intact holoenzymes. *Science* **2017**, *356*, 1288-1293.

207. Johnstone, T.B.; Agarwal, S.R.; Harvey, R.D.; Ostrom, R.S. cAMP Signaling Compartmentation: Adenylyl Cyclases as Anchors of Dynamic Signaling Complexes. *Mol Pharmacol* **2018**, *93*, 270-276.

208. Mery, P.F.; Pavoine, C.; Belhassen, L.; Pecker, F.; Fischmeister, R. Nitric oxide regulates cardiac Ca^{2+} current. Involvement of cGMP-inhibited and cGMP-stimulated

phosphodiesterases through guanylyl cyclase activation. *J Biol Chem* **1993**, *268*, 26286-26295.

209. Subramanian, H.; Froese, A.; Jonsson, P.; Schmidt, H.; Gorelik, J.; Nikolaev, V.O. Distinct submembrane localisation compartmentalises cardiac NPR1 and NPR2 signalling to cGMP. *Nat Commun* **2018**, *9*, 2446.

210. Piggott, L.A.; Hassell, K.A.; Berkova, Z.; Morris, A.P.; Silberbach, M.; Rich, T.C. Natriuretic peptides and nitric oxide stimulate cGMP synthesis in different cellular compartments. *J Gen Physiol* **2006**, *128*, 3-14.

211. Cawley, S.M.; Sawyer, C.L.; Brunelle, K.F.; van der Vliet, A.; Dostmann, W.R. Nitric oxide-evoked transient kinetics of cyclic GMP in vascular smooth muscle cells. *Cell Signal* **2007**, *19*, 1023-1033.

212. Nausch, L.W.; Ledoux, J.; Bonev, A.D.; Nelson, M.T.; Dostmann, W.R. Differential patterning of cGMP in vascular smooth muscle cells revealed by single GFP-linked biosensors. *Proc Natl Acad Sci U S A* **2008**, *105*, 365-370.

213. Cairrao, E.; Santos-Silva, A.J.; Verde, I. PKG is involved in testosterone-induced vasorelaxation of human umbilical artery. *Eur J Pharmacol* **2010**, *640*, 94-101.

214. Wilson, L.S.; Guo, M.; Umana, M.B.; Maurice, D.H. Distinct phosphodiesterase 5A-containing compartments allow selective regulation of cGMP-dependent signalling in human arterial smooth muscle cells. *Cell Signal* **2017**, *36*, 204-211.

215. Tsai, E.J.; Kass, D.A. Cyclic GMP signaling in cardiovascular pathophysiology and therapeutics. *Pharmacol Ther* **2009**, *122*, 216-238.

216. Zhang, Y.; Moreland, S.; Moreland, R.S. Regulation of vascular smooth muscle contraction: myosin light chain phosphorylation dependent and independent pathways. *Can J Physiol Pharmacol* **1994**, *72*, 1386-1391.

217. Martinsen, A.; Dessy, C.; Morel, N. Regulation of calcium channels in smooth muscle: new insights into the role of myosin light chain kinase. *Channels (Austin)* **2014**, *8*, 402-413.

218. Woodrum, D.A.; Brophy, C.M. The paradox of smooth muscle physiology. *Molecular and Cellular Endocrinology* **2001**, *177*, 135-143.

219. Jackson, W.F. Ion channels and vascular tone. *Hypertension* **2000**, *35*, 173-178.

220. Dolphin, A.C. A short history of voltage-gated calcium channels. *Br J Pharmacol* **2006**, *147 Suppl 1*, S56-62.

221. Wray, S. Calcium Signaling in Smooth Muscle. In *Handbook of Cell Signaling (Second Edition)*; Academic Press: Physiology Department, School of Biomedical Sciences, University of Liverpool, Liverpool, England, UK, 2010; pp. 1009-1025.

222. Ringer, S.; Morshead, E.A. The Influence on the Afferent Nerves of the Frog's Leg from the Local Application of the Chlorides, Bromides, and Iodides of Potassium, Ammonium, and Sodium. *J Anat Physiol* **1877**, *12*, 58-72.

223. Ringer, S. Concerning the Influence exerted by each of the Constituents of the Blood on the Contraction of the Ventricle. *J Physiol* **1882**, *3*, 380-393.

224. Ringer, S. A further Contribution regarding the influence of the different Constituents of the Blood on the Contraction of the Heart. *J Physiol* **1883**, *4*, 29-42 23.

225. Ringer, S. Regarding the Action of Lime Potassium and Sodium Salts on Skeletal Muscle. *J Physiol* **1887**, *8*, 20-24.

226. Miller, D.J. Sydney Ringer; physiological saline, calcium and the contraction of the heart. *J Physiol* **2004**, *555*, 585-587.

227. Brini, M.; Ottolini, D.; Cali, T.; Carafoli, E. Calcium in health and disease. *Met Ions Life Sci* **2013**, *13*, 81-137.

228. Tivane, C.; Rodrigues, M.N.; Favaron, P.O.; Assis Neto, A.C.d.; Birgel Júnior, E.H.; Miglino, M.A. Mechanisms of calcium transport across the placenta: Review. *Open Journal of Animal Sciences* **2013**, *03*, 13-20.

229. Kon, N.; Fukada, Y. [Cognitive Function and Calcium. Ca^{2+}-dependent regulatory mechanism of circadian clock oscillation and its relevance to neuronal function]. *Clin Calcium* **2015**, *25*, 201-208.

230. Brozovich, F.V.; Nicholson, C.J.; Degen, C.V.; Gao, Y.Z.; Aggarwal, M.; Morgan, K.G. Mechanisms of Vascular Smooth Muscle Contraction and the Basis for Pharmacologic Treatment of Smooth Muscle Disorders. *Pharmacol Rev* **2016**, *68*, 476-532.

231. Tykocki, N.R.; Boerman, E.M.; Jackson, W.F. Smooth Muscle Ion Channels and Regulation of Vascular Tone in Resistance Arteries and Arterioles. *Compr Physiol* **2017**, *7*, 485-581.

232. Rosenbaum, D.M.; Rasmussen, S.G.; Kobilka, B.K. The structure and function of G-protein-coupled receptors. *Nature* **2009**, *459*, 356-363.

233. Toth, A.D.; Turu, G.; Hunyady, L.; Balla, A. Novel mechanisms of G-protein-coupled receptors functions: AT1 angiotensin receptor acts as a signaling hub and focal point of receptor cross-talk. *Best Pract Res Clin Endocrinol Metab* **2018**, *32*, 69-82.

234. Berridge, M.J. The Inositol Trisphosphate/Calcium Signaling Pathway in Health and Disease. *Physiol Rev* **2016**, *96*, 1261-1296.

235. Oner, S.S.; Blumer, J.B.; Lanier, S.M. Group II activators of G-protein signaling: monitoring the interaction of Galpha with the G-protein regulatory motif in the intact cell. *Methods Enzymol* **2013**, *522*, 153-167.

236. Hoeflich, K.P.; Ikura, M. Calmodulin in Action. *Cell* **2002**, *108*, 739-742.

237. Webb, R.C. Smooth muscle contraction and relaxation. *Adv Physiol Educ* **2003**, *27*, 201-206.

238. Bar-Sagi, D.; Hall, A. Ras and Rho GTPases. *Cell* **2000**, *103*, 227-238.

239. Schwartz, M.A. Integrins and extracellular matrix in mechanotransduction. *Cold Spring Harb Perspect Biol* **2010**, *2*, a005066.

240. Fukata, Y.; Kaibuchi, K.; Amano, M.; Kaibuchi, K. Rho–Rho-kinase pathway in smooth muscle contraction and cytoskeletal reorganization of non-muscle cells. *Trends in Pharmacological Sciences* **2001**, *22*, 32-39.

241. H.Tsui., Q.Z., K.Chen., X.Zhang. Rho-Associated Protein Kinase. In *Current Topics in Developmental Biology*; 2017.

242. Liao, J.K.; Seto, M.; Noma, K. Rho kinase (ROCK) inhibitors. *J Cardiovasc Pharmacol* **2007**, *50*, 17-24.

243. Amano, M.; Nakayama, M.; Kaibuchi, K. Rho-kinase/ROCK: A key regulator of the cytoskeleton and cell polarity. *Cytoskeleton (Hoboken)* **2010**, *67*, 545-554.

244. Muranyi, A.; Derkach, D.; Erdodi, F.; Kiss, A.; Ito, M.; Hartshorne, D.J. Phosphorylation of Thr695 and Thr850 on the myosin phosphatase target subunit: inhibitory effects and occurrence in A7r5 cells. *FEBS Lett* **2005**, *579*, 6611-6615.

245. McConnell, J.L.; Wadzinski, B.E. Targeting protein serine/threonine phosphatases for drug development. *Mol Pharmacol* **2009**, *75*, 1249-1261.

246. Carvajal, J.A.; Germain, A.M.; Huidobro-Toro, J.P.; Weiner, C.P. Molecular mechanism of cGMP-mediated smooth muscle relaxation. *J Cell Physiol* **2000**, *184*, 409-420.

247. Baumann, F.; Bauer, M.S.; Rees, M.; Alexandrovich, A.; Gautel, M.; Pippig, D.A.; Gaub, H.E. Increasing evidence of mechanical force as a functional regulator in smooth muscle myosin light chain kinase. *Elife* **2017**, *6*.

248. Zhu, Y.; Qu, J.; He, L.; Zhang, F.; Zhou, Z.; Yang, S.; Zhou, Y. Calcium in Vascular Smooth Muscle Cell Elasticity and Adhesion: Novel Insights Into the Mechanism of Action. *Front Physiol* **2019**, *10*, 852.

249. Inesi, G.; Prasad, A.M.; Pilankatta, R. The Ca2+ ATPase of cardiac sarcoplasmic reticulum: Physiological role and relevance to diseases. *Biochem Biophys Res Commun* **2008**, *369*, 182-187.

250. Stafford, N.; Wilson, C.; Oceandy, D.; Neyses, L.; Cartwright, E.J. The Plasma Membrane Calcium ATPases and Their Role as Major New Players in Human Disease. *Physiol Rev* **2017**, *97*, 1089-1125.

251. Philipson, K.D.; Nicoll, D.A. Sodium-calcium exchange: a molecular perspective. *Annu Rev Physiol* **2000**, *62*, 111-133.

252. Bootman, M.D.; Collins, T.J.; Peppiatt, C.M.; Prothero, L.S.; MacKenzie, L.; De Smet, P.; Travers, M.; Tovey, S.C.; Seo, J.T.; Berridge, M.J.; et al. Calcium signalling-an overview. *Semin Cell Dev Biol* **2001**, *12*, 3-10.

253. Robertson, S.Y.T.; Wen, X.; Yin, K.; Chen, J.; Smith, C.E.; Paine, M.L. Multiple Calcium Export Exchangers and Pumps Are a Prominent Feature of Enamel Organ Cells. *Front Physiol* **2017**, *8*, 336.

254. Morgado, M.; Cairrao, E.; Santos-Silva, A.J.; Verde, I. Cyclic nucleotide-dependent relaxation pathways in vascular smooth muscle. *Cell Mol Life Sci* **2012**, *69*, 247-266.

255. Shaul, P.W. Regulation of endothelial nitric oxide synthase: location, location, location. *Annu Rev Physiol* **2002**, *64*, 749-774.

256. Akata, T. Cellular and molecular mechanisms regulating vascular tone. Part 2: regulatory mechanisms modulating Ca2+ mobilization and/or myofilament Ca^{2+} sensitivity in vascular smooth muscle cells. *J Anesth* **2007**, *21*, 232-242.

257. Polson, J.B.; Strada, S.J. Cyclic nucleotide phosphodiesterases and vascular smooth muscle. *Annu Rev Pharmacol Toxicol* **1996**, *36*, 403-427.

258. Coats, P. Signalling mechanisms underlying the myogenic response in human subcutaneous resistance arteries. *Cardiovascular Research* **2001**, *49*, 828-837.

259. Karaki, H. Historical techniques: cytosolic Ca2+ and contraction in smooth muscle. *Trends Pharmacol Sci* **2004**, *25*, 388-393.

260. Ledoux, J.; Werner, M.E.; Brayden, J.E.; Nelson, M.T. Calcium-activated potassium channels and the regulation of vascular tone. *Physiology (Bethesda)* **2006**, *21*, 69-78.

261. Ets, H.K.; Seow, C.Y.; Moreland, R.S. Sustained Contraction in Vascular Smooth Muscle by Activation of L-type Ca(2+) Channels Does Not Involve Ca(2+) Sensitization or Caldesmon. *Front Pharmacol* **2016**, *7*, 516.

262. Arsalan U. Syed, T.L., Manuel F. Navedo, Madeline Nieves-Cintrón. Ion Channels and Their Regulation in Vascular Smooth Muscle. In *Basic and Clinical Understanding of Microcirculation*, Shad, K.F., Ed.; intechopen: 2020; p. 166.

263. Nieves-Cintron, M.; Syed, A.U.; Nystoriak, M.A.; Navedo, M.F. Regulation of voltage-gated potassium channels in vascular smooth muscle during hypertension and metabolic disorders. *Microcirculation* **2018**, *25*.

264. Cheng, J.; Wen, J.; Wang, N.; Wang, C.; Xu, Q.; Yang, Y. Ion Channels and Vascular Diseases. *Arterioscler Thromb Vasc Biol* **2019**, *39*, e146-e156.

265. Di Naro, E.; Ghezzi, F.; Raio, L.; Franchi, M.; D'Addario, V. Umbilical cord morphology and pregnancy outcome. *Eur J Obstet Gynecol Reprod Biol* **2001**, *96*, 150-157.

266. Arutyunyan, I.; Elchaninov, A.; Makarov, A.; Fatkhudinov, T. Umbilical Cord as Prospective Source for Mesenchymal Stem Cell-Based Therapy. *Stem Cells Int* **2016**, *2016*, 6901286.

267. Campesi, I.; Franconi, F.; Montella, A.; Dessole, S.; Capobianco, G. Human Umbilical Cord: Information Mine in Sex-Specific Medicine. *Life (Basel)* **2021**, *11*.

268. Predanic, M.; Perni, S.C.; Chasen, S.T.; Baergen, R.N.; Chervenak, F.A. Assessment of umbilical cord coiling during the routine fetal sonographic anatomic survey in the second trimester. *J Ultrasound Med* **2005**, *24*, 185-191; quiz 192-183.

269. Bosselmann, S.; Mielke, G. Sonographic Assessment of the Umbilical Cord. *Geburtshilfe Frauenheilkd* **2015**, *75*, 808-818.

270. Moshiri, M.; Zaidi, S.F.; Robinson, T.J.; Bhargava, P.; Siebert, J.R.; Dubinsky, T.J.; Katz, D.S. Comprehensive Imaging Review of Abnormalities of the Umbilical Cord. *RadioGraphics* **2014**, *34*, 179-196.

271. Cairrao, E.; Santos-Silva, A.J.; Alvarez, E.; Correia, I.; Verde, I. Isolation and culture of human umbilical artery smooth muscle cells expressing functional calcium channels. *In Vitro Cell Dev Biol Anim* **2009**, *45*, 175-184.

272. Ferguson, V.L.; Dodson, R.B. Bioengineering aspects of the umbilical cord. *Eur J Obstet Gynecol Reprod Biol* **2009**, *144 Suppl 1*, S108-113.

273. Spurway, J.; Logan, P.; Pak, S. The development, structure and blood flow within the umbilical cord with particular reference to the venous system. *Australas J Ultrasound Med* **2012**, *15*, 97-102.

274. Kellow, Z.S.; Feldstein, V.A. Ultrasound of the Placenta and Umbilical Cord. *Ultrasound Quarterly* **2011**, *27*, 187-197.

275. Sobolewski, K.; Malkowski, A.; Bankowski, E.; Jaworski, S. Wharton's jelly as a reservoir of peptide growth factors. *Placenta* **2005**, *26*, 747-752.

276. Nanaev, A.K.; Kohnen, G.; Milovanov, A.P.; Domogatsky, S.P.; Kaufmann, P. Stromal differentiation and architecture of the human umbilical cord. *Placenta* **1997**, *18*, 53-64.

277. Mott, J.D.; Werb, Z. Regulation of matrix biology by matrix metalloproteinases. *Curr Opin Cell Biol* **2004**, *16*, 558-564.

278. Corrao, S.; La Rocca, G.; Lo Iacono, M.; Corsello, T.; Farina, F.; Anzalone, R. Umbilical cord revisited: from Wharton's jelly myofibroblasts to mesenchymal stem cells. *Histol Histopathol* **2013**, *28*, 1235-1244.

279. Lorigo. M., M.M., Feiteiro. J., Cairrao. E. . Human Umbilical Artery Smooth Muscle Cells: Vascular Function and Clinical Importance. In *Horizons in World Cardiovascular Research*; Nova Science Publishers: 2019; Volume 16.

280. Blache, G.; Garba, A.; Frairot, P.; Vancina, S.; Gaja, R. [Prognostic value of a single umbilical artery. 87 cases]. *J Gynecol Obstet Biol Reprod (Paris)* **1995**, *24*, 522-528.

281. Locatelli, A.; Incerti, M.; Ghidini, A.; Greco, M.; Villa, E.; Paterlini, G. Factors associated with umbilical artery acidemia in term infants with low Apgar scores at 5 min. *Eur J Obstet Gynecol Reprod Biol* **2008**, *139*, 146-150.

282. Bordoni., J.R.H.B. *Embryology, Umbilical Cord*; Creighton University School of Medicine and Foundation Don Carlo Gnocchi IRCCS, 2021.

283. Larque, E.; Ruiz-Palacios, M.; Koletzko, B. Placental regulation of fetal nutrient supply. *Curr Opin Clin Nutr Metab Care* **2013**, *16*, 292-297.

284. Gloria, S.; Marques, J.; Feiteiro, J.; Marcelino, H.; Verde, I.; Cairrao, E. Tributyltin role on the serotonin and histamine receptors in human umbilical artery. *Toxicol In Vitro* **2018**, *50*, 210-216.

285. Feiteiro, J.; Santos-Silva, A.J.; Verde, I.; Cairrao, E. Testosterone and atrial natriuretic peptide share the same pathway to induce vasorelaxation of human umbilical artery. *J Cardiovasc Pharmacol* **2014**, *63*, 461-465.

286. Lorigo, M.; Cairrao, E. Fetoplacental vasculature as a model to study human cardiovascular endocrine disruption. *Mol Aspects Med* **2021**, 101054.

287. Aird, W.C. Endothelium. In *Consultative Hemostasis and Thrombosis (Third Edition)*, Kitchens, C.S., Kessler, C.M., Konkle, B.A., Eds.; W.B. Saunders: Philadelphia, 2013; pp. 33-41.

288. Frismantiene, A.; Philippova, M.; Erne, P.; Resink, T.J. Smooth muscle cell-driven vascular diseases and molecular mechanisms of VSMC plasticity. *Cell Signal* **2018**, *52*, 48-64.

289. Ringvold, H.C.; Khalil, R.A. Chapter Six - Protein Kinase C as Regulator of Vascular Smooth Muscle Function and Potential Target in Vascular Disorders. In *Advances in Pharmacology*, Khalil, R.A., Ed.; Academic Press: 2017; Volume 78, pp. 203-301.

290. Fernandez-Alfonso, M.S. Regulation of vascular tone: the fat connection. *Hypertension* **2004**, *44*, 255-256.

291. Landry, D.W.; Anubkumar, S.; Oliver, J.A. Chapter 4 - Vascular Tone. In *Clinical Critical Care Medicine*, Albert, R.K., Slutsky, A.S., Ranieri, V.M., Takala, J., Torres, A., Eds.; Mosby: Philadelphia, 2006; pp. 31-39.

292. Lorigo, M.; Mariana, M.; Feiteiro, J.; Cairrao, E. How is the human umbilical artery regulated? *J Obstet Gynaecol Res* **2018**, *44*, 1193-1201.

293. Santos-Silva, A.J.; Cairrao, E.; Marques, B.; Verde, I. Regulation of human umbilical artery contractility by different serotonin and histamine receptors. *Reprod Sci* **2009**, *16*, 1175-1185.

294. Santos-Silva, A.J.; Cairrao, E.; Verde, I. Study of the mechanisms regulating human umbilical artery contractility. *Health* **2010**, *02*, 321-331.

295. Martin, P.; Rebolledo, A.; Palomo, A.R.; Moncada, M.; Piccinini, L.; Milesi, V. Diversity of potassium channels in human umbilical artery smooth muscle cells: a review of their roles in human umbilical artery contraction. *Reprod Sci* **2014**, *21*, 432-441.

296. Lorigo, M.; Oliveira, N.; Cairrao, E. Clinical Importance of the Human Umbilical Artery Potassium Channels. *Cells* **2020**, *9*.

297. Feiteiro, J.; Rocha, S.M.; Mariana, M.; Maia, C.J.; Cairrao, E. Pathways involved in the human vascular Tetrabromobisphenol A response: Calcium and potassium channels and nitric oxide donors. *Toxicology* **2022**, *470*, 153158.

298. Vest, A.R.; Cho, L.S. Hypertension in pregnancy. *Curr Atheroscler Rep* **2014**, *16*, 395.

299. Naderi, S.; Tsai, S.A.; Khandelwal, A. Hypertensive Disorders of Pregnancy. *Curr Atheroscler Rep* **2017**, *19*, 15.

300. Filipek, A.; Jurewicz, E. [Preeclampsia - a disease of pregnant women]. *Postepy Biochem* **2018**, *64*, 232-229.

301. Folk, D.M. Hypertensive Disorders of Pregnancy: Overview and Current Recommendations. *J Midwifery Womens Health* **2018**, *63*, 289-300.

302. McLaughlin, K.; Snelgrove, J.W.; Sienas, L.E.; Easterling, T.R.; Kingdom, J.C.; Albright, C.M. Phenotype-Directed Management of Hypertension in Pregnancy. *J Am Heart Assoc* **2022**, e023694.

303. Peres, G.M.; Mariana, M.; Cairrao, E. Pre-Eclampsia and Eclampsia: An Update on the Pharmacological Treatment Applied in Portugal. *J Cardiovasc Dev Dis* **2018**, *5*.

304. Vesna D Garovic, R.D., Thomas Easterling, S Ananth Karumanchi, Suzanne McMurtry Baird, Laura A Magee, Sarosh Rana, Jane V Vermunt, Phyllis August, . Correction to: Hypertension in Pregnancy: Diagnosis, Blood Pressure Goals, and Pharmacotherapy: A Scientific Statement From the American Heart Association. *Hypertension* **2022**, *79*, e70.

305. Gupta, S.; Hanff, L.M.; Visser, W.; Steegers, E.A.; Saxena, P.R.; Vulto, A.G.; MaassenVanDenBrink, A. Functional reactivity of 5-HT receptors in human umbilical cord and maternal subcutaneous fat arteries after normotensive or pre-eclamptic pregnancy. *J Hypertens* **2006**, *24*, 1345-1353.

306. Sabolovic Rudman, S.; Mustapic, M.; Kosec, V.; Pivac, N.; Rudman, F.; Muck-Seler, D. Serotonin risk factors for the development of hypertension in pregnancy. *Arch Gynecol Obstet* **2015**, *291*, 779-785.

307. Gumusoglu, S.; Scroggins, S.; Vignato, J.; Santillan, D.; Santillan, M. The Serotonin-Immune Axis in Preeclampsia. *Curr Hypertens Rep* **2021**, *23*, 37.

308. Feng, X.; Zhang, Y.; Tao, J.; Lu, L.; Zhang, Y.; Liu, J.; Zhao, M.; Guo, J.; Zhu, D.; Zhu, J.; et al. Comparison of Vascular Responses to Vasoconstrictors in Human Placenta in Preeclampsia between Preterm and Later Term. *Curr Pharm Biotechnol* **2020**, *21*, 727-733.

309. Bolte, A.C.; van Geijn, H.P.; Dekker, G.A. Pathophysiology of preeclampsia and the role of serotonin. *Eur J Obstet Gynecol Reprod Biol* **2001**, *95*, 12-21.

310. Brew, O.; Sullivan, M.H. The links between maternal histamine levels and complications of human pregnancy. *J Reprod Immunol* **2006**, *72*, 94-107.

311. Pennington, K.A.; Schlitt, J.M.; Jackson, D.L.; Schulz, L.C.; Schust, D.J. Preeclampsia: multiple approaches for a multifactorial disease. *Dis Model Mech* **2012**, *5*, 9-18.

312. Chaiworapongsa, T.; Chaemsaithong, P.; Yeo, L.; Romero, R. Pre-eclampsia part 1: current understanding of its pathophysiology. *Nat Rev Nephrol* **2014**, *10*, 466-480.

313. Turpin, C.A.; Sakyi, S.A.; Owiredu, W.K.; Ephraim, R.K.; Anto, E.O. Association between adverse pregnancy outcome and imbalance in angiogenic regulators and oxidative stress biomarkers in gestational hypertension and preeclampsia. *BMC Pregnancy Childbirth* **2015**, *15*, 189.

314. Lamarca, B. Endothelial dysfunction. An important mediator in the pathophysiology of hypertension during pre-eclampsia. *Minerva Ginecol* **2012**, *64*, 309-320.

315. Opichka, M.A.; Rappelt, M.W.; Gutterman, D.D.; Grobe, J.L.; McIntosh, J.J. Vascular Dysfunction in Preeclampsia. *Cells* **2021**, *10*.

316. Rutherford, R.A.; McCarthy, A.; Sullivan, M.H.; Elder, M.G.; Polak, J.M.; Wharton, J. Nitric oxide synthase in human placenta and umbilical cord from normal, intrauterine growth-retarded and pre-eclamptic pregnancies. *Br J Pharmacol* **1995**, *116*, 3099-3109.

317. Myatt, L.; Webster, R.P. Vascular biology of preeclampsia. *J Thromb Haemost* **2009**, *7*, 375-384.

318. Bueno-Pereira, T.O.; Nunes, P.R.; Matheus, M.B.; Vieira da Rocha, A.L.; Sandrim, V.C. Nebivolol Increases Nitric Oxide Synthase via beta3 Adrenergic Receptor in Endothelial Cells Following Exposure to Plasma from Preeclamptic Patients. *Cells* **2022**, *11*.

319. Boron, D.; Kornacki, J.; Wender-Ozegowska, E. The Assessment of Maternal and Fetal Intima-Media Thickness in Perinatology. *J Clin Med* **2022**, *11*.

320. Leung, S.W.; Quan, A.; Lao, T.T.; Man, R.Y. Efficacy of different vasodilators on human umbilical arterial smooth muscle under normal and reduced oxygen conditions. *Early Hum Dev* **2006**, *82*, 457-462.

321. Rockelein, G.; Schneider, R. [Three-dimensional analysis of the tunica media of umbilical arteries. Scanning electron microscopy study]. *Z Geburtshilfe Perinatol* **1992**, *196*, 266-272.

322. Junek, T.; Baum, O.; Lauter, H.; Vetter, K.; Matejevic, D.; Graf, R. Pre-eclampsia associated alterations of the elastic fibre system in umbilical cord vessels. *Anat Embryol (Berl)* **2000**, *201*, 291-303.

323. Inan, S.; Sanci, M.; Can, D.; Vatansever, S.; Oztekin, O.; Tinar, S. Comparative morphological differences between umbilical cords from chronic hypertensive and preeclamptic pregnancies. *Acta Med Okayama* **2002**, *56*, 177-186.

324. Thomas, M.R.; Bhatia, J.K.; Kumar, S.; Boruah, D. The histology and histomorphometry of umbilical cord cross section in preeclampsia and normal pregnancies: a comparative study. *J Histotechnol* **2020**, *43*, 109-117.

325. Saw, S.N.; Dai, Y.; Yap, C.H. A Review of Biomechanics Analysis of the Umbilical-Placenta System With Regards to Diseases. *Front Physiol* **2021**, *12*, 587635.

326. Kuo, I.Y.; Wolfle, S.E.; Hill, C.E. T-type calcium channels and vascular function: the new kid on the block? *J Physiol* **2011**, *589*, 783-795.

327. Sonkusare, S.; Palade, P.T.; Marsh, J.D.; Telemaque, S.; Pesic, A.; Rusch, N.J. Vascular calcium channels and high blood pressure: pathophysiology and therapeutic implications. *Vascul Pharmacol* **2006**, *44*, 131-142.

328. Pinterova, M.; Kunes, J.; Zicha, J. Altered neural and vascular mechanisms in hypertension. *Physiol Res* **2011**, *60*, 381-402.

329. Joseph, B.K.; Thakali, K.M.; Moore, C.L.; Rhee, S.W. Ion channel remodeling in vascular smooth muscle during hypertension: Implications for novel therapeutic approaches. *Pharmacol Res* **2013**, *70*, 126-138.

330. Sobey, C.G. Potassium channel function in vascular disease. *Arterioscler Thromb Vasc Biol* **2001**, *21*, 28-38.

331. Korovkina, V.P.; England, S.K. Detection and implications of potassium channel alterations. *Vascul Pharmacol* **2002**, *38*, 3-12.

332. Cox, R.H.; Fromme, S.J.; Folander, K.L.; Swanson, R.J. Voltage gated K+ channel expression in arteries of Wistar-Kyoto and spontaneously hypertensive rats. *Am J Hypertens* **2008**, *21*, 213-218.

333. Cox, R.H. Changes in the expression and function of arterial potassium channels during hypertension. *Vascul Pharmacol* **2002**, *38*, 13-23.

334. Cox, R.H. Molecular determinants of voltage-gated potassium currents in vascular smooth muscle. *Cell Biochem Biophys* **2005**, *42*, 167-195.

335. Brown, B.M.; Shim, H.; Christophersen, P.; Wulff, H. Pharmacology of Small- and Intermediate-Conductance Calcium-Activated Potassium Channels. *Annu Rev Pharmacol Toxicol* **2020**, *60*, 219-240.

336. Amberg, G.C.; Bonev, A.D.; Rossow, C.F.; Nelson, M.T.; Santana, L.F. Modulation of the molecular composition of large conductance, Ca(2+) activated K(+) channels in vascular smooth muscle during hypertension. *J Clin Invest* **2003**, *112*, 717-724.

337. Amberg, G.C.; Santana, L.F. Downregulation of the BK channel beta1 subunit in genetic hypertension. *Circ Res* **2003**, *93*, 965-971.

338. Zhao, G.; Zhao, Y.; Pan, B.; Liu, J.; Huang, X.; Zhang, X.; Cao, C.; Hou, N.; Wu, C.; Zhao, K.S.; et al. Hypersensitivity of BKCa to Ca2+ sparks underlies hyporeactivity of arterial smooth muscle in shock. *Circ Res* **2007**, *101*, 493-502.

339. Nelson, M.T.; Cheng, H.; Rubart, M.; Santana, L.F.; Bonev, A.D.; Knot, H.J.; Lederer, W.J. Relaxation of arterial smooth muscle by calcium sparks. *Science* **1995**, *270*, 633-637.

340. Eichhorn, B.; Dobrev, D. Vascular large conductance calcium-activated potassium channels: functional role and therapeutic potential. *Naunyn Schmiedebergs Arch Pharmacol* **2007**, *376*, 145-155.

341. Dietrich, A.; Chubanov, V.; Kalwa, H.; Rost, B.R.; Gudermann, T. Cation channels of the transient receptor potential superfamily: their role in physiological and pathophysiological processes of smooth muscle cells. *Pharmacol Ther* **2006**, *112*, 744-760.

342. Inoue, R.; Jensen, L.J.; Shi, J.; Morita, H.; Nishida, M.; Honda, A.; Ito, Y. Transient receptor potential channels in cardiovascular function and disease. *Circ Res* **2006**, *99*, 119-131.

343. Nilius, B.; Owsianik, G.; Voets, T.; Peters, J.A. Transient receptor potential cation channels in disease. *Physiol Rev* **2007**, *87*, 165-217.

344. Karadas, B.; Kaya, T.; Cetin, M.; Parlak, A.; Durmus, N.; Bagcivan, I.; Gulturk, S. Effects of formoterol and BRL 37344 on human umbilical arteries in vitro in normotensive and pre-eclamptic pregnancy. *Vascul Pharmacol* **2007**, *46*, 360-366.

345. Lucas, K.A.; Pitari, G.M.; Kazerounian, S.; Ruiz-Stewart, I.; Park, J.; Schulz, S.; Chepenik, K.P.; Waldman, S.A. Guanylyl Cyclases and Signaling by Cyclic GMP. **2000**, *52*, 375-414.

346. Martin, E.; Berka, V.; Tsai, A.L.; Murad, F. Soluble guanylyl cyclase: the nitric oxide receptor. *Methods Enzymol* **2005**, *396*, 478-492.

347. Mergia, E.; Friebe, A.; Dangel, O.; Russwurm, M.; Koesling, D. Spare guanylyl cyclase NO receptors ensure high NO sensitivity in the vascular system. *J Clin Invest* **2006**, *116*, 1731-1737.

348. Ruetten, H.; Zabel, U.; Linz, W.; Schmidt, H.H. Downregulation of soluble guanylyl cyclase in young and aging spontaneously hypertensive rats. *Circ Res* **1999**, *85*, 534-541.

349. Kloss, S.; Bouloumie, A.; Mulsch, A. Aging and chronic hypertension decrease expression of rat aortic soluble guanylyl cyclase. *Hypertension* **2000**, *35*, 43-47.

350. Uehata, M.; Ishizaki, T.; Satoh, H.; Ono, T.; Kawahara, T.; Morishita, T.; Tamakawa, H.; Yamagami, K.; Inui, J.; Maekawa, M.; et al. Calcium sensitization of smooth muscle mediated by a Rho-associated protein kinase in hypertension. *Nature* **1997**, *389*, 990-994.

351. Behuliak, M.; Bencze, M.; Vaneckova, I.; Kunes, J.; Zicha, J. Basal and Activated Calcium Sensitization Mediated by RhoA/Rho Kinase Pathway in Rats with Genetic and Salt Hypertension. *Biomed Res Int* **2017**, *2017*, 8029728.

352. Friel, A.M.; Sexton, D.J.; O'Reilly M, W.; Smith, T.J.; Morrison, J.J. Rho A/Rho kinase: human umbilical artery mRNA expression in normal and pre eclamptic pregnancies and functional role in isoprostane-induced vasoconstriction. *Reproduction* **2006**, *132*, 169-176.

353. Friel, A.M.; Hynes, P.G.; Sexton, D.J.; Smith, T.J.; Morrison, J.J. Expression levels of mRNA for Rho A/Rho kinase and its role in isoprostane-induced vasoconstriction of human placental and maternal vessels. *Reprod Sci* **2008**, *15*, 179-188.

354. Yang, S.M.; Peng, W.; Ye, Y.H.; Zhan, Y. [Expression and significance of Rho-associated protein kinase II in preeclamptic placenta and umbilical artery]. *Zhonghua Fu Chan Ke Za Zhi* **2008**, *43*, 32-35.

355. Lorigo, M.; Quintaneiro, C.; Maia, C.J.; Breitenfeld, L.; Cairrao, E. UV-B filter octylmethoxycinnamate impaired the main vasorelaxant mechanism of human umbilical artery. *Chemosphere* **2021**, *277*, 130302.

356. Lorigo, M.; Quintaneiro, C.; Breitenfeld, L.; Cairrao, E. UV-B Filter Octylmethoxycinnamate Alters the Vascular Contractility Patterns in Pregnant Women with Hypothyroidism. *Biomedicines* **2021**, *9*.

Chapter 2

Introduction- Part B- An overview of the TBBPA effect: From environmental to human exposure

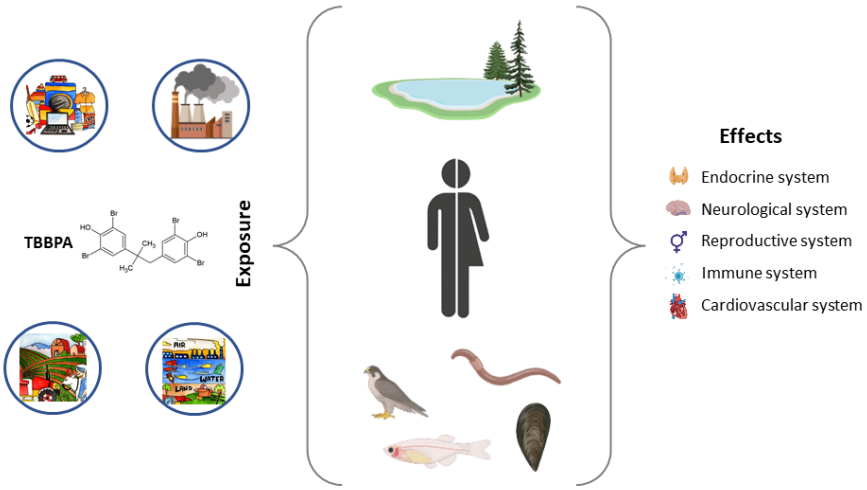

This chapter is adapted from the review article:

Joana Feiteiro, Melissa Mariana, Elisa Cairrão (2021). Health toxicity effects of Brominated Flame Retardants: From environmental to human exposure. Environmental Pollution. Volume 285, 15 September 2021, 117475, https://doi.org/10.1016/j.envpol.2021.117475.

2. Tetrabromobisphenol A (TBBPA)

2.1. Physical-chemical properties of TBBPA

TBBPA (tetrabromobisphenol A or 2,6-Dibromo-4-[2-(3,5-dibromo-4-hydroxyphenyl)propan-2yl]phenol) (Figure 2.1), as previously described, is one of the most prevalent bromo flame retardants (BFRs) in the world. Its main application is in epoxy resin used to produce printed circuit boards, in which the bromine content can reach 20 % by weight. About 90 % is a reactive BFR covalently bound to the polymer structure, therefore TBBPA is less likely to be released into the environment than additive BFRs [1-5]. Its structure is due to bromination of bisphenol A, with a molecular weight of 543.9 g/mol, and at 20 °C, TBBPA is an off-white crystalline powder [2,3,5,6]. TBBPA is considered a lipophilic (log Kow=4.5) compound, with high volatility and low solubility in water (0.72 mg/mL). Generally, TBBPA is not found in water samples, being measured in the air [1], sediment and soil [7,8]. An important chemical property is the aromatic structure of TBBPA containing two phenolic groups with a pka1 and pka2 values of 7.5 and 8.5, respectively [9], which allows that, in neutral environmental conditions, TBBPA is in the dissociation phase. Its chemical properties have an important effect on the distribution and behaviour of TBBPA in different environmental and biotic systems [10]. For example, when the pH increases the TBBPA solubility increases, this solubility value is higher than in the other BFRs namely PBDEs and HBCD [11,12] at neutral pH [13]. Thus, these unique characteristics of TBBPA must be considered when studying the effect of these BFRs on the environment, as well as the analytical methodology used to measure their levels in several biotic and abiotic samples [14,15]. In biological samples, TBBPA has been found in umbilical cord serum, human milk, and egg of birds. TBBPA can also be used as a base compound to produce other commercial flame retardants, such as Tetrabromobisphenol A dihydroxyethly ether (TBBPA-DHEE), Tetrabromobisphenol A-bis (2,3-dibromopropyleter) (TBBPA-DBPE) and Tetrabromobisphenol A bis (alkyl ether) (TBBPA-BAE) [14]. Regarding to their physical-chemical properties, these derivatives present a molecular weight of 632, 624 and 944 g/mol, respectively. The Log Kow value for TBBPA-DHEE is 6.02 ± 0.68, for TBBPA-DBPE is 9.99 ± 1.56 and for TBBPA-BAE is 6.24 ± 1.03. These low production volume chemicals are highly hydrophobic and have low volatility, hence they have a low long-range atmospheric transport [14,16,17]. Nevertheless, these TBBPA derivates can also have adverse effects on health since they are biologically active.

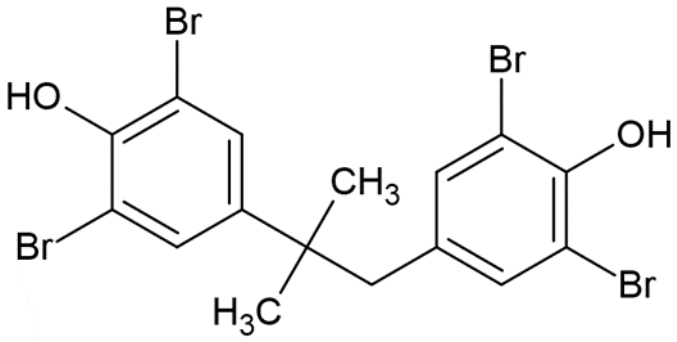

Figure 2.1. Chemical structure of Tetrabromobisphenol (TBBPA)

2.2. TBBPA in the environment

Regarding the environment TBBPA has been detected in water, dust, air, soil and consequently in fish and aquatic food [18-32]. Several studies show that China is the country where higher levels of TBBPA are detected [33]. For instance, it has detected in soils ranging from 1.64 to 7758 ng/g dw [18], in office air at 511 pg/m3 and in dust up to 59.140 ng/g dw [21]. In addition, TBBPA has been found in food, for example, in aquatic food samples the levels of this compound range from 3.05-207.3 ng/g lw, in meat 1.78 ng/g lw, in eggs 3.12 ng/g lw and 5.76 ng/g lw in milk [33-35]. These are very perturbing results since, besides being found in the environment, the detection in these food samples increases the human exposure to this compound and its adverse effects.

TBBPA is discharged into the aquatic environment through the migration from TBBPA-based products, and the effluent from wastewater treatment plants and landfill sites [36]. Again, most of these studies were carried out in China and the levels of TBBPA detected in waters were lower than 10 ng/L except for Yellow River (320 ng/L) [37], Qinghe River (23.9- 224 ng/L) [38] and Chaohu Lake (850-4870 ng/L) [39]. TBBPA is detrimental to a variety of aquatic organisms, with adverse effects on survival, reproduction, and development at very low concentrations [40]. However, the concentrations of TBBPA in the aquatic environment in China were well below the thresholds, since in terms of aquatic exposure, the Chinese criterion maximum concentration (CMC) is 0.1475 mg/L and criterion continuous concentration (CCC) is 0.0126 mg/L [29].

In dust matrices of a typical PCB (printed circuit board) manufacturing plant, in Eastern China, Zhou *et al.* quantified the TBBPA concentration, being 2660 ng/g dw. These values indicated that the TBBPA contamination occurred primarily in the form of sedimentary dust rather than suspended particular matter in PCB production [41]. The electronic waste recycling is another type of TBBPA polluted areas. Wu *et al.* noted that the average concentration of indoor TBBPA at e-waste recycling site from Taizhou (3435 ng/g dw) was much higher compared to the outdoor (1998 ng/g dw) [22]. Other studies showed that the mean concentration of TBBPA near to a garbage dumpling site from Wuhan was up to 24.030 ng/g dw, ranging from 17.510-39.620 ng/g dw [21,42]. However, the highest TBBPA concentration was 2300 ng/g dw and was observed in dust samples from Chinese houses. These results suggested that TBBPA has been identified in occupational, household, and environmental dust samples, thus posing a potential risk from oral, dermal and inhalation exposures, especially among children via hand-to-mouth contact [43].

When it comes to air samples, there are very few reports on concentrations of TBBPA, as expected, since TBBPA has low vapor pressure and high lipophilicity. Ni *et al.* investigated the TBBPA levels in particulate phase of indoor air from Shenzhen, China, while Zhou *et al.* conducted the study at the PCB plant in Eastern China (mentioned above), reporting TBBPA concentrations of 12.3-1640 pg/m and 6.26-511 pg/m, respectively [21,41]. In addition, in an e-waste recycling site of Guiyu, China, extremely high concentrations of TBBPA were found (66.010-95.040 pg/m) [44]. Several authors determined that the TBBPA levels in indoor air were significantly higher than those in outdoor air, suggesting that the potential emission sources of TBBPA can be from indoor electrical and electronic equipment, furnishing materials and textiles [2,28,45-47].

The soil would be expected to constitute the major TBBPA contamination site. The high levels of TBBPA contamination have been reported in soil around an electronic waste recycling of Qingyuan, China [23,48], reaching up to 780 ng/g dw. Furthermore, the concentrations of TBBPA in soils changed between different types of land used, for example, dismantling sites, industrial areas, residential area and farmland soils. TBBPA was also detected in soils of the Tibetan Plateau [23], in industrial soils from Spain [49] and in soils from an e-waste recycling workshop in Vietnam [50]. In China, the soil TBBPA concentrations were generally higher than the concentrations found in Spain [49] but lower than those of Vietnam [50].

According to the data presented above, indoor dust would be the environmental matrix where TBBPA accumulates the most. This is a worrying fact, since the human being spends a considerably amount of time indoor, being more exposed to TBBPA and increasing the risk of adverse health outcomes.

2.3. Exposure pathways and bioaccumulation of TBBPA

Several researchers have been studying the main exposure pathways of TBBPA, among which are inhalation, ingestion and, in a less extent, dermal contact. Regarding this latter pathway, Makinen *et al.* performed a study to quantify the levels of TBBPA in workers of an electronics dismantling facility and a circuit board factory in Finland. They found low levels of TBBPA in patch samples attached to workers' clothes (<0.09– 63 ng/cm2) and it was undetectable in handwash samples (<2 ng/hands) [51]. A different study, using human skin models in vitro, showed that the absorption of TBBPA depends on several factors, including the contact time and the applied dose, concluding that the absorption of TBBPA ranged between 5.4-6.8 % of the applied dose [43,52]. Corroborating these values, another in vitro study performed by Knudsen and co-workers, determined a penetration of TBBPA through skin of 3.5 % in 24h [53-55]. It was also demonstrated that, when applied at 2 mg/cm2, the bioavailability of TBBPA was <2 % (in 24 hours, 0.73 % penetrated and 0.9 % accumulated in the skin) [56]. In an ex vivo study, the values of relative penetration and absorption in human skin were 0.2 % and 53 %, respectively [54]. Even if dermal absorption is low, it is important to consider that the half-life of TBBPA in human plasma is relatively long (48-72 hours) and that upon absorption TBBPA is rapidly metabolized [57,58]. Despite the low levels of penetration and absorption, TBBPA dermal exposure is an important exposure pathway, mainly in children due to high levels of household dust and being often on the

floor. So, more studies in human skin should be performed to better elucidate this exposure pathway.

Regarding exposure to TBBPA through food ingestion, there are still few studies, however, exposure to TBBPA through breastfeeding has been reported. In 2009, Shi and collaborators quantified the estimated daily intake (EDI) of TBBPA in Chinese breastfeeding babies, from 1-6 months old. The results showed an EDI ranging from 2.5–290.5 ng/day, with an average of 39.7 ng/day [32]. In a different study, the average TBBPA daily intake through breastfeeding was 1 ng/kg bw for a 1-month-old UK infant [59], ranging from 0.04 to 3.1 ng/kg bw in a USA infant, and, more recently, Fujii *et al.* determined the daily intake in Japanese infants, being 3.4 ng/kg bw [60]. Considering that the provisional tolerable daily intake (TDI) is 1 mg/kg bw/day, all these studies show that the exposure of infants to TBBPA through breast milk is very low. On the other hand, it has been demonstrated a pre-natal exposure to TBBPA, since this compound has been detected in umbilical cord from Japanese pregnant women [61]. In a less extent, the exposure though the intake of food of animal origin has been less studied and less detected. In mussels, oysters, and scallops from Scotland, TBBPA has not been detected [62], nor in several fish and shellfish samples from the Netherlands [63]. In a Chinese study, it was reported that meat products are the main source of TBBPA, with the average daily intake of TBBPA of diet samples being 256 pg/kg bw for an adult [32]. Although TBBPA is not detected in some animal food species or is detected in other species at low levels, the studies presented, in addition to being few, have small sample sizes, making it difficult to reach a conclusion regarding the exposure of TBBPA by food intake.

TBBPA metabolism studies in humans showed that, 2-6 hours upon oral ingestion of 0.1 mg/kg bw of TBBPA, there was a peak concentration of the main compound and its conjugate, suffering a decrease to the limit of detection at 8 hours [58].

Another route of exposure is inhalation, which can occur by air, dust and diet. In a UK population-based study, the average of indoor and outdoor air inhaled from adults and children were 6.4 % and 2 % to the daily intake, respectively [28]. The same way, since dust can either be inhaled or ingested, these authors determined that the average daily intake of TBBPA ingested was 34 % for adults and 90 % for children [28]. Later, Batterman *et al.* quantified the levels of TBBPA in air, dust, ventilation system filters and carpets of several buildings in a city of the USA, concluding that this compound was only found in 30 % of the buildings tested in a range of 12-86 pg/m3 [64].

Takigami *et al.* compared the inhaled and the ingested dust in Japanese people. Inhabitants of two houses were exposed to different doses of TBBPA, in house 1 the doses were 67 pg/day and 37 pg/day, for adults and children, respectively, and house 2 were 210 pg/day and 114 pg/day. The authors concluded that inhalation of TBBPA, compared to ingestion, has a small contribution to overall exposure [47]. However, this study does not present a significant sample, with only habitants of two houses being tested. In an adult Chinese population, the inhaled and ingested dust from air-conditioner filters was quantified. The results of this study are in accordance with Takigami *et al.*, showing a much higher intake of TBBPA from ingested dust, 966 pg/kg bw/day, compared to the inhaled, 18 pg/kg bw/day. Besides, the authors also revealed that 29 pg/kg bw/day ($PM_{2.5}$) bound TBBPA can be inhaled deep into the lungs and 15 pg/kg bw/day (PM_{10}) bound

TBBPA stays in the upper respiratory system [21]. Occupational exposure of Chinese workers in an electronic factory also showed a higher exposure through ingestion (1930 pg/kg bw/day) than dermal absorption (431 pg/kg bw/day) or inhalation (96.5 pg/kg bw/day) [41].

As mentioned, several studies point to a greater exposure to TBBPA by dust ingestion, thus many epidemiological research have focused on this pathway. In 2009, Geens *et al.* determined the levels of house and office dust ingested by adults and children in Belgium. The authors found an average intake of TBBPA in adults of 0.2 ng/day with a maximum of 34 ng/day, while in children the average was 0.5 ng/day with the highest value 138 ng/day [65]. In a Chinese region, samples from electronic waste recycling were tested for TBBPA, having much higher concentration in indoor dust than outdoor dust, 3435 and 1998 ng/g, dw, respectively [22]. In addition, the authors also tested TBBPA levels in adults and children from that region, reporting high concentrations of this flame retardant, ranging from 0.04–7.50 ng/kg bw/day for adults and 0.31–58.54 ng/kg bw/day for children [22]. In the same way, and having results that corroborate the studies mentioned, Wang *et al.* performed a much broader study, quantifying TBBPA in indoor dust of 12 different countries. With an estimated daily intake 10 times higher than in other countries are infants and children from Japan, South Korea, and China. Overall, the intake of TBBPA is proportional to age, being higher in babies (0.01-3.4 ng/kg bw/day) and children (0.01 to 1.2 ng/kg bw/day) and decreasing in adolescents (0.003 to 0.61 ng/kg bw/day) and adults (0.001 to 0.28 ng/kg bw/day) [66]. Although it is understandable why children are more susceptible to ingest more TBBPA than adults, due to walking on the floor and the hand-to-mouth behaviour, it is a much more worrying fact, due to their body weight and weaker defences.

When it comes to animals, there are still few studies relating the TBBPA and most of them is performed in fish. It has been shown that this compound is rapidly accumulated and absorbed in several aquatic organisms, including scallop, bluegill sunfish and zebrafish [67-69], with rates of bioaccumulation and metabolism of 19.33 % and 8.88 %, respectively [69]. Regarding dermal absorption, Yu *et al.* have focused on the relative absorption of TBBPA. *In vivo* studies using Wistar rats dermally exposed to a maximum of 600 mg/kg for 6 hours/day (90 days), the relative absorption was 3-11 % and 3-13 % in male and female rats, respectively. At 24 hours after exposure, the relative absorption was 24.7 % for male and 20.1 % for female rats [70-72]. Knudsen and colleagues demonstrated a penetration of TBBPA through skin of 1 % with an absorption of 26 %, in an *in vivo* study performed in rats [55]. It has been demonstrated that TBBPA has a low dermal bioavailability when compared to other BFRs. Upon exposure (100 nmol/cm^2) for 24 h, TBBPA bioavailability is around 1-2 %, being <1 % for a 10-fold higher dose [54], while, for bisphenol A (nonbrominated TBBPA analogue) is 9 % [73].

Dermal and oral exposure of TBBPA have similar disposition and kinetic profiles in rats [54,55,73]. *In vivo* studies performed in rats have shown that upon oral administration TBBPA is rapidly absorbed [53,74,75]. After 4-6 hours, TBBPA and its main metabolites (TBBPA-glucuronide (TBBPA-GA) and TBBPA-sulfate (TBBPA-S)) levels reach their maximum, being then rapidly eliminated [58]. In 2001, Szymanska and collaborators, tested the effects of a single dose of TBBPA in male rats. Upon intraperitoneal injection of 250 mg/kg of TBBPA-[14C]-labelled, the authors detected a 14C peak in 1 hour, and the highest concentrations were found in fat tissue, liver, sciatic

nerve, muscles, and adrenals [76]. Similarly, in 2006, male rats were orally administered a TBBPA dose of 300 mg/kg, with the concentration peak of TBBPA (103 mmol/L) and TBBPA-GA (25 mmol/L) being observed in 3 hours, and TBBPA-S (694 mmol/L) in 6 hours [58]. It has been demonstrated that the higher TBBPA dose administered the higher the concentration of TBBPA and its metabolites in the liver, plasma, and uterine tissue [77]. A more recent study showed that TBBPA administration to pregnant and nursing Wistar rats will affect the foetus and offspring [78]. It is now important to discover how will this maternal exposure affect the next generation. As it was previously mentioned, the TBBPA main metabolites are TBBPA-GA and TBBPA-S that derive from the conjugation of TBBPA with glucuronic acid and with sulfate, by glucuronyl- and sulfotransferases in the liver. In addition, TBBPA can suffer a reduction through intestinal microflora originating tribromobisphenol A, that can suffer a conjugation with glucuronic acid. These metabolites are excreted in the faeces, bile, and in a small part in urine, after TBBPA conjugates undergo enterohepatic recirculation. In humans, an effective elimination in the bile will originate a decrease in the TBBPA systemic bioavailability [58].

Regarding excretion of TBBPA, it has been demonstrated that the main route are the faeces. In 2000, Hakk *et al.* showed that 92 % of total TBBPA administered to male rats were excreted in faeces with only 0.3 % in urine (72 hours) [79]. Later, Kuester and collaborators performed a similar study in female rats orally exposed to different doses of TBBPA (25, 250, and 1000 mg/kg), obtaining an excretion > 90 % in faeces and 2 % in urine at 72 hours [53]. It has also been demonstrated a delayed and slower faecal excretion after a single, high dose of TBBPA (1000 mg/kg) [74]. Overall, from the reports described previously, the most important exposure pathway of TBBPA is dust ingestion, however, in children dermal contact should also be considered due to high levels of household dust and being often on the floor. Besides, another important feature of TBBPA exposure is the age, since the intake of TBBPA has been reported to be higher in babies and children than in adolescents and adults, which may be due to walking on the floor and the hand-to-mouth behaviour. On the other hand, in rats, dermal and oral exposure have similar disposition and kinetics, and the administration of TBBPA to pregnant and nursing rats will affect the future generation. Despite these studies are pointing in the same direction, with similar conclusions, more experiments regarding absorption, metabolism and excretion should be performed, both in humans and animals.

2.4. Toxicity studies in animals

Several studies about toxicity effects of TBBPA were developed and performed in different animals, mainly in rodents. In fish and vertebrates, TBBPA exerts a small acute toxicity. Some studies in rats showed that TBBPA has an endocrine activity which can alter thyroid hormone levels. In addition to this activity, TBBPA causes neurotoxicity, nephrotoxicity and hepatotoxicity, and carcinogenicity studies suggest that TBBPA increases the incidence of uterine tumours in rats. Exposure to TBBPA can also cause reproductive, development and neurobehavioral effects. All the TBBPA effects in animals described in this review are summarized in table 2.1.

Godfrey *et al.* used zebrafish embryos to study the acute toxicity of TBBPA and observed that after 96 hours exposure to TBBPA the lethal concentration (LC50) was 1.3 mg/L [80]. These LC50 values were similar to those found for fathead minnow *Pimephales promelas* [81,82] and rainbow trout *Oncorhynchus mykiss* with 96 h LC50 values ranging from of 0.54-1.1 mg/L [82]. Wollenberger *et al.* reported a 48 h LC50 of 0.40 mg/L (0.37–0.43 mg/L) for the copepod *Acartia tonsa* [83]. Other studies in *Eisenia fetida* and earthworm species *Metaphire guillelmi*, found that the 14-day LC50 for TBBPA was >500 mg/ kg and 39 mg/kg, respectively [84].

Using rats and mice, Covaci and his co-workers performed oral administration studies and demonstrated that TBBPA has a low acute toxicity in these animals, with LD50 > 5 for rats and >4 g/kg for mice [4,85]. This low toxicity of TBBPA in rodents is consistent with the low availability [4], however, studies of oral toxicity in these animals have shown that TBBPA induces changes in thyroid hormone. Kitamura *et al.* performed toxicity studies regarding thyroid hormonal activity of TBBPA in rat pituitary cell lines (GH3 cells), isolated from pituitary tumour, and enhanced the proliferation of GH3 cells [86]. In addition, TBBPA also increased rat pituitary cell lines (MtT/E-2 cells) proliferation, and this growth was oestrogen-dependent. So, Kitamura and his co-workers suggested that TBBPA acts as thyroid hormone agonist, as well as oestrogen agonist [86]. These results are similar to other studies that showed that TBBPA effect is thyroid hormone-like and oestrogen receptor mediated [87-91]. Namely, Ghirsari *et al.* observed that TBBPA potentially disrupt the steroid hormone function including thyroid hormone dependent growth of GH3 cells [88]. In addition, *in vitro* studies have shown that TBBPA can inhibit oestradiol sulfation through oestrogen sulfotransferase, leading to increased oestradiol bioavailability [87]. On the other hand, in Chinese hamster ovary cells and African green monkey kidney cell line CV-1 transiently transfected with T3 receptors, TBBPA induces an antagonizing effect of the thyroid, and an inhibition of the binding of triiodothyronine (T3) to thyroid hormone receptors [92,93]. Furthermore, studies using male Wistar WU rats microsomes demonstrated that TBBPA is a strong inhibitor for the binding of T4 to transthyretin and this binding was greater than that of the natural ligand T4 [94].

Several studies have indicated that TBBPA did not affect the neurological system. Studies conducted in neonatal mice exposed to 0.75 or 11.5 mg/kg bw of TBBPA for 10 days, demonstrated that this flame retardant did not result in neurobehavioral changes in adult mice, with no effects on motor activity, spatial learning and memory [95-97]. However, neurological impairments have been observed in animals exposed to TBBPA. In rats exposed to 250 mg/kg/day of TBBPA for 50 days, there were alterations in the neurobehavior of offspring, with changes in habituation of activity, learning and memory [98,99], being consistent with a similar study performed by Lilienthal *et al.* (2008), where the same dose orally administered for 50 days led to impaired habituation of activity and spatial learning [97]. *In vitro* studies, using different neuronal cell cultures, have also confirmed the TBBPA neuronal toxicity [33,100,101]. In 2003, Mariussen *et. al* concluded that an exposure of 3 mM of TBBPA led to a reduction of dopamine and GABA uptake in brain synaptosomes [102]. In cerebellar granule cells primary neurons, it was demonstrated that TBBPA leads to an increase in intracellular [Ca^{2+}] and to cell death, which is reduced by NMDA receptors antagonists [103]. Ogunbayo *et al.* also observed that TBBPA led to cell death through

Ca^{2+} release via RyR in mouse TM4 Sertoli cells [104]. These two studies are in agreement with the one performed by Zieminska *et al.*, where the release of intracellular Ca^{2+} concentrations ($[Ca^{2+}]_i$) by RyR and the increase of neurons $[Ca^{2+}]_i$ by NMDA receptors are part of the TBBPA mechanism in cerebellar granule cells [105]. From these studies reported, it is possible to conclude TBBPA leads to intracellular calcium imbalance, which may be part of TBBPA neuronal excitotoxicity mechanism.

Regarding nephrotoxicity and hepatotoxicity of TBBPA, few studies have been published to date. Fukuda *et al.* tested an exposure of 200 and 600 mg/kg of TBBPA in new-born rats, which resulted in the formation of polycystic lesions, demonstrating TBBPA nephrotoxicity [106]. In contrast, Kang *et al.* did not demonstrate this toxicity of TBBPA. In this study, Sprague-Dawley rats (male) were exposed to different concentrations of TBBPA for 14 days and the nephrotoxic potential and its toxicokinetics were evaluated. The results proposed that at high concentrations TBBPA may produce transient oxidative stress in kidneys. Still, this response may not be toxic, since the half-life of TBBPA is short, it was completely eliminated in faeces and had a low distribution in the kidneys [107]. In addition to being contradictory, these studies should not be comparable, since they used rats of different ages, which implies a different physiology, and consequently TBBPA promotes different responses. So, more studies must be performed to understand if TBBPA is nephrotoxic or not. In ICR mice (specific pathogen-free male Crlj:CD1 mice), a prenatal and postnatal exposure to 1 % TBBPA led to hepatic and kidney lesions, and, upon an exposure of 350 and 1400 mg/kg bw for 14 days, there was an increase in the livers' weight and focal necrosis, or slight enlargement of hepatocytes were also observed [108,109]. Using rat hepatocytes exposed to 0.25 and 1.0 mM of TBBPA, Nakagawa *et al.* observed a decrease in intracellular ATP, adenine nucleotides, glutathione, and protein thiols [110]. Suh *et al.*, using rat pancreatic β-cells (the RIN-m5F cell line), investigated the effects of TBBPA and observed that it increased the levels of inflammatory cytokines (Factor de necrose tumoral alfa (TNF-α) and interleukin 1 beta (IL-1β)), nitric oxide, intracellular ROS and mitochondrial superoxide. Consistently, exposure to TBBPA damages pancreatic β-cells by triggering mitochondrial dysfunction and inducing apoptosis [111]. Canesi *et al.* determined the possible effects and mechanisms of TBBPA on the immune cells, and for that the authors used haemocytes of the marine mussel Mytilus galloprovincialis [112], and showed that TBBPA, in the low concentrations, induced haemocyte lysosomal membrane destabilization. The effect was reduced or prevented by haemocyte pre-treatment by specific inhibitors of mitogen-activated protein kinase (MAPK) and protein kinase C (PKC), so, these researchers concluded that TBBPA activates the immune function by kinase-mediated cell signalling and that common transduction pathways are involved in mediating the effects of this BFR in mammalian and aquatic invertebrate cells [112]. Choi *et al.* carried out experiments to analyse the possible involvement of TBBPA in the oxidative stress in osteoblastic MC3T3-E1 cells [113]. The authors measured cell viability, apoptosis, ROS, mitochondrial superoxide and mitochondrial parameters. The results showed that TBBPA induced cardiolipin peroxidation, cytochrome c release and decreased cyclophilin A and B, ATP levels which induced apoptosis or necrosis and decreased the differentiation markers, collagen synthesis, alkaline phosphatase activity, and calcium deposition in these cells. Therefore, TBBPA inhibits

osteoblast function and has effects on osteoblasts through a pathway involving mitochondrial dysfunction and oxidative stress [113]. Recently, a study performed by Park *et al.* in RAW264.7 mouse macrophage cell line, a well-known in vitro model of osteoclastogenesis [114], showed that TBBPA enhanced TRAP (marker enzyme for osteoclasts) activity and osteoclast differentiation. This TBBPA pathway might include increased expression of several genes involved in osteoclast differentiation and reactive oxygen species production [115].

In general, it can be said that TBBPA induces chronic toxicity in several animal species, including zebrafish, fathead minnow, rainbow trout, copepod, *Eisenia fetida*, earthworm and marine mussel. In rodents, TBBPA has been shown to have low acute toxicity and low availability. Being consistent with several reports, TBBPA is suggested to act as thyroid hormone and oestrogen agonist. Besides, it was demonstrated that this compound affects the osteoblasts through a pathway involving mitochondrial dysfunction and oxidative stress. On the other hand, inconsistent results have been shown regarding neuronal toxicity and nephrotoxicity of TBBPA. Some authors point to an impaired motor activity, spatial learning, and memory upon exposure to TBBPA, while others reported no neurobehavioral changes. The same occurs for the renal system, so new studies, mainly in these two systems, are needed to understand if TBBPA has adverse effects.

Table 2.1. Overview of the tetrabromobisphenol effects in animals.

Animal	Effect	References
Zebrafish embryos	• Induces toxicity after 96 h of exposure (LC50 = 1.3 mg/L)	[80,81]
fathead minnow *Pimephales promelas*	• Induces toxicity after 96 h of exposure (LC50 = 1.3 mg/L)	[82]
Rainbow trout *Oncorhynchus mykiss*	• Induces toxicity after 96 h of exposure (LC50 = 0.54-1.1 mg/L)	[82]
Copepod *Acartia tonsa*	• Induces toxicity after 48 h of exposure (LC50 = 0.37-0.43 mg/L)	[83]
***Eisenia fetida* (redworm)**	• Induces toxicity after 14 days of exposure (LC50 > 500 mg/L)	[83]
Earthworm species *Metaphire guillelmi*	• Induces toxicity after 14 days of exposure (LC50 > 39 mg/L)	[84]
Marine mussel *Mytilus galloprovincialis*	• Induces hemocyte lysosomal membrane destabilization (low concentrations) • Activates immune function by kinase-mediated cell signaling	[112]
Rats	• Induces low toxicity (LD50 > 5 g/kg)	[4]
	• Induces neurological and neurobehavior impairments (offspring) • Changes activity habituation, learning and memory	[97-99]
Mice	• Induces low toxicity (LD50 > 4 g/kg)	[4]
Neonatal mice	• No effect in neurobehavioral changes	[95-97]
Newborn rats	• Induces nephrotoxicity	[106]

Table 2.1. Overview of the tetrabromobisphenol effects in animals (continued).

Animal	Effect	References
Sprague-Dawley rats (male)	• Produces transient oxidative stress in kidneys	[107]
ICR mice model	• Increases liver weight • Increases focal necrosis or light enlargement of hepatocytes	[108-109]
Rat pituitary cell lines (MtT/E-2 cells)	• Increases cell proliferation (estrogen-dependent) • Estrogenic activity	[86]
Rat pituitary tumor cell line (GH3)	• Changes thyroid hormone activity • Disrupts steroid hormone function • Disrupts TH-dependent cell growth	[88]
Chinese hamster ovary cells	• Antagonizes thyroid effect • Inhibits T3 binding to thyroid hormone receptors	[92]
African green monkey kidney cell line	• Antagonizes thyroid effect • Inhibits T3 binding to thyroid hormone receptors	[93]
Rat cerebellar granule cells (CGC)	• Increases $[Ca^{2+}]_i$ • Increases cell death (reduced by NMDA receptor antagonists)	[103,105]
Mouse Sertoli cells (TM4)	• Induces cell death (through Ca^{2+} release via ryanodine receptors)	[104,105]

Table 2.1. Overview of the tetrabromobisphenol effects in animals (continued).

Animal	Effect	References
Rat pancreatic β-cells (RIN-m5F cell line)	• Increases inflammatory cytokines (TNF-α and IL-1β), nitric oxide, intracellular ROS and mitochondrial superoxide levels • Damages pancreatic β-cells by triggering mitochondrial dysfunction • Induces cell apoptosis	[111]
Mouse osteoblastic cells line (MC3T3-E1 cells)	• Induces cardiolipin peroxidation, cytochrome c release • Decreased ATP, cyclophilin A and B levels • Induces cell apoptosis or necrosis • Decreases differentiation markers, collagen synthesis, alkaline phosphatase activity and calcium deposition • Inhibits osteoblast function	[113]
Mouse macrophage cell line (RAW264.7 cell line)	• Increases TRAP activity and osteoclast differentiation • Increases expression of several genes involved in osteoclast differentiation • Increases ROS production	[115]
Male Wistar WU rats microsomes	• Inhibits T4 binding to transthyretin	[94]
Rat brain synaptosomes and vesicles	• Reduces dopamine and GABA uptake in brain synaptosomes	[102]

Table 2.1. Overview of the tetrabromobisphenol in animals (continued).

Animal	Effect	References
Rat hepatocytes	• Decreases intracellular ATP, adenine nucleotides, glutathione, and protein thiols	[110]

2.5. Toxicity studies in humans

When it comes to human health, it is still unclear which potential health impacts of TBBPA on the general population. However, toxicological, and human exposure data suggest a relationship between TBBPA exposure and human health injure. All the TBBPA effects described below are summarized in table 2.2.

In human airway epithelial cells (A549) Wu *et al.* observed that TBBPA increased caspase-3 activities, ROS generation and lipid peroxidation (MDA) content. After TBBPA exposure (0, 10, and 40 μg/mL) there was a seriously injured mitochondria and a dilated smooth endoplasmic reticulum [116]. These effects of TBBPA may contribute to the pathogenesis of several lung diseases. Studies in human mesenchymal stem cells (hMSCs) showed that TBBPA, through a peroxisome proliferator-activated receptor gamma (PPARγ)-dependent mechanism, increased the number of lipid droplets and upregulated the expression of adipocyte-related mRNA, adipocyte-specific protein 2 (aP2) and alkaline phosphatase (LPL). With these results the authors concluded that TBBPA induced lipogenesis in osteoblast differentiation, which may be dependent on increased PPARγ expression [117]. Moreover, in epithelial ovarian cancer cell line (OVCAR-3) TBBPA upregulated apelin expression and secretion, which is regulated by the PPARγ [118]. Furthermore, the apelin receptor expression level was lower in granulosa tumour cells than in epithelial cancer cells, whereas it was the reverse for apelin expression and secretion [118].

Regarding the immune system, Reistad *et al.* investigated the effect of TBBPA on the formation of ROS and Ca^{2+} levels in human neutrophil granulocytes. The results showed that this compound potently activates the nicotinamide adenine dinucleotide phosphate (NADPH) oxidase primarily through elevation of intracellular Ca^{2+}, activation of PKC and MAPK pathway, being dependent of TBBPA concentration [119,120]. TBBPA has been shown to alter the tumour killing function of NK lymphocytes, and the secretion of the inflammatory cytokines interferon gamma (IFNγ) and IL-1β [121-124]. In other study, after exposure of human immune cells (NK, monocyte-depleted (MD) and peripheral blood mononuclear cells (PBMCs)) to TBBPA there was a decrease in the secretion of TNF and interfered with NK cell lytic function by decreasing the ability of NK cells to bind to target cells [121,124,125]. In human first trimester extravillous trophoblast cells (HTR-8/SVneo cells), TBBPA (10 mM) increased the expression of interleukin (IL)-6, IL-8, and prostaglandin E2, and the transforming growth factor beta 1 (TGF-β) release was suppressed [126]. Koike *et al.* observed that human bronchial epithelial cells exposure to TBBPA increased the expression of ICAM- 1 and IL-6. Consistently, TBBPA can disrupt the expression of proinflammatory proteins in bronchial epithelial cells by stimulate epidermal growth factor receptor (EGFR) related protein phosphorylation or by disrupt nuclear receptor signalling pathways [127].

Other health effects associated with the exposure to TBBPA include cancer disorders. In human hepatocellular liver carcinoma cell line (HepG2), Lyu *et al.* showed that TBBPA induced migration and invasion by affecting the number and distribution of lysosomes in HepG2 cells in a dose-dependent manner. Intracellularly, TBBPA decreased protein levels of Beta-Hexosaminidase

(HEXB), Cathepsin B (CTSB) and D (CTSD), on other hand it increased the extracellular CTSB and CTSD. Thus, the authors concluded that TBBPA exposure could promote the lysosomal exocytosis in cancer cells [128]. Moreover, the molecular docking results of this study suggested that TBBPA could bind to transient receptor potential mucolipin-1 (TRPML1), and this complex (TBBPA-TRPML1) regulated the calcium-mediated lysosomal exocytosis, promoting the metastasis in liver cancer cells [128]. In oestrogen-dependent human breast cancer cell line MCF-7, Samuelsen *et al.* performed studies that compared the estrogenic potency of TBBPA and other derivates and showed that these compounds competed with 17beta-estradiol for binding to the oestrogen receptor. However, the binding of these endocrine disruptors to the oestrogen receptor is weaker than that of 17beta-estradiol [90].

Overall, the results from the few studies on human health suggest that TBBPA may contribute to the pathogenesis of some lung diseases and to the lipogenesis in osteoblast differentiation, through increased PPARγ expression. Likewise in rats, TBBPA also effects the osteoblast function, through mitochondrial dysfunction and oxidative stress. Besides, this compound may affect the immune system by interfering with the tumour killing function of NK lymphocytes, the secretion of the inflammatory cytokines and the ability of NK cells to bind to the target. In cancer cell lines, TBBPA can promote lysosomal exocytosis and metastasis in the liver. In addition, TBBPA has also been shown to be involved in the binding to oestrogen receptors, which is consistent with the effects obtain in rats. However, there are still few studies on this matter, so more investigations should be performed to enlighten the potential health impacts of TBBPA on the general population health.

Table 2.2. Overview of the tetrabromobisphenol effects in humans.

Human cell type	Effect	References
Airway epithelial cells (A549)	• Increases caspase-3 activities • Increases ROS generation and MDA content • Damages mitochondria • Dilates smooth endoplasmic reticulum • Induces pathogenesis of several lung diseases	[116]
Mesenchymal stem cells (hMSCs)	• Increases the number of lipid droplets • Upregulates expression of adipocyte-related mRNA, aP2 and LPL • Induces lipogenesis in osteoblast differentiation (dependent of increased PPARγ expression)	[117]
Epithelial ovarian cancer cell line (OVCAR-3)	• Upregulates apelin expression and secretion (by PPARγ)	[118]
Immune cells (NK cells, MD and PBMCs.	• Changes tumor killing function of NK lymphocytes • Interferes with NK cell lytic function • Decreases the ability of NK cells to bind to target cells • Changes secretion of the IFNγ and IL-1β • Decreases secretion of TNF	[121,124,125]

Table 2.2. Overview of the tetrabromobisphenol effects in humans (continued).

Human cell type	Effect	References
Bronchial epithelial cells	• Disrupts expression of proinflammatory proteins by stimulating EGFR-related protein phosphorylation or disrupting nuclear receptor signaling pathways	[127]
Hepatocellular liver carcinoma cell line (HepG2)	• Induces liver cancer disorders • Induces migration and invasion by affecting the number and distribution of lysosomes • Decreases intracellular levels of Beta-Hexosaminidase (HEXB), Cathepsin B (CTSB) and D (CTSD) • Increases extracellular levels of CTSB and CTSD • Promotes lysosomal exocytosis • Binds to transient receptor potential mucolipin-1 (TRPML1) • TBBPA-TRPML1 complex regulates the calcium-mediated lysosomal exocytosis • Promotes liver cancer cells metastasis	[128]
Breast cancer cell line (MCF-7)	• Competes with 17beta-estradiol for binding to the estrogen receptor	[90]
Neutrophil granulocytes	• Actives NADPH oxidase (by increasing [Ca^{2+}] and activating PKC and MAP kinase pathway)	[119,120]

2.6. Authors statement

Joana Feiteiro: Conceptualization; Investigation; Roles/Writing-original draft; Writing - review & editing. Melissa Mariana: Roles/Writing - original draft; Writing - review & editing. Elisa Cairrão: Conceptualization; Funding acquisition; Project administration; Supervision; Visualization; Writing - review & editing.

2.7. Declaration of competing interests

The authors declare that they have no known competing financial interests or personal relationships that could have appeared to influence the work reported in this paper.

2.8. Acknowledgments

This research was supported by FEDER funds through the POCI-COMPETE 2020—Operational Program Competitiveness and Internationalisation in Axis I-Strengthening research, technological development and innovation (Project POCI-01-0145-FEDER007491) and National Funds by FCT—Foundation for Science and Technology (Project UID/Multi/00709/2019). J.F. acknowledges the PhD fellowship from FCT (Reference: SFRH/BD/131665/2017) and M.M. acknowledges the PhD fellowship from FCT (Reference: 2020.07020.BD).

2.9. References

1. Zweidinger, R.A.; Cooper, S.D.; Erickson, M.D.; Michael, L.C.; Pellizzari, E.D. Sampling and Analysis for Semivolatile Brominated Organics in Ambient Air. In *Monitoring Toxic Substances*; ACS Symposium Series; AMERICAN CHEMICAL SOCIETY: 1979; Volume 94, pp. 217-231.

2. Bergman, A.M., Wehler, E.K., Sjodin, A. Environmental levels (air and soil) of other organohalogen and dioxins, polybrominated environmental pollutants: ,human and wildlife exposures. *Organohalogen Compd.* **1999**, *43*, 89-92.

3. Birnbaum, L.S.; Staskal, D.F. Brominated flame retardants: cause for concern? *Environ Health Perspect* **2004**, *112*, 9-17.

4. Covaci, A.; Voorspoels, S.; Abdallah, M.A.; Geens, T.; Harrad, S.; Law, R.J. Analytical and environmental aspects of the flame retardant tetrabromobisphenol-A and its derivatives. *J Chromatogr A* **2009**, *1216*, 346-363.

5. Birnbaum, L.S.; Bergman, A. Brominated and chlorinated flame retardants: the San Antonio Statement. *Environ Health Perspect* **2010**, *118*, A514-515.

6. Cruz, R.; Cunha, S.C.; Casal, S. Brominated flame retardants and seafood safety: a review. *Environ Int* **2015**, *77*, 116-131.

7. Watanabe, I.; Kashimoto, T.; Tatsukawa, R. The flame retardant tetrabromobisphenol-A and its metabolite found in river and marine sediments in Japan. *Chemosphere* **1983**, *12*, 1533-1539.

8. Watanabe, I.; Sakai, S. Environmental release and behavior of brominated flame retardants. *Environ Int* **2003**, *29*, 665-682.

9. WHO. Tetrabromobisphenol A and derivatives. . **1995**, *Environmental Health Criteria 172*.

10. Abou-Elwafa Abdallah, M. Environmental occurrence, analysis and human exposure to the flame retardant tetrabromobisphenol-A (TBBP-A)-A review. *Environ Int* **2016**, *94*, 235-250.

11. KEMI. RISK ASSESSMENT: Hexabromocyclododecane **2008**.

12. EPA, U. Technical fact sheet – polybrominated diphenyl ethers (PBDEs) and polybrominated biphenyls (PBBs). . **2014**.

13. ECHA. European Union Risk Assessment Report on 2,2′,6,6′-tetrabromo-4,4`isopropylidenediphenol(tetrabromobisphenol-A or TBBP-A). **2008**.

14. Covaci, A.; Harrad, S.; Abdallah, M.A.; Ali, N.; Law, R.J.; Herzke, D.; de Wit, C.A. Novel brominated flame retardants: a review of their analysis, environmental fate and behaviour. *Environ Int* **2011**, *37*, 532-556.

15. Papachlimitzou, A.; Barber, J.L.; Losada, S.; Bersuder, P.; Law, R.J. A review of the analysis of novel brominated flame retardants. *J Chromatogr A* **2012**, *1219*, 15-28.

16. Jonsson, S.; Hörsing, M. Investigation of sorption phenomena by solid phase extraction and liquid chromatography for the determination of some ether derivatives of tetrabromobisphenol A. *Journal of Physical Organic Chemistry* **2009**, *22*, 1120-1126.

17. Harju, M.; Heimstad, E.S.; Herzke, D.; Sandanger, T.; Posner, S.; Wania, F. Emerging "new" brominated flame retardants in flame retarded products and the environment **2009**, *Report 2462*, 113 pp.

18. Zhu, Z.C.; Chen, S.J.; Zheng, J.; Tian, M.; Feng, A.H.; Luo, X.J.; Mai, B.X. Occurrence of brominated flame retardants (BFRs), organochlorine pesticides (OCPs), and polychlorinated biphenyls (PCBs) in agricultural soils in a BFR-manufacturing region of North China. *Sci Total Environ* **2014**, *481*, 47-54.

19. Li, F.; Jin, J.; Tan, D.; Wang, L.; Geng, N.; Cao, R.; Gao, Y.; Chen, J. Hexabromocyclododecane and tetrabromobisphenol A in sediments and paddy soils from Liaohe River Basin, China: Levels, distribution and mass inventory. *J Environ Sci (China)* **2016**, *48*, 209-217.

20. Tang, J.; Feng, J.; Li, X.; Li, G. Levels of flame retardants HBCD, TBBPA and TBC in surface soils from an industrialized region of East China. *Environ Sci Process Impacts* **2014**, *16*, 1015-1021.

21. Ni, H.G.; Zeng, H. HBCD and TBBPA in particulate phase of indoor air in Shenzhen, China. *Sci Total Environ* **2013**, *458-460*, 15-19.

22. Wu, Y.; Li, Y.; Kang, D.; Wang, J.; Zhang, Y.; Du, D.; Pan, B.; Lin, Z.; Huang, C.; Dong, Q. Tetrabromobisphenol A and heavy metal exposure via dust ingestion in an e-waste recycling region in Southeast China. *Sci Total Environ* **2016**, *541*, 356-364.

23. Wang, J.; Liu, L.; Wang, J.; Pan, B.; Fu, X.; Zhang, G.; Zhang, L.; Lin, K. Distribution of metals and brominated flame retardants (BFRs) in sediments, soils and plants from an informal e-waste dismantling site, South China. *Environ Sci Pollut Res Int* **2015**, *22*, 1020-1033.

24. Lu, J.F.; He, M.J.; Yang, Z.H.; Wei, S.Q. Occurrence of tetrabromobisphenol a (TBBPA) and hexabromocyclododecane (HBCD) in soil and road dust in Chongqing, western China, with emphasis on diastereoisomer profiles, particle size distribution, and human exposure. *Environ Pollut* **2018**, *242*, 219-228.

25. Wang, R.; Tang, J.; Xie, Z.; Mi, W.; Chen, Y.; Wolschke, H.; Tian, C.; Pan, X.; Luo, Y.; Ebinghaus, R. Occurrence and spatial distribution of organophosphate ester flame retardants and plasticizers in 40 rivers draining into the Bohai Sea, north China. *Environ Pollut* **2015**, *198*, 172-178.

26. Barghi, M.; Shin, E.S.; Kim, J.C.; Choi, S.D.; Chang, Y.S. Human exposure to HBCD and TBBPA via indoor dust in Korea: Estimation of external exposure and body burden. *Sci Total Environ* **2017**, *593-594*, 779-786.

27. Abafe, O.A.; Martincigh, B.S. Determination and human exposure assessment of polybrominated diphenyl ethers and tetrabromobisphenol A in indoor dust in South Africa. *Environ Sci Pollut Res Int* **2016**, *23*, 7038-7049.

28. Abdallah, M.A.; Harrad, S.; Covaci, A. Hexabromocyclododecanes and tetrabromobisphenol-A in indoor air and dust in Birmingham, U.K: implications for human exposure. *Environ Sci Technol* **2008**, *42*, 6855-6861.

29. Yang, S.W.; Yan, Z.G.; Xu, F.F.; Wang, S.R.; Wu, F.C. Development of freshwater aquatic life criteria for tetrabromobisphenol A in China. *Environ Pollut* **2012**, *169*, 59-63.

30. Xu, J.; Zhang, Y.; Guo, C.; He, Y.; Li, L.; Meng, W. Levels and distribution of tetrabromobisphenol A and hexabromocyclododecane in Taihu Lake, China. *Environ Toxicol Chem* **2013**, *32*, 2249-2255.

31. Liu, A.F.; Qu, G.B.; Yu, M.; Liu, Y.W.; Shi, J.B.; Jiang, G.B. Tetrabromobisphenol-A/S and Nine Novel Analogs in Biological Samples from the Chinese Bohai Sea: Implications for Trophic Transfer. *Environ Sci Technol* **2016**, *50*, 4203-4211.

32. Shi, Z.X.; Wu, Y.N.; Li, J.G.; Zhao, Y.F.; Feng, J.F. Dietary exposure assessment of Chinese adults and nursing infants to tetrabromobisphenol-A and hexabromocyclododecanes: occurrence measurements in foods and human milk. *Environ Sci Technol* **2009**, *43*, 4314-4319.

33. Liu, K.; Li, J.; Yan, S.; Zhang, W.; Li, Y.; Han, D. A review of status of tetrabromobisphenol A (TBBPA) in China. *Chemosphere* **2016**, *148*, 8-20.

34. Shi, Z.; Zhang, L.; Zhao, Y.; Sun, Z.; Zhou, X.; Li, J.; Wu, Y. Dietary exposure assessment of Chinese population to tetrabromobisphenol-A, hexabromocyclododecane and decabrominated diphenyl ether: Results of the 5th Chinese Total Diet Study. *Environ Pollut* **2017**, *229*, 539-547.

35. Shi, Z.; Zhang, L.; Li, J.; Wu, Y. Legacy and emerging brominated flame retardants in China: A review on food and human milk contamination, human dietary exposure and risk assessment. *Chemosphere* **2018**, *198*, 522-536.

36. Report, E.U.R.A. 2,2',6,6'-TETRABROMO-4,4'-ISOPROPYLIDENEDIPHENOL (TETRABROMOBISPHENOL-A or TBBP-A) Part II – Human Health **2006**.

37. Li, Y.; Zhou, Q.; Wang, Y.; Xie, X. Fate of tetrabromobisphenol A and hexabromocyclododecane brominated flame retardants in soil and uptake by plants. *Chemosphere* **2011**, *82*, 204-209.

38. Yin, J.; Meng, Z.; Zhu, Y.; Song, M.; Wang, H. Dummy molecularly imprinted polymer for selective screening of trace bisphenols in river. *Anal Methods* **2011**, *3*, 173-180.

39. Yang, S.; Wang, S.; Liu, H.; Yan, Z. Tetrabromobisphenol A: tissue distribution in fish, and seasonal variation in water and sediment of Lake Chaohu, China. *Environ Sci Pollut Res Int* **2012**, *19*, 4090-4096.

40. Canada, G. Screening Assessment Report: Phenol, 4,40-(1-methylethylidene) bis [2,6-dibromo- (Chemical Abstracts Service Registry Number79-94-7), Ethanol,2,20-[(1-methylethylidene)bis[(2,6-dibromo-4,1-phenylene)oxy]]bis (ChemicalAbstracts Service Registry Number 4162-45-2), Benzene, 1,10-(1methylethylidene) bis[3,5- dibromo-4-(2-propenyloxy)- (Chemical Abstracts Service Registry Number 25327-89-3). . **2013**.

41. Zhou, X.; Guo, J.; Zhang, W.; Zhou, P.; Deng, J.; Lin, K. Tetrabromobisphenol A contamination and emission in printed circuit board production and implications for human exposure. *J Hazard Mater* **2014**, *273*, 27-35.

42. Yu, C.; Hu, B. Novel combined stir bar sorptive extraction coupled with ultrasonic assisted extraction for the determination of brominated flame retardants in environmental samples using high performance liquid chromatography. *J Chromatogr A* **2007**, *1160*, 71-80.

43. Abdallah, M.A.; Pawar, G.; Harrad, S. Evaluation of in vitro vs. in vivo methods for assessment of dermal absorption of organic flame retardants: a review. *Environ Int* **2015**, *74*, 13-22.

44. Xiao, X., Chen, D.Y., Mei, J., Hu, J.F., Peng, P.A.,. Particle-bound PCDD/Fs, PBDD/Fs and TBBPA in the atmosphere around an electronic waste dismantling site in Guiyu, China. *Acta Scien. Circum.* **2012**, *32*, 1142-1148.

45. Sjodin, A.; Carlsson, H.; Thuresson, K.; Sjolin, S.; Bergman, A.; Ostman, C. Flame retardants in indoor air at an electronics recycling plant and at other work environments. *Environ Sci Technol* **2001**, *35*, 448-454.

46. Takigami, H., Suzuki, G., Hirai, Y., Sakai, S.I.,. Comparison of brominated flame retardants in indoor air and dust samples from two homes in Japan. *Organohalogen Compd.* **2017**, *69*, 2785-2792.

47. Takigami, H.; Suzuki, G.; Hirai, Y.; Sakai, S. Brominated flame retardants and other polyhalogenated compounds in indoor air and dust from two houses in Japan. *Chemosphere* **2009**, *76*, 270-277.

48. Huang, D.Y.; Zhao, H.Q.; Liu, C.P.; Sun, C.X. Characteristics, sources, and transport of tetrabromobisphenol A and bisphenol A in soils from a typical e-waste recycling area in South China. *Environ Sci Pollut Res Int* **2014**, *21*, 5818-5826.

49. Sanchez-Brunete, C.; Miguel, E.; Tadeo, J.L. Determination of tetrabromobisphenol-A, tetrachlorobisphenol-A and bisphenol-A in soil by ultrasonic assisted extraction and gas chromatography-mass spectrometry. *J Chromatogr A* **2009**, *1216*, 5497-5503.

50. Matsukami, H.; Tue, N.M.; Suzuki, G.; Someya, M.; Tuyen le, H.; Viet, P.H.; Takahashi, S.; Tanabe, S.; Takigami, H. Flame retardant emission from e-waste recycling operation in northern Vietnam: environmental occurrence of emerging organophosphorus esters used as alternatives for PBDEs. *Sci Total Environ* **2015**, *514*, 492-499.

51. Makinen, M.S.; Makinen, M.R.; Koistinen, J.T.; Pasanen, A.L.; Pasanen, P.O.; Kalliokoski, P.J.; Korpi, A.M. Respiratory and dermal exposure to organophosphorus flame retardants and tetrabromobisphenol A at five work environments. *Environ Sci Technol* **2009**, *43*, 941-947.

52. Abdallah, M.A.; Pawar, G.; Harrad, S. Evaluation of 3D-human skin equivalents for assessment of human dermal absorption of some brominated flame retardants. *Environ Int* **2015**, *84*, 64-70.

53. Knudsen, G.A.; Sanders, J.M.; Sadik, A.M.; Birnbaum, L.S. Disposition and kinetics of Tetrabromobisphenol A in female Wistar Han rats. *Toxicol Rep* **2014**, *1*, 214-223.

54. Knudsen, G.A.; Hughes, M.F.; McIntosh, K.L.; Sanders, J.M.; Birnbaum, L.S. Estimation of tetrabromobisphenol A (TBBPA) percutaneous uptake in humans using the parallelogram method. *Toxicol Appl Pharmacol* **2015**, *289*, 323-329.

55. Knudsen, G.A.; Hughes, M.F.; Birnbaum, L.S. Dermal disposition of Tetrabromobisphenol A Bis(2,3-dibromopropyl) ether (TBBPA-BDBPE) using rat and human skin. *Toxicol Lett* **2019**, *301*, 108-113.

56. ECHA. 2,2',6,6'-tetrabromo-4,4'-isopropylidenediphenol, Toxicological Information,Toxicokinetics, Metabolism and Distribution, Dermal Absorption. **2005**.

57. Hagmar, L.; Sjödin, A.; Höglund, P.; Thuresson, K.; Rylander, L.; Bergman, A.J.O.c. Biological half-lives of polybrominated diphenyl ethers and tetrabromobisphenol a in exposed workers. **2000**, *47*, 198-201.

58. Schauer, U.M.; Volkel, W.; Dekant, W. Toxicokinetics of tetrabromobisphenol a in humans and rats after oral administration. *Toxicol Sci* **2006**, *91*, 49-58.

59. Abdallah, M.A.; Harrad, S. Tetrabromobisphenol-A, hexabromocyclododecane and its degradation products in UK human milk: relationship to external exposure. *Environ Int* **2011**, *37*, 443-448.

60. Fujii, Y.; Nishimura, E.; Kato, Y.; Harada, K.H.; Koizumi, A.; Haraguchi, K. Dietary exposure to phenolic and methoxylated organohalogen contaminants in relation to their concentrations in breast milk and serum in Japan. *Environ Int* **2014**, *63*, 19-25.

61. Kawashiro, Y.; Fukata, H.; Omori-Inoue, M.; Kubonoya, K.; Jotaki, T.; Takigami, H.; Sakai, S.; Mori, C. Perinatal exposure to brominated flame retardants and polychlorinated biphenyls in Japan. *Endocr J* **2008**, *55*, 1071-1084.

62. Fernandes, A.; Dicks, P.; Mortimer, D.; Gem, M.; Smith, F.; Driffield, M.; White, S.; Rose, M. Brominated and chlorinated dioxins, PCBs and brominated flame retardants in Scottish shellfish: methodology, occurrence and humandietary exposure. *Mol. Nutr. Food* **2008**, *52*, 238 - 249.

63. van Leeuwen, S.P.; de Boer, J. Brominated flame retardants in fish and shellfish - levels and contribution of fish consumption to dietary exposure of Dutch citizens to HBCD. *Mol Nutr Food Res* **2008**, *52*, 194-203.

64. Batterman, S.; Godwin, C.; Chernyak, S.; Jia, C.; Charles, S. Brominated flame retardants in offices in Michigan, USA. *Environ Int* **2010**, *36*, 548-556.

65. Geens, T.; Roosens, L.; Neels, H.; Covaci, A. Assessment of human exposure to Bisphenol-A, Triclosan and Tetrabromobisphenol-A through indoor dust intake in Belgium. *Chemosphere* **2009**, *76*, 755-760.

66. Wang, W.; Abualnaja, K.O.; Asimakopoulos, A.G.; Covaci, A.; Gevao, B.; Johnson-Restrepo, B.; Kumosani, T.A.; Malarvannan, G.; Minh, T.B.; Moon, H.B.; et al. A comparative assessment of human exposure to tetrabromobisphenol A and eight bisphenols including bisphenol A via indoor dust ingestion in twelve countries. *Environ Int* **2015**, *83*, 183-191.

67. Hu, F.; Pan, L.; Xiu, M.; Liu, D. Dietary accumulation of tetrabromobisphenol A and its effects on the scallop Chlamys farreri. *Comp Biochem Physiol C Toxicol Pharmacol* **2015**, *167*, 7-14.

68. Hakk, H.; Letcher, R.J. Metabolism in the toxicokinetics and fate of brominated flame retardants--a review. *Environ Int* **2003**, *29*, 801-828.

69. Liu, H.; Ma, Z.; Zhang, T.; Yu, N.; Su, G.; Giesy, J.P.; Yu, H. Pharmacokinetics and effects of tetrabromobisphenol a (TBBPA) to early life stages of zebrafish (Danio rerio). *Chemosphere* **2018**, *190*, 243-252.

70. Yu, G.; Bu, Q.; Cao, Z.; Du, X.; Xia, J.; Wu, M.; Huang, J. Brominated flame retardants (BFRs): A review on environmental contamination in China. *Chemosphere* **2016**, *150*, 479-490.

71. Yu, Y.; Li, L.; Li, H.; Yu, X.; Zhang, Y.; Wang, Q.; Zhou, Z.; Gao, D.; Ye, H.; Lin, B.; et al. In vivo assessment of dermal adhesion, penetration, and bioavailability of tetrabromobisphenol A. *Environ Pollut* **2017**, *228*, 305-310.

72. Yu, Y.; Ma, R.; Yu, L.; Cai, Z.; Li, H.; Zuo, Y.; Wang, Z.; Li, H. Combined effects of cadmium and tetrabromobisphenol a (TBBPA) on development, antioxidant enzymes activity and thyroid hormones in female rats. *Chem Biol Interact* **2018**, *289*, 23-31.

73. Demierre, A.L.; Peter, R.; Oberli, A.; Bourqui-Pittet, M. Dermal penetration of bisphenol A in human skin contributes marginally to total exposure. *Toxicol Lett* **2012**, *213*, 305-308.

74. Knudsen, G.A.; Jacobs, L.M.; Kuester, R.K.; Sipes, I.G. Absorption, distribution, metabolism and excretion of intravenously and orally administered tetrabromobisphenol A [2,3-dibromopropyl ether] in male Fischer-344 rats. *Toxicology* **2007**, *237*, 158-167.

75. Kuester, R.K.; Solyom, A.M.; Rodriguez, V.P.; Sipes, I.G. The effects of dose, route, and repeated dosing on the disposition and kinetics of tetrabromobisphenol A in male F-344 rats. *Toxicol Sci* **2007**, *96*, 237-245.

76. Szymanska, J.A.; Sapota, A.; Frydrych, B. The disposition and metabolism of tetrabromobisphenol-A after a single i.p. dose in the rat. *Chemosphere* **2001**, *45*, 693-700.

77. Borghoff, S.J.; Wikoff, D.; Harvey, S.; Haws, L. Dose- and time-dependent changes in tissue levels of tetrabromobisphenol A (TBBPA) and its sulfate and glucuronide conjugates following repeated administration to female Wistar Han Rats. *Toxicol Rep* **2016**, *3*, 190-201.

78. Knudsen, G.A.; Hall, S.M.; Richards, A.C.; Birnbaum, L.S. TBBPA disposition and kinetics in pregnant and nursing Wistar Han IGS rats. *Chemosphere* **2018**, *192*, 5-13.

79. Hakk, H.; Larsen, G.; Bergman, A.; Orn, U. Metabolism, excretion and distribution of the flame retardant tetrabromobisphenol-A in conventional and bile-duct cannulated rats. *Xenobiotica* **2000**, *30*, 881-890.

80. Godfrey, A.; Abdel-Moneim, A.; Sepulveda, M.S. Acute mixture toxicity of halogenated chemicals and their next generation counterparts on zebrafish embryos. *Chemosphere* **2017**, *181*, 710-712.

81. Laboratories, S. The subchronic toxicity of sediment-sorbed tetrabromobisphenol A to Chironomus tentans under flow-through conditions. **1989**.

82. Pittinger, C.A.; Pecquet, A.M. Review of historical aquatic toxicity and bioconcentration data for the brominated flame retardant tetrabromobisphenol A (TBBPA): effects to fish, invertebrates, algae, and microbial communities. *Environ Sci Pollut Res Int* **2018**, *25*, 14361-14372.

83. Wollenberger, L.; Dinan, L.; Breitholtz, M. Brominated flame retardants: activities in a crustacean development test and in an ecdysteroid screening assay. *Environ Toxicol Chem* **2005**, *24*, 400-407.

84. Chen, X.; Gu, J.; Wang, Y.; Gu, X.; Zhao, X.; Wang, X.; Ji, R. Fate and O-methylating detoxification of Tetrabromobisphenol A (TBBPA) in two earthworms (Metaphire guillelmi and Eisenia fetida). *Environ Pollut* **2017**, *227*, 526-533.

85. Criteria, E.H. Tetrabromobisphenol A and Derivatives,. In Proceedings of the International Programme on Chemical Safety, World Health Organization,, Geneva, 1995.

86. Kitamura, S.; Jinno, N.; Ohta, S.; Kuroki, H.; Fujimoto, N. Thyroid hormonal activity of the flame retardants tetrabromobisphenol A and tetrachlorobisphenol A. *Biochem Biophys Res Commun* **2002**, *293*, 554-559.

87. Kester, M.H.; Bulduk, S.; van Toor, H.; Tibboel, D.; Meinl, W.; Glatt, H.; Falany, C.N.; Coughtrie, M.W.; Schuur, A.G.; Brouwer, A.; et al. Potent inhibition of estrogen sulfotransferase by hydroxylated metabolites of polyhalogenated aromatic hydrocarbons reveals alternative mechanism for estrogenic activity of endocrine disrupters. *J Clin Endocrinol Metab* **2002**, *87*, 1142-1150.

88. Ghisari, M.; Bonefeld-Jorgensen, E.C. Impact of environmental chemicals on the thyroid hormone function in pituitary rat GH3 cells. *Mol Cell Endocrinol* **2005**, *244*, 31-41.

89. Meerts, I.A.; Letcher, R.J.; Hoving, S.; Marsh, G.; Bergman, A.; Lemmen, J.G.; van der Burg, B.; Brouwer, A. In vitro estrogenicity of polybrominated diphenyl ethers, hydroxylated PDBEs, and polybrominated bisphenol A compounds. *Environ Health Perspect* **2001**, *109*, 399-407.

90. Samuelsen, M.; Olsen, C.; Holme, J.A.; Meussen-Elholm, E.; Bergmann, A.; Hongslo, J.K. Estrogen-like properties of brominated analogs of bisphenol A in the MCF-7 human breast cancer cell line. *Cell Biol Toxicol* **2001**, *17*, 139-151.

91. Olsen, C.M.; Meussen-Elholm, E.T.; Samuelsen, M.; Holme, J.A.; Hongslo, J.K. Effects of the environmental oestrogens bisphenol A, tetrachlorobisphenol A, tetrabromobisphenol A, 4-hydroxybiphenyl and 4,4'-dihydroxybiphenyl on oestrogen receptor binding, cell proliferation and regulation of oestrogen sensitive proteins in the human breast cancer cell line MCF-7. *Pharmacol Toxicol* **2003**, *92*, 180-188.

92. Kitamura, S.; Kato, T.; Iida, M.; Jinno, N.; Suzuki, T.; Ohta, S.; Fujimoto, N.; Hanada, H.; Kashiwagi, K.; Kashiwagi, A. Anti-thyroid hormonal activity of tetrabromobisphenol A, a flame retardant, and related compounds: Affinity to the mammalian thyroid hormone receptor, and effect on tadpole metamorphosis. *Life Sci* **2005**, *76*, 1589-1601.

93. Sun, H.; Shen, O.X.; Wang, X.R.; Zhou, L.; Zhen, S.Q.; Chen, X.D. Anti-thyroid hormone activity of bisphenol A, tetrabromobisphenol A and tetrachlorobisphenol A in an improved reporter gene assay. *Toxicol In Vitro* **2009**, *23*, 950-954.

94. Meerts, I.A.; van Zanden, J.J.; Luijks, E.A.; van Leeuwen-Bol, I.; Marsh, G.; Jakobsson, E.; Bergman, A.; Brouwer, A. Potent competitive interactions of some brominated flame retardants and related compounds with human transthyretin in vitro. *Toxicol Sci* **2000**, *56*, 95-104.

95. Eriksson, P.; Jakobsson, E.; Fredriksson, A. Brominated flame retardants: a novel class of developmental neurotoxicants in our environment? *Environ Health Perspect* **2001**, *109*, 903-908.

96. Viberg, H.; Eriksson, P. Differences in neonatal neurotoxicity of brominated flame retardants, PBDE 99 and TBBPA, in mice. *Toxicology* **2011**, *289*, 59-65.

97. Lilienthal, H.; Verwer, C.M.; van der Ven, L.T.; Piersma, A.H.; Vos, J.G. Exposure to tetrabromobisphenol A (TBBPA) in Wistar rats: neurobehavioral effects in offspring from a one-generation reproduction study. *Toxicology* **2008**, *246*, 45-54.

98. Altmann, L.; Welge, P.; Mensing, T.; Lilienthal, H.; Voss, B.; Wilhelm, M. Chronic exposure to trichloroethylene affects neuronal plasticity in rat hippocampal slices. *Environ Toxicol Pharmacol* **2002**, *12*, 157-167.

99. Saegusa, Y.; Fujimoto, H.; Woo, G.H.; Inoue, K.; Takahashi, M.; Mitsumori, K.; Hirose, M.; Nishikawa, A.; Shibutani, M. Developmental toxicity of brominated flame retardants, tetrabromobisphenol A and 1,2,5,6,9,10-hexabromocyclododecane, in rat offspring after maternal exposure from mid-gestation through lactation. *Reprod Toxicol* **2009**, *28*, 456-467.

100. Wojtowicz, A.K.; Szychowski, K.A.; Kajta, M. PPAR-gamma agonist GW1929 but not antagonist GW9662 reduces TBBPA-induced neurotoxicity in primary neocortical cells. *Neurotox Res* **2014**, *25*, 311-322.

101. Diamandakis, D.; Zieminska, E.; Siwiec, M.; Tokarski, K.; Salinska, E.; Lenart, J.; Hess, G.; Lazarewicz, J.W. Tetrabromobisphenol A-induced depolarization of rat cerebellar granule cells: ex vivo and in vitro studies. *Chemosphere* **2019**, *223*, 64-73.

102. Mariussen, E.; Fonnum, F. The effect of brominated flame retardants on neurotransmitter uptake into rat brain synaptosomes and vesicles. *Neurochem Int* **2003**, *43*, 533-542.

103. Reistad, T.; Mariussen, E.; Ring, A.; Fonnum, F. In vitro toxicity of tetrabromobisphenol-A on cerebellar granule cells: cell death, free radical formation, calcium influx and extracellular glutamate. *Toxicol Sci* **2007**, *96*, 268-278.

104. Ogunbayo, O.A.; Lai, P.F.; Connolly, T.J.; Michelangeli, F. Tetrabromobisphenol A (TBBPA), induces cell death in TM4 Sertoli cells by modulating Ca^{2+} transport proteins and causing dysregulation of Ca2+ homeostasis. *Toxicol In Vitro* **2008**, *22*, 943-952.

105. Zieminska, E.; Stafiej, A.; Toczylowska, B.; Albrecht, J.; Lazarewicz, J.W. Role of Ryanodine and NMDA Receptors in Tetrabromobisphenol A-Induced Calcium Imbalance and Cytotoxicity in Primary Cultures of Rat Cerebellar Granule Cells. *Neurotox Res* **2015**, *28*, 195-208.

106. Fukuda, N.; Ito, Y.; Yamaguchi, M.; Mitumori, K.; Koizumi, M.; Hasegawa, R.; Kamata, E.; Ema, M. Unexpected nephrotoxicity induced by tetrabromobisphenol A in newborn rats. *Toxicol Lett* **2004**, *150*, 145-155.

107. Kang, M.J.; Kim, J.H.; Shin, S.; Choi, J.H.; Lee, S.K.; Kim, H.S.; Kim, N.D.; Kang, G.W.; Jeong, H.G.; Kang, W.; et al. Nephrotoxic potential and toxicokinetics of tetrabromobisphenol A in rat for risk assessment. *J Toxicol Environ Health A* **2009**, *72*, 1439-1445.

108. Tada, Y.; Fujitani, T.; Ogata, A.; Kamimura, H. Flame retardant tetrabromobisphenol A induced hepatic changes in ICR male mice. *Environ Toxicol Pharmacol* **2007**, *23*, 174-178.

109. Tada, Y.; Fujitani, T.; Yano, N.; Takahashi, H.; Yuzawa, K.; Ando, H.; Kubo, Y.; Nagasawa, A.; Ogata, A.; Kamimura, H. Effects of tetrabromobisphenol A, brominated flame retardant, in ICR mice after prenatal and postnatal exposure. *Food Chem Toxicol* **2006**, *44*, 1408-1413.

110. Nakagawa, Y.; Suzuki, T.; Ishii, H.; Ogata, A. Biotransformation and cytotoxicity of a brominated flame retardant, tetrabromobisphenol A, and its analogues in rat hepatocytes. *Xenobiotica* **2007**, *37*, 693-708.

111. Suh, K.S.; Choi, E.M.; Rhee, S.Y.; Oh, S.; Kim, S.W.; Pak, Y.K.; Choe, W.; Ha, J.; Chon, S. Tetrabromobisphenol A induces cellular damages in pancreatic beta-cells in vitro. *J Environ Sci Health A Tox Hazard Subst Environ Eng* **2017**, *52*, 624-631.

112. Canesi, L.; Lorusso, L.C.; Ciacci, C.; Betti, M.; Gallo, G. Effects of the brominated flame retardant tetrabromobisphenol-A (TBBPA) on cell signaling and function of Mytilus hemocytes: involvement of MAP kinases and protein kinase C. *Aquat Toxicol* **2005**, *75*, 277-287.

113. Choi, E.M.; Suh, K.S.; Rhee, S.Y.; Oh, S.; Kim, S.W.; Pak, Y.K.; Choe, W.; Ha, J.; Chon, S. Exposure to tetrabromobisphenol A induces cellular dysfunction in osteoblastic MC3T3-E1 cells. *J Environ Sci Health A Tox Hazard Subst Environ Eng* **2017**, *52*, 561-570.

114. Hsu, H.; Lacey, D.L.; Dunstan, C.R.; Solovyev, I.; Colombero, A.; Timms, E.; Tan, H.L.; Elliott, G.; Kelley, M.J.; Sarosi, I.; et al. Tumor necrosis factor receptor family member RANK mediates osteoclast differentiation and activation induced by osteoprotegerin ligand. *Proc Natl Acad Sci U S A* **1999**, *96*, 3540-3545.

115. Park, S.Y.; Choi, E.M.; Suh, K.S.; Kim, H.S.; Chin, S.O.; Rhee, S.Y.; Kim, D.Y.; Oh, S.; Chon, S. Tetrabromobisphenol A Promotes the Osteoclastogenesis of RAW264.7 Cells Induced by Receptor Activator of NF-kappa B Ligand In Vitro. *J Korean Med Sci* **2019**, *34*, e267.

116. Wu, S.; Wu, M.; Qi, M.; Zhong, L.; Qiu, L. Effects of novel brominated flame retardant TBBPA on human airway epithelial cell (A549) in vitro and proteome profiling. *Environ Toxicol* **2018**, *33*, 1245-1253.

117. Kakutani, H.; Yuzuriha, T.; Akiyama, E.; Nakao, T.; Ohta, S. Complex toxicity as disruption of adipocyte or osteoblast differentiation in human mesenchymal stem cells under the mixed condition of TBBPA and TCDD. *Toxicol Rep* **2018**, *5*, 737-743.

118. Hoffmann, M.; Fiedor, E.; Ptak, A. Bisphenol A and its derivatives tetrabromobisphenol A and tetrachlorobisphenol A induce apelin expression and secretion in ovarian cancer cells through a peroxisome proliferator-activated receptor gamma-dependent mechanism. *Toxicol Lett* **2017**, *269*, 15-22.

119. Reistad, T.; Mariussen, E.; Fonnum, F. The effect of a brominated flame retardant, tetrabromobisphenol-A, on free radical formation in human neutrophil granulocytes: the involvement of the MAP kinase pathway and protein kinase C. *Toxicol Sci* **2005**, *83*, 89-100.

120. Strack, S.; Detzel, T.; Wahl, M.; Kuch, B.; Krug, H.F. Cytotoxicity of TBBPA and effects on proliferation, cell cycle and MAPK pathways in mammalian cells. *Chemosphere* **2007**, *67*, S405-411.

121. Hurd, T.; Whalen, M.M. Tetrabromobisphenol A decreases cell-surface proteins involved in human natural killer (NK) cell-dependent target cell lysis. *J Immunotoxicol* **2011**, *8*, 219-227.

122. Anisuzzaman, S.; Whalen, M.M. Tetrabromobisphenol A and hexabromocyclododecane alter secretion of IL-1beta from human immune cells. *J Immunotoxicol* **2016**, *13*, 403-416.

123. Almughamsi, H.; Whalen, M.M. Hexabromocyclododecane and tetrabromobisphenol A alter secretion of interferon gamma (IFN-gamma) from human immune cells. *Arch Toxicol* **2016**, *90*, 1695-1707.

124. Yasmin, S.; Whalen, M. Flame retardants, hexabromocyclododecane (HCBD) and tetrabromobisphenol a (TBBPA), alter secretion of tumor necrosis factor alpha (TNFalpha) from human immune cells. *Arch Toxicol* **2018**, *92*, 1483-1494.

125. Kibakaya, E.C.; Stephen, K.; Whalen, M.M. Tetrabromobisphenol A has immunosuppressive effects on human natural killer cells. *J Immunotoxicol* **2009**, *6*, 285-292.

126. Park, H.R.; Kamau, P.W.; Korte, C.; Loch-Caruso, R. Tetrabromobisphenol A activates inflammatory pathways in human first trimester extravillous trophoblasts in vitro. *Reprod Toxicol* **2014**, *50*, 154-162.

127. Koike, E.; Yanagisawa, R.; Takano, H. Brominated flame retardants, hexabromocyclododecane and tetrabromobisphenol A, affect proinflammatory protein expression in human bronchial epithelial cells via disruption of intracellular signaling. *Toxicol In Vitro* **2016**, *32*, 212-219.

128. Lyu, L.; Jin, X.; Li, Z.; Liu, S.; Li, Y.; Su, R.; Su, H. TBBPA regulates calcium-mediated lysosomal exocytosis and thereby promotes invasion and migration in hepatocellular carcinoma. *Ecotoxicol Environ Saf* **2020**, *192*, 110255.

Chapter 3

Global Aims

3. Global aims

TBBPA is a brominated phenolic compound that has been used as a flame retardant. It can contaminate the environment, thus exposing the human being to it. Over the last years, this compound has raised some concerns regarding human health since it can act as an endocrine disrupting compounds (EDCs) interfering with hormonal function. Given its wide presence in the environment and its potentially adverse effects on human health, several studies propose a correlation between TBBPA exposure and adverse health outcomes, such as thyroid, neurobehavior, development, oncological, immunological, cardiac, and reproductive disorders. In addition, studies showed that TBBPA affects oxidative stress, cell proliferation, and intracellular calcium levels. This compound has already been detected in biological samples such as human serum, urine, and breast milk, and umbilical cord of Japanese pregnant women. Despite the multiple adverse effects of TBBPA, the vascular consequences of TBBPA exposure are still poorly understood. In this sense, it is important to analyse how the TBBPA exposure effects the vascular tonus and if the endocrine disrupting effects from that exposure can be detected in future generations Therefore, in this doctoral project, several approaches were developed and applied to lead to a better understanding of the role of TBBPA in vascular homeostasis and to understand the mechanistic pathways underlying of TBBPA effects.

According to other studies, EDCs induce smooth muscle relaxation involving the activation of sGC with increases in the cGMP intracellular levels and inactivation of L-Type VGCC. In addition, long-term exposure to EDCs showed interference with the NO/sGC/cGMP/PKG pathway. Considering these results, the study of the compartmentation of cyclic nucleotides was established as an intermediate task. Although this study of the cGMP compartmentation was not initially one of the goals set, the results obtained in this intermediate task showed to be promising.

This doctoral thesis was developed based on one main general objective: to study the effect of TBBPA on arterial contractility and analyse the possible mechanisms involved in this effect.
To reach this main goal, specific aims were defined and performed throughout this project, including:

1. To characterize and to compare in real-time the changes in subsarcolemmal cGMP concentration in response to activation of sGC and pGC. For that purpose, the HUASMC were infected with adenovirus containing mutants of the rat olfactory cyclic nucleotide–gated (Ad-CNGA2). The whole cell configuration of patch clamp technique was used to measure the cGMP-gated current (I_{CNG}) and the potassium current (I_K) in HUASMC. (**Research Work 1**).

2. To analyse the TBBPA direct effects and the 24 h exposure on the HUA and the HUASMC, and to investigate for the first time how the exposure to TBBPA impairs vascular homeostasis in HUA. Using these arteries, it was possible to 1) analyse the vascular contractility, 2) observe the effects of TBBPA on cGMP signalling pathway, and 3) observe the effects of TBBPA on the activity of L-type Ca^{2+} channels. Using cultured HUASMC it

was possible to 1) analyse the HUASMC viability after 24 h exposure to TBBPA and 2) analyse mRNA expression levels of Cav1.2, BK_{Ca} β_1, BK_{Ca} 1.1α, $Gucci_{\alpha}$ and PRKG 1α after 24 h exposure to TBBPA. (**Research Work 2**).

3. To evaluate the effects of TBBPA in rat aortic smooth muscle, and to investigate its signalling pathway. *Ex vivo* and *in vitro* experiments in rat aorta were performed. Resorting to these arteries, the vascular contractility was analysed and using cultured A7r5 cells it was possible to 1) analyse the A7r5 cells viability after 24h exposure to TBBPA, 2) observe the TBBPA effects in Ca^{2+} current and 3) analyse mRNA expression levels of Cav1.2, BK_{Ca} β_1, BK_{Ca} 1.1α, $Gucci_{\alpha}$ and PRKG 1α after 24 h exposure to TBBPA (**Research Work 3**).

Chapter 4

Research Work 1

Cyclic guanosine monophosphate compartmentation in human vascular smooth muscle cells

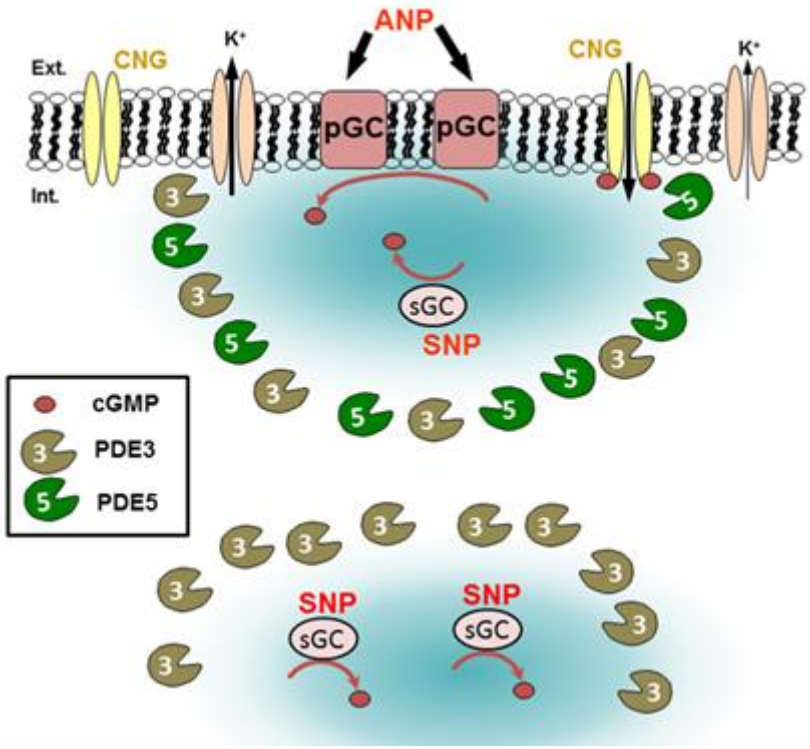

This chapter corresponds to the original research article:

Joana Feiteiro, Ignacio Verde, Elisa Cairrão (2016). *Cyclic guanosine monophosphate compartmentation in human vascular smooth muscle cells*. Cellular Signalling. Volume 28, Issue 3, March 2016, Pages 109-116, https://doi.org/10.1016/j.cellsig.2015.12.004.

4.1. Abstract

Aims: The role of different vascular subtypes of phosphodiesterases (PDE) in cGMP compartmentalization was evaluated in human smooth muscle cells.

Methods and results: To understand how the cGMP conveys different information we infected smooth muscle cells with adenovirus containing mutants of the rat olfactory cyclic nucleotide–gated (CNG) channel-subunit and we recorded the associated cGMP-gated current (I_{CNG}). The whole cell configuration of patch clamp technique was used to measure the I_{CNG} and also the potassium current (I_K) in human umbilical artery smooth muscle cells (HUASMC). ANP (0.1μM) induced a clear activation of basal I_{CNG}, whereas SNP (100μM) had a slight effect. The nonselective PDE inhibitor (IBMX; 100μM), the PDE5 inhibitor (T0-156; 1μM) and the PDE3 inhibitor (cilostamide; 10μM), all had a tiny effect on the basal I_{CNG} current. Concerning potassium channels, we observed that ANP and testosterone induced activation of I_K and this activation is bigger than that elicited by SNP, cilostamide and T0-156. Cilostamide and T0-156 decreased the CNG stimulation induced by ANP and testosterone, suggesting that pGC pool is controlled by PDE3 and 5. Thus, the effects of SNP show the existence of two separated pools, one localized next to the plasma membrane and controlled by the PDE5 and PDE3, and a second pool localized in the cytosol of the cells that is regulated mainly by PDE3.

Conclusions: Our results show the existence of cGMP compartmentalization in human vascular smooth muscle cells and this phenomenon can open new perspectives concerning the examination of PDE families as therapeutic targets.

Keywords: Compartmentalization, Cyclic nucleotide-gated channels, Cyclic GMP, Potassium current, Phosphodiesterases

4.2. Introduction

CNG channels have been used in the last years to monitor and to define the spatial and temporal changes in cyclic nucleotides in living cells. The CNGA2, translate changes in intracellular cyclic nucleotide concentration in electrical response and/ or a sign of Ca^{2+} intracellular because they open by the direct binding of cAMP and cGMP [1].

In living cells, the cGMP synthesis is controlled by two types of guanylyl cyclases that differ in their cellular location and in their activation by specific ligands. The particulate guanylyl cyclases (pGC) localized at the plasma membrane, which is activated by natriuretic peptides such as atrial (ANP), brain (BNP) and C-type natriuretic peptides [2-4]. The soluble guanylyl cyclase (sGC) is present in the cytosol and is activated by nitric oxide (NO) [4,5]. Although both cyclases synthetise cGMP, the consequences of activating pGC or sGC often lead to dissimilar functional effects. One explanation for these divergent effects is that different stimuli induce cGMP rises in distinct and specific subcellular locations, hence regulating dissimilar targets in different parts of the cells [6-10]. Thus, the increase of cGMP induced by natriuretic peptides and by NO donors may occur in different subcellular compartments [6,7,11].

The existence of subcellular compartments of cyclic nucleotides cAMP was discovered some decades ago [12] and explains different effects observed in cardiomyocytes [13-16]. Some authors suggested that this phenomenon is due to a physical barrier formed by parts of the endoplasmic reticulum located near the plasma membrane [14]. Other authors suggested that this phenomenon depends on the location of various components associated with signal transduction pathways cyclic nucleotide [17]. The cyclic nucleotides localized signals are important to determine the speed and the specificity of events mediated by the cyclic nucleotides. This allows the cells to respond differently to different external stimuli which act on the same second messenger. Thus, changes in cyclic nucleotide concentration in subcellular places may orchestrate a variety of cellular responses [14]. Several years ago, it was demonstrated that PDE, the enzymes degrading cyclic nucleotides, participate in its compartmentalization [13,15,18-20]. Different effects between after stimulation of the ANP and SNP pathways in human umbilical artery smooth muscle cells (HUASMC) concerning the stimulation of potassium currents were also observed [21]. Moreover, Santos-Silva *et al* [22] in HUASMC demonstrated that the two major PDE isoforms bind and hydrolyse intracellular cGMP: PDE3, which hydrolyses preferentially cAMP and is inhibited by cGMP; and PDE5, which is highly specific for cGMP. Our data and that obtained in cardiomyocytes suggest the existence of subcellular compartments of cyclic nucleotides in vascular smooth muscle cells. However, few information was obtained concerning compartmentalization of cyclic nucleotides in vascular smooth muscle cells.

In this study, our aim was to characterize and compare in real time the changes in subsarcolemmal cGMP concentration in response to activation of sGC and pGC. For that purpose, we used the wild-type (WT) α-subunit of the rat olfactory cyclic nucleotide–gated channel (CNGA2) as real-time sensor for subsarcolemmal cGMP [23]. This channel binds cGMP with a >10-fold higher affinity than cAMP [23]. Here we describe experiments performed on HUASMC infected with an adenovirus encoding the WT CNGA2 (Ad-CNGA2). Using this model, we analysed the effect

of atrial natriuretic peptide (ANP, a stimulator of particulate GC) and sodium nitroprusside (SNP, a stimulator of soluble GC) and we provide evidence for cGMP compartmentalization and identify PDE3 and PDE5 isoforms as key elements in this phenomenon.

4.3. Methods

4.3.1. Tissue preparation

Pieces (3–7 cm) of the umbilical cord were obtained from normal term pregnancies after vaginal delivery with the consent of the donor mothers. All the procedures performed with the umbilical cords in the present study were approved by the Ethics Committee of Centro Hospitalar da Cova da Beira (Covilhã, Portugal) and conformed to the tenets of the Declaration of Helsinki.

Umbilical cord samples were collected in sterile physiological saline solution (PSS; composition (in mmol/L): NaCl 110; CaCl2 0.15; KCl 5; MgCl2 2; HEPES 10; NaHCO3 10; KH2PO4 0.5; NaH2PO4 0.5; glucose 10; EDTA 0.49). To avoid contamination and tissue degradation, penicillin (5 U/mL), streptomycin (5 μg/mL), amphotericin B (12.5 ng/mL) and antiproteases (leupeptin 0.45 mg/L, benzamidine 26mg/L and trypsin inhibitor 10mg/L) were added to the PSS. Umbilical arteries were isolated from the surrounding connective tissue and cut into 3–5 mm rings. The human umbilical artery (HUA) rings were cut up into rectangular pieces with scissors so that the smooth muscle layers from the tunica media could be retrieved using surgical forceps and a scalpel. The smooth muscle layers were used for subsequent cell dissociation and culture (see below).

4.3.2. Cell dissociation and culture

Smooth muscle cells were isolated from the HUA as previously described [24]. Briefly, the layers extracted from the tunica media were cut into small fragments and placed in PSS (without antiproteases but containing 1–2 mg/mL collagenase V, 0.3–0.5 mg/mL elastase, 0.6 mg/mL trypsin inhibitor and 1.25 mg/mL taurine) for 10min at 37 °C. The hydrolytic action of the enzymes was stopped by the addition of Dulbecco's modified Eagle's medium (DMEM)–F12 cell culture medium containing 10% fetal bovine serum (FBS). The digested tissue was subjected to gentle shaking for 10 min, after which it was filtered through a 500 μm mesh. The filtered solution, containing isolated HUA smooth muscle cells, was centrifuged at 150 g for 5 min at 21° C. The supernatant was discarded, and the pellet was suspended in plating medium, consisting of DMEM-F12 containing 5 % FBS, 5 μg/mL epidermal growth factor (EGF), 0.5 ng/mL fibroblast growth factor (FGF), 2μg/mL heparin and 5 μg/mL insulin. Cells were plated in collagen-coated culture dishes at 37°C under an atmosphere of 95 % air and 5 % CO2. The culture medium was changed every 2–3 days and confluent cultures were obtained after 15–20 days. Confluent cells were subcultured until passage 7.

4.3.3. Infection

The infection of HUASMC with WT CNGA2 encoding adenovirus (Ad-CNGA 2) was performed as previously described [25]. The confluent cultures of HUASMC were placed for 1h in the FBS-free cell culture medium DMEM-F12. After this time, the medium is replaced by 400 μL of free-FBS medium containing WT CNGA2 encoding adenovirus (Ad-CNGA2), used at a multiplicity of infection (MOI) of 5000 plaque forming units per cell (pfu/cell). The Ad-CNGA2 was a generous gift from Dr Dermot Cooper (University of Cambridge, United Kingdom)

After infection, the cells are placed in an incubator for 24 h. After this period the medium is replaced by DMEM-F12 containing 5 % FBS and placed 12h in an incubator. After that the cells were used to perform the experiments.

4.3.4. Immunocytochemistry

The HUASMC attached onto coverslips (1 × 104 cells/dish) were fixed, permeabilized and incubated with a mouse monoclonal antibody against CNGA2 as previously described [13,24]. This antibody was a generous gift of Drs. F. Mueler and B. Kaupp (Juelich, Germany). Cells were revealed with Alexa fluor 488 goat anti-mouse. After mounting the samples, the expressed proteins were localized using a Confocal fluorescence imaging with a confocal laser scanning (Carl Zeiss, LSM510 Meta) with 488 nm laser excitation for the fluorescein isothiocyanate (FITC) channels. A 40× ApoChromat,1.4-NA objective (Carl Zeiss) was used to ensure high-resolution images. DIC images were collected simultaneously with transmitted light by excitation at 633 nm. Images were processed with LSM Image Browser (Zeiss) and Adobe Photoshop.

4.3.5. Electrophysiology experiments

Cells from the first to the sixth passages were trypsinized and used to perform the electrophysiology experiments.

The CNGA2 current (I_{CNG}) in HUASMC was analysed in the whole cell configuration of the patch clamp technique. The cells were maintained at 0 mV holding potential and routinely hyperpolarized every 8s to -50mV test potential during 200ms. I_{CNG} was recorded in the absence of divalent cations in the extracellular solutions contains (mM): NaCl 107, CsCl 20, HEPES 10, Glucose 5 and pH 7.4; allowing monovalent cations to flow through the channels in a non-specific manner. Patch electrodes (2.8-4.2MΩ) were made of soft glass and filled with control internal solution (Reagent 5, Portugal) and filled with control internal solution containing (in mM): HEPES 20, EGTA 20, Glucose 5, TEA 5, CsCl 113.8, MgCl2 2.5, CaCl2 0.062, Na2ATP 3.1, Na2GTP 0.42, adjusted to pH 7.3 with CsOH. Basal I_{CNG} were measured 5-10 min after patch break to allow the equilibration between pipette and intracellular solutions.

The potassium current (I_K) was analysed in HUASMC using the amphotericin B-performed whole-cell patch-clamp methodology [26]. The cells were maintained at a holding potential of −80mV and routinely depolarised every 8s to 60mV test potential during 350ms to measure I_K. The external solution contained (mM): NaCl 134.3, CaCl2 1.0, HEPES 5.0, KCl 5.4 and glucose 6.0, pH

7.4 adjusted with NaOH. The internal solution contained (mM): KCl 125.0, MgCl2 1.0, Na-ATP 5.0, Na-GTP 0.5, EGTA 0.1, HEPES 20.0 and glucose 10.0, pH 7.3 adjusted with KOH.

Currents I_{CNG} and I_K were not compensated for capacitance and leak currents. All experiments were done at room temperature (21–25 °C) and the temperature did not vary by more than 1 °C in a given experiment. The cells were voltage clamped using the patch-clamp amplifier Axopatch 200B (Axon instruments, USA). Currents were sampled at 10kHz frequency and filtered at 0.05kHz using the analogy-digital interface Digidata 1322A (Axon Instruments, USA) connected to a compatible computer with the Pclamp8 software (Axon Instruments, USA). Patch electrodes of 2–4 MΩ made of soft borosilicate glass capillaries (GC150T-15, Harvard apparatus, UK) were filled with the internal solution. The external solution was applied to the cell proximity by placing the cell at the opening of a 250μm inner diameter capillary tube flowing at a rate of 20 μL/min. The basal I_{CNG} was studied in the presence of ANP (0.1 μM), SNP (100 μM), IBMX (100 μM), T0-156 (0.01-10 μM), cilostamide (0.1-10 μM) e 8-Sp (100 μM). Moreover, the basal I_K was studied in the presence of ANP (0.1 μM), SNP (100 μM), T0-156 (1 μM) e cilostamide (10 μM). The I_K stimulatory or inhibitory effect elicited by the drugs is given in percentage of increase or decrease on basal I_K.

4.3.6. Drugs and chemicals

All drugs and chemicals were purchased from Sigma-Aldrich Chemistry (Sintra, Portugal). Testosterone, cilostamide, 3-isobutyl-1-methylxanthine (IBMX) and T0-156 were initially dissolved in ethanol, and final solutions were obtained by dilution with the extracellular solutions. ANP, SNP, 8- ((4-Chlorophenylthio) guanosine- 3', 5'-cyclic monophosphate) (Sp-8, an analog of the natural signal molecule cyclic GMP) were dissolved in distilled water.

4.3.7. Data analysis

I_{CNG} amplitude is time-independent and was measured at the end of the 200ms pulse. In a total of 199 cells, mean membrane capacitance (Cm) was 53.52 ± 4.40 pF. I_{CNG} density (dI_{CNG}) which represents the ratio of current amplitude to Cm was average 7.0±0.5 pA/pF. In each experimental condition, the responses of d I_{CNG} to a drug was expressed relative to the "basal current" obtained in control extracellular solution following the relation: "response" = (I_{CNG} - "Basal current")/Cm.

The amphotericin B- was used to perform whole-cell patch-clamp methodology technique to analyse potassium current (I_K) in HUASMC. Basal I_K amplitude was on average 284±13.38 pA at 60mV membrane potential. In total of mean cell capacitance values were on average 28.0±0.89 pF (n=238).

All results are expressed as mean ± SEM of n experiments. Statistical significance between two groups was analysed using Student´s t-test. Comparison among multiple groups was analysed by using a one-way ANOVA followed by Tuckey and Dunnet's test, post-hoc test to determine significant differences among the means. Probability levels lower than 5% were considered significant ($p<0.05$). Statistical analysis of data was performed using the SigmaStat Statistical Analysis System, version 3.5 (2007).

4.4. Results

4.4.1. Subsarcolemmal localization of recombinant CNGA2 channels in HUASMC

CNGA2 expression in HUASMC was investigated by immunofluorescence after 36 h of culture. Native or Ad-CNGA2 cells were labelled with primary antibody against CNGA2 and visualized with fluorophore conjugated secondary antibody (Alexa 488). The Figure 4.1 shows images of representative cells in Ad-CNGA2-infected and Figure 4.2 shows cells not infected. Infected cells show a strong fluorescent signal in the plasmatic membrane. These results revealed that the cells are infected with WT CNGA2 encoding adenovirus (Ad-CNGA2).

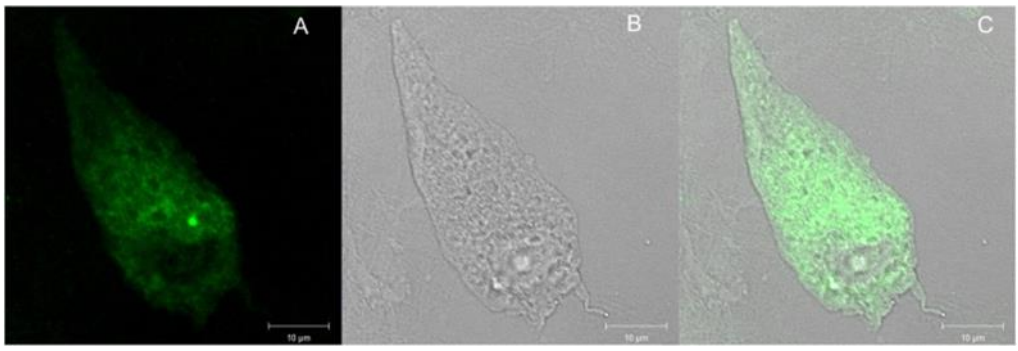

Figure 4.1. Representative confocal microscopy imagens of the recombinant WT-CNGA2 channels in HUASMC. **(A)** Confocal fluorescence (FL), **(B)** Transmitted light (TL), **(C)** and overlay image (FL + TL). The smooth muscle cells were infected with an adenovirus encoding the wild type (WT) α-subunit of rat olfactory CNG channels and labelled with ant-CNGA2 antibody after 36 h of culture. Images were processed with LSM Image Browser (Zeiss) and Adobe Photoshop.

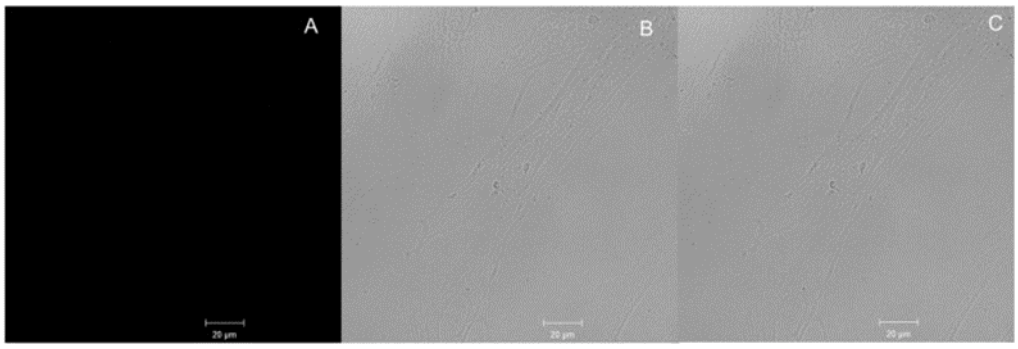

Figure 4.2. Representative confocal microscopy imagens of the recombinant WT-CNGA2 channels in non-infected HUASMC. **(A)** Confocal fluorescence (FL), **(B)** Transmitted light (TL), **(C)** and overlay image (FL + TL). Images were processed with LSM Image Browser (Zeiss) and Adobe Photoshop.

4.4.2. Functional expression of CNGA2 channels in HUASMC

The CNGA2 current (I_{CNG}) was recorded 36 hours after cell infection. This methodology induced a time-independent inward current at −50 mV in Ad-CNGA2 cells. Such current was not detected in non-infected HUASMC, and the application of Sp-8 (100 μmol/L) did not change I_{CNG} density (0.3±0.3 pA/pF; n = 4), but Sp-8 induced a large increase in infected HUASMC (13.0±2.7

pA/pF; n =26). The membrane permeable cGMP-analogue Sp-8 (100 µmol/L) was used as positive control of the stimulation of CNG channels and elicited a maximal effect.

The cGMP effect has been analysed after activation of pGC and sGC by the stimulation of CNGA2 channels. We used the ANP as activator of pGC and SNP as sGC activator. The results show that, either ANP (0.1 µmol/L) or SNP (100 µmol/L) increase I_{CNG} and the effect induced by ANP (9.12±1.26 pA/pF, n = 18) was not significantly different than that of Sp-8 100µmol/L (12.37±2.53 pA/pF, n = 6) that corresponds to the maximal amplitude of I_{CNG} in infected HUASMC, as show in Figure 4.3A. The effect induced SNP (6.29±1.04 pA/pF, n = 23) is significantly smaller than the effect caused by the Sp-8 100µmol/L (12.59±1.83 pA/pF, n = 8), as show in Figure 4.3B.

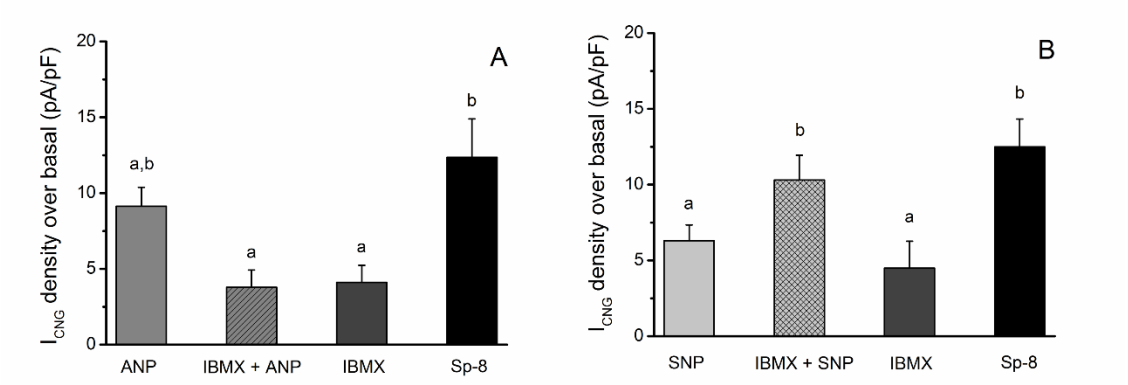

Figure 4.3. Effect of unspecific inhibition of PDE on CNG current density. The bars show the CNG density of current (pA/pF) elicited by Sp-8 (100 µmol/L; positive control) and IBMX (100 µmol/L) alone and in presence of **(A)** ANP (0.1 µmol/L) and **(B)** SNP (100 µmol/L). The bars represent the mean and the lines the SEM, n = 6–23 of cell studied from at least 5 different human umbilical arteries. Distinct letters (a, b) indicate significant differences ($p < 0.05$ one-way ANOVA with Tukey post hoc test and Dunnett's post hoc test.).

4.4.3. Effect of PDE on CNGA2 activity in presence and in absence of ANP and SNP

4.4.3.1. Effect of the non-selective PDE inhibitor on CNGA2 activity

To start studding effect of PDE in compartmentalisation, initially we used a non-selective PDE inhibitor, the IBMX (3-Isobutyl-1-methylxanthine; 100 µmol/L), which by its own caused a small I_{CNG} stimulation. Regarding pGC stimulation, when associated ANP (0.1 µmol/L) with IBMX a small decrease in de I_{CNG} occurred, however this decrease is not significant than that the observed by ANP, as show in Figure 4.3A. The association of SNP (100 µmol/L) with IBMX stimulated significantly I_{CNG} when compared with SNP and with IBMX, as shown in Figure 4.3B. The different response of IBMX in presence of ANP and SNP suggests that in some way the PDE limit the cGMP pool next to the plasma membrane.

4.4.3.2. Role of PDE3 and PDE5 on CNGA2 activated by pGC

In the following experiments, our aim was to analyse if the more relevant PDE subtypes are involved in cGMP compartmentalization. We used selective inhibitors for these two PDE isoforms: cilostamide that inhibits PDE3 and To-156 that inhibits PDE5, and they induced only small increase I_{CNG} ($p < 0.05$, Figure 4.4). As shown in the Figure 4.4, ANP and Sp-8 increase similarly I_{CNG}, ANP is a direct activator of pGC, which induces the production of cGMP near the membrane. So, we analysed what would be the role of PDE3 in the modulation of cGMP levels close to the membrane when its production is stimulated by pGC. Figure 4.4A shows that ANP induces a clear stimulation of I_{CNG}, but when associated with cilostamide (0.1, 1 and 10 μmol/L) this stimulation was reduced ($p < 0.05$), suggesting a role of PDE3 in cGMP compartmentalization.

We also analysed what would be the role of PDE5 in the modulation of cGMP levels generated by ANP. Figure 4.4B show that the stimulatory effect of ANP (0.1 μmol/L) on I_{CNG} decreases in presence of a low concentration of the PDE5 inhibitor (0.01 μmol/L). The I_{CNG} stimulation induced by the association of ANP (0.1 μmol/L) and higher concentrations of To-156 (0.1 and 1 μmol/L) is not significantly different from the stimulation obtained either by ANP alone or by Sp-8 ($p > 0.05$). The Figure 4.5 shows a typical experiment of the ANP (0.1 μmol/L) alone and with To-156 (To; 0.01-1 μmol/L), and Sp-8 (100 μmol/L), the membrane permeable cGMP analogue.

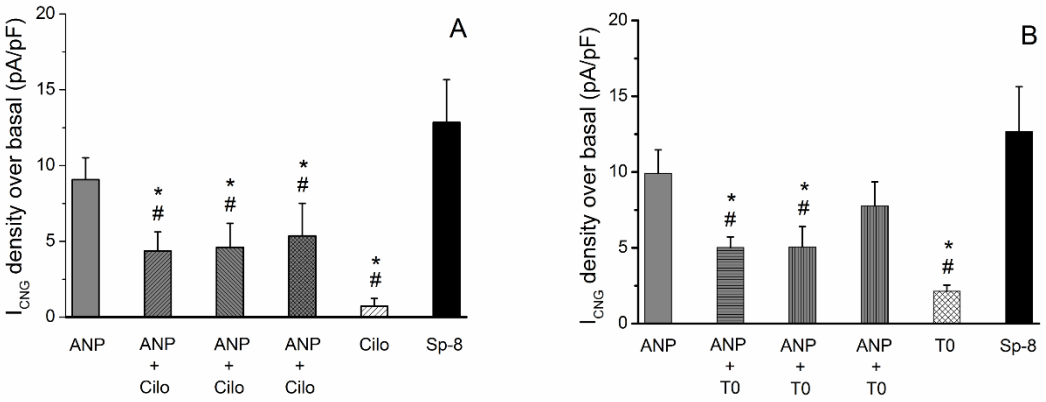

Figure 4.4. Effect of PDE3 and PDE5 inhibitors on ANP stimulated CNG current density. The bars show the ANP (0.1 μmol/L) stimulated CNG density of current (pA/pF) elicited by **(A)** cilostamide (Cilo; 0.1-10 μmol/L, PDE3 inhibitor) and **(B)** To-156 (To; 0.01-1 μmol/L, PDE5 inhibitor). The bars represent the mean and the lines the SEM, n = 3–14 cell studied from at least 3 different human umbilical arteries. * $p < 0.05$ versus the Sp-8 effect and # $p < 0.05$ versos ANP effect, one-way ANOVA with Tukey post hoc test and Dunnett's post hoc test.

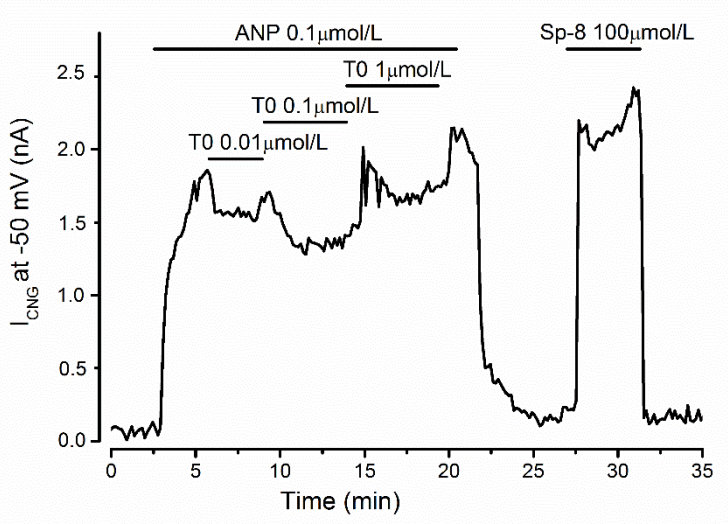

Figure 4.5. A time course of CNGA2 current (I_{CNG}) amplitude at -50 mV in an Ad-CNGA2 infected human umbilical smooth muscle cells. The cell was the challenged with ANP (0.1 μmol/L), and with ANP plus To-156 (To; 0.01-1 μmol/L), and with 8-pCPT as an internal control for WT-CNGA2.

4.4.3.3. Role of PDE3 and PDE5 on CNGA2 activated by sGC

SNP is a NO donor which activates sGC and stimulates production of cytosolic cGMP. We analysed the role of PDE3 in modulation of cGMP signals generated by SNP. In figure 4.6A we can observe that the stimulation of I_{CNG} induced by SNP significantly decreases in presence of lower concentrations of cilostamide (0.1 and 1 μmol/L) ($p < 0.05$). However, this decrease does not occur when the cilostamide concentration was 10 μmol/L.

Concerning to contribution of PDE5 to the control of the cGMP pool generated by activation of sGC, the PDE5 inhibitor (0.01, 0.1 and 1 μmol/L) caused slightly and not significant decrease of the SNP I_{CNG} stimulation (Figure 4.6B). The I_{CNG} stimulation induced by SNP, either alone or in presence of To-156, is significantly lower than that caused by Sp-8 ($p < 0.05$).

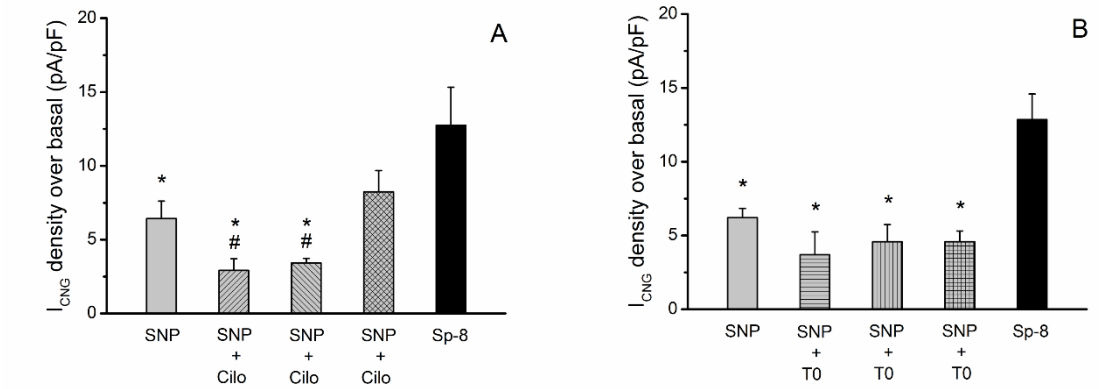

Figure 4.6. Effect of PDE3 and PDE5 inhibitors on SNP stimulated CNG current density. The bars show the SNP (100 μmol/L) stimulated CNG density of current (pA/pF) elicited by **(A)** cilostamide (Cilo; 0.1-10 μmol/L, PDE3 inhibitor) and **(B)** To-156 (To; 0.01-1 μmol/L, PDE5 inhibitor). The bars represent the mean and the lines the SEM, n = 7–13 cell studied from at least 5 different human umbilical arteries. * $p < 0.05$ versus the Sp-8 effect and # $p < 0.05$ versos SNP effect, one-way ANOVA with Tukey post hoc test and Dunnett's post hoc test.

4.4.4. Effect of PDE inhibitors on potassium current (I_K) stimulated by pGC activator and testosterone.

We analysed the effect of PDE3 and PDE5 inhibition on I_{CNG} stimulated by ANP (pGC activator) and testosterone by an unknown pathway also stimulates pGC, supposed to as previously described [25]. Figure 4.7 shows the effect of ANP and testosterone alone or in the presence of the PDE3 and PDE5 inhibitors. ANP (0.1 µmol/L) stimulated I_K and cilostamide (10 µmol/L) or T0-156 (1 µmol/L) significantly decreased the ANP effect. This I_K decline was more prominent when PDE3 was inhibited. The I_K stimulation induced by ANP and testosterone are similar ($p > 0.05$). On the other hand, testosterone alone (0.1 µmol/L) activated I_K, and the PDE5 or PDE3 inhibitors significantly decreased this effect ($p < 0.05$). The results also show that, by its own, cilostamide 10 µmol/L (-0.98±1.49, n = 40) and T0-156 1 µmol/L (-1.61±0.93, n = 42) does not modify the I_K.

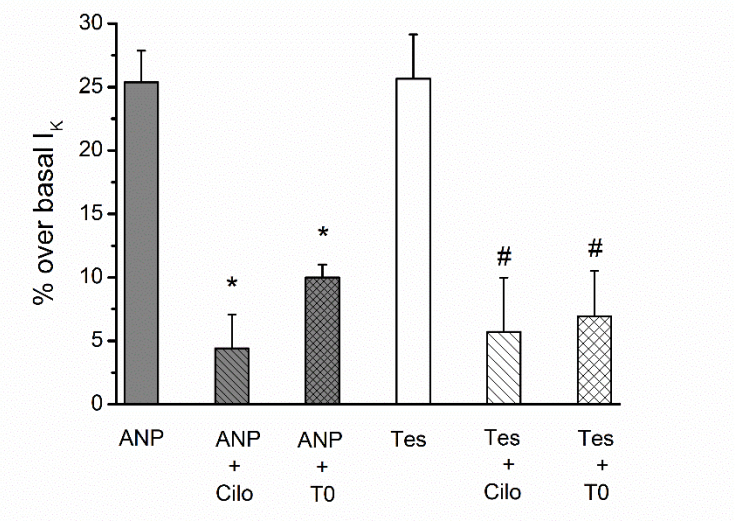

Figure 4.7. Effect of PDE3 and PDE5 specific inhibitors on pGC activator and testosterone stimulated potassium current. The bars show the percent of I_K elicited by ANP (0.1µmol/L) and testosterone (Tes; 0.1µmol/L) alone or in the presence of cilostamide (10 µmol/L; Cilo) and T0-156 (T0; 1µmol/L). The bars represent the mean and the lines the SEM, n = 5–28 cell studied from at least 5 different human umbilical arteries. * p <0.05 versus the ANP effect and # p <0.05 versos testosterone effect, one-way ANOVA with Dunnett's post hoc test.

4.4.5. Effects of PDE3 and PDE5 inhibitors on SNP potassium current (I_K) stimulation

Figure 4.8 shows the effect of SNP alone or in the presence of PDE inhibitors: cilostamide (10 µmol/L) and T0-156 (1 µmol/L).

The soluble guanylate cyclase activator induced stimulation of I_K (figure 4.8), and this effect is not modified in the presence of PDE3 or PDE5 inhibitors, however in the presence of PDE3 inhibitor the I_K is not significantly stimulated ($p = 0.07$, one-way ANOVA).

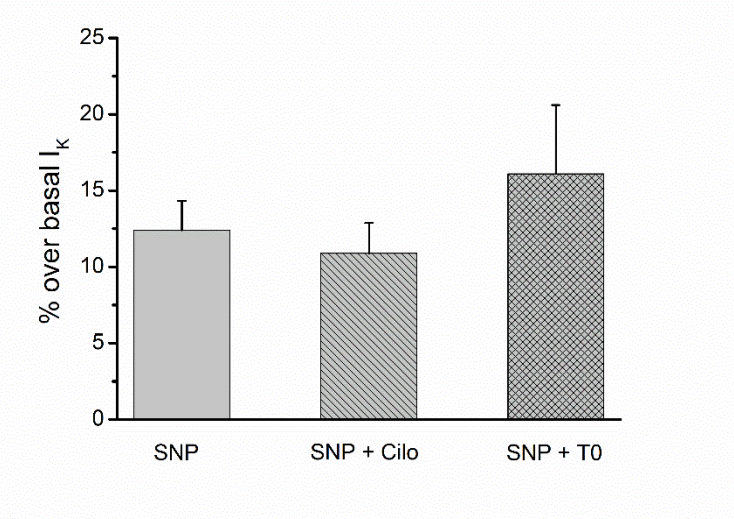

Figure 4.8. Effect of PDE3 and PDE5 specific inhibitors on sGC activator stimulated potassium current. The bars show the percent of I_K elicited by SNP (100 μmol/L) alone or in the presence of cilostamide (10 μmol/L; Cilo) and T0-156 (T0; 1 μmol/L). The bars represent the mean and the lines the SEM, n = 9–21 cell studied from at least 5 different human umbilical arteries.

4.5. Discussion

In the present study we have used CNG channels as cGMP biosensors in HUASMC to study the role of PDE3 and PDE5 on cGMP compartmentalization. We applied the whole cell configuration of patch clamp technique to measure CNG current in infected HUASMC and also to measure potassium channels activity (I_K) in HUASMC. Previously, we already had demonstrated that the I_K is stimulated by ANP and testosterone, and this effect corresponds to the activation of BK_{Ca} and K_V channels through an increase of cGMP and PKG activation [25]. Our data reveal differences in spatiotemporal distribution of intracellular cGMP depending on activation two cyclases differently localized: 1) when pGC is activated by ANP, cGMP rises near the membrane; 2) when sGC is activated by NO donors (SNP), cGMP increases in the cytosol and also near the membrane. These suggest that when a cyclase is activated, besides its hydrosolubility, intracellular cGMP is not uniformly distributed within the cell, and it is probably clustered in specific sites. We found that PDEs play a key role in this compartmentation, because different PDE subtypes (PDE3 and PDE5) regulate particulate and cytosolic cGMP pools. We observed that PDE5 appears to control the particulate but not the soluble pool and the soluble cGMP pool is under the exclusive control of PDE3.

Ours previous results are performed in human umbilical arteries; however, this vessel transports deoxygenated blood, contrarily to the observed with the umbilical vein. Umbilical and placental vessels lack autonomic innervation and regulation of its vascular tone depends on the release of vasoactive substances, which are locally produced or transported through the circulation system. However, the HUASMC seems to play a major role in controlling the fetoplacental blood flow [27,28]. The vascular smooth muscle cells are responsible for the vascular tone by responding to various hormonal and haemodynamic stimuli. The use of these cells is essential to study several

signalling processes implicated in this control, as calcium metabolism and different pathways involved in the modulation of vascular reactivity [29]. Thus, the used of HUASMC may be used to generalize to the other smooth muscle cells present of other arteries. But this generalization can see allows controversy, not only by the type of blood that transports, that principally by the main function of this artery that is limited in the time.

Several studies have shown differential effects of cGMP produced by sGC and pGC concerning the regulation of various cell functions. In pig airway smooth muscle cells, stimulation of pGC and not sCG, causes relaxation exclusively by decreasing intracellular Ca^{2+} concentrations and Ca^{2+} sensitivity of the myofilaments [7]. In a human epithelial cell line, activation of pGC and not sGC is coupled to the inhibition of Ca^{2+} efflux, whereas activation of sGC and not pGC is involved in stimulation of Ca^{2+} sequestration into the intracellular Ca^{2+} stores [6]. In human endothelial cells from umbilical vein, activation of sGC induces relaxation in a more efficient manner than does activation of pGC [10]. Differences between pGC and sGC activation have also been reported in cardiac preparations. In frog ventricular myocytes, sGC activation causes a pronounced inhibition of the L-type Ca^{2+} current ($I_{Ca,L}$), whereas pGC activation had little effect [30]. In rabbit atria, activation of pGC caused a larged cAMP accumulation (via PDE3 inhibition), cGMP efflux, and ANP release than activation of sGC [8]. In mouse ventriculares myocytes, pGC activation caused a decrease in intracellular Ca^{2+}, whereas sGC activation had little effect [9].

To our knowledge, the present study provides the first direct evidence for intracellular cGMP compartmentalization in vascular SMC. To explain this compartmentation, some authors suggest the existence of a physical barrier formed by elements of the endoplasmic reticulum, located near the plasma membrane [14]. Other authors suggest that this phenomenon depends on the location of various components associated with signal transduction pathways of cyclic nucleotides. More recently, it was also suggested that PDE have a crucial role for the existence of different concentrations of cAMP and/or cGMP in distinct cell locations [31,32]. Furthermore, Castro *et al.* (2006) demonstrated that in rat cardiomyocytes the particulate cGMP pool is readily accessible at the plasma membrane, whereas the soluble is not. These authors also demonstrated that PDE5 controls the soluble but not the particulate pool, whereas the particulate pool is under the exclusive control of PDE2 [13].

We took advantage of the method developed by Rich and co-workers [23] in HEK293 cells that follow in real time cGMP changes beneath the sarcolemma membrane using the WT-CNGA2 as readout. We previously confirmed by immunocytochemistry that this channel is not normal expressed in native HUASMC [25] but becomes functionally expressed 24 hours after infection of the HUASMC with the Ad-CNGA2 constructer developed by Fagan *et al.* [33].

The WT-CNGA2 channel responds to cGMP changes with threshold at 0.1 to 0.5 μmol/L concentration, a K1/2 of 1.4 μmol/L, and a maximal amplitude obtained at 5 to 10 μmol/ cGMP [23]. With the use of these parameters and the amplitude of the CNG current measured at the end of each experiment after applications of a saturating concentration (100 μmol/L) of the cGMP analogue Sp-8, it was possible to give a rough estimate of the subsarcolemmal cGMP concentration reached in each of the experimental condition tested here.

Ours results obtained with WT-CNGA2 channel in the HUASMC clearly indicate that the homogeneous distribution of cGMP is stopped by the activity of PDE, because when we block the activity of PDE with IBMX the I_{CNG} decreases, so the intracellular cGMP is highly compartmentalized within HUASMC, and that homogeneous distribution is controlled by PDE activity.

In 2008, Santos Silva *et al.* concluded that the PDE that are expressed on human umbilical artery smooth muscle cells are PDE1, PDE3, PDE4 and PDE5, however only PDE3 and PDE5 hydrolyse cGMP [22]. All PDE isoforms are inhibited by IBMX, and different drugs have been developed as selective inhibitors of PDE3 and PDE5. In this study we used cilostamide as specific PDE3 inhibitor and T0-156 as specific PDE5 inhibitor and we observed that by its own both inhibitors have little effect on I_{CNG}. Concerning the I_K, the PDE5 and PDE3 inhibitor did not change the potassium current activity.

The CNG stimulation by ANP decreases in the presence of the inhibitor of PDE3 (cilostamide) and PDE5 (T0-156). The cGMP decreases next to membrane due to the break of the membrane pool and cGMP diffuses abroad the cell. This diffusion of cGMP into the inner of the cell has been observed by Nausch *et al.* (2008) with confocal imaging techniques (non-FRET biosensors) with ANP and sildenafil (PDE5 inhibitor) [34]. Nevertheless, this effect is more pronounced with cilostamide, suggesting that inhibition of PDE5 causes small cGMP dispersion near the membrane. These results can be explained because the regulation of the PDE3 is quite different than that the PDE5. Several authors show that PDE3 can function differently dependent of the cGMP concentration and seems that this effect can modified the cAMP concentrations and activated/inhibited other PDEs [8,35,36] however this pathway need to be further analysed. A similar effect was obtained measuring I_K current in HUASMC. Castro *et al.* (2006) also observed in rat cardiomyocytes that a particulate cGMP pool near the plasma membrane, but in their cells the PDE2 is the only PDE responsible for this phenomenon [13].

Our results whether on I_{CNG} and I_K current seems to suggest that SNP produces two separate effects: one more localized near the membrane, which is controlled by the PDE3 and PDE5, and other more localized inside the cells and this effect is regulate only by PDE3. These results are in agreement with those obtained previously by Cawley *et al.* [37] in rat aortic SMC, that observed transient increases in the concentration of cGMP produced by sGC. Moreover, Nausch *et al.* [34] observed the existence of subcellular compartments of cGMP in rat aortic SMC and suggested that PDE5 differentially regulates the effects of NO donors and natriuretic peptides.

We previously demonstrated that the rapid effects of testosterone in HUASMC are due to the activation of pGC, which increase cGMP close to the membrane and activates the CNG channels. We also demonstrated that testosterone activates the CNG channels that are sensible to cGMP and that the stimulation of these channels by testosterone is similar to that induced by ANP [21,25]. Our data show that testosterone and ANP effect decreases in presence of the PDE3 and PDE5 inhibitors, suggesting that this effect is controlled by PDE3 e PDE5 in a similarly way.

The results led us to propose a model for intracellular cGMP compartmentation which is illustrated in Figure 4.9. The activation of the receptor by ANP leads to pGC activity and cGMP production that activated CNG channel to produce I_{CNG} current. The cGMP induce by ANP also

activates PKG, which activated the potassium channels and are directly depends on the concentration of cGMP next to the potassium channels. When PDE3 or PDE5 are inhibited, the cGMP decreases next to membrane due to the break of the membrane pool and cGMP diffuses abroad the cell. This diffusion of cGMP into the inner of the cell has been observed by Nausch *et al.* (2008) with confocal imaging techniques (non-FRET biosensors) with ANP and sildenafil (PDE5 inhibitor) [34]. The activation of sGC leads to cGMP generation in two different compartments, one next to the membrane and other in the inner of the cell. The PDE3 inhibition induces two different effects: 1) the diffusion of cGMP from the inner of the cell to the compartment next to the membrane, but the PDE5 may, in some way, form a barrier next to the membrane and 2) the diffusion of the cGMP from the compartment next to the membrane to other places inside the cell. On the contrary, the PDE5 inhibition does not modified the concentration of cGMP- dependent of the activation of sGC. On the other hand, several authors show that PDE3 can function differently dependent of the cGMP concentration and seems that this effect can modified the cAMP concentrations and activated/inhibited other PDEs [8,35,36] however this pathway need to be further analysed.

In summary, this work is the first to prove that cGMP is compartmentalizated in human vascular muscle. Our study also reveals for the first time that the compartmentation of cGMP is controlled by PDE3 and PDE5. The particulate cGMP pool formed near plasma membrane and is controlled by PDE5 and PDE3 and the cGMP pool localised in the cytosol is exclusively controlled by PDE3.

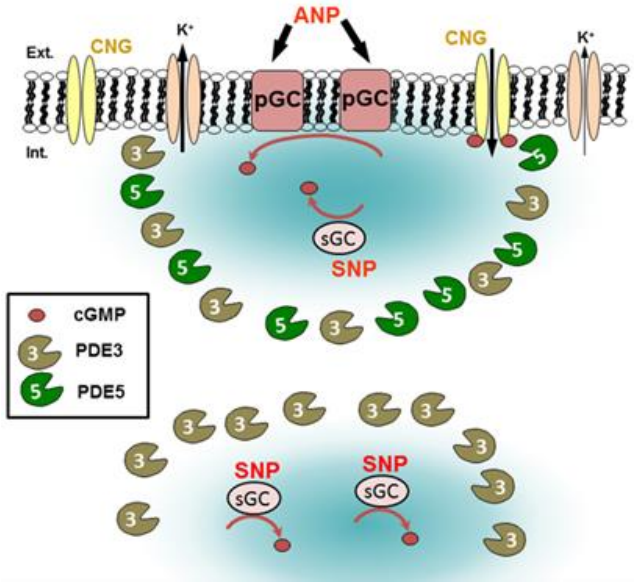

Figure 4.9. Schematic representation of cGMP compartmentation PDE3 and PDE5-dependent of in the HUASMC. The diagram represents the endoplasmic membrane, with CNG channels, potassium channels and NP receptor inserted. Activation of the receptor by ANP leads to pGC activity and cGMP production that activated CNG channel to produce I_{CNG} current. The cGMP induce by ANP also activates PKG, which activated the potassium channels. When the PDE3 or PDE5 inhibits, the cGMP decrease net to membrane, because to the diffusion of cGMP to the inner of the cell. Activation of sGC by NO leads to cGMP generation in two different compartment, one next to the membrane and other in the inner of the cell. The PDE3 inhibition leads to different effects 1) the diffusion of cGMP from the inner of the cell to the compart next to the membrane, but the PDE5 may, in some way, form a barrier next to the membrane and 2) the diffusion of the cGMP from the compartment next to the membrane.

4.6. Conflict of interest

The authors declare that they have no conflicts of interest.

4.7. Acknowledgments

We thank the donor mothers and the Gynaecology-Obstetrics Department staff of "Centro Hospitalar da Cova da Beira" (Covilhã, Portugal) for their disinterested collaboration and to Dr. Dermot Cooper (University of Cambridge, United Kingdom) for the adenovirus encoding CNGA2. This work was partially supported by the Portuguese Foundation for Science and Technology (FCT) under Program COMPETE(PEst-OE/SAU/UI0709/2014).

4.8. References

1. Kaupp, U.B.; Seifert, R. Cyclic nucleotide-gated ion channels. *Physiol Rev* **2002**, *82*, 769-824.

2. D'Souza, S.P.; Davis, M.; Baxter, G.F. Autocrine and paracrine actions of natriuretic peptides in the heart. *Pharmacol Ther* **2004**, *101*, 113-129.

3. Kuhn, M. Structure, regulation, and function of mammalian membrane guanylyl cyclase receptors, with a focus on guanylyl cyclase-A. *Circ Res* **2003**, *93*, 700-709.

4. Padayatti, P.S.; Pattanaik, P.; Ma, X.; van den Akker, F. Structural insights into the regulation and the activation mechanism of mammalian guanylyl cyclases. *Pharmacol Ther* **2004**, *104*, 83-99.

5. Pyriochou, A.; Papapetropoulos, A. Soluble guanylyl cyclase: more secrets revealed. *Cell Signal* **2005**, *17*, 407-413.

6. Zolle, O.; Lawrie, A.M.; Simpson, A.W. Activation of the particulate and not the soluble guanylate cyclase leads to the inhibition of Ca^{2+} extrusion through localized elevation of cGMP. *J Biol Chem* **2000**, *275*, 25892-25899.

7. Rho, E.H.; Perkins, W.J.; Lorenz, R.R.; Warner, D.O.; Jones, K.A. Differential effects of soluble and particulate guanylyl cyclase on Ca(2+) sensitivity in airway smooth muscle. *J Appl Physiol* **2002**, *92*, 257-263.

8. Wen, J.F.; Cui, X.; Jin, J.Y.; Kim, S.M.; Kim, S.Z.; Kim, S.H.; Lee, H.S.; Cho, K.W. High and low gain switches for regulation of cAMP efflux concentration: distinct roles for particulate GC- and soluble GC-cGMP-PDE3 signaling in rabbit atria. *Circ Res* **2004**, *94*, 936-943.

9. Su, J.; Scholz, P.M.; Weiss, H.R. Differential effects of cGMP produced by soluble and particulate guanylyl cyclase on mouse ventricular myocytes. *Exp Biol Med (Maywood)* **2005**, *230*, 242-250.

10. Rivero-Vilches, F.J.; de Frutos, S.; Saura, M.; Rodriguez-Puyol, D.; Rodriguez-Puyol, M. Differential relaxing responses to particulate or soluble guanylyl cyclase activation on endothelial cells: a mechanism dependent on PKG-I alpha activation by NO/cGMP. *Am J Physiol Cell Physiol* **2003**, *285*, C891-898.

11. Zhang, Q.; Scholz, P.M.; He, Y.; Tse, J.; Weiss, H.R. Cyclic GMP signaling and regulation of SERCA activity during cardiac myocyte contraction. *Cell Calcium* **2005**, *37*, 259-266.

12. Corbin, J.D.; Sugden, P.H.; Lincoln, T.M.; Keely, S.L. Compartmentalization of adenosine 3':5'-monophosphate and adenosine 3':5'-monophosphate-dependent protein kinase in heart tissue. *J Biol Chem* **1977**, *252*, 3854-3861.

13. Castro, L.R.V.; Verde, I.; Cooper, D.M.F.; Fischmeister, R. Cyclic GMP compartmentation in rat cardiac myocytes. *Circulation* **2006**, *113*, 2221-2228.

14. Piggott, L.A.; Hassell, K.A.; Berkova, Z.; Morris, A.P.; Silberbach, M.; Rich, T.C. Natriuretic peptides and nitric oxide stimulate cGMP synthesis in different cellular compartments. *J Gen Physiol* **2006**, *128*, 3-14.

15. Conti, M.; Beavo, J. Biochemistry and Physiology of Cyclic Nucleotide Phosphodiesterases: Essential Components in Cyclic Nucleotide Signaling. *Annu Rev Biochem* **2007**, *76*, 481-511.

16. Zaccolo, M.; Magalhaes, P.; Pozzan, T. Compartmentalisation of cAMP and Ca^{2+} signals. *Curr Opin Cell Biol* **2002**, *14*, 160-166.

17. Karpen, J.W.; Rich, T.C. The fourth dimension in cellular signaling. *Science* **2001**, *293*, 2204-2205.

18. Dodge-Kafka, K.L.; Langeberg, L.; Scott, J.D. Compartmentation of cyclic nucleotide signaling in the heart: the role of A-kinase anchoring proteins. *Circ Res* **2006**, *98*, 993-1001.

19. Fischmeister, R.; Castro, L.R.; Abi-Gerges, A.; Rochais, F.; Jurevicius, J.; Leroy, J.; Vandecasteele, G. Compartmentation of cyclic nucleotide signaling in the heart: the role of cyclic nucleotide phosphodiesterases. *Circ Res* **2006**, *99*, 816-828.

20. Lissandron, V.; Zaccolo, M. Compartmentalized cAMP/PKA signalling regulates cardiac excitation-contraction coupling. *J Muscle Res Cell Motil* **2006**, *27*, 399-403.

21. Cairrao, E.; Santos-Silva, A.J.; Verde, I. PKG is involved in testosterone-induced vasorelaxation of human umbilical artery. *Eur J Pharmacol* **2010**, *640*, 94-101.

22. Santos-Silva, A.J.; Cairrao, E.; Morgado, M.; Álvarez, E.; Verde, I. PDE4 and PDE5 regulate cyclic nucleotides relaxing effects in human umbilical arteries. *Eur J Pharmacol* **2008**, *582*, 102-109.

23. Rich, T.C.; Tse, T.E.; Rohan, J.G.; Schaack, J.; Karpen, J.W. In vivo assessment of local phosphodiesterase activity using tailored cyclic nucleotide-gated channels as cAMP sensors. *J Gen Physiol* **2001**, *118*, 63-78.

24. Cairrao, E.; Santos-Silva, A.J.; Alvarez, E.; Correia, I.; Verde, I. Isolation and culture of human umbilical artery smooth muscle cells expressing functional calcium channels. *In Vitro Cellular & Developmental Biology - Animal* **2009**, *45*, 175-184.

25. Feiteiro, J.; Santos-Silva, A.J.; Verde, I.; Cairrao, E. Testosterone and atrial natriuretic Peptide share the same pathway to induce vasorelaxation of human umbilical artery. *J Cardiovasc Pharmacol* **2014**, *63*, 461-465.

26. Rae, J.; Cooper, K.; Gates, P.; Watsky, M. Low access resistance perforated patch recordings using amphotericin B. *J Neurosci Methods* **1991**, *37*, 15-26.

27. Haugen, G.; Mellembakken, J.; Stray-Pedersen, S. Characterization of the vasodilatatory response to serotonin in human umbilical arteries perfused in vitro. The influence of the endothelium. *Early Hum Dev* **1997**, *47*, 185-193.

28. Errasti, A.E.; del-Rey, G.; Cesio, C.E.; Souza, G.; Nowak, W.; Pelorosso, F.G.; Daray, F.M.; Rothlin, R.P. Expression and functional evidence of the prostaglandin F2alpha receptor mediating contraction in human umbilical vein. *Eur J Pharmacol* **2009**, *610*, 68-74.

29. Rebecca R.Pauly, C.B., Linda Cheng, Robert Monticone, Michael T. Crow. Vascular Smooth Muscle Cell Cultures. In *Methods Cell Biol*, Charles P. Emerson Jr., H.L.S., Ed.; Vascular Biology Group Laboratory of Cardiovascular Science National Institute on Aging—National Institutes of Health Baltimore, Maryland 21224, 1997; Volume Volume 52, pp. Pages 133-154.

30. Gisbert, M.P.; Fischmeister, R. Atrial natriuretic factor regulates the calcium current in frog isolated cardiac cells. *Circ Res* **1988**, *62*, 660-667.

31. Rybalkin, S.D.; Yan, C.; Bornfeldt, K.E.; Beavo, J.A. Cyclic GMP phosphodiesterases and regulation of smooth muscle function. *Circ Res* **2003**, *93*, 280-291.

32. Morgado, M.; Cairrao, E.; Santos-Silva, A.J.; Verde, I. Cyclic nucleotide-dependent relaxation pathways in vascular smooth muscle. *Cell. Mol. Life Sci.* **2012**, *69*, 247-266.

33. Fagan, K.A.; Rich, T.C.; Tolman, S.; Schaack, J.; Karpen, J.W.; Cooper, D.M. Adenovirus-mediated expression of an olfactory cyclic nucleotide-gated channel regulates the endogenous Ca^{2+}-inhibitable adenylyl cyclase in C6-2B glioma cells. *J Biol Chem* **1999**, *274*, 12445-12453.

34. Nausch, L.W.; Ledoux, J.; Bonev, A.D.; Nelson, M.T.; Dostmann, W.R. Differential patterning of cGMP in vascular smooth muscle cells revealed by single GFP-linked biosensors. *Proc Natl Acad Sci U S A* **2008**, *105*, 365-370.

35. Zaccolo, M.; Movsesian, M.A. cAMP and cGMP signaling cross-talk: role of phosphodiesterases and implications for cardiac pathophysiology. *Circ Res* **2007**, *100*, 1569-1578.

36. Gotz, K.R.; Sprenger, J.U.; Perera, R.K.; Steinbrecher, J.H.; Lehnart, S.E.; Kuhn, M.; Gorelik, J.; Balligand, J.L.; Nikolaev, V.O. Transgenic mice for real-time visualization of cGMP in intact adult cardiomyocytes. *Circ Res* **2014**, *114*, 1235-1245.

37. Cawley, S.M.; Sawyer, C.L.; Brunelle, K.F.; van der Vliet, A.; Dostmann, W.R. Nitric oxide-evoked transient kinetics of cyclic GMP in vascular smooth muscle cells. *Cell Signal* **2007**, *19*, 1023-1033.

Chapter 5

Research Work 2

Pathways involved in the human vascular Tetrabromobisphenol A response: calcium and potassium channels and nitric oxide donors

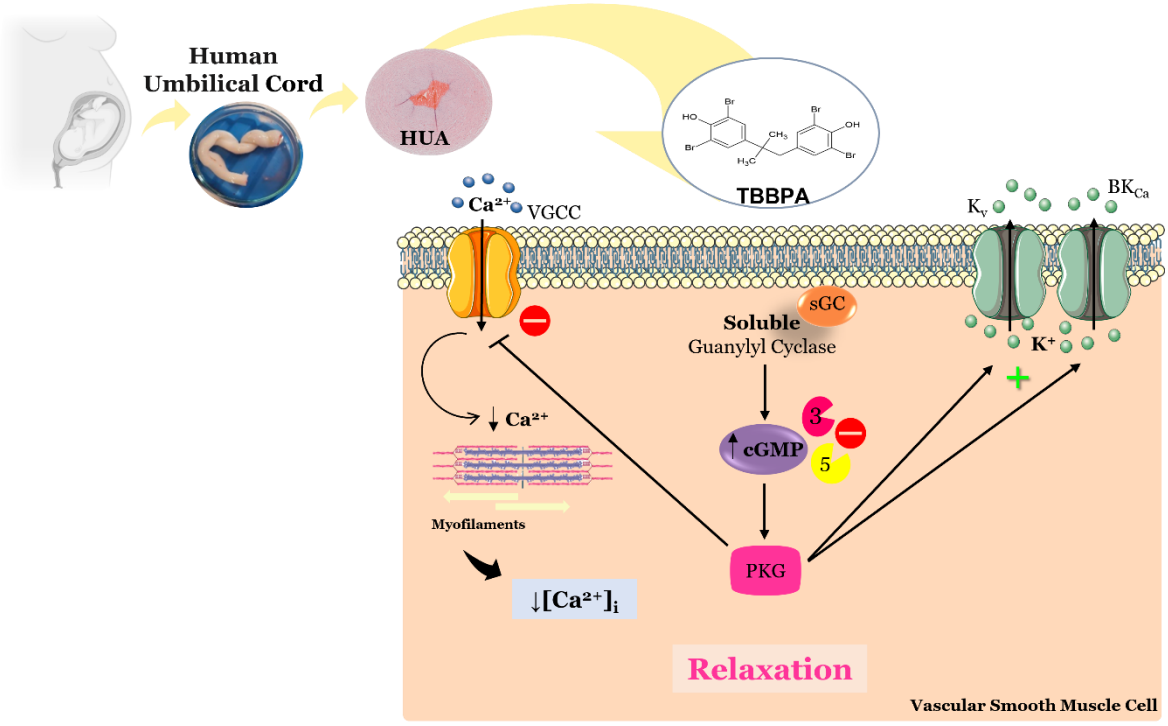

This chapter corresponds to the original research article:

Joana Feiteiro, Sandra M Rocha, Melissa Mariana, Cláudio J Maia, Elisa Cairrão. *Pathways involved in the human vascular Tetrabromobisphenol A response: calcium and potassium channels and nitric oxide donors*. Toxicology. Volume 470, 30 March 2022, 153158, https://doi.org/10.1016/j.tox.2022.153158.

5.1. Abstract

Tetrabromobisphenol A (TBBPA) is a flame retardant that can contaminate the environment and human being, acting as an endocrine disruptor. Several studies propose a correlation between TBBPA exposure and adverse health outcomes, however, at vascular level TBBPA effects are still poorly understood. Thus, considering that the vascular tonus is regulated by vasoactive substances (serotonin and histamine) which are involved in some pathological processes, this work aimed to analyse the direct effects and the 24 hours exposure of TBBPA on the human umbilical artery (HUA) and to investigate its signalling pathway. Using organ bath technique, endothelium-denuded HUA rings were contracted with serotonin (5-HT, 1 μM), histamine (His, 10 μM) and potassium chloride (KCl, 60mM), and the exposure (0-24 h) of different concentrations of TBBPA (1, 10 and 50 μM) were evaluated. Besides, the vascular mode of action of TBBPA was studied through the analysis of cyclic guanosine monophosphate and calcium channels activity, pathways involved in relaxation and contraction of HUA, respectively. Our results demonstrated that the direct effects of TBBPA induce a vasorelaxation of HUA. The maximum relaxant effect was observed at 100 μM of TBBPA with 63.74, 64.24 and 30.05 %, for 5-HT-, His- or KCl-contracted arteries respectively. The 24 hours TBBPA exposure altered the vasorelaxant response pattern of sodium nitroprusside and nifedipine. This effect is due to the involvement of TBBPA with the NO/sGC/cGMP/PKG pathway and the interference in calcium influx. Furthermore, using the real-time quantitative polymerase chain reaction, TBBPA clearly modulates L-type calcium and large-conductance Ca^{2+} 1.1 α- and β1 -subunit channels, and soluble guanylyl cyclase and protein Kinase G. So, at vascular level TBBPA induces changes in HUA after TBBPA exposure.

Keywords: Tetrabromobisphenol A, Endocrine disruptor compound, Vascular homeostasis, Ionic channels, Nitric oxide donors

5.2. Introduction

Endocrine disrupting compounds (EDCs) are exogenous agents that interfere with the secretion, binding, transport, synthesis, action, or elimination of natural hormones in the body [1,2]. Flame retardants (FRs) are considered as EDCs and include a diverse group of chemicals, such as bromine and chlorine [3]. These compounds are used in electronics, clothes, children´s toys, carpets, mattresses, housing and wiring TV sets, computers and mobile phones, motor vehicles, as well as in electrical kitchen appliances, upholstery and textiles, building materials and many plastics, in order to reduce their flammability [4-8].

Tetrabromobisphenol A (TBBPA or 2,6-Dibromo-4-[2-(3,5-dibromo-4-hydroxyphenyl)propan-2yl]phenol) is a brominated phenolic compound that has been used as a flame retardant in plastic, textile and paper, being one of the most prevalent brominated flame retardants in the world [9,10]. Several studies have shown that the levels of TBBPA in the environment and humans are increasing, and their harmful effects in human health can be related to their persistency, bioaccumulation and biomagnification [11,12]. So, TBBPA has been shown to have effects on thyroid, neurological and reproduction function [5,13-16]. Besides, its exposure can be related with some cardiovascular disorders, such as diabetes and obesity [17-19]. TBBPA has also been detected in biological samples such as human serum (maximum concentration detected was 0.4574 μg/g lipid in children) [9], urine (maximum concentration detected was 127.24 μg/g in adults) [20], and breast milk (maximum concentration detected was 0.0125 μg/g lipid) [9]. Furthermore, it was also detected in the umbilical cord of Japanese pregnant women, proving a prenatal exposure to this compound [21,22], which corroborates that TBBPA can cross the human placenta [23,24]. So, can the endocrine disrupting effects resulting from the exposure to TBBPA be correlated with vascular complications? The present study aimed to investigate for the first time how the exposure to TBBPA impairs vascular homeostasis in human umbilical artery (HUA). According to other studies, this artery is used as a model to investigate the effects of EDCs on the vascular system and to understand their vascular implications in pregnancy [25,26]. Furthermore, the regulation of the contractile mechanism of the human umbilical artery smooth muscle cells (HUASMC) is essential for gas and nutrient exchange between the foetus and the placenta. Thus, we resorted to the HUA to analyse the direct effects and the 24 h exposure of TBBPA on vascular contractility, as well as the expression of some genes related to the vascular function, including potassium (K^+) and calcium (Ca^{2+}) channels, soluble guanylate cyclase (sGC) and cyclic guanosine monophosphate (cGMP)-dependent protein kinase.

5.3. Methods

5.3.1. Ethics statement

All the biological samples were obtained from the obstetrics units of “Centro Hospitalar Universitário da Cova da Beira E.P.E” (CHUCB, Covilhã) and “Hospital Sousa Martins-Unidade Local da Guarda” (ULS, Guarda). The hospitals’ ethic committees (CHUCB, No.33/2018, July 18,

2018, and ULS-Guarda, No.02324/2019, February 27, 2019) approved this study and all pregnant women gave written informed consent following the Declaration of Helsinki principles.

5.3.2. Sample collection

Human umbilical cord samples were collected from normal full-term pregnancies after vaginal delivery. All donor mothers were under medication with folic acid during the first trimester or iron supplementation during the last trimester of gestation. The collection of samples and informed consent was performed by professionals (doctors, nurses, health technicians, and assistants) present in the hospital delivery room. These samples were collected in sterile physiological saline solution (PSS; composition (in mM): NaCl 110; $CaCl_2$ 0.15; KCl 5; $MgCl_2$ 2; HEPES 10; $NaHCO_3$ 10; KH_2PO_4 0.5; NaH_2PO_4 0.5; glucose 10; and EDTA 0.49) with penicillin (5 U/mL), streptomycin (5 mg/mL), amphotericin B (12.5 ng/mL) and antiproteases (leupeptin 0.45 mg/L, benzamidine 26 mg/L and trypsin inhibitor 10 mg/L) to avoid contamination and degradation of the tissue, and then stored at 4 °C for 4-24 h. To ensure genetic variability, all the experiments were performed with several HUA rings from at least six/seven different human umbilical cords.

5.3.3. Tissue preparation

Tissue preparation was performed according to Cairrao *et al.* 2010 [27]. Human umbilical arteries (HUA) were isolated from the surrounding connective tissue and cut into 3–5 mm rings. The contractility experiments were performed with HUA without endothelium, which was mechanically removed inserting a cotton thread into the arterial lumen.

5.3.4. Contractility experiments in HUA rings

The organ bath technique was used to analyse the direct and the 24 h exposure of TBBPA effects on umbilical arteries. The isometric tension recordings of HUA were according to our previous works [25,28]. Briefly, the HUA was isolated and after the vascular endothelium was removed it was cut into small rings (3–5 mm). Then, these rings were placed between two parallel stainless-steel wires and into the organ bath to measure the tension. The artery rings are carboned throughout the experience (95 % O2 and 5 % CO2) and subjected to a resting tension (2-2.5 g). After the equilibration time (45 min), the viability of the arterial rings was tested contracting them with a maximum concentration of serotonin (5-HT, 1 μM) and the rings in which the tension did not reach 1 g were not used in the study.

Firstly, the direct effects of TBBPA (0.01, 0.1, 1, 10, 30, 50 and 100 μM) over the basal were analysed. In an independent experiment, the HUA rings were contracted with 5-HT (1 μM), histamine (His, 10 μM) and potassium chloride (KCl, 60 mM) and then different concentrations of TBBPA (0.01- 100 μM) were added to analyse the direct effects. Ethanol (vehicle) was used to perform control experiments at same percentage used to dissolve TBBPA. The final concentration of the vehicle never exceeded 0.1 %.

To determine the 24 h exposure of TBBPA effects, HUA rings were placed in Dulbecco's modified Eagle's medium (DMEM)-F12 for 24 h in the presence of TBBPA (1, 10 and 50 μM). After this incubation period, HUA rings were contracted with the contractile agents (5-HT,1 μM; His, 10 μM and KCl, 60 mM). A stable contraction was achieved with these different vasoactive agents, and then the rings were submitted to sodium nitroprusside (SNP, 1 or 10 μM) and nifedipine (Nif, 0.1-10 μM) and the vasorelaxation of these drugs was analysed. Each experiment was conducted in several HUA rings from at least five different arteries. All experiences were performed in the absence of light since SNP and Nif are photodegradable agents.

5.3.5. Cell dissociation and culture of human umbilical artery smooth muscle cells

Smooth muscle cells (SMC) were isolated from the HUA as described previously [29]. All procedures were performed inside a laminar flow chamber in an aseptic environment and using sterile materials, solutions and instruments. The culture medium was changed every 2-3 days and after 15-20 days confluent cultures were obtained. Subcultures of SMC were performed until the fourth passage to maintain the same genetic, morphological, and electrophysiological characteristics as those observed in HUA tissues. These cells were used for cell viability assays, extraction of total RNA and determination of gene expression. Before RNA extraction, confluent cells were placed in a culture medium without FBS (24 h) to express their contractile phenotype.

5.3.6. Assessment of viability (MMT assay)

The MTT assay allows the evaluation of cell viability and proliferation *in vitro* of a cell population in response to an external factor. This assay was performed according to the methodology described by Gloria *et al.* [25]. It measures the reduction of MTT (tetrazolium salt) to the purple formazan by cellular dehydrogenase enzymes of living cells. The ability of formazan production serves as cell viability marker. Thus, confluent cells in 96 well plates were exposed to different concentrations of TBBPA (0.01, 0.1, 1, 10, 30, 50, 100, 500 and 1000 μM) for 24 h. At the end of the incubation period, 200 μL MTT solution (0.5 mg/mL) were added to each well and after 3 h (37 °C, 5 % CO_2 and 95 % of humidity) the MTT solution was removed and 200 μL dimethyl sulfoxide solution were added to solubilize the purple formazan crystals. The relative amount of formazan production was measured through the absorbance at 570 nm with a photometer (EZ Read 400, Microplate Reader, Biochrom).

5.3.7. Real-time quantitative polymerase chain reaction

The mRNA expression of L-type calcium channel (LTCC) α1c-subunit (Cav1.2), BK_{Ca} 1.1 α- and β_1- subunits, sGC ($Gucci_{\alpha}$) and protein kinase cGMP-dependent 1 α-subunit (PRKG 1α) in HUASMC was analysed using the real time quantitative polymerase chain reaction (qPCR) in response to 24 h exposure to different concentrations of TBBPA (0.01, 1, 10, 50 and 100 μM). Ion

channel expression was normalized with human β-actin, used as an internal control. The primers sequence used in the present study are provided in Table 5.1.

To each set of primers, the gene expression studies, and the optimization strategy (amplifications, concentrations, and annealing temperature of the primers and cycling conditions) were according to Saldanha *et al.* and Gloria *et al.* [25,30]. Briefly, total RNA was extracted from HUASMC using TRI reagent ™. The concentration and purity of RNA were assessed using a spectrophotometer (Pharmacia Biotech, Ultrospec 3000, Cambridge, England), determining the absorbance at 260 nm and the absorbance ratio (260/280 nm), respectively. Using the electrophoresis technique (1 % agarose) the integrity of extracted RNA was evaluated. For cDNA synthesis, 1 μg of total RNA was reverse transcribed using random hexamer mix (0.5 mg/mL) and M-MuLV Reverse Transcriptase (200 U/mL) (NZYTech, Lisboa, Portugal) in a final volume of 20 μL. For the gene expression analysis, each qPCR reaction required 1 μL of cDNA, gene-specific primers (Table 5.1) and SYBR Green/Fluorescein qPCR Master Mix (NZYTech, Lisboa, Portugal). Triplicates were made for all samples, and following the mathematical model proposed by Pfaffl using the formula $2^{-\Delta\Delta Ct}$ [31] the fold differences in mRNA expression were calculated.

Table 5.1. Oligonucleotide primers used in the present study for real-time polymerase chain reaction.

Gene	GenBank accession no.	Primer (5´- 3´)	Annealing T (C°)
β-actin	NM_001101.5	Fw: 5-CAT CCT CAC CCT GAA GTA CCC-3 Rv: 5-AGC CTG GAT AGC AAC GTA CAT G-3	60
Cav1.2	XM_034935167.1	Fw: 5-CAT CAT CAT CTA CGC CAT CAT CGC -3 Rv: 5-GGT CAT CTT CTG CTG GAA CAT CTG-3	60
BK_{Ca} β_1	XM_003830649.4	Fw: 5-CAA TGT GGT GAA CGC AGC C-3 Rv: 5-TGT GAT GCT GAG GCG TGA A-3	60
BK_{Ca} 1.1α	XM_034930944.1	Fw: 5-AAG CAA CGG AAT GGA GGC AT-3 Rv: 5-CCA GTG AAA CAT CCC AGT AGA GT-3	60
$Gucci_{\alpha}$	NM_001379671.1	Fw: 5-GAT AGC ACT GAT GGC CCT GAA-3 Rv: 5-GTA GTC CAA TTC GCA TCT TGA TAG G-3	60
PRKG 1α	NM_001098512	Fw: 5-GGC TGT CAG AGA AGG AGG AAG -3 Rv: 5-GGA AGG ACC TGT ACG TCT GC -3	60

5.3.8. Drugs and chemicals

All drugs and chemicals were purchased from Sigma-Aldrich Chemistry (Sintra, Portugal) except the products used in qPCR technique, that were purchased from NZYTech (Lisboa, Portugal) and the TRI reagent ™ that was purchased from Grisp (Porto, Portugal). Regarding the contractility experiments, the stock solutions of 5-HT, Hist and SNP were prepared in distilled water. Nif and TBBPA were dissolved in absolute ethanol and final solutions were obtained by dilution with Krebs' solution. These dilutions were carried out daily according to each experiment. Concerning the preparation of the TBBPA solution, all HUA were incubated at different concentrations of TBBPA (1, 10 and 50 μM) dissolved in 10 mL of DMEM-F12 medium with no additives, for 24 h. Concerning the MTT assay and qPCR technique, the TBBPA initial solution was also dissolved in

absolute ethanol and final solutions were obtained by dilution FBS-free culture medium. In all experiments the final concentration of the solvent (ethanol) never exceeded 0.1 %.

5.3.9. Statistical analysis

The graphic design was performed using the Software Origin 8.5.1. and the statistical analysis using SigmaStat Statistical Analysis System version 4.0 (2016) for a significance level of 0.05. All results are expressed as mean ± standard deviation of mean (SD) of n experiments. Different statistical methods were chosen according to the number and type of variables tested. Statistical significance between two groups was analysed using Student's t-test. Comparison between different concentrations of TBBPA and control for cell viability was analysed using one-way analysis of variance (ANOVA) followed by Dunnett's post hoc tests to determine significant differences among the means. Comparison between all concentrations of TBBPA was analysed using one way ANOVA followed by Tukey post hoc tests to determine significant differences among the means. Significant differences in tension induced by the contractile agents were determined through the nonparametric method Kruskal–Wallis followed by Dunn's post-hoc tests, since the results did not achieve the normality criterium. Two-way ANOVA with interaction followed by the Holm-Sidak post-hoc tests were used to evaluate the effect of TBBPA on incubated HUA contracted with 5-HT, His and KCl, and to evaluate the effect on the activity of SNP and Nif. Differences in the mRNA expression were calculated against the control using one-way ANOVA followed by Dunnett's multiple comparison test. In all cases the statistical significance was found for *p*-value lower than 0.05. When possible, data sets were $\log_{10}$ transformed to achieve normal distribution.

5.4. Results

This study focused on the direct effects and the 24 h exposure of TBBPA on HUA contractility. The direct effects are rapid actions caused by TBBPA in the HUA, that is, there is no incubation of the HUA. Concerning the exposure time of TBBPA, the HUA and HUASMC were incubated with TBBPA for 24 h, according to previous studies performed by our research group [25,30,32]. These authors demonstrated that 24 h of incubation is enough for genomic changes to occur. These changes are the result of modifications in the modulation of gene expression, which can result from differences in the contractile properties of the arteries.

5.4.1. Assessment of cell viability (MTT assay)

MTT assay was used to investigate the cellular viability of HUASMC under the effect of TBBPA. The cells were exposed to different concentrations of TBBPA (0.01, 0.1, 1, 10, 30, 50, 100, 500 and 1000 μM), to the culture medium (control) and to ethanol (solvent used to dissolve TBBPA, vehicle). As shown in Figure 5.1, only the two highest TBBPA concentrations (500 and 1000 μM) induced a significant decrease in cell viability ($p < 0.01$ and $p < 0.001$, respectively). At the remaining concentrations, no differences were observed when compared to the control and the

vehicle. Thus, in all the following experiments, the TBBPA concentrations used were 0.01, 0.1, 1, 10, 30, 50 and 100 μM.

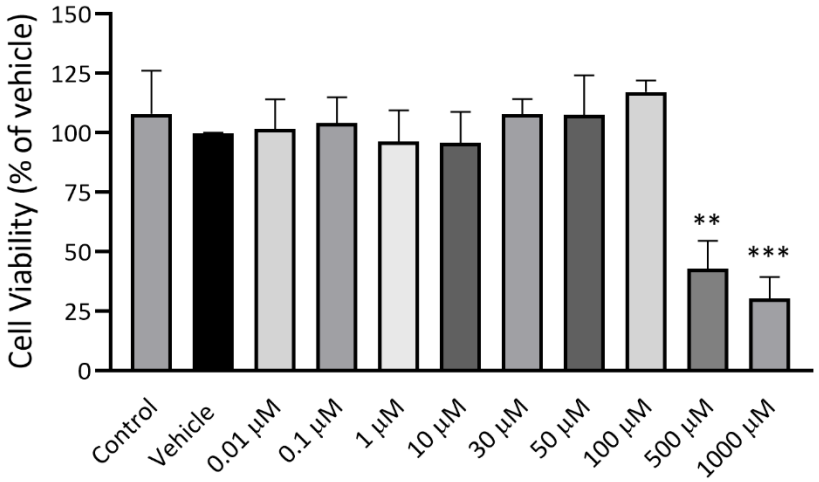

Figure 5.1. Percentage of cell viability of HUASMC under the effect of TBBPA. Data are expressed as percentage (%) of cellular viability. Each bar represents the mean values and vertical lines the SD * Represents statistical differences between TBBPA and Vehicle (**p < 0.01 and ***p < 0.001, one-way ANOVA followed by Dunnett's post hoc test).

5.4.2. Direct effects of TBBPA on HUA

To analyse the direct effects of TBBPA, the HUA rings without endothelium were contracted with two different receptors agonists (5-HT and His) and by depolarization with isosmotic KCl (60 mM) solution. First, the effect of TBBPA over the resting tension in the HUA was analysed. The obtained results show that the different concentrations of TBBPA (0.01–100 μM) did not induce an increase in the basal tension of HUA (data not shown). Then, the vascular effect of TBBPA (0.01–100 μM) was analysed upon HUA contraction with 5-HT (1 μM), His (1 μM) and KCl (60 mM).

As show in Figure 5.2, TBBPA induced a concentration-dependent relaxant effect in the HUA rings contracted with either 5-HT (Figure 5.2A), His (Figure 5.2B) or KCl (Figure 5.2C). In all contractile agents (5-HT, His and KCl), TBBPA effects were significant at all concentrations (0.01-100 μM) (p < 0.001), evidencing a monotonic response. For 5-HT contractions, the three highest TBBPA concentrations (30, 50 and 100 μM) caused a significant vasorelaxation compared with the two lowest concentrations (p < 0.001), while in His contractions, the TBBPA concentrations that caused a significant vasorelaxation were 10, 30, 50 and 100 μM (p < 0.001). Regarding the KCl contractions, the three highest TBBPA concentrations (30-100 μM) caused a significant vasorelaxation compared to the two lowest concentration (p < 0.001).

Overall, the maximum relaxant effect induced by TBBPA was observed at the highest concentration tested (100 μM). The relaxation elicited by this concentration of TBBPA on 5-HT-, His- or KCl-contracted arteries were 63.74 ± 22.07 %, 64.24 ± 7.4 % and 30.05 ± 13.28 %, respectively. The obtained results show that the relaxant effects of TBBPA are more prominent in 5-HT and His-contracted HUA rings, suggesting that TBBPA effects may be dependent on the contractile agent used. Regarding the vehicle, it did not have significant effects on contracted

arteries at the concentrations used, as shown in Figure 5.2. After washing with Krebs' solution, all vascular effects were reversible (data not shown).

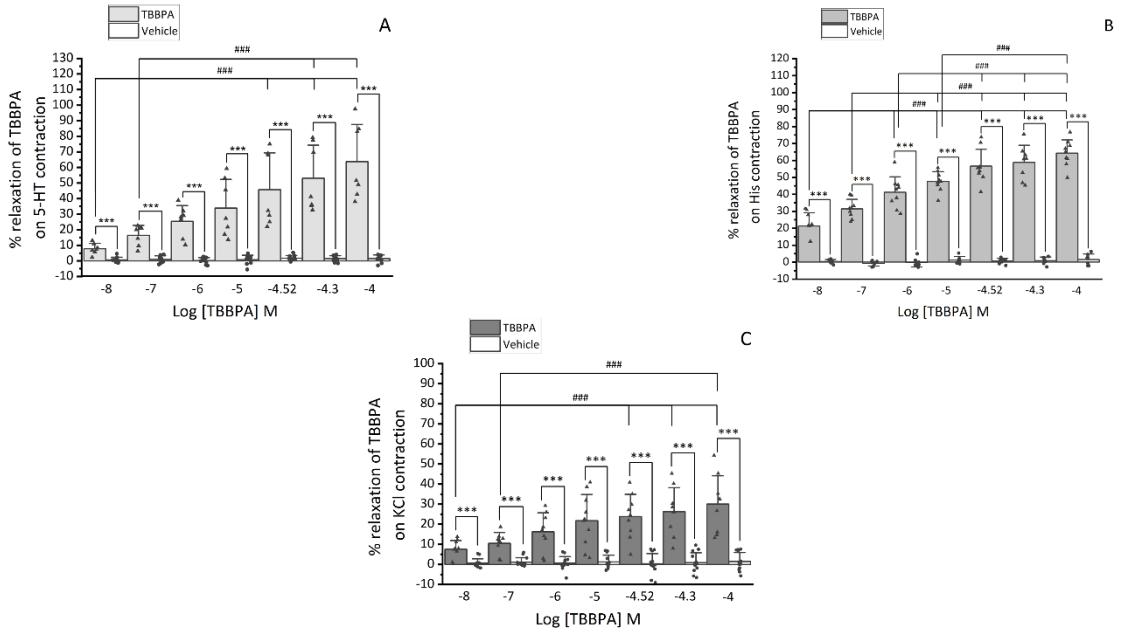

Figure 5.2. Vasorelaxant effects of TBBPA (0.01–100 μM) contracted with **(A)** serotonin (5-HT, 1 μM, n=6), **(B)** histamine (His, 10 μM, n=6) and **(C)** KCl (60 mM, n=7). Data are expressed as percentage (%) of relaxation on contractile effects. Each bar represents the mean values, the vertical lines the SD and the dots the replicates for each n. *** Represents statistical differences between each TBBPA concentrations and the respective vehicle ($p < 0.001$, Student's t-test) and ### represents statistical differences between all TBBPA concentrations ($p < 0.001$, one-way ANOVA followed by Tukey's post hoc tests).

5.4.3. Effects of 24 hours exposure of TBBPA in the contractility of HUA

To investigate the effects of 24 h exposure of TBBPA (at different concentrations - 1, 10 and 50 μM - for 24h) in the contractile properties of the HUA, the HUA rings without endothelium were contracted with 5-HT, His and KCl.

In Figure 5.3, we observe that the tensions of HUA contracted with 5-HT and His were similar for 1 and 10 μM TBBPA incubation when compared with non-incubated HUA rings ($p > 0.05$). However, when incubated with 50 μM of TBBPA, the tensions of HUA contracted with 5-HT and His significantly decreased ($p < 0.001$). Regarding the tensions of HUA contracted with KCl, the tension of incubated HUA rings with 1 μM of TBBPA was significantly higher than the tension of non-incubated arteries ($p < 0.05$). On the other hand, the tension of incubated arteries with 50 μM of TBBPA was significantly lower than the tension of non-incubated HUA rings ($p < 0.001$). Concerning the tension of non-incubation HUA rings, it was higher in HUA rings contracted with 5-HT and KCl than His.

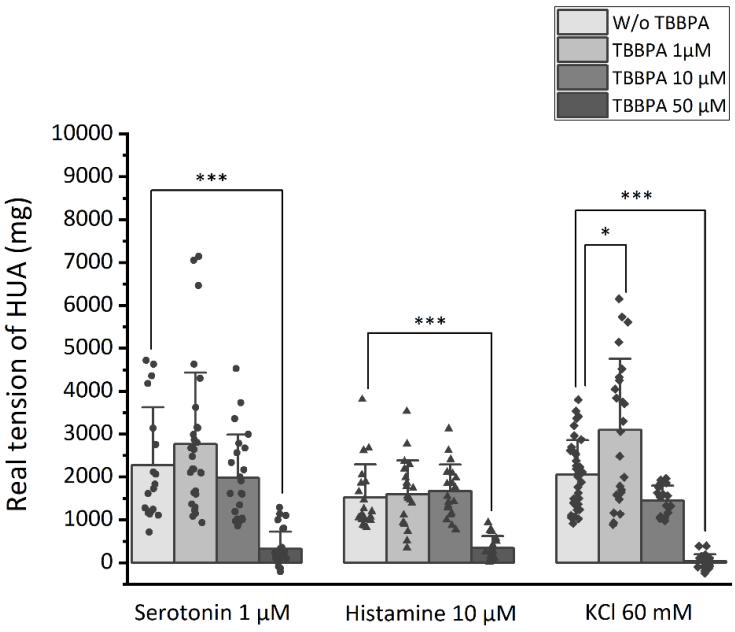

Figure 5.3. Real Tension (mg) of the endothelium-denuded HUA rings non- and incubated (24 h) with TBBPA (1, 10 and 50 µM) and then contracted with serotonin (5-HT, 1 µM, n=7), histamine (His, 10 µM, n=7) and KCl (60 mM, n=7). Each bar represents the mean values, vertical lines the SD and the dots the replicates for each n. *Represents statistical differences on the tension of each contractile agent in comparison to control HUA rings (W/o TBBPA): * ($p < 0.05$) and *** ($p < 0.001$), Kruskal–Wallis method followed by Dunn's post-hoc tests.

5.4.4. Effects of TBBPA on cGMP signalling pathway

We analysed the involvement of TBBPA on cGMP signalling pathway. SNP, a stimulator of sGC, was used to determine the involvement of this pathway in the mechanism underlying TBBPA-induced relaxation in HUA rings, non-incubated and incubated with 1 and 10 µM TBBPA for 24 h. Figure 5.4 shows the % of relaxation of incubated denuded HUA rings contracted with 5-HT, His and KCl and exposed to different concentrations of SNP (1 and 10 µM), and we observed that there was a statistical interaction between the HUA rings incubated with TBBPA and SNP for His (p = 0.001) and KCl (p = 0.026) contractions, however there was not a statistical interaction for 5-HT contraction (p = 0.834).

Concerning the HUA rings contracted with 5-HT (Figure 5.4A), we observed that SNP induced relaxation in both control group (W/o TBBPA) and incubated HUA (1 and 10 µM TBBPA). However, the relaxation induced by 1 µM of SNP in HUA incubated with 1 and 10 µM of TBBPA was significantly higher ($p < 0.01$ and $p < 0.001$, respectively) than the relaxation observed in those W/o TBBPA. Moreover, the relaxant effect of SNP (10 µM) was significantly different from the control group in HUA incubated with 10 µM TBBPA ($p < 0.01$).

Regarding the HUA rings contracted with His (Figure 5.4B), we also observed that SNP induced relaxation in these HUA rings in both groups (W/o TBBPA, 1 and 10 µM of TBBPA). In HUA incubated with 10 µM of TBBPA, the relaxant effect induced by SNP (1 µM) was significantly higher ($p < 0.01$) than the relaxation observed in those W/o TBBPA.

In relation to HUA rings contracted with KCl (Figure 5.4C), SNP also led to relaxation of the HUA rings from W/o TBBPA, 1 and 10 μM of TBBPA groups. In HUA incubated with 1 μM of TBBPA, our results showed a significantly higher relaxation induced by 1 and 10 μM of SNP when compared to the relaxation observed in HUA rings from the W/o TBBPA group ($p < 0.001$). Moreover, the relaxation induced by 1 and 10 μM of SNP in HUA incubated with 10 μM of TBBPA was also significantly higher ($p < 0.001$) when compared to the relaxation observed in HUA from the control group.

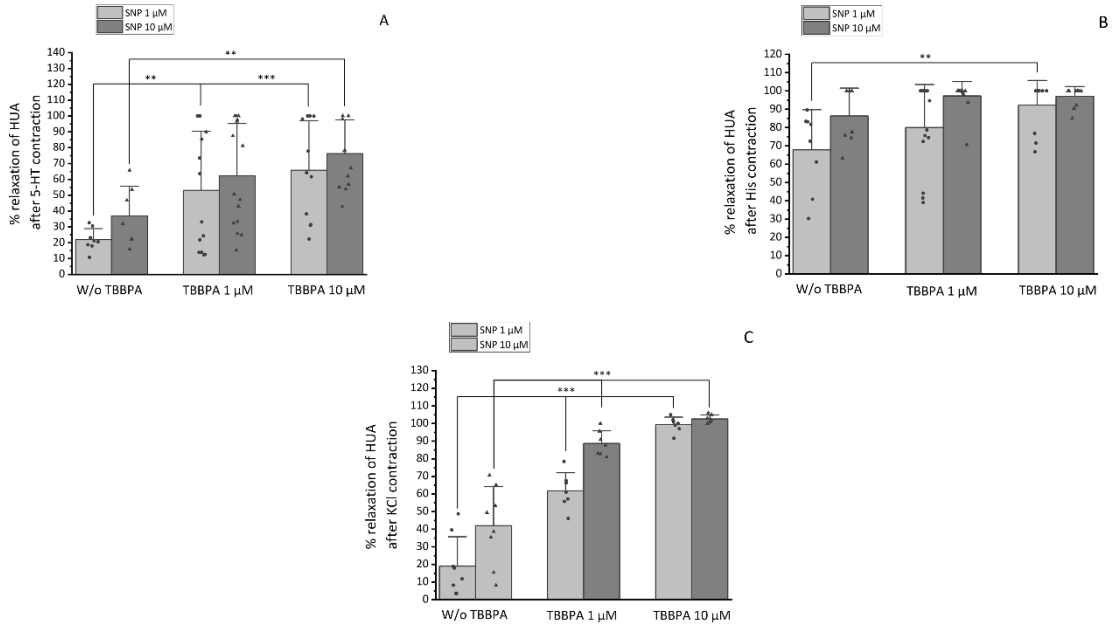

Figure 5.4. Percentage of relaxation of HUA rings non- and incubated (24 h) with TBBPA (1 and 10 μM), contracted with **(A)** serotonin (5-HT, 1 μM, n=8), **(B)** histamine (His, 10 μM, n=8) and **(C)** KCl (60 mM, n=7) and exposed to cumulative concentrations of SNP (1 and 10 μM). Each bar represents the mean values, vertical lines the SD and the dots the replicates for each n. * Represents a significant difference in comparison to control HUA rings (W/oTBBPA): ** ($p < 0.01$) and *** ($p < 0.001$). Data were analysed using two-way ANOVA followed by Holm-Sidak post-hoc test.

5.4.5. Effects of TBBPA on the activity of L-type Ca^{2+} channels

We analysed the effect of TBBPA on Ca^{2+} influx by ion channels. Nif, an inhibitor of LTCC, was used to determine the involvement of these channels in the mechanism underlying TBBPA-induced relaxation, both in the control group (W/o TBBPA) and incubation (1 and 10 μM TBBPA) for 24 h. Figure 5.5 shows the % of relaxation of cumulative concentrations of Nif (0.1–10 μM) in incubated HUA rings contracted with 5-HT, His and KCl, and we only observed an interaction between the HUA rings incubated with TBBPA and the effect triggered by Nif treatment for KCl contraction ($p = 0.023$). Concerning the HUA rings contracted with 5-HT (Figure 5.5A), results showed a significant relaxation ($p < 0.05$) induced by 1 μM of Nif in arteries incubated with 10 μM of TBBPA when compared to the rings W/o TBBPA. Moreover, there was also a significant vasorelaxation ($p < 0.05$) for 10 μM Nif in arteries incubated with 1 and 10 μM of TBBPA. Regarding the HUA rings contracted with His (Figure 5.5B) there was a significant decrease in the

relaxation induced by Nif 0.1, 1 and 10 μM ($p < 0.01$) when the arteries were incubated with 10 μM compared to those W/o TBBPA. In relation to HUA rings contracted with KCl (Figure 5.5C), the relaxation induced by Nif (0.1 μM) in HUA incubated with 1 and 10 μM of TBBPA was significantly lower ($p < 0.001$) than the relaxation observed in those W/o TBBPA.

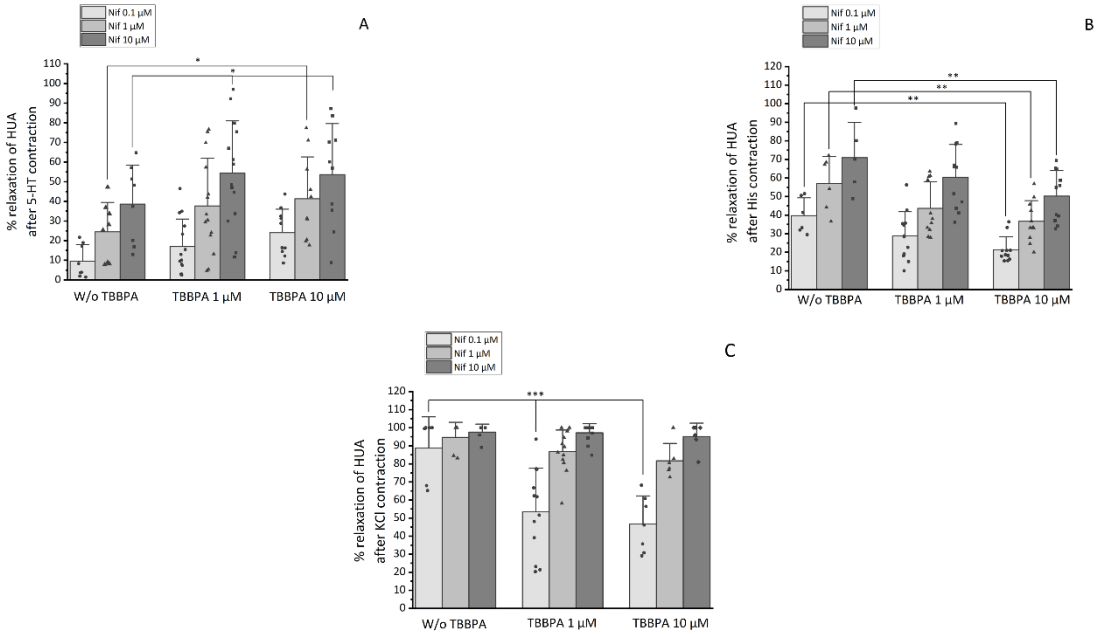

Figure 5.5. Percentage of relaxation of HUA rings non- and incubated (24 h) with TBBPA (1 and 10 μM), contracted with **(A)** serotonin (5-HT, 1 μM, n=8), **(B)** histamine (His, 10 μM, n=7) and **(C)** KCl (60 mM, n=7) and exposed to cumulative concentrations of Nif (0.1–10 μM). Each bar represents the mean values, vertical lines the SD and the dots the replicates for each n. * Represents a significant difference in comparison to control HUA rings (W/oTBBPA): * ($p < 0.05$), ** ($p < 0.01$) and *** ($p < 0.001$). Data were analysed using two-way ANOVA followed by Holm-Sidak post-hoc test.

5.4.6. Effects of TBBPA on the expression of channels and proteins involved on the contractile property of HUASMC

qPCR was used to evaluate the expression of some ion channel subunits and some proteins in HUA. Figure 5.6 shows the effects of TBBPA on mRNA expression of channels (Cav1.2, $BK_{Ca}\beta_1$ and BK_{Ca} 1.1α) and proteins involved in the contractile process of HUA ($Gucci_{\alpha}$ and PRKG 1α). Concerning the Cav1.2 channels, mRNA expression was significantly higher in HUASMC incubated with 1 μM ($p < 0.01$), 10 μM ($p < 0.05$) and 100 μM ($p < 0.001$) in comparison to the control (Figure 5.6A). Regarding the $BK_{Ca}\beta_1$ subunit, 50 and 100 μM of TBBPA significantly increased the mRNA expression when compared to the control in HUASMC ($p < 0.05$ and $p < 0.001$ respectively, Figure 5.6B). In relation to the BK_{Ca} 1.1α subunit, mRNA expression was significantly higher in HUASMC incubated with 1, 50 and 100 μM in comparison to the control ($p < 0.001$, $p < 0.01$ and $p < 0.01$ respectively, Figure 5.6C). In the mRNA expression of $Gucci_{\alpha}$, it was observed a significant increase of its expression in HUASMC incubated with 10 and 100 μM of TBBPA when compared to

the control (p < 0.001, Figure 5.6D). At last, the mRNA expression of PRKG 1α was significantly higher for HUASMC incubations of 1 and 100 μM of TBBPA in comparison to the control (p < 0.01 and p < 0.001 respectively, Figure 5.6E).

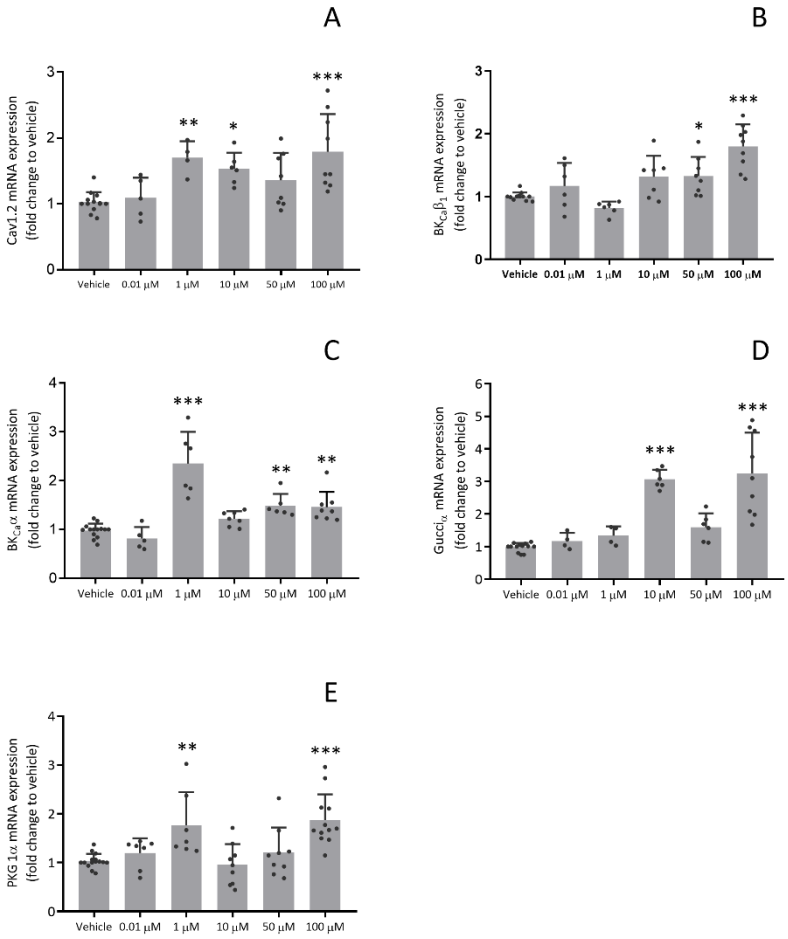

Figure 5.6. Relative expression in HUASMC exposed to TBBPA (0.01 – 100 μM) (24 h) **(A)** Cav1.2 channels, **(B)** BK_{Ca} β_1 subunit channels, **(C)** BK_{Ca} 1.1α subunit channels, **(D)** sGC ($Gucci_{\alpha}$) and **(E)** PRKG 1α subunit. Human β-actin was used as housekeeping gene to normalize the mRNA expression. Each horizontal line represents the mean values and vertical lines the SD of four independent experiments performed in triplicate. * Represents statistical differences in comparison to control (Vehicle): * (p < 0.05), ** (p < 0.01), *** (p < 0.001). Data were analysed using ANOVA followed by Dunnett's multiple comparison test.

5.5. Discussion

HUA is easily obtained from the umbilical cord and an excellent source of vascular SMC. It has been used as a model to analyse the effects of EDCs on the vascular system and to understand the vascular implications of exposure to these compounds in pregnancy [25,26]. Studying the exposure to EDCs during pregnancy is of vital importance, since it is a sensitive time of development, so the fetoplacental vasculature can help to estimate the exposure to these compounds during pregnancy and to understand the implications for the child and the mother [24]. Besides that, the mechanisms regulating the contractile state of the HUASMC are crucial for

gas and nutrient exchange between the foetus and the placenta. Since the umbilical cord is not innervated, the umbilical blood flow and the HUA tonus are controlled by vasoactive substances, that can be locally released or present in the circulation, such as 5-HT and His [26], that are involved in some pathological processes that disturb the umbilical circulation [33,34].

The purpose of this study was to analyse the direct effects and the 24 h exposure of TBBPA on vascular contractility in HUA, and if vascular homeostasis of this artery is affected by TBBPA. Some studies performed in zebrafish, fathead minnow, rainbow trout, Eisenia fetida and earthworm species, demonstrated that TBBPA was able to induce chronic toxicity after 14 and 96 h exposure [35-38]. Therefore, and as a first approach, the cell viability of HUASMC was analysed and cells exposed to high concentrations of TBBPA (500 and 1000 μM) showed a decrease in the cell viability of approximately 57 % and 70 %, respectively, indicating a toxic effect of TBBPA in the vascular SMC. However, the contractility results showed that the HUA rings incubated with 50 μM of TBBPA are not responsive to the contractile agents, suggesting that TBBPA concentrations about 10 times lower than the toxicity dose may already affect the HUA contractility, and this effect is not due to the toxicity induced by TBBPA. Considering these results, we analysed the effect of non-toxic TBBPA concentrations (0.01–100 μM) in HUA vascular tone. For this the HUA rings were contracted with 5-HT, His and KCl, and then cumulative concentrations of TBBPA were added to the contracted artery. To the best of our knowledge, our results showed for the first time that the TBBPA direct effects induced a dose-dependent relaxation on denuded HUA rings contracted either with 5-HT, His or KCl (60 mM). This effect is more prominent in HUA contracted with 5-HT and His than KCl, indicating that it depends on the contractile agent. Consequently, these results may suggest that different mechanisms of action may be involved in vasorelaxation induced by TBBPA. Moreover, these differences can be explained based on the pathways of each of the contractile agent. The contractile capacity of 5-HT in HUA is associated with the activation of 5-HT_{2A} and 5-HT_{1B}/5-HT_{1D} receptors expressed in the smooth muscle of this artery [39]. The 5-HT_{2A} receptor is coupled to the Gq protein and activates phospholipase C, leading to an increase of inositol trisphosphate (IP_3) levels, following an increase of intracellular Ca^{2+} levels ($[Ca^{2+}]_i$). On the other hand, the 5-HT_{1B}/5-HT_{1D} receptors are coupled to the Gi/o protein that leads to an inhibition of adenyl cyclase, leading to an decrease in cAMP levels and an increase of $[Ca^{2+}]_i$ [33,39-43]. Therefore, our results suggested that the TBBPA effects are due to the modulation of 5-HT_{2A} and 5-HT_{1B}/5-HT_{1D} receptors and involve Ca^{2+} channels inhibition or K^+ channels activation. Regarding the contractility capacity of His, the contraction is achieved by activating H_1 receptor, which is coupled to Gi/o protein, activating the PLC/IP_3 signalling cascade, and leading to an increase of the $[Ca^{2+}]_i$ [39,44,45]. The H_2 receptor is also expressed in HUA smooth muscle, causing an increase in cAMP levels due to the Gs activation, and consequently to the HUA relaxation. Although the effect of activation of the H_1 receptor is predominant, the activation of the receptor H_2 can also induce less potent contractions, suggesting that the contractile capacity may also be influenced by this receptor [46]. Thus, we may suggest that the TBBPA acts in H_1 and H_2 receptors and induces the inhibition of Ca^{2+} channels or the activation of K^+ channels. The KCl contraction is mainly due to the influx of extracellular Ca^{2+}, with membrane depolarization and opening of voltage-gated calcium channels (VGCC), mainly L-Type, that are involved in the regulation of arterial tonus [33,47,48]. So, the

muscle contraction results from VGCC opening and increasing $[Ca^{2+}]_i$. It is important to note that $[Ca^{2+}]_i$ is a key to the HUA vascular smooth muscle contraction/relaxation [26,47,48], and our results suggest that the vasorelaxation caused by TBBPA is mainly due to the inhibition of VGCC.

The next point was to analyse the effects of 24 h exposure of TBBPA in the contractility of HUA. For this, the HUA rings were incubated with 1, 10 and 50 μM of TBBPA for 24 h, and then contracted with 5-HT, His and KCl. Concerning the HUA rings contracted with 5-HT, our results demonstrated that the incubation with 50 μM of TBBPA induced a very low capacity to contract when compared to the control. However, the contractile capacity in the HUA rings incubated with 1 and 10 μM of TBBPA is similar to the control. So, these results suggest that a continued exposure to high concentrations of TBBPA can modulate vascular homeostasis by interference with 5-HT receptors (5-HT_{2A} and 5-HT_{1B}/5-HT_{1D}). In relation to the contractile capacity of His in incubated HUA rings with 1 and 10 μM of TBBPA, it is similar to the non-incubated HUA rings. However, when incubated with 50 μM of TBBPA, the contractile effect of His is very small. Facing these results, we may suggest that a continuous exposure to high concentrations of TBBPA modifies the contractile effect of His, possibly due to an interaction with the H_1 and H_2 receptors. Concerning the HUA rings contracted with KCl, the results of 1 μM incubation showed an increased contractile effect of KCl. The HUA rings incubated with 50 μM of TBBPA did not have the capacity to contract in the presence of KCl, suggesting a correlation between the effect of KCl and the concentrations of TBBPA. This means that the contractile capacity of KCl depends on the exposure to different TBBPA concentrations. Moreover, taking into account that the $[Ca^{2+}]_i$ is a key factor in the HUA vascular smooth muscle contraction/relaxation [26,47,48], our results suggest that TBBPA also modulates vascular homeostasis by interfering with the Ca^{2+} channels. The results described above suggest that the use of the different contractile agents may allow to understand the different signalling pathways triggered by TBBPA, and consequently their effects at the vascular level. Facing these results, we intended to analyse how the exposure to TBBPA harms vascular homeostasis of HUA through these signalling pathways.

It is well described that the cGMP signalling is the main pathway responsible for the HUA relaxation [26,27,49]. Thus, we used the SNP (stimulator of sGC) to analyse TBBPA involvement on cGMP signalling pathway. Our results showed that the highest concentration of SNP induces a greater relaxation in the HUA, either for 5-HT, His and KCl contracted arteries. In addition, the incubation with TBBPA causes an increase in the SNP relaxation response, which increases with cumulative concentrations of TBBPA incubation. So, these results suggest that the effects induced by SNP depend on TBBPA incubation concentrations, since there was an interaction between the effects of SNP and TBBPA incubation for His and KCl contractions. For this reason, we can hypothesize that the 24 h exposure effects of TBBPA seems to involve the NO/sGC/cGMP/PKG signalling pathway.

The involvement of TBBPA on Ca^{2+} influx by ion channels was analysed using a specific inhibitor of L-type VGCC, Nif. Our results showed that the response to Nif depends on the TBBPA incubation of the arteries since there was an interaction between Nif response and TBBPA incubation concentrations. Concerning the 5-HT-contracted HUA rings, incubation with TBBPA leads to a significantly increase in the vasodilation induced by Nif (1 and 10 μM) for HUA rings

incubated with 1 and 10 μM of TBBPA. Regarding the His-contracted HUA rings, incubation with TBBPA leads to a vasodilation induced by Nif similar to the non-incubated HUA rings. However, a decreased vasodilatation by Nif (0.1 μM) was observed in HUA incubated with 10 μM of TBBPA. A similar effect was observed in KCl-contracted HUA rings, where an incubation with TBBPA clearly modifies the Nif effect, decreasing the vasorelaxant response induced by Nif (0.1 μM). These observations indicate that TBBPA modifies the action mechanisms of Nif, interfering in the Ca^{2+} influx. However, TBBPA effects on expression of ion channels showed that the mRNA expression levels of Cav1.2 channels in HUASMC increased after exposure to TBBPA. Besides, we analysed the expression of other ion channels (K_v and BK_{Ca} channels) and proteins (sGC and PKG) involved in the HUA vascular contractility mechanism. Our research group showed that the potassium channels are also involved in the vasodilator effects in HUA. The PKG activation due to increased cGMP levels, induces the activation of these channels, mainly K_v and BK_{Ca} channels [27,49-51]. As mentioned previously, the vasorelaxation induced by TBBPA may be due to an increase in the potassium channels. Based on these results, we observed that the mRNA expression levels of BK_{Ca} 1.1α- and β_1- subunits and PRKG 1α subunit are increased in response to TBBPA incubation. Besides, TBBPA effect in mRNA expression levels of sGC ($Gucci_{\alpha}$), showed an increased expression in TBBPA incubation when compared to control. Considering these results, TBBPA clearly modulates these proteins and ion channels expression.

Our research suggests that TBBPA modifies the contractile response of 5-HT, His and KCl by interference with 5-HT and His receptors and the involvement of Ca^{2+} and K^+ channels. Taking into account that hypertensive disorders in pregnancy are associated with a variation in 5-HT or His release and with the sensitivity of the HUA to these mediators, that leads to changes in vascular resistance [43,52-54]. In fact, some epidemiological studies have associated the exposure to EDCs, including flame retardants, with the development of cardiovascular diseases [24,55]. However, more studies are needed to understand this involvement and the associated mechanisms. Since we are daily exposed to products containing EDCs, studying how and by what mechanisms these compounds can disrupt the normal physiological regulation of HUA is fundamental to the treatment and prevention of cardiovascular diseases.

5.6. Conclusions

In summary, our results showed for the first time that the direct effects of TBBPA induce a vasorelaxation in HUA. Concerning the effects of 24 h exposure of TBBPA, these are dependent on the contractile agents (5-HT, His and KCl) and the incubation concentration of this compound. In addition, these effects of TBBPA modified the vasorelaxant response of sodium nitroprusside and nifedipine, impairing the main HUA vasorelaxant mechanism.

The genomic effects of TBBPA induced an increase in vasodilation, and this effect may be due to the involvement of TBBPA in the NO/sGC/cGMP/PKG signalling pathway. Moreover, TBBPA clearly modulated the L-type Ca^{2+} and the BK_{Ca} 1.1 α- and β_1 -subunit channels, and the sGC and PKG protein. Taken together, these observations suggest that TBBPA exposure alters vascular homeostasis of HUA.

5.7. Funding

This work was supported by European Regional Development Fund (ERDF) funds through the POCICOMPETE 2020—Operational Program Competitiveness and Internationalisation in Axis I-Strengthening research, technological development and innovation (Project POCI-01- 0145-FEDER007491) and National Funds by FCT—Foundation for Science and Technology (Project UID/Multi/00709/2019). J.F. acknowledges the PhD fellowship from FCT (Reference: SFRH/BD/131665/ 2017), S.R. acknowledges the PhD fellowship from FCT (SFRH/BD/ 115693/2016) and M.M. acknowledges the PhD fellowship from FCT (Reference: 2020.07020. BD).

5.8. Credit authorship contribution statement

Joana Feiteiro: Conceptualization, Methodology, Formal analysis, Investigation, Writing – original draft, Visualization. Sandra M Rocha: Formal analysis, Writing – review & editing. Melissa Mariana: Formal analysis, Writing – review & editing. Cláudio J Maia: Methodology, Formal analysis, Software, Validation, Writing – review & editing, Supervision. Elisa Cairrão: Conceptualization, Visualization, Methodology, Formal analysis, Software, Validation, Writing – review & editing, Supervision, Funding acquisition.

5.9. Declaration of competing interest

The authors declare that they have no known competing financial interests or personal relationships that could have appeared to influence the work reported in this paper.

5.10. Acknowledgements

The authors would like to thank all donors' mothers who agreed to participate in this study and all the technical staff from Gynaecology–Obstetrics Department staff of "Centro Hospitalar Universitário da Cova da Beira E.P.E." (CHUCB, Covilhã, Portugal) and from maternity of "Unidade de Saúde Local da Guarda" (ULS, Guarda, Portugal), particularly to all medical, nurses and health technicians for their disinterested collaboration.

5.11. References

1. Kavlock, R.J.; Daston, G.P.; DeRosa, C.; Fenner-Crisp, P.; Gray, L.E.; Kaattari, S.; Lucier, G.; Luster, M.; Mac, M.J.; Maczka, C.; et al. Research needs for the risk assessment of health and environmental effects of endocrine disruptors: a report of the U.S. EPA-sponsored workshop. *Environ Health Perspect* **1996**, *104 Suppl 4*, 715-740.

2. Sabir, S.; Akhtar, M.F.; Saleem, A. Endocrine disruption as an adverse effect of non-endocrine targeting pharmaceuticals. *Environ Sci Pollut Res Int* **2018**.

3. Legler, J.; Brouwer, A. Are brominated flame retardants endocrine disruptors? *Environ Int* **2003**, *29*, 879-885.

4. van der Veen, I.; de Boer, J. Phosphorus flame retardants: properties, production, environmental occurrence, toxicity and analysis. *Chemosphere* **2012**, *88*, 1119-1153.

5. Chan, W.K.; Chan, K.M. Disruption of the hypothalamic-pituitary-thyroid axis in zebrafish embryo-larvae following waterborne exposure to BDE-47, TBBPA and BPA. *Aquat Toxicol* **2012**, *108*, 106-111.

6. Chen, S.J.; Ma, Y.J.; Wang, J.; Chen, D.; Luo, X.J.; Mai, B.X. Brominated flame retardants in children's toys: concentration, composition, and children's exposure and risk assessment. *Environ Sci Technol* **2009**, *43*, 4200-4206.

7. Dirtu, A.C.; Covaci, A. Estimation of daily intake of organohalogenated contaminants from food consumption and indoor dust ingestion in Romania. *Environ Sci Technol* **2010**, *44*, 6297-6304.

8. Abafe, O.A.; Martincigh, B.S. Determination and human exposure assessment of polybrominated diphenyl ethers and tetrabromobisphenol A in indoor dust in South Africa. *Environ Sci Pollut Res Int* **2016**, *23*, 7038-7049.

9. Abou-Elwafa Abdallah, M. Environmental occurrence, analysis and human exposure to the flame retardant tetrabromobisphenol-A (TBBP-A)-A review. *Environ Int* **2016**, *94*, 235-250.

10. Covaci, A.; Voorspoels, S.; Abdallah, M.A.; Geens, T.; Harrad, S.; Law, R.J. Analytical and environmental aspects of the flame retardant tetrabromobisphenol-A and its derivatives. *J Chromatogr A* **2009**, *1216*, 346-363.

11. Kim, Y.R.; Harden, F.A.; Toms, L.M.; Norman, R.E. Health consequences of exposure to brominated flame retardants: a systematic review. *Chemosphere* **2014**, *106*, 1-19.

12. Feiteiro, J.; Mariana, M.; Cairrao, E. Health toxicity effects of brominated flame retardants: From environmental to human exposure. *Environ Pollut* **2021**, *285*, 117475.

13. Cope, R.B.; Kacew, S.; Dourson, M. A reproductive, developmental and neurobehavioral study following oral exposure of tetrabromobisphenol A on Sprague-Dawley rats. *Toxicology* **2015**, *329*, 49-59.

14. Huang, G.Y.; Ying, G.G.; Liang, Y.Q.; Zhao, J.L.; Yang, B.; Liu, S.; Liu, Y.S. Hormonal effects of tetrabromobisphenol A using a combination of in vitro and in vivo assays. *Comp Biochem Physiol C Toxicol Pharmacol* **2013**, *157*, 344-351.

15. Kitamura, S.; Jinno, N.; Ohta, S.; Kuroki, H.; Fujimoto, N. Thyroid hormonal activity of the flame retardants tetrabromobisphenol A and tetrachlorobisphenol A. *Biochem Biophys Res Commun* **2002**, *293*, 554-559.

16. Kitamura, S.; Kato, T.; Iida, M.; Jinno, N.; Suzuki, T.; Ohta, S.; Fujimoto, N.; Hanada, H.; Kashiwagi, K.; Kashiwagi, A. Anti-thyroid hormonal activity of tetrabromobisphenol A, a flame retardant, and related compounds: Affinity to the mammalian thyroid hormone receptor, and effect on tadpole metamorphosis. *Life Sci* **2005**, *76*, 1589-1601.

17. Ongono, J.S.; Dow, C.; Gambaretti, J.; Severi, G.; Boutron-Ruault, M.C.; Bonnet, F.; Fagherazzi, G.; Mancini, F.R. Dietary exposure to brominated flame retardants and risk of type 2 diabetes in the French E3N cohort. *Environ Int* **2018**, *123*, 54-60.

18. McDonald, T.A. A perspective on the potential health risks of PBDEs. *Chemosphere* **2002**, *46*, 745-755.

19. Muller, M.H.; Polder, A.; Brynildsrud, O.B.; Lie, E.; Loken, K.B.; Manyilizu, W.B.; Mdegela, R.H.; Mokiti, F.; Murtadha, M.; Nonga, H.E.; et al. Brominated flame retardants (BFRs) in breast milk and associated health risks to nursing infants in Northern Tanzania. *Environ Int* **2015**, *89-90*, 38-47.

20. Ho, K.L.; Yuen, K.K.; Yau, M.S.; Murphy, M.B.; Wan, Y.; Fong, B.M.; Tam, S.; Giesy, J.P.; Leung, K.S.; Lam, M.H. Glucuronide and sulfate conjugates of tetrabromobisphenol A (TBBPA): Chemical synthesis and correlation between their urinary levels and plasma TBBPA content in voluntary human donors. *Environ Int* **2017**, *98*, 46-53.

21. Kawashiro, Y.; Fukata, H.; Omori-Inoue, M.; Kubonoya, K.; Jotaki, T.; Takigami, H.; Sakai, S.; Mori, C. Perinatal exposure to brominated flame retardants and polychlorinated biphenyls in Japan. *Endocr J* **2008**, *55*, 1071-1084.

22. Tung, E.W.; Yan, H.; Lefevre, P.L.; Berger, R.G.; Rawn, D.F.; Gaertner, D.W.; Kawata, A.; Rigden, M.; Robaire, B.; Hales, B.F.; et al. Gestational and Early Postnatal Exposure to an Environmentally Relevant Mixture of Brominated Flame Retardants: General Toxicity and Skeletal Variations. *Birth Defects Res B Dev Reprod Toxicol* **2016**, *107*, 157-168.

23. Darnerud, P.O. Toxic effects of brominated flame retardants in man and in wildlife. *Environ Int* **2003**, *29*, 841-853.

24. Lorigo, M.; Cairrao, E. Fetoplacental vasculature as a model to study human cardiovascular endocrine disruption. *Mol Aspects Med* **2021**, 101054.

25. Gloria, S.; Marques, J.; Feiteiro, J.; Marcelino, H.; Verde, I.; Cairrao, E. Tributyltin role on the serotonin and histamine receptors in human umbilical artery. *Toxicol In Vitro* **2018**, *50*, 210-216.

26. Lorigo, M.; Mariana, M.; Feiteiro, J.; Cairrao, E. How is the human umbilical artery regulated? *J Obstet Gynaecol Res* **2018**, *44*, 1193-1201.

27. Cairrao, E.; Santos-Silva, A.J.; Verde, I. PKG is involved in testosterone-induced vasorelaxation of human umbilical artery. *Eur J Pharmacol* **2010**, *640*, 94-101.

28. Cairrao, E.; Santos-Silva, A.J.; Alvarez, E.; Correia, I.; Verde, I. Isolation and culture of human umbilical artery smooth muscle cells expressing functional calcium channels. *In Vitro Cell Dev Biol Anim* **2009**, *45*, 175-184.

29. Lorigo, M.; Quintaneiro, C.; Lemos, M.C.; Martinez-de-Oliveira, J.; Breitenfeld, L.; Cairrao, E. UV-B Filter Octylmethoxycinnamate Induces Vasorelaxation by Ca(2+) Channel Inhibition and Guanylyl Cyclase Activation in Human Umbilical Arteries. *Int J Mol Sci* **2019**, *20*.

30. Saldanha, P.A.; Cairrao, E.; Maia, C.J.; Verde, I. Long- and short-term effects of androgens in human umbilical artery smooth muscle. *Clin Exp Pharmacol Physiol* **2013**, *40*, 181-189.

31. Pfaffl, M.W. A new mathematical model for relative quantification in real-time RT–PCR. *Nucleic Acids Research* **2001**, *29*, e45-e45.

32. Lorigo, M.; Quintaneiro, C.; Maia, C.J.; Breitenfeld, L.; Cairrao, E. UV-B filter octylmethoxycinnamate impaired the main vasorelaxant mechanism of human umbilical artery. *Chemosphere* **2021**, *277*, 130302.

33. Tufan, H.; Ayan-Polat, B.; Tecder-Unal, M.; Polat, G.; Kayhan, Z.; Ogus, E. Contractile responses of the human umbilical artery to KCl and serotonin in Ca-free medium and the effects of levcromakalim. *Life Sci* **2003**, *72*, 1321-1329.

34. Leung, S.W.; Quan, A.; Lao, T.T.; Man, R.Y. Efficacy of different vasodilators on human umbilical arterial smooth muscle under normal and reduced oxygen conditions. *Early Hum Dev* **2006**, *82*, 457-462.

35. Godfrey, A.; Abdel-Moneim, A.; Sepulveda, M.S. Acute mixture toxicity of halogenated chemicals and their next generation counterparts on zebrafish embryos. *Chemosphere* **2017**, *181*, 710-712.

36. Laboratories, S. The subchronic toxicity of sediment-sorbed tetrabromobisphenol A to Chironomus tentans under flow-through conditions. **1989**.

37. Pittinger, C.A.; Pecquet, A.M. Review of historical aquatic toxicity and bioconcentration data for the brominated flame retardant tetrabromobisphenol A (TBBPA): effects to fish, invertebrates, algae, and microbial communities. *Environ Sci Pollut Res Int* **2018**, *25*, 14361-14372.

38. Chen, X.; Gu, J.; Wang, Y.; Gu, X.; Zhao, X.; Wang, X.; Ji, R. Fate and O-methylating detoxification of Tetrabromobisphenol A (TBBPA) in two earthworms (Metaphire guillelmi and Eisenia fetida). *Environ Pollut* **2017**, *227*, 526-533.

39. Santos-Silva, A.J.; Cairrao, E.; Marques, B.; Verde, I. Regulation of human umbilical artery contractility by different serotonin and histamine receptors. *Reprod Sci* **2009**, *16*, 1175-1185.

40. Lovren, F.; Li, X.F.; Lytton, J.; Triggle, C. Functional characterization and m-RNA expression of 5-HT receptors mediating contraction in human umbilical artery. *Br J Pharmacol* **1999**, *127*, 1247-1255.

41. Karlsson, C.; Bodelsson, G.; Bodelsson, M.; Stjernquist, M. Characterization of 5-hydroxytryptamine receptors mediating circular smooth muscle contraction in the human umbilical artery. *Gynecol Obstet Invest* **1999**, *47*, 102-107.

42. Jahnichen, S.; Glusa, E.; Pertz, H.H. Evidence for 5-HT2B and 5-HT7 receptor-mediated relaxation in pulmonary arteries of weaned pigs. *Naunyn Schmiedebergs Arch Pharmacol* **2005**, *371*, 89-98.

43. Gupta, S.; Hanff, L.M.; Visser, W.; Steegers, E.A.; Saxena, P.R.; Vulto, A.G.; MaassenVanDenBrink, A. Functional reactivity of 5-HT receptors in human umbilical cord and maternal subcutaneous fat arteries after normotensive or pre-eclamptic pregnancy. *J Hypertens* **2006**, *24*, 1345-1353.

44. Hawley, J.; Rubin, P.C.; Hill, S.J. Distribution of receptors mediating phosphoinositide hydrolysis in cultured human umbilical artery smooth muscle and endothelial cells. *Biochem Pharmacol* **1995**, *49*, 1005-1011.

45. Santos-Silva, A.J.; Cairrao, E.; Morgado, M.; Alvarez, E.; Verde, I. PDE4 and PDE5 regulate cyclic nucleotides relaxing effects in human umbilical arteries. *Eur J Pharmacol* **2008**, *582*, 102-109.

46. Schneider, A.; Riess, P.; Elbers, A.; Neugebauer, E.; Schaefer, U. Polyclonal anti-histamine H2 receptor antibodies detect differential expression of H2 receptor protein in primary vascular cell types. *Inflamm Res* **2004**, *53*, 223-229.

47. Cribbs, L.L. T-type Ca2+ channels in vascular smooth muscle: multiple functions. *Cell Calcium* **2006**, *40*, 221-230.

48. Santos-Silva, A.J.; Cairrao, E.; Verde, I. Study of the mechanisms regulating human umbilical artery contractility. *Health* **2010**, *02*, 321-331.

49. Feiteiro, J.; Verde, I.; Cairrao, E. Cyclic guanosine monophosphate compartmentation in human vascular smooth muscle cells. *Cell Signal* **2016**, *28*, 109-116.

50. Cairrao, E.; Alvarez, E.; Santos-Silva, A.J.; Verde, I. Potassium channels are involved in testosterone-induced vasorelaxation of human umbilical artery. *Naunyn Schmiedebergs Arch Pharmacol* **2008**, *376*, 375-383.

51. Lorigo, M.; Oliveira, N.; Cairrao, E. Clinical Importance of the Human Umbilical Artery Potassium Channels. *Cells* **2020**, *9*.

52. Brew, O.; Sullivan, M.H. The links between maternal histamine levels and complications of human pregnancy. *J Reprod Immunol* **2006**, *72*, 94-107.

53. Sonkusare, S.; Palade, P.T.; Marsh, J.D.; Telemaque, S.; Pesic, A.; Rusch, N.J. Vascular calcium channels and high blood pressure: pathophysiology and therapeutic implications. *Vascul Pharmacol* **2006**, *44*, 131-142.

54. Kuo, I.Y.; Wolfle, S.E.; Hill, C.E. T-type calcium channels and vascular function: the new kid on the block? *J Physiol* **2011**, *589*, 783-795.

55. Eslami, B.; Malekafzali, H.; Rastkari, N.; Rashidi, B.H.; Djazayeri, A.; Naddafi, K. Association of serum concentrations of persistent organic pollutants (POPs) and risk of pre-eclampsia: a case-control study. *J Environ Health Sci Eng* **2016**, *14*, 17.

Chapter 6

Research Work 3

Vascular response of tetrabromobisphenol A in rat aorta: Calcium channels inhibition and potassium channels activation

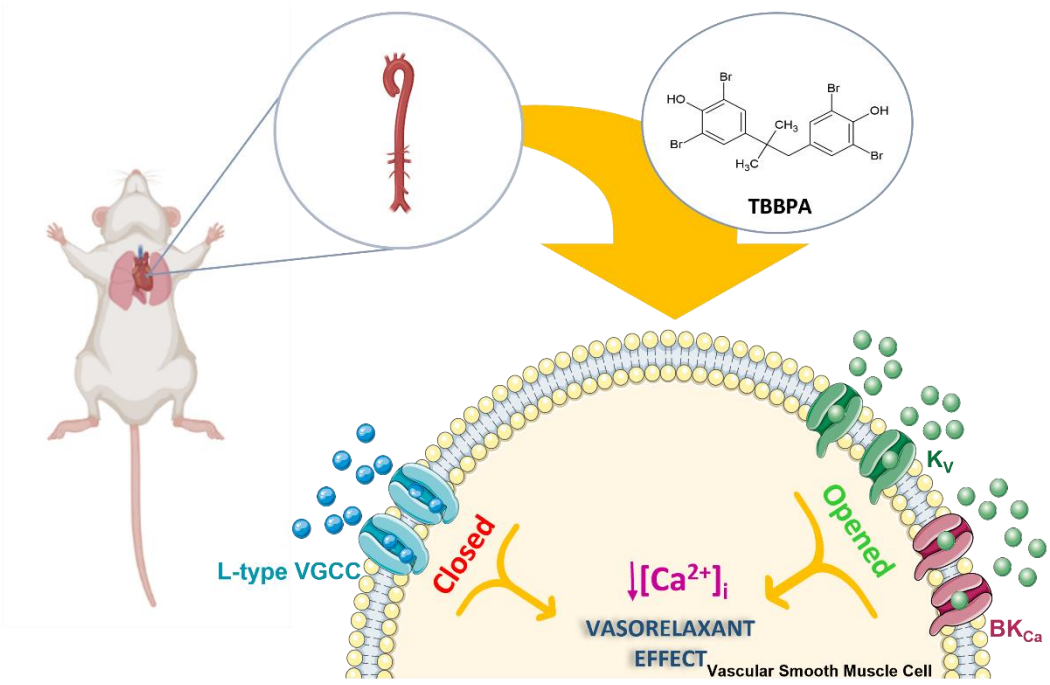

This chapter corresponds to the original research article:

Joana Feiteiro, Sandra M Rocha, Melissa Mariana, Cláudio J Maia, Elisa Cairrão. *Vascular response of tetrabromobisphenol A in rat aorta: Calcium channels inhibition and potassium channels activation*. Toxics. Volume 10(9):529, 9 September 2022, https://doi.org/10.3390/toxics10090529

6.1. Abstract

Abstract: Tetrabromobisphenol A (TBBPA) is a flame retardant widely used to reduce flammability. Being an endocrine disruptor and due to a constant human exposure, some concerns have been raised in human health. Studies showed that TBBPA affects oxidative stress, cell proliferation, and intracellular calcium levels. However, the vascular consequences of TBBPA exposure are still scarce. Hence, this work aimed to analyse TBBPA effects on rat aortic smooth muscle and its action mechanisms. Through an *ex vivo* approach Wistar rat aortas were used in an organs bath to evaluate the vascular effect of TBBPA (0.01–100 μM). In addition, TBBPA's mode of action was studied through calcium and potassium channel inhibitors. Resorting to *in vitro* studies, A7r5 cells were used to analyse L-Type voltage-gated calcium channels (VGCC) activity through the whole-cell configuration of Patch clamp technique, and the mRNA expression of proteins and ion channels involved in vascular contractility. The results showed a vasorelaxation of rat aorta induced by TBBPA exposure, involving the inactivation of L-Type VGCC and activation of potassium channels, and the modulation of mRNA expression of L-type calcium and large-conductance calcium 1.1 and the BK_{Ca} 1.1 α- and β_1 -subunit channels, soluble guanylyl cyclase and protein Kinase G.

Keywords: Tetrabromobisphenol A, Relaxation, Calcium channels, Potassium channels, Rat aortic, A7r5 cells

6.2. Introduction

One of the most prevalent brominated flame retardant is tetrabromobisphenol A (TBBPA or 2,6-Dibromo-4-[2-(3,5-dibromo-4-hydroxyphenyl)propan-2yl]phenol), used in plastic, textile and paper [1]. This compound is considered an endocrine disruptor and it has been already found in food, dust, water, air, soil, and consequently, in animals and humans [1].

So far, most of the studies have been performed in animals, mainly in rodents, showing an association between TBBPA exposure and reproductive, development and neurobehavioral effects [2-4]. Besides, it was also demonstrated that this compound can alter thyroid hormone levels [5,6], and has been related with nephrotoxicity, hepatotoxicity, and carcinogenicity [7-9]. Specifically, TBBPA leads to an increase in intracellular calcium levels ($[Ca^{2+}]_i$) and to cell death in cerebellar granule cells´ primary neurons [10]. Moreover, in rat pancreatic β-cells, TBBPA can also affect some parameters of oxidative stress, namely nitric oxide (NO) and intracellular reactive oxygen species (ROS), and mitochondrial superoxide levels [11]. These results showed that the disruption of calcium (Ca^{2+}) homeostasis is involved in the formation of ROS and cell death, mechanisms in which TBBPA is involved.

It is known that vascular tone is regulated by the $[Ca^{2+}]_i$, which is the main factor of vascular smooth muscle cells´ (SMC) contractility, and NO [12,13]. In rat small mesenteric arteries and rabbit cerebral arteries it is suggested that NO may activate large-conductance Ca^{2+}-activated K^+ (BK_{Ca}) channels in a cyclic guanosine monophosphate (cGMP)-independent manner and may modulate the frequency of Ca^{2+} sparks affecting the activity of BK_{Ca} channels [14,15].

Giving these observations, it is important to analyse how TBBPA exposure affects the vascular tonus and to understand the mechanistic pathways underlying these effects. Thus, the aim of this work was to assess the effects of TBBPA in rat aortic smooth muscle and to investigate its potential signalling pathway. For that purpose, the TBBPA effect on contracted endothelium-denuded rat aorta was analysed by *ex vivo* organ bath experiments. Using A7r5 cells, TBBPA effects on voltage dependent Ca^{2+} current ($I_{Ca,L}$) were analysed through the whole cell configuration of the patch clamp technique and after 24 h TBBPA exposure, the expression of potassium (K^+) and Ca^{2+} channels, soluble guanylate cyclase (sGC) and cGMP-dependent protein kinase (PKG) was evaluated.

6.3. Methods

6.3.1. Drugs and chemicals

The drugs used in cell culture and contractility, MTT, and electrophysiology ex-periments were purchased from Sigma-Aldrich Chemistry (Sintra, Portugal). The reagents for RT-qPCR technique were bought NZYTech (Lisboa, Portugal), and Grisp (Porto, Portugal). In addition, the bovine serum albumin (BSA) was purchased from Fisher Scientific and the foetal bovine serum (FBS) from Biochrom. The stock solutions of Phenylephrine (Phenyl), Noradrenaline (NA), tetraethylammonium (TEA) and 4-aminopyridine (4-AP) were made in distilled water, while TBBPA, Nifedipine (Nif), glybenclamide (Gly) and Bay-K 8644 were dissolved in absolute ethanol

and stored at -20 ºC. Appropriate dilutions were prepared before the experiments in each specific solution, Krebs' solution to be used in organ bath, electrophysiology external solution in patch clamp technique and FBS-free culture medium in MTT assay and RT-qPCR technique. The final concentrations of ethanol (vehicle) did not exceed 0.1 %.

6.3.2. *Ex Vivo* studies

6.3.2.1. Contractility experiments in isolated rat thoracic aorta rings

The use of male adult Wistar rats (Charles-River, Barcelona, Spain) was approved by the Animal Research Committee of University of Beira Interior (CICS-UBI, Covilhã, Portugal) and follows the regulations of the European Convention for the Protection of Vertebrate Animals Used for Experimental and Other Scientific Purposes (Directive 2010/63/EU). The procedures for euthanasia, thoracotomy and organs bath technique were performed as previously by our group [16,17]. After confirming the absence of endothelium using acetylcholine (1 μM), the rat aorta rings were contracted with Phenyl (1 μM), NA (1 μM) and isosmotic KCl (60 mM) solution. Upon each contraction the effects of TBBPA (0.01–100 μM) were evaluated. Besides, to analyse the influence of Ca^{2+} and K^+ channels, different inhibitors were added:

- Nif (0.001 and 1 μM), an inhibitor of voltage-gated calcium channels (VGCC);
- TEA (1000 μM), an inhibitor of conductance Ca^{2+}-activated K^+ (BK_{Ca}) channel;
- 4-AP (1000 μM), an inhibitor of voltage-gated potassium channels (K_v);
- Gly (10 μM), an inhibitor of ATP-sensitive potassium (K_{ATP}).

In these experiments, before contraction, the rat aorta rings were incubated 15 minutes with these K^+ channels inhibitors and the effects of TBBPA and Nif in the presence of these drugs were analysed. Ethanol was used as control at the same percentage used to dissolve TBBPA. Each experiment was conducted in several rat aorta rings from at least five different rats.

6.3.3. *In Vitro* studies

6.3.3.1. Culture of A7r5 cells

A7r5 cell line is a commercial vascular smooth muscle cell line obtained from embryonic rat aorta (Sigma-Aldrich, Portugal) and a suitable model to study the contractile function, mainly the calcium homeostasis. The culture of the cells was performed according to Mariana *et al.* [16]. After confluence, the cells were maintained in a culture medium without FBS for 24 h. Before each experiment, the cells were trypsinized using a commercial trypsin-EDTA solution (0.025 %). These cells were used to perform MTT assay, electrophysiology, and real-time quantitative polymerase chain reaction (RT-qPCR) experiments.

6.3.3.2. Cell viability

A7r5 cells´viability and proliferation in response to TBBPA exposure were measured using the MTT assay. This assay was performed according to the methodology described by Feiteiro *et al.* [18]. Confluent cells were treated for 24 h with different concentrations of TBBPA (0.01, 0.1, 1, 10, 30, 50, 100, 500 and 1000 μM), after which 200 μL MTT solution (0.5 mg/mL) were added. After 4 h (37 °C, 5 % CO2 and 95 % of humidity) of exposure to MTT, it was removed, and the formazan crystals were dissolved in DMSO and converted into a purple colour indicating the amount of formazan production. Colour intensity was measured at 570 nm using a photometer (EZ Read 400, Microplate Reader, Biochrom).

6.3.3.3. Electrophysiology experiments

For the electrophysiological experiments, the cells were kept at 4 °C in medium without FBS until the initiation of the experience. To analyse the L-type VGCC current ($I_{Ca,L}$), the patch clamp technique was used in the whole-cell configuration, as described by Cairrao *et al.* [19] and Mariana *et al.* [16]. Different concentrations of TBBPA (0.01, 1, 10, 50 and 100 μM) dissolved in external solution, were studied in basal and BAY K8644-stimulated (0.01 μM) $I_{Ca,L}$.

6.3.3.4. Real-time quantitative polymerase chain reaction (RT-qPCR)

RT-qPCR was the technique used to assess the mRNA expression of L-type calcium channel a1C-subunit (Cav1.2), BK_{Ca} 1.1 α- and β_1- subunits (BK_{Ca} 1.1α and BKCa β_1), sGC ($Gucci_{\alpha}$) and protein kinase cGMP-dependent 1 α-subunit (PRKG 1α) in response to TBBPA after 24 hours of treatment. This procedure was performed according to Feiteiro *et al.* [18]. For these cells cyclophilin A (Cyc A) was used as internal control to normalize gene expression. The efficiency of the amplification (CFX Connect; Real-Time System; BioRad, Hercules, CA, USA) was defined for all primer sets using serial dilutions of cDNA samples (1:1, 1:5 and 1:25). For the qPCR, a 20 μL reaction was pre-pared (1 μL cDNA, 0.3 μM of each primer, except for L-type (0.4 μM), and 10 μL SYBR Green/Fluorescein qPCR Master Mix). Then, initial denaturation at 95 °C for 5 min was followed by 40 cycles of 95 °C (10 sec), 60 °C the annealing temperature (30 sec) and at 72 °C (10 sec). The amplified PCR fragments (60 °C to 95 °C at a rate of 0.05 °C/s) were verified by melting curve analysis. All samples were run in triplicated for each qPCR assay. The normalized mRNA expression value was calculated following the mathematical model proposed by Pfaffl using the formula $2^{-\Delta\Delta Ct}$ [20]. All oligonucleotide primers are indicated in Table 6.1.

Table 6.1. Oligonucleotide primers used for real-time polymerase chain reaction.

Gene	GenBank accession no.	Primer (5´- 3´)	Concentration (μM)
Cyc A	NM_017090.2	Fw: 5- CAA GAC TGA GTG GCT GGA TGG -3 Rv: 5-GCC CGC AAG TCA AAG AAA TTA GAG -3	0.3
Cav1.2	NM_012517.2	Fw: 5- CTC GAA GTT GGG AGA ACA GC -3 Rv: 5- GAC GAA ACC CAC GAA GAT GT -3	0.4
BK_{Ca} β_1	NM_019273.1	Fw: 5- CCA GGA ATC CAC CTG TCA CT -3 Rv: 5- TCA CAT CAA CCA AGG CTG TC -3	0.3
BK_{Ca} 1.1 α	NM_031828.1	Fw: 5- GTC TGC ATC TTT GGG GAT GT -3 Rv: 5- GGG GAA GTT GTG CAG TGT TT -3	0.3
$Gucci_{\alpha}$	NM_017090.2	Fw: 5- GTG TGC CTC GGA AAA TCA AT -3 Rv: 5- ATC TCG GGG TGA ACA CAA AG -3	0.3
PRKG 1α	NM_001105731.3	Fw: 5- CGT GAG GCT ATA CCG GAC AT -3 Rv: 5- GCA AAC GCT TCT ACC ACA CA -3	0.3

6.3.4. Statistical analysis

According to the number and type of the variables tested in this work different and specific statistical methods were applied. For cell viability, a comparison between different concentrations of TBBPA and control was analysed using a one-way analysis of variance (ANOVA) followed by Dunnett's post hoc test to determine significant differences among the means. In the contractility experiments, statistical significance between two groups was analysed using Student's t-test, while a comparison between different concentrations of TBBPA was analysed using one-way ANOVA followed by Tukey post hoc test. Additionally, to analyse the statistical difference of the effect of Nif and K^+ channels inhibitors on TBBPA effect, the Two-way ANOVA with interaction followed by the Holm-Sidak post-hoc tests were applied. In the electrophysiology experiments, comparison between different concentrations of TBBPA was analysed using one-way ANOVA followed by Tukey post hoc test to determine significant differences. Finally, to evaluate the statistical differences in the mRNA expression one-way ANOVA followed by Dunnett's multiple comparison test was used.

In all cases the statistical significance was considered for a *p*-value lower than 0.05 and all values are presented as the mean ± SD (standard deviation) of number of experiments. Software Origin 8.5.1. was used for the graphic design and SigmaStat Statistical Analysis System version 4.0 (2016) for data analysis.

6.4. Results

This research study assessed how TBBPA affects the rat aorta smooth muscle. The TBBPA-mediated vascular effects were analysed a functional (through the organ bath and patch-clamp) and genomic levels (24 h exposure of TBBPA in A7r5 cells). The design of this study was chosen in accordance with previous works performed by our research group [16,17,21,22], in which bisphenol A (BPA), an analogue of TBBPA, was one of the compounds analysed in those studies. These authors demonstrated that this experimental design is adequate to analyse how these hazardous compounds impair the vascular function. A wide range of concentrations is appropriate to study

toxic effects of environmental contaminants, so in this study we used 0.01-1000 µM of TBBPA that are in accordance with a recent study [18], that demonstrated that only the highest concentrations decreased the viability of human umbilical smooth muscle cells.

6.4.1. *Ex Vivo* studies

6.4.1.1. Effects of TBBPA on isolated rat aorta

To evaluate the effects of TBBPA on rat aorta contractility, after removing the endothelium, the aortic rings were first exposed to Phenyl (1 µM), NA (1 µM) and KCl (60 mM) solution. The maximum contractions promoted by these three contractile agents were 2.02± 0.7 g, 2.01 ± 0.7 g and 2.01 ± 0.6 g, respectively, and were not statistically significant (p = 0.997). However, when TBBPA was added to the resting tension the results showed that none TBBPA concentrations (0.01–100 µM) affected the basal tension (data not shown).

Afterwards, the TBBPA effects were analysed over the contractions the Phenyl (1 µM), NA (1 µM) and KCl (60 mM). As displayed in Figure 1, TBBPA provoked a concentration-dependent relaxation over the precontracted aortic rings, either with Phenyl (Figure 2A), NA (Figure 2B) or KCl (Figure 2C), with a maximum effect at 100 µM (the highest concentration). The relaxations elicited by this concentration of TBBPA on Phenyl- NA- or KCl-contracted rat aorta were 44 ± 6.3 %, 53.35 ± 4.23 % and 34.43 ± 3.8 %, respectively. In Phenyl and NA-contracted rat aorta the relaxant effects of TBBPA are more prominent, indicating that the contractile agent used can modulate the TBBPA response. Also in Figure 6.1, it is shown that the vehicle did not have significant effects on contracted arteries in any of the concentrations used.

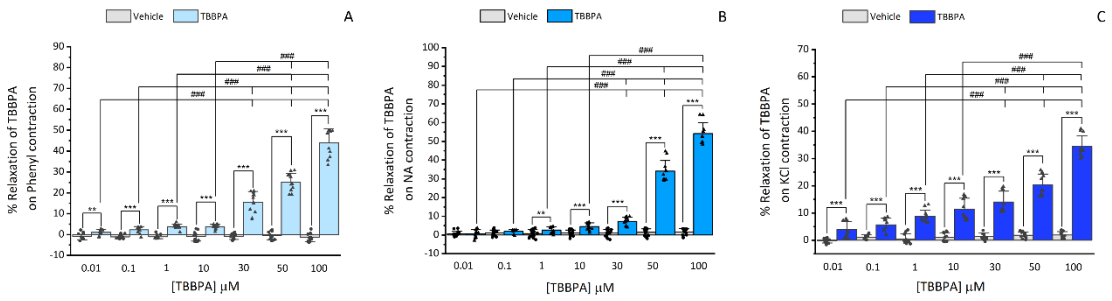

Figure 6.1. TBBPA vasorelaxation (0.01–100 µM) in rat aorta rings contracted with **(A)** Phenylephrine (Phenyl, 1 µM, number of rat aortas = 7) **(B)** Noradrenaline (NA, 1 µM, number of rat aortas = 7) and **(C)** KCl (60 mM, number of rat aortas = 6). Results are expressed as a percentage (%) of relaxation on contractility. Each bar represents the mean values, the vertical lines the SD and the dots the replicates for each n. * Represents significant statistical differences between each TBBPA concentrations and the respective vehicle (** $p < 0.01$ and *** $p < 0.001$, Student's t-test) and ### represents statistical differences between all TBBPA concentrations ($p < 0.001$, one-way ANOVA followed by Tukey's post hoc tests).

6.4.1.2. Influence of L-type Ca^{2+} channels on TBBPA-induced vasorelaxation on isolated rat aorta

To analyse the involvement of L-type VGCC in the TBBPA vasorelaxant effect, after contraction with Phenyl (1 µM), NA (1 µM) and isosmotic KCl (60 mM) solution, the arteries were exposed to Nif (0.001 and 1 µM) and the TBBPA (0.01–100 µM). Isosmotic KCl solution induces contraction by extracellular Ca^{2+} influx, through depolarisation and opening of L-type VGCC. Nif, being a specific blocker of these channels, when added at a concentration of 1 µM it leads to a relaxation of almost 100 % (data not shown). Thus, a lower concentration (0.001 µM) had to be used in KCl contracted arteries to better analyse the effect of the TBBPA plus Nif. Figure 6.2 shows that Nif caused vasorelaxation in all Phenyl, NA, and KCl contracted arteries with a statistically significant interaction between the different concentrations of TBBPA and the effect triggered by Nif treatment ($p \leq 0.001$). Concerning the rat aorta contracted with Phenyl and NA (Figure 6.2A and 6.2B), the vasorelaxation induced by the combined application Nif and TBBPA (0.01-50 µM) was significantly higher than the individual TBBPA effect ($p < 0.001$). However, at 100 µM the vasorelaxation induced by Nif plus TBBPA was lower than the individual TBBPA effect ($p < 0.001$). While in KCl-contracted arteries (Figure 6.2C), the vasorelaxation induced by Nif plus TBBPA was significantly higher than the individual TBBPA effect in all concentrations ($p < 0.001$). The vasorelaxation induced by Nif plus TBBPA was similar to the individual effect of Nif ($p > 0.05$), in all conditions and TBBPA concentrations. Regardless of the contractile agent, the inactivation of L-type VGCC seems to be involved in the TBBPA vasorelaxant effect.

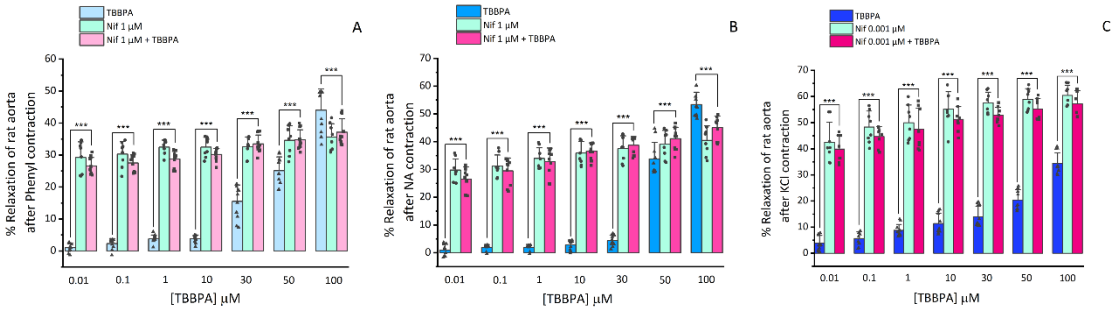

Figure 6.2. Relaxation of rat aortas with TBBPA (0.01–100 µM), Nif (0.1 and 1 µM) and Nif plus TBBPA upon contraction with **(A)** Phenylephrine (Phenyl, 1 µM, number of rat aortas = 8) **(B)** Noradrenaline (NA, 1 µM, number of rat aortas = 8) and **(C)** KCl (60 mM, number of rat aortas = 8). Results are expressed as a percentage (%) of relaxation on contractility. Each bar represents the mean values, the vertical lines the SD and the dots, squares and triangles the replicates for each n. *** Represents significant statistical differences between TBBPA and Nif + TBBPA: *** $p < 0.001$. Data were analysed using two-way ANOVA followed by Holm-Sidak post-hoc test.

6.4.1.3. Influence of K^+ channels on TBBPA-induced vasorelaxation on isolated rat aorta

Considering the previous results, the following approach was to analyse the involvement of K^+ channels in the vasorelaxation mechanism induced by TBBPA in rat aorta. Thus, TEA, 4-AP, and

Gly were used as different K^+ channels inhibitors. Firstly, before contraction, rat aorta rings were exposed for 15 min to TEA (1000 μM), 4-AP (1000 μM) and Gly (10 μM), and we observed that these inhibitors did not cause a significant effect on Phenyl and NA (1 μM) contraction (data not shown). After that, the Nif (1 μM) effect and cumulative concentrations of TBBPA (0.01–100 μM) were analysed, as shown in Figure 6.3. A statistical interaction was observed between the TBBPA levels, and the effect triggered by Nif plus TEA, 4-AP and Gly treatment for Phenyl and NA contractions ($p \leq 0.001$).

The following results for Phenyl contracted arteries will be summarized in Figure 6.3A and the statistics represented in Table 6.2, in which TBBPA will be called *Ct1*, Nif of *Ct2* and K^+ inhibitors plus Nif of *Ct3*. The obtained results showed that the synergetic effect of Nif and TBBPA was significantly higher than *Ct1* effect at 0.01–50 μM of TBBPA ($p < 0.001$), but at 100 μM of TBBPA, the combined application of Nif and TBBPA was significantly lower than *Ct1* ($p < 0.001$). Moreover, the effects induced by K^+ channels inhibitors with TBBPA were significantly lower than Ct1 at 0.01–100 μM and the combined application of K^+ channels inhibitors, Nif and TBBPA was significantly higher than *Ct1* (0.01–100 μM). The *Ct2* effect was not statistically significant neither with Nif plus TBBPA, nor with the effect of joint application of K^+ channels inhibitors, Nif and TBBPA ($p > 0.05$). However, the effect of *Ct2* was significantly higher compared to the effect induced by the K^+ channels inhibitors with TBBPA ($p < 0.001$). In addition, the application of *Ct3* at 0.01, 0.1, 1 and 10 μM of TBBPA was significantly higher than effect induced by Nif plus TBBPA ($p < 0.05$), while the effect induced by K^+ channels inhibitors with TBBPA was significantly lower than *Ct3* ($p < 0.001$). However, the *Ct3* effect was not significantly different compared to the effect of the combined application of K^+ channels inhibitors, Nif and TBBPA ($p > 0.05$).

In the same way as Phenyl, the results and statistics related to NA will be presented in Figure 6.3B and in Table 6.3, with the same designations *Ct1*, *Ct2* and *Ct3*. The results showed that combined application of Nif and TBBPA was significantly higher than *Ct1* at 0.01–50 μM of TBBPA ($p < 0.001$). However, at 100 μM the effect was significantly lower than *Ct1* ($p < 0.001$). The effect of K^+ channels inhibitors plus TBBPA was significantly lower than *Ct1*, at the three highest TBBPA concentrations (30, 50 and 100 μM) ($p < 0.01$ and $p < 0.001$), as well as the combined application K^+ channels inhibitors, Nif and TBBPA at 0.01, 1, 10 and 50 ($p < 0.001$) and 30 μM ($p < 0.01$) that was also significantly lower than *Ct1* effect ($p < 0.001$). On the contrary, at 100 μM concentrations of TBBPA, the effect of *Ct1* was significantly higher than the combined application of K^+ channels inhibitors, Nif and TBBPA ($p < 0.001$). Regarding *Ct2*, the effect induced by K^+ channels inhibitors plus TBBPA and combined applications of K^+ channels inhibitors, Nif and TBBPA were significantly lower than the vasorelaxation caused by *Ct2* ($p < 0.001$), at all concentrations of TBBPA. The effect of *Ct3* was significantly lower than the combined application of Nif and TBBPA ($p < 0.001$), and higher when compared to the combined applications of K^+ channels inhibitors and TBBPA ($p < 0.001$). Further-more, the *Ct3* effect was only significantly higher for TBBPA at 0.01 and 0.1 μM of TBBPA than the combined applications of K^+ channels inhibitors, Nif and TBBPA ($p < 0.05$).

Table 6.2. Statistical differences in the relaxation of rat aortas contracted with Phenyl (1 µM) in different conditions. *Ct1* represents the individual TBBPA effect; *Ct2* represents the individual Nif effect; *Ct3* represents the potassium channels inhibitors with Nif. * Represents significant statistical differences between different controls and other conditions: * $p < 0.05$, *** $p < 0.001$, n.s. represents no significant differences ($p > 0.05$). Data were analysed using two-way ANOVA followed by Holm-Sidak post-hoc test.

				[TBBPA] µM						
				0.01	0.1	1	10	30	50	100
Contraction with Phenylephrine (1 µM)	TBBPA (*Ct1*)	*vs*	Nif 1 µM + TBBPA	***	***	***	***	***	***	***
			K^+ channels inhibitors + TBBPA	*	*	***	***	***	***	***
			K^+ channels inhibitors + Nif 1 µM + TBBPA	***	***	***	***	***	***	*
	Nif 1 µM (*Ct2*)	*vs*	Nif 1 µM + TBBPA	n.s	n.s	n.s	n.s	n.s	n.s	n.s
			K^+ channels inhibitors + TBBPA	***	***	***	***	***	***	***
			K^+ channels inhibitors + Nif 1 µM + TBBPA	n.s	n.s	n.s	n.s	n.s	n.s	n.s
	K^+ channels inhibitors + Nif 1 µM (*Ct3*)	*vs*	Nif 1 µM + TBBPA	*	*	*	*	n.s	n.s	n.s
			K^+ channels inhibitors + TBBPA	***	***	***	***	***	***	***
			K^+ channels inhibitors + Nif 1 µM + TBBPA	n.s	n.s	n.s	n.s	n.s	n.s	n.s

(* p-value < 0.05; *** p-value < 0.001; n.s – no significant difference, p-value > 0.05)

Table 6.3. Statistical differences in the relaxation of rat aortas contracted with NA (1 µM) in different conditions. *Ct1* represents the individual TBBPA effect; *Ct2* represents the individual Nif effect; *Ct3* represents the potassium channels inhibitors with Nif. * Represents significant statistical differences between different controls and other conditions: * $p < 0.05$, ** $p < 0.01$, *** $p < 0.001$, n.s. represents no significant differences ($p > 0.05$). Data were analysed using two-way ANOVA followed by Holm-Sidak post-hoc test.

				[TBBPA] µM						
				0.01	0.1	1	10	30	50	100
Contraction with Noradrenaline (1 µM)	TBBPA (*Ct1*)	*vs*	Nif 1 µM + TBBPA	***	***	***	***	***	***	***
			K^+ channels blockage + TBBPA	n.s	n.s	n.s	n.s	**	***	***
			K^+ channels blockage + Nif 1 µM + TBBPA	***	***	***	***	**	***	***
	Nif 1 µM (*Ct2*)	*vs*	Nif 1 µM + TBBPA	n.s	n.s	n.s	n.s	n.s	n.s	n.s
			K^+ channels blockage + TBBPA	***	***	***	***	***	***	***
			K^+ channels blockage + Nif 1 µM + TBBPA	***	***	***	***	***	***	***
	K^+ channels + Nif 1 µM (*Ct3*)	*vs*	Nif 1 µM + TBBPA	***	***	***	***	***	***	***
			K^+ channels blockage + TBBPA	***	***	***	***	***	***	***
			K^+ channels blockage + Nif 1 µM + TBBPA	*	*	n.s	n.s	n.s	n.s	n.s

(* p-value < 0.05; ** p-value < 0.01; *** p-value < 0.001; n.s – no significant difference p-value > 0.05)

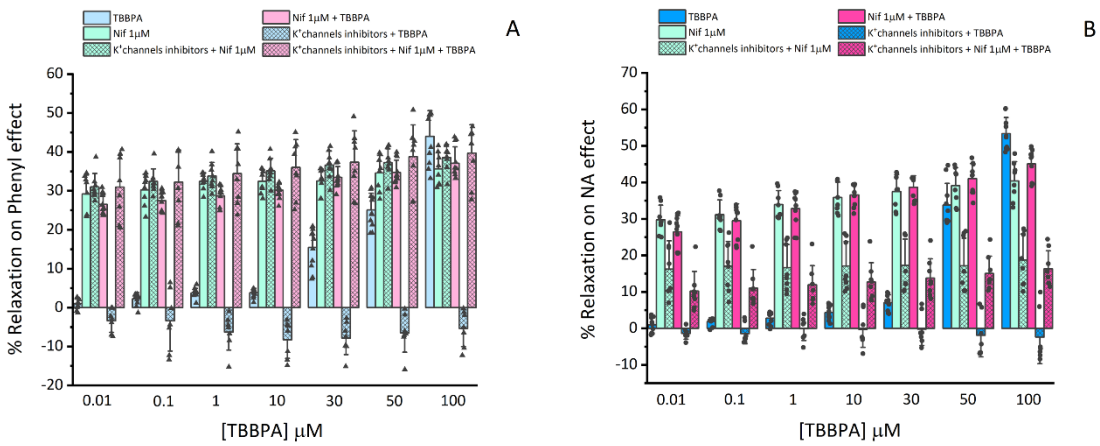

Figure 6.3. Vasorelaxant effects of TBBPA (0.01–100 µM), nifedipine (Nif, 1 µM), K^+ channels inhibitors (TEA, 1000 µM; 4-4-AP, 1000 µM and Gly, 10 µM), with Nif, Nif with TBBPA, and K^+ channels inhibitors with Nif and TBBPA on rat aorta rings contracted with **(A)** Phenylephrine (Phenyl, 1 µM, number of rat aortas = 7) **(B)** Noradrenaline (NA, 1 µM, number of rat aortas = 7). Each bar represents the mean values, the vertical lines the SD and the dots the replicates for each n.

6.4.2. *In Vitro* studies

6.4.2.1 Assessment of viability (MTT assay)

The cellular viability of A7r5 cells exposed to TBBPA (0.01, 0.1, 1, 10, 30, 50, 100, 500 and 1000 µM) was analysed using MTT assay. Besides TBBPA, the cells were exposed to the culture medium, as control, and to ethanol, the solvent used to dissolve TBBPA (vehicle) for 24 h. As shown in Figure 6.4, TBBPA at 500 and 1000 µM significantly decreased the cell viability ($p < 0.0001$). Thus, in all the experiments, the TBBPA concentrations used were 0.01, 0.1, 1, 10, 30, 50 and 100 µM.

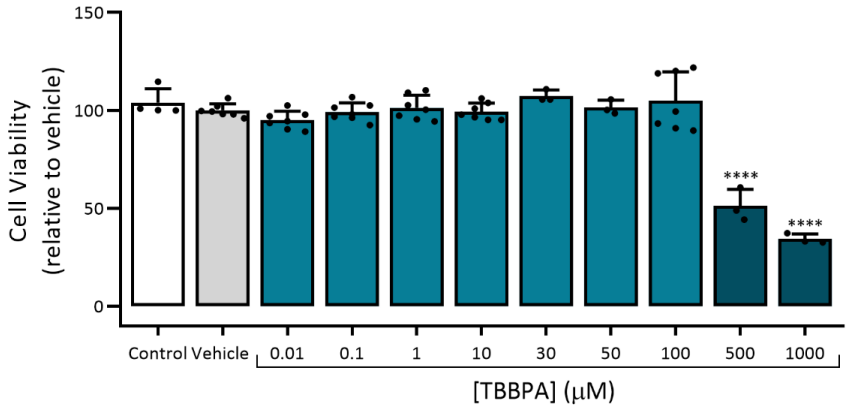

Figure 6.4. A7r5 cell viability under the effect of TBBPA. Data are expressed as a percentage (%) of cellular viability. Each bar represents the mean values and vertical lines the SD and the dots the replicates for each n. * Represents statistical differences between TBBPA and Vehicle (**** $p < 0.0001$, one-way ANOVA followed by Dunnett's post hoc test).

6.4.2.2. Effects of TBBPA on $I_{Ca,L}$ in A7r5 cells

In A7r5 cells, L-type VGCC current ($I_{Ca,L}$) was analysed through the whole-cell patch clamp technique. Figure 5A showed the effect of the TBBPA concentrations used in this study on $I_{Ca,L}$. of which 50 and 100 µM significantly inhibited basal $I_{Ca,L}$ ($p < 0.001$). This inhibition was reversible after washout. The $I_{Ca,L}$ density mean value was -1.82 ± 1.26 pA/pF (n = 33).

In order to analyse TBBPA effect on stimulated $I_{Ca,L}$, we resorted to BAY K8644 (0.01 µM), as a potent and specific activator of the L-type VGCC, which stimulated the calcium current by 60.40 ± 30.22 % above the basal level. Considering that Bay effects returned to the initial levels after washout we confirmed that the current analysed was $I_{Ca,L}$. Figure 6.5B summarizes the effects of TBBPA on the calcium current, in which a significant inhibition was observed for concentrations of 10, 50 and 100 µM ($p < 0.01$ and $p < 0.001$), with maximum values of 34.96 ± 4.45 %, 57.95 ± 3.80 %, and 64.24 ± 2.72 % respectively. The vehicle used to dissolve TBBPA, ethanol, did not affect basal or stimulated $I_{Ca,L}$ (-1.8 ± 2.75 %) (data not shown).

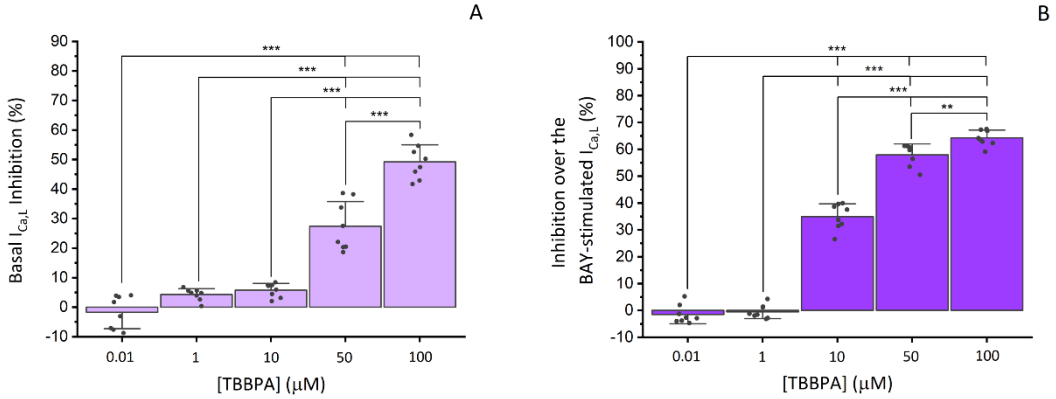

Figure 6.5. Effects of TBBPA (0.01–100 µM) on $I_{Ca,L}$ in A7r5 cells. **(A)** Inhibitory effects of TBBPA on basal $I_{Ca,L}$ expressed in percent variation over the amplitude of basal $I_{Ca,L}$ **(B)** inhibitory effects of TBBPA on the $I_{Ca,L}$ stimulated by BAY (0.01 µM), expressed in percent variation over the amplitude of BAY-stimulated $I_{Ca,L}$. Each bar represents the mean values, the vertical lines the SD and the dots the replicates for each n. * Represents statistical differences between TBBPA concentrations: ** $p < 0.01$, *** $p < 0.001$. Data were analysed using two-way ANOVA followed by Holm-Sidak post-hoc test.

6.4.2.3. Effects of TBBPA on the expression of Cav1.2, BK_{Ca} β_1, BK_{Ca} 1.1α, $Gucci_{\alpha}$ and PRKG 1α

The expression of ion channels and proteins implicated in the regulation of vascular tone, interfering with the contraction and relaxation mechanisms of the SMC, were evaluated using RT-qPCR. The effects of TBBPA on mRNA expression of channels' subunits (Cav1.2, BK_{Ca} β_1 and BK_{Ca} 1.1α) and proteins ($Gucci_{\alpha}$ and PRKG 1α) are represented in Figure 6.6.

Concerning the ion channels the mRNA expression was significantly increased when A7r5 cells were incubated with TBBPA 0.01 and 50 µM for Cav1.2 channels ($p < 0.001$ and $p < 0.05$, Figure 6.6A), TBBPA 1 and 10 µM for BK_{Ca} β_1 subunit ($p < 0.01$ and $p < 0.001$ respectively, Figure

6.6B) and TBBPA 50 µM for BK_{Ca} 1.1α subunit ($p < 0.001$, Figure 6.6C). Similarly, mRNA expression of $Gucci_{\alpha}$, was significantly higher for TBBPA 0.01 e 1 µM ($p < 0.01$ and $p < 0.001$, respectively, Figure 6.6D), while for PRKG 1α it was for TBBPA 50 µM ($p < 0.01$, Figure 6E). All these results were compared to the vehicle (control group).

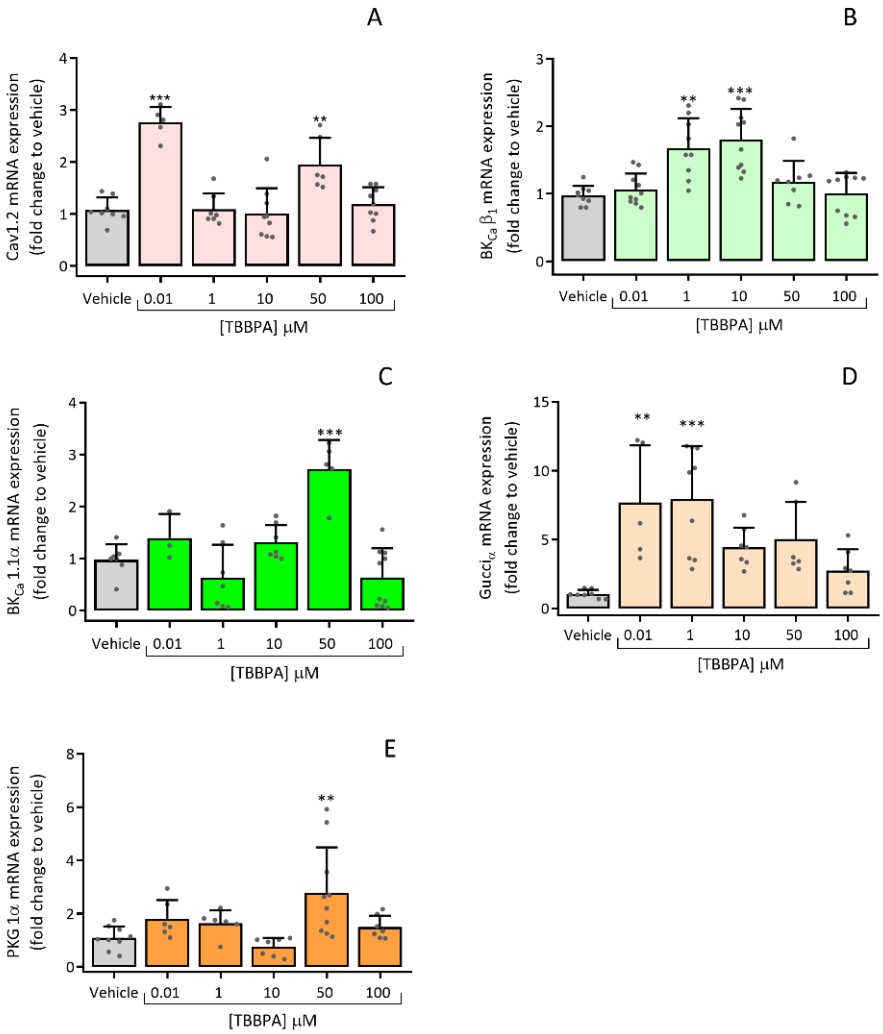

Figure 6.6. Relative expression in A7r5 cells exposed to TBBPA (0.01 – 100 µM) (24 h) **(A)** Cav1.2 channels, **(B)** BK_{Ca} β_1 subunit channels, **(C)** BK_{Ca} 1.1α subunit channels, **(D)** sGC ($Gucci_{\alpha}$) and **(E)** PRKG 1α subunit. Cyc A was used as a housekeeping gene to normalize the mRNA expression. Each bar represents the mean values and vertical lines the SD of four independent experiments performed in triplicate and the dots the n. * Represents significant statistical differences in comparison to vehicle (control): ** $p < 0.01$, *** $p < 0.001$. Data were analysed using ANOVA followed by Dunnett's multiple comparison test.

6.5. Discussion

TBBPA´s endocrine-disrupting properties are currently under European Chemicals Agency assessment [23]. However, according to the harmonized classification (European Union) TBBPA is already considered extremely toxic to aquatic life and this effect can be long lasting [24].

The adverse effects of TBBPA in *Ex vivo* and *In vitro* models have been demonstrated in several studies. Recently, it was demonstrated that TBBPA induces vasorelaxation of the human

umbilical artery (HUA) involving the NO/sGC/cGMP/PKG pathway and the influx of calcium, suggesting that TBBPA exposure modifies the HUA vascular homeostasis [18]. In order to provide a clarification of these results, there was the need to analyse TBBPA effects in rat aorta, since this sample is considered a universal model at the vascular level. Furthermore, studies carried out in the rat aorta using a TBBPA analogue considered to be more toxic at the vascular level, the BPA, showed that it inhibits the calcium channels [17].

Experimental studies using animal models can offer a quicker and more flexible approach for the study of TBBPA effects on human health and contribute to unravel the mechanism of action and dose–response characteristics [1]. ECHA has also identified TBBPA as suspected of causing cancer, since it has been classified as category 1B (Carc1B) based on animal studies. Most of those studies considered TBBPA as a carcinogenic compound in rodents, with possible mechanisms being disruption of oestrogen homeostasis and thyroid hormone pathway, oxidative stress, inflammation, and immunosuppression [23]. In addition, TBBPA also leads to an increase in intracellular [Ca^{2+}] and affects NO, ROS, and mitochondrial superoxide levels [10,11,25]. As already mentioned, the intracellular [Ca^{2+}] and NO are vital for the vascular tonus regulation and considering that TBBPA affects these parameters, the main goal of this work was to understand the real impact of TBBPA at a vascular level. For that purpose, *ex vivo* and *in vitro* experiments on rat aorta were performed. Regarding these arteries, the vascular contractility was analysed, and using cultured A7r5 cells it was possible to 1) observe the TBBPA effects in Ca^{2+} current and 2) analyse mRNA expression levels of Cav1.2, BK_{Ca} β_1, BK_{Ca} 1.1α, $Gucci_{\alpha}$ and PRKG 1α after 24 h exposure of TBBPA.

Several studies using zebrafish, fathead minnow, rainbow trout, Eisenia fetida and earthworm species, showed that TBBPA can induce chronic toxicity after 14 and 96 h exposure [26-29]. However, in rodents, TBBPA induces small acute toxicity and has low availability [30]. Therefore, by analysing the A7r5 cells viability it was found that after exposure to 500 and 1000 μM TBBPA, there was a decrease in cell viability of 66 and 49 %, respectively. These results indicate that high concentrations of TBBPA have toxic effects on vascular smooth muscle cells. Considering these results, we excluded the concentrations 500 and 1000 μM in all the experiments.

Through the *ex vivo* studies, it was possible to show for the first time that TBBPA induces relaxation on rat aorta rings pre-contracted either with Phenyl, NA or KCl (60 mM). We can suggest that, in addition to having a dose-dependent effect, it is not NO production dependent, since the arteries are devoid of endothelium. Thus, TBBPA was the unique responsible for the relaxation effect. It should be noted that the vasorelaxation induced by TBBPA was less pronounced in arteries contracted with KCl than those contracted with Phenyl or NA, which can be explained by the different vascular pathways of these three contractile agents. NA mediates vascular contractility through the activation of the α1A-, α1B-, α1D-, β1-, and β2-adrenoceptors [31,32], which act differently. The α1- adrenoceptors are coupled to the Gq protein activation leading to an increase of $[Ca^{2+}]_i$ from the sarcoplasmic reticulum and causing contraction [33-35]. On the other hand, β1- and β2-adrenoceptors will lead to vasorelaxation. These receptors are coupled to Gs protein inducing the activation of adenylate cyclase and increasing the intracellular cAMP concentration [36,37]. Also associated with the NA contraction is the influx of extracellular Ca^{2+} via voltage- or receptor-operated Ca^{2+} channels [38]. In the case of Phenyl, it causes contraction by binding only to

α1-adrenoreceptors. As described above, these adrenoreceptors are associated with Gq protein, causing the increase in $[Ca^{2+}]_i$, which results in contraction [35,39,40]. Considering these results TBBPA effects may be mediated by α1-, β1-, and β2-adrenoceptors receptors activation and by ion channels involved in the vascular response, namely Ca^{2+} and K^+ channels. Regarding the KCl contraction, it is mainly triggered by membrane depolarization and consequently opening of VGCC, mainly L-Type, promoting the entry of extracellular Ca^{2+} [16,17]. Our results suggest that the decrease of Ca^{2+} influx by blockage of L-type VGCC is the main pathway involved in the TBBPA vasorelaxation.

The L-type VGCC are the main Ca^{2+} channels responsible for the contractile or re-laxant effects [12,41]. So, to understand the involvement of TBBPA on Ca^{2+} influx by ion channels, Nif, a specific inhibitor of L-type VGCC, was used on the contracted endothelium-denuded rat aorta rings followed by TBBPA. The results demonstrated that Nif causes relaxation in rat aorta precontracted with Phenyl (1 μM), NA (1 μM) and KCl (60 mM). Even using a lower concentration of Nif (0.001 μM) in the arteries contracted with KCl, the induced relaxation was superior to that induced by Nif (1 μM) in the arteries contracted by Phenyl and NA, which proves that the KCl-contraction is due to the opening of the L-type VGCC.

From the results on TBBPA effects, it was clear that the vasorelaxation induced by the combined exposure to Nif and TBBPA was significantly higher than the individual TBBPA effect, but identical to the individual Nif effect, suggesting that TBBPA may share the same mechanism as Nif, or act by an interrelated pathway involving the in-activation of L-type VGCC. Despite the fact that there are no significant differences, in contractions with Phenyl and NA, the individual effect of TBBPA at 100 μM was higher than the individual Nif effect demonstrating that K^+ channels may also be involved in the TBBPA mechanism. The K^+ channels contribute to relaxation in vascular smooth muscle by repolarization of the plasma membrane, leading to the closure of L-type VGCC channels [42].

Considering the possible K^+ channels involvement, the next approach was to analyse the influence of these channels on vasorelaxation induced by TBBPA on isolated rat aorta. For that different K^+ channels inhibitors, TEA (inhibitor of BK_{Ca} channels, 1000 μM), 4-AP (inhibitor of K_v channels 1000 μM) and Gly (inhibitor of K_{ATP} channels, 10 μM) were used prior to Phenyl and NA contractions. Concerning the arteries contracted with Phenyl, our results demonstrated that the individual TBBPA effect was higher than the combined application of K^+ channels inhibitors and TBBPA, and it was lower than the effect triggered by K^+ channels inhibitors, Nif and TBBPA; moreover, the combined application of K^+ channels inhibitors and Nif was higher than the effect of the K^+ channels inhibitors plus TBBPA. These results suggest that TEA, 4-AP and Gly clearly inhibit the TBBPA effect, modifying the vasorelaxant response of this compound in rat aorta. These results show that activation of K^+ channels is another path-way involved in vasorelaxation induced by TBBPA, whose increment of cGMP leads to the activation of PKG and consequently to a decrease in $[Ca^{2+}]_i$ [17,42]. The results obtained for rat aorta rings contracted with NA demonstrate that TBBPA individual effect (30, 50 and 100 μM) was higher than K^+ channels inhibitors plus TBBPA and at all concentrations, it was lower than the combined application of K^+ channels inhibitors, Nif and TBBPA. Additionally, the relaxation induced by K^+ channels inhibitors with TBBPA and by the

combined applications of K^+ channels inhibitors, Nif and TBBPA were significantly lower than vasorelaxation caused by the individual Nif effect. Overall, in arteries contracted with NA the K^+ inhibitors also modify the vasorelaxant response of TBBPA in a concentration dependent manner. These data indicate that TBBPA vasorelaxation may occur either by inactivation of L-type VGCC channels or by activation of K^+ channels, mainly through BK_{Ca}, K_v and K_{ATP}.

Taking into account the *ex vivo* results obtained, to confirm if the mechanisms of TBBPA-induced vasorelaxation were L-type VGCC dependent, patch clamp experiments in A7r5 cells were performed. In fact, TBBPA can inhibit L-type VGCC activity in vascular smooth muscle cells from rat aorta, with more notable effects at 50 and 100 μM, corresponding to 27.44 and 49.21 % of inhibition, respectively. Furthermore, it also inhibits BAY-stimulated $I_{Ca,L}$, with the maximum effect observed for the same concentrations (57.95 and 64.24 %, respectively), confirming the TBBPA inhibitory effect on $I_{Ca,L}$. These results are in accordance with a previous study performed by our research group, in which bisphenol A (BPA), that is an analogue of TBBPA, leads to vasorelaxation of rat aorta by inhibition of the L-type VGCC [17].

Regarding the TBBPA effects on the expression of these channels, the results showed an increase in mRNA expression levels of Cav1.2 channels in A7r5 cells increased after exposure to TBBPA, suggesting that this compound may interfere with Ca^{2+} homeostasis. These findings are in accordance with a study performed by Reistad *et. al*, in which rat cerebellar granule cells exposed to TBBPA increased the $[Ca^{2+}]_i$ and reduced by NMDA receptor antagonists, increasing cell death [10]. As mentioned previously, besides the inhibition of Ca^{2+} channels the vasorelaxation induced by TBBPA may also be due to an increase in the K^+ channels´ activity. Based on this proposition, the mRNA expression levels of BK_{Ca} 1.1 α- and β_1- subunits were also analysed, showing an increased response to TBBPA incubation. Similarly, the mRNA expression levels of sGC ($Gucci_\alpha$) and PRKG 1α subunits were also increased when compared to control, indicating that TBBPA modulates these proteins´ expression.

These are promising findings, which may lead to a better understand of TBBPA vascular toxicity and the methods by which it affects the human health. Thus far, few studies have related TBBPA exposure with cardiac health. When evaluating TBBPA cardiac developmental toxicity in zebrafish embryos and larvae, it was found that this compound led to ROS production and cardiomyocyte apoptosis [43] and to cardiac and blood circulation system impairment [44]. On the other hand, also available in the literature are several studies regarding the *in vivo* effects of BPA, demonstrating that it can lead to cardiovascular toxic events, including hypertension, arrhythmias, atherosclerosis, cardiac ischaemia and anomalies [45-51]. Considering that BPA, being an analogue of TBBPA, is involved in several cardiac complications, further *in vivo* studies are needed to demonstrate whether TBBPA affects the cardiovascular system the same way, and that the *in vitro* and *ex vivo* effects revealed in this study can lead to possible diseases.

6.6. Conclusions

In this work, we demonstrated, for the first time, that TBBPA induces vasorelaxation of the rat aorta. Specifically, we were able to discover part of the mechanism of action of TBBPA, which may be interrelated with the pathway involving L-type VGCC inactivation, or even share the same mechanism of action as Nif. However, the presence of K^+ inhibitors modified the effect of TBBPA, which leads us to conclude that the activation of K^+ channels may be another pathway involved in the TBBPA vasorelaxation. These data were corroborated by the results obtained in the analysis of mRNA expression, in which it was observed that TBBPA modulates the expression of proteins and ion channels involved in vascular contractility. Overall, these remarks suggest that TBBPA exposure interferes with vascular homeostasis, through Ca^{2+} and K^+ channels.

6.7. Author Contributions

J.F.: Methodology; Formal analysis; Investigation; Writing—original draft; Visualization. S.M.R.: Formal analysis; Writing-review & editing. M.M.: Formal analysis; Writing—review & editing. C.J.M.: Methodology; Formal analysis; Software; Validation; Writing—review & editing. E.C.: Conceptualization; Visualization; Methodology; Formal analysis; Software; Validation; Writing—review & editing; Supervision; Funding acquisition. All authors have read and agreed to the published version of the manuscript.

6.8. Funding

J.F. acknowledges the PhD fellowship from FCT (Reference: SFRH/BD/131665/2017 and COVID/BD/151940/2021), S.R. acknowledges the PhD fellowship from FCT (SFRH/BD/115693/2016 and COVID/BD/151732/2021) and M.M. acknowledges the PhD fellowship from FCT (Reference: 2020.07020.BD). This work was developed within the scope of the CICS-UBI projects UIDB/00709/2020 and UIDP/00709/2020, financed by national funds through the Portuguese Foundation for Science and Technology/MCTES.

6.9. Institutional Review Board Statement

All experiments were according to the Animal Care guidelines endorsed by UBI, University of Beira Interior (Institutional Review Board approval number T0023), and were conformed to the European Parliament Directive (nº 2010/63/EU) concerning the animals' protection for scientific purposes.

6.10. Informed Consent Statement

Not applicable.

6.11. Data Available Statement

Not applicable.

6.12. Conflicts of Interest

The authors declare that they have no known competing financial interests or personal relationships that could have appeared to influence the work reported in this paper.

6.13. References

1. Feiteiro, J.; Mariana, M.; Cairrao, E. Health toxicity effects of brominated flame retardants: From environmental to human exposure. *Environ Pollut* **2021**, *285*, 117475.

2. Altmann, L.; Welge, P.; Mensing, T.; Lilienthal, H.; Voss, B.; Wilhelm, M. Chronic exposure to trichloroethylene affects neuronal plasticity in rat hippocampal slices. *Environ Toxicol Pharmacol* **2002**, *12*, 157-167.

3. Lilienthal, H.; Verwer, C.M.; van der Ven, L.T.; Piersma, A.H.; Vos, J.G. Exposure to tetrabromobisphenol A (TBBPA) in Wistar rats: neurobehavioral effects in offspring from a one-generation reproduction study. *Toxicology* **2008**, *246*, 45-54.

4. Saegusa, Y.; Fujimoto, H.; Woo, G.H.; Inoue, K.; Takahashi, M.; Mitsumori, K.; Hirose, M.; Nishikawa, A.; Shibutani, M. Developmental toxicity of brominated flame retardants, tetrabromobisphenol A and 1,2,5,6,9,10-hexabromocyclododecane, in rat offspring after maternal exposure from mid-gestation through lactation. *Reprod Toxicol* **2009**, *28*, 456-467.

5. Kitamura, S.; Kato, T.; Iida, M.; Jinno, N.; Suzuki, T.; Ohta, S.; Fujimoto, N.; Hanada, H.; Kashiwagi, K.; Kashiwagi, A. Anti-thyroid hormonal activity of tetrabromobisphenol A, a flame retardant, and related compounds: Affinity to the mammalian thyroid hormone receptor, and effect on tadpole metamorphosis. *Life Sci* **2005**, *76*, 1589-1601.

6. Sun, H.; Shen, O.X.; Wang, X.R.; Zhou, L.; Zhen, S.Q.; Chen, X.D. Anti-thyroid hormone activity of bisphenol A, tetrabromobisphenol A and tetrachlorobisphenol A in an improved reporter gene assay. *Toxicol In Vitro* **2009**, *23*, 950-954.

7. Kitamura, S.; Jinno, N.; Ohta, S.; Kuroki, H.; Fujimoto, N. Thyroid hormonal activity of the flame retardants tetrabromobisphenol A and tetrachlorobisphenol A. *Biochem Biophys Res Commun* **2002**, *293*, 554-559.

8. Fukuda, N.; Ito, Y.; Yamaguchi, M.; Mitumori, K.; Koizumi, M.; Hasegawa, R.; Kamata, E.; Ema, M. Unexpected nephrotoxicity induced by tetrabromobisphenol A in newborn rats. *Toxicol Lett* **2004**, *150*, 145-155.

9. Ghisari, M.; Bonefeld-Jorgensen, E.C. Impact of environmental chemicals on the thyroid hormone function in pituitary rat GH3 cells. *Mol Cell Endocrinol* **2005**, *244*, 31-41.

10. Reistad, T.; Mariussen, E.; Ring, A.; Fonnum, F. In vitro toxicity of tetrabromobisphenol-A on cerebellar granule cells: cell death, free radical formation, calcium influx and extracellular glutamate. *Toxicol Sci* **2007**, *96*, 268-278.

11. Suh, K.S.; Choi, E.M.; Rhee, S.Y.; Oh, S.; Kim, S.W.; Pak, Y.K.; Choe, W.; Ha, J.; Chon, S. Tetrabromobisphenol A induces cellular damages in pancreatic beta-cells in vitro. *J Environ Sci Health A Tox Hazard Subst Environ Eng* **2017**, *52*, 624-631.

12. Tykocki, N.R.; Boerman, E.M.; Jackson, W.F. Smooth Muscle Ion Channels and Regulation of Vascular Tone in Resistance Arteries and Arterioles. *Compr Physiol* **2017**, *7*, 485-581.

13. Lorigo, M.; Mariana, M.; Feiteiro, J.; Cairrao, E. How is the human umbilical artery regulated? *J Obstet Gynaecol Res* **2018**, *44*, 1193-1201.

14. Weidelt, T.; Boldt, W.; Markwardt, F.J.T.J.o.P. Acetylcholin... induced K+ currents in smooth muscle cells of intact rat small arteries. **1997**, *500*.

15. Jewell, R.P.; Saundry, C.M.; Bonev, A.D.; Tranmer, B.I.; Wellman, G.C. Inhibition of Ca++ sparks by oxyhemoglobin in rabbit cerebral arteries. *J Neurosurg* **2004**, *100*, 295-302.

16. Mariana, M.; Feiteiro, J.; Cairrao, E. Cardiovascular Response of Rat Aorta to Di-(2-ethylhexyl) Phthalate (DEHP) Exposure. *Cardiovasc Toxicol* **2018**, *18*, 356-364.

17. Feiteiro, J.; Mariana, M.; Gloria, S.; Cairrao, E. Inhibition of L-type calcium channels by Bisphenol A in rat aorta smooth muscle. *J Toxicol Sci* **2018**, *43*, 579-586.

18. Feiteiro, J.; Rocha, S.M.; Mariana, M.; Maia, C.J.; Cairrão, E. Pathways involved in the human vascular Tetrabromobisphenol A response: Calcium and potassium channels and nitric oxide donors. *Toxicology* **2022**, *470*.

19. Cairrao, E.; Alvarez, E.; Carvas, J.M.; Santos-Silva, A.J.; Verde, I. Non-genomic vasorelaxant effects of 17beta-estradiol and progesterone in rat aorta are mediated by L-type Ca2+ current inhibition. *Acta Pharmacol Sin* **2012**, *33*, 615-624.

20. Pfaffl, M.W. A new mathematical model for relative quantification in real-time RT–PCR. *Nucleic Acids Research* **2001**, *29*, e45-e45.

21. Feiteiro, J.; Mariana, M.; Verde, I.; Cairrão, E. Tributyltin Affects Rat Vascular Contractility Through L-Type Calcium Channels. *International Journal of Environmental Research* **2018**, *12*, 215-221.

22. Lorigo, M.; Cairrao, E. UV-B filter octylmethoxycinnamate-induced vascular endothelial disruption on rat aorta: In silico and in vitro approach. *Chemosphere* **2022**, *307*, 135807.

23. ECHA. Opinion of the committee for risk assessment on a dossier proposing harmonised classification and labelling at EU level. **2021**.

24. ECHA, E.C.A.-. 2,2',6,6'-tetrabromo-4,4'-isopropylidenediphenol. Available online: https://echa.europa.eu/substance-information/-/substanceinfo/100.001.125 (accessed on

25. Choi, E.M.; Suh, K.S.; Rhee, S.Y.; Oh, S.; Kim, S.W.; Pak, Y.K.; Choe, W.; Ha, J.; Chon, S. Exposure to tetrabromobisphenol A induces cellular dysfunction in osteoblastic MC3T3-E1 cells. *J Environ Sci Health A Tox Hazard Subst Environ Eng* **2017**, *52*, 561-570.

26. Godfrey, A.; Abdel-Moneim, A.; Sepulveda, M.S. Acute mixture toxicity of halogenated chemicals and their next generation counterparts on zebrafish embryos. *Chemosphere* **2017**, *181*, 710-712.

27. Laboratories, S. The subchronic toxicity of sediment-sorbed tetrabromobisphenol A to Chironomus tentans under flow-through conditions. **1989**.

28. Pittinger, C.A.; Pecquet, A.M. Review of historical aquatic toxicity and bioconcentration data for the brominated flame retardant tetrabromobisphenol A (TBBPA): effects to fish, invertebrates, algae, and microbial communities. *Environ Sci Pollut Res Int* **2018**, *25*, 14361-14372.

29. Chen, S.J.; Ma, Y.J.; Wang, J.; Chen, D.; Luo, X.J.; Mai, B.X. Brominated flame retardants in children's toys: concentration, composition, and children's exposure and risk assessment. *Environ Sci Technol* **2009**, *43*, 4200-4206.

30. Covaci, A.; Voorspoels, S.; Abdallah, M.A.; Geens, T.; Harrad, S.; Law, R.J. Analytical and environmental aspects of the flame retardant tetrabromobisphenol-A and its derivatives. *J Chromatogr A* **2009**, *1216*, 346-363.

31. Guimaraes, S.; Moura, D. Vascular adrenoceptors: an update. *Pharmacol Rev* **2001**, *53*, 319-356.

32. Xiao, R.-P. The Adrenergic Receptors in the 21st Century. *Circulation* **2006**, *113*.

33. Wang, Y.; Hou, R.; Li, P.; Li, J.; Yan, J.; Yin, F.; Han, C.; Zhang, Y. Gene expression profiles in response to the activation of adrenoceptors in A7r5 aortic smooth muscle cells. *Clin Exp Pharmacol Physiol* **2004**, *31*, 602-607.

34. Carbajal-Garcia, A.; Reyes-Garcia, J.; Montano, L.M. Androgen Effects on the Adrenergic System of the Vascular, Airway, and Cardiac Myocytes and Their Relevance in Pathological Processes. *Int J Endocrinol* **2020**, *2020*, 8849641.

35. Hewitt, S.C.; Grimm, S.A.; Wu, S.P.; DeMayo, F.J.; Korach, K.S. Estrogen receptor alpha (ERalpha)-binding super-enhancers drive key mediators that control uterine estrogen responses in mice. *J Biol Chem* **2020**, *295*, 8387-8400.

36. Weihua, Z.; Saji, S.; Makinen, S.; Cheng, G.; Jensen, E.V.; Warner, M.; Gustafsson, J.A. Estrogen receptor (ER) beta, a modulator of ERalpha in the uterus. *Proc Natl Acad Sci U S A* **2000**, *97*, 5936-5941.

37. Traupe, T.; Stettler, C.D.; Li, H.; Haas, E.; Bhattacharya, I.; Minotti, R.; Barton, M. Distinct roles of estrogen receptors alpha and beta mediating acute vasodilation of epicardial coronary arteries. *Hypertension* **2007**, *49*, 1364-1370.

38. Perusquia, M.; Hernandez, R.; Morales, M.A.; Campos, M.G.; Villalon, C.M. Role of endothelium in the vasodilating effect of progestins and androgens on the rat thoracic aorta. *Gen Pharmacol* **1996**, *27*, 181-185.

39. Sedin, J.; Dahlgren, D.; Sjoblom, M.; Nylander, O. The Impact of alpha-Adrenoceptors in the Regulation of the Hypotonicity-Induced Increase in Duodenal Mucosal Permeability In Vivo. *Pharmaceutics* **2021**, *13*.

40. Bojic, M.G.; Todorovic, L.; Santrac, A.; Mian, M.Y.; Sharmin, D.; Cook, J.M.; Savic, M.M. Vasodilatory effects of a variety of positive allosteric modulators of GABAA receptors on rat thoracic aorta. *Eur J Pharmacol* **2021**, *899*, 174023.

41. Kuo, I.Y.; Wolfle, S.E.; Hill, C.E. T-type calcium channels and vascular function: the new kid on the block? *J Physiol* **2011**, *589*, 783-795.

42. Lorigo, M.; Oliveira, N.; Cairrao, E. Clinical Importance of the Human Umbilical Artery Potassium Channels. *Cells* **2020**, *9*.

43. Yang, S.; Wang, S.; Sun, F.; Zhang, M.; Wu, F.; Xu, F.; Ding, Z. Protective effects of puerarin against tetrabromobisphenol a-induced apoptosis and cardiac developmental toxicity in zebrafish embryo-larvae. *Environ Toxicol* **2015**, *30*, 1014-1023.

44. Wu, S.; Ji, G.; Liu, J.; Zhang, S.; Gong, Y.; Shi, L. TBBPA induces developmental toxicity, oxidative stress, and apoptosis in embryos and zebrafish larvae (Danio rerio). *Environ Toxicol* **2016**, *31*, 1241-1249.

45. Patel, B.B.; Raad, M.; Sebag, I.A.; Chalifour, L.E. Lifelong exposure to bisphenol a alters cardiac structure/function, protein expression, and DNA methylation in adult mice. *Toxicol Sci* **2013**, *133*, 174-185.

46. Saura, M.; Marquez, S.; Reventun, P.; Olea-Herrero, N.; Arenas, M.I.; Moreno-Gomez-Toledano, R.; Gomez-Parrizas, M.; Munoz-Moreno, C.; Gonzalez-Santander, M.; Zaragoza, C.; et al. Oral administration of bisphenol A induces high blood pressure through angiotensin II/CaMKII-dependent uncoupling of eNOS. *FASEB J* **2014**, *28*, 4719-4728.

47. Kim, M.J.; Moon, M.K.; Kang, G.H.; Lee, K.J.; Choi, S.H.; Lim, S.; Oh, B.C.; Park, D.J.; Park, K.S.; Jang, H.C.; et al. Chronic exposure to bisphenol A can accelerate atherosclerosis in high-fat-fed apolipoprotein E knockout mice. *Cardiovasc Toxicol* **2014**, *14*, 120-128.

48. Belcher, S.M.; Gear, R.B.; Kendig, E.L. Bisphenol A alters autonomic tone and extracellular matrix structure and induces sex-specific effects on cardiovascular function in male and female CD-1 mice. *Endocrinology* **2015**, *156*, 882-895.

49. Reventun, P.; Sanchez-Esteban, S.; Cook, A.; Cuadrado, I.; Roza, C.; Moreno-Gomez-Toledano, R.; Munoz, C.; Zaragoza, C.; Bosch, R.J.; Saura, M. Bisphenol A induces coronary endothelial cell necroptosis by activating RIP3/CamKII dependent pathway. *Sci Rep* **2020**, *10*, 4190.

50. Brown, A.R.; Green, J.M.; Moreman, J.; Gunnarsson, L.M.; Mourabit, S.; Ball, J.; Winter, M.J.; Trznadel, M.; Correia, A.; Hacker, C.; et al. Cardiovascular Effects and Molecular Mechanisms of Bisphenol A and Its Metabolite MBP in Zebrafish. *Environ Sci Technol* **2019**, *53*, 463-474.

51. Sui, Y.; Park, S.H.; Wang, F.; Zhou, C. Perinatal Bisphenol A Exposure Increases Atherosclerosis in Adult Male PXR-Humanized Mice. *Endocrinology* **2018**, *159*, 1595-1608.

Chapter 7

Concluding remarks and future perspectives

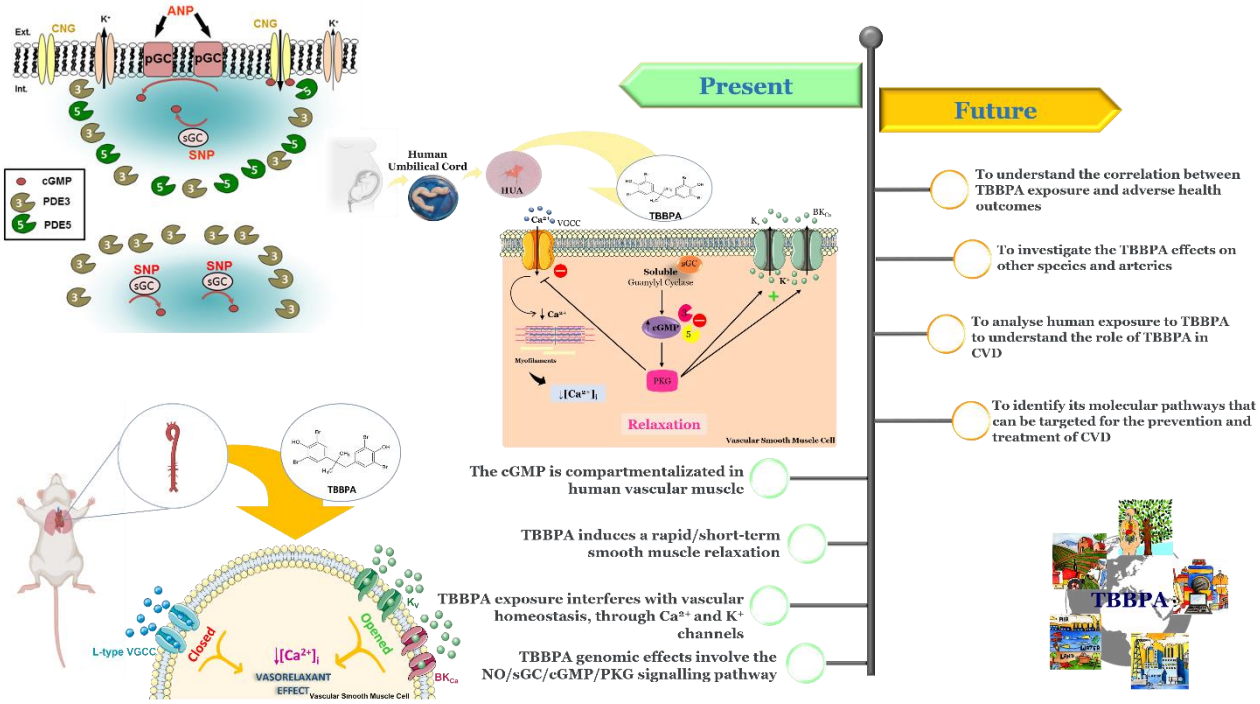

7.1. Concluding remarks

TBBPA is a brominated flame retardant widely used in a variety of industrial and consumer products to reduce flammability. It can contaminate the environment, mainly water, dust, air and soil, from which human exposure occurs. This constant exposure has raised some concerns about human health. This compound can act as an endocrine disruptor, a property that gives it the ability to interfere with hormonal function and quantity when TBBPA binds target tissues in the body. Studies in humans and animals suggest a correlation between TBBPA exposure and adverse health outcomes.

Despite all studies in *Ex vivo* and *In vitro* models, the vascular adverse effects of TBBPA remain to be understood, as well as the upstream mechanisms that disrupt the vascular homeostasis. Taking this into account, this thesis addressed the effect of TBBPA exposure and the influence of TBBPA on homeostatic mechanisms in the vascular function. This analysis was performed in two different study models, HUA, and rat aorta. The use of rat aorta in basic studies is standard practice. This animal model is a good starting point for studying human biological processes, given that, most of the time, it allows to extrapolate the results to human models. In this sense, HUA and rat aorta were used in this study. The HUA is a very specific artery since it is the main function is limited in time. Thus, it presents unique histological and morphological characteristics, which prevents us from considering it a universal model at the vascular level. In this sense, to get an overview at the vascular level we used the rat aorta as a universal model. Thus, the combination of these two models is essential to study several signalling processes implicated in this control, as calcium metabolism and different pathways involved in the modulation of vascular reactivity, providing a better clarification of the effects of TBBPA exposure in animals and humans.

In the first original article presented in this thesis (Cyclic guanosine monophosphate compartmentation in human vascular smooth muscle cells), our results prove, for the first time, that cGMP is compartmentalized in VSMC. This cGMP compartmentation is controlled by two PDEs subtypes, PDE3 and PDE5. The particulate cGMP pool formed near the plasma membrane is controlled by PDE5 and PDE3 and the cGMP pool located in the cytosol is exclusively controlled by PDE3.

In Chapter 5, our results showed that the TBBPA direct effects induce a dose-dependent relaxation on HUA. However, this effect is more prominent in HUA contracted with 5-HT and His than KCl, indicating that it depends on the contractile agent, thus suggesting that different action mechanisms may be involved in vasorelaxation induced by TBBPA. Furthermore, the pathways of each of the contractile agents may explain the differences observed. In this sense, our results suggested that the TBBPA effects are due to the modulation of 5-HT (5-HT_{2A}, 5-HT_{1B}/5-HT_{1D}) and His receptors (H_1 and H_2). In addition, it was also shown that vasorelaxation caused by TBBPA is mainly due to the inhibition of VGCC or K^+ channels activation, thus demonstrating that TBBPA not only modulates vascular homeostasis by interference with 5-HT and His receptors, but also interferes with the Ca^{2+} channels. Taking this into account, the way the exposure to TBBPA harms vascular homeostasis of HUA through of cGMP signalling pathway and Ca^{2+} influx by ion channels was analysed, since these are the main pathways responsible for the HUA vascular smooth muscle

relaxation/contraction [1-4]. The obtained results showed that a 24 h exposure to TBBPA causes an increase in the SNP relaxation response, which increases with cumulative concentrations of TBBPA incubation, thus suggesting that the effects induced by SNP depend on TBBPA incubation concentrations. Therefore, it can be hypothesized that the genomic effects of TBBPA induced an increase in vasodilation and seems to involve the NO/sGC/cGMP/PKG signalling pathway. It was also demonstrated that TBBPA modifies the action mechanisms of Nif, interfering in the Ca^{2+} influx since after a 24 h exposure to TBBPA, the Nif relaxation response changed. Moreover, it is worth noticing that the mRNA expression levels of Cav1.2 channels in HUASMC increased after exposure to TBBPA. Furthermore, previous studies showed that the K^+ channels are also involved in the vasodilator effects in HUA. The increase of cGMP levels induces the PKG activation and consequently the activation of these channels, mainly K_v and BK_{Ca} channels [2,3,5,6]. In this context, the expression of BK_{Ca} channels and proteins (sGC and PKG) involved in HUA vascular contractility mechanism was also analysed. The obtained results demonstrated that the mRNA expression levels of BK_{Ca} 1.1 α- and β_1- subunits, PRKG 1α subunit and $Gucci_{\alpha}$ are increased in response to TBBPA exposure. Considering these results, TBBPA clearly modulates the PKG and sGC proteins and ion channels expression. In short, these results suggest that TBBPA exposure alters the vascular homeostasis of HUA.

In Chapter 6, we aimed to explore the role of TBBPA in rat aorta. Firstly, we demonstrated for the first time that TBBPA induced a relaxation on rat aorta rings pre-contracted either with Phenyl, NA or KCl and this effect was dose-dependent. Once the arteries were devoid of the endothelium, the results suggested that TBBPA was the unique responsible for the relaxation effect, possibly through the inhibition of L-type VGCC and not due to NO production. Then, and to confirm this hypothesis, Patch clamp studies were performed with A7r5 cells and the effect of TBBPA on L-type Ca^{2+} channels activity was analysed. The obtained results showed that TBBPA induces a rapid and concentration dependent inhibition of the basal activity of Ca^{2+} channels in A7r5 cells. In addition, these results also demonstrated for the first time that TBBPA inhibits BAY-stimulated Ca^{2+} currents, thus confirming the TBBPA inhibitory effect on L-type VGCC currents. Taking this into account, the functionality of TBBPA on Ca^{2+} influx by ion channels using Nif was analysed. The obtained results showed that the vasorelaxation induced by the combined exposure of Nif and TBBPA was significantly higher than the individual TBBPA effect and similar to the individual Nif effect. Thus, the results suggested that TBBPA act through an interrelated pathway that involves the inactivation of L-type VGCC, or even share the same mechanism of action as Nif. However, in rat aorta contracted with Phenyl and NA, at 100 μM, the individual Nif effect and the combined exposure Nif and TBBPA appears to be smaller than the individual effect of TBBPA which confirmed that other pathways may be involved in TBBPA mechanism such as activation of K^+ channels. According to the literature, the activation of K^+ channels in vascular smooth muscle may induce repolarization of the plasma membrane, which leads to the closure of L-type VGCC channels, after the increase of cGMP and activation of PKG, thus contributing to vascular relaxation [6,7]. In this sense, in Phenyl- and NA-contractions, different K^+ channels inhibitors (TEA, 4-4-AP and Gly) were selected to analyse the influence of K^+ channels on TBBPA vasorelaxation on isolated rat aorta. The obtained results showed that all these K^+ channels inhibitors clearly inhibit the

TBBPA vasorelaxation, thus suggesting that K^+ channels are also involved in the vasorelaxant effect of TBBPA in the rat aorta. In addition, in this research, it was found that TBBPA increased the expression of L-type Ca^{2+} and BK_{Ca} 1.1 α- and β_1- subunits channels and the sGC and PKG, ion channels and proteins involved in mechanisms of vascular contractility.

Overall, the results presented in this doctoral thesis show evidence of cGMP compartmentalization in human vascular smooth muscle cells and this phenomenon can open new perspectives concerning the examination of PDE families as therapeutic targets. Furthermore, our results demonstrate that TBBPA induces a rapid/short-term smooth muscle relaxation acting through an endothelium-independent mode of action (MOA), involving an sGC activation that increases the cGMP intracellular levels, an inhibition of L-Type VGCC and an activation of K^+ channels. Moreover, it is expected that this research can be useful in the future to understand the correlation between TBBPA exposure and adverse health outcomes.

7.2. Future Trends

Despite the scientific advances achieved through the experimental work carried out in this thesis, the obtained results represent a whole new and promising perspective for the future. Yet, much work will still be needed to increase the knowledge about the effects of TBBPA at the vascular level and its complexity in environmental and human exposure. Epidemiological studies have associated the exposure to EDCs with the development of hypertension in pregnancy or preeclampsia. In fact, using serum samples from mothers, some researchers have associated a type of flame retardants (PBDEs) with the occurrence of preeclampsia [8,9].

According to the literature, hypertensive disorders in pregnancy are associated with a variation in 5-HT or His release and with the sensitivity of the HUA to these mediators that leads to changes in vascular resistance [10-14]. In addition, the dysregulation of the normal functioning of the Ca^{2+} channels, such as an increase in its activity, has been also associated with cardiovascular complications, mainly hypertension and/or preeclampsia [15]. This result is supported by studies showing that increased L-Type VGCC expression and activity are related to hypertension in rats [16,17]. This effect may be related to the increase in Ca^{2+} currents and the number of open functional Ca^{2+} channels and not to the modification of the channel properties. In addition, during hypertension the expression/activity of BK_{Ca} were increased in SMC [16-19]. Thus, considering that TBBPA modifies the contractile response of 5-HT, His and KCl by interference with 5-HT and His receptors and the involvement of Ca^{2+} and K^+ channels, can TBBPA enhance the development of hypertensive disorders? In this sense more studies should be performed to understand this involvement and the associated mechanisms.

Additionally, sGC and PKG activation seems to contribute to the development of hypertension [20-23]. A study using hypertensive mice, showed that the mRNA expression levels of sGC are lower when compared to normotensive mice, thus suggesting a decrease in sGC levels [24], which is opposite to our results in which sGC and PKG proteins expression was increased in the presence of TBBPA. Consequently, it seems important to also investigate the TBBPA effects on

other species and arteries (such as HUA samples from pregnant women with hypertension) to uncover the cardiovascular toxicity of this compound. In addition, we pioneered in characterizing the compartmentation of cGMP signalling in human vascular smooth muscle cells. The cGMP/PKG compartmentation is recognized as an essential signalling element in vascular physiology and pathophysiology, due to the critical role of cyclic nucleotide signalling [7,25]. It is known that the genomic effects of TBBPA induced an increase in vasodilation, and this effect may be due to the involvement of TBBPA in the NO/sGC/cGMP/PKG signalling pathway. So, it is expected that future studies will unravel the underlying mechanisms of TBBPA actions in compartmentation of cGMP signalling to understand the involvement of TBBPA in the development of hypertensive diseases and to know its impact on health and disease.

Consequently, due to its presence in the environment and its potentially adverse effects on human health, in the future, it would be interesting to analyse human exposure to TBBPA to understand the role of TBBPA in cardiovascular diseases and to identify its molecular pathways that can be targeted for the prevention and treatment of these disorders.

7.3. References

1. Santos-Silva, A.J.; Cairrao, E.; Verde, I. Study of the mechanisms regulating human umbilical artery contractility. *Health* **2010**, *02*, 321-331.

2. Cairrao, E.; Santos-Silva, A.J.; Verde, I. PKG is involved in testosterone-induced vasorelaxation of human umbilical artery. *Eur J Pharmacol* **2010**, *640*, 94-101.

3. Feiteiro, J.; Verde, I.; Cairrao, E. Cyclic guanosine monophosphate compartmentation in human vascular smooth muscle cells. *Cell Signal* **2016**, *28*, 109-116.

4. Lorigo, M.; Mariana, M.; Feiteiro, J.; Cairrao, E. How is the human umbilical artery regulated? *J Obstet Gynaecol Res* **2018**, *44*, 1193-1201.

5. Cairrao, E.; Alvarez, E.; Santos-Silva, A.J.; Verde, I. Potassium channels are involved in testosterone-induced vasorelaxation of human umbilical artery. *Naunyn Schmiedebergs Arch Pharmacol* **2008**, *376*, 375-383.

6. Lorigo, M.; Oliveira, N.; Cairrao, E. Clinical Importance of the Human Umbilical Artery Potassium Channels. *Cells* **2020**, *9*.

7. Morgado, M.; Cairrao, E.; Santos-Silva, A.J.; Verde, I. Cyclic nucleotide-dependent relaxation pathways in vascular smooth muscle. *Cell Mol Life Sci* **2012**, *69*, 247-266.

8. Eslami, B.; Malekafzali, H.; Rastkari, N.; Rashidi, B.H.; Djazayeri, A.; Naddafi, K. Association of serum concentrations of persistent organic pollutants (POPs) and risk of pre-eclampsia: a case-control study. *J Environ Health Sci Eng* **2016**, *14*, 17.

9. Lorigo, M.; Cairrao, E. Fetoplacental vasculature as a model to study human cardiovascular endocrine disruption. *Mol Aspects Med* **2021**, 101054.

10. Redman, C.W.; Sargent, I.L. Latest advances in understanding preeclampsia. *Science* **2005**, *308*, 1592-1594.

11. Brew, O.; Sullivan, M.H. The links between maternal histamine levels and complications of human pregnancy. *J Reprod Immunol* **2006**, *72*, 94-107.

12. Feinberg, B.B. Preeclampsia: the death of Goliath. *Am J Reprod Immunol* **2006**, *55*, 84-98.

13. Gupta, S.; Hanff, L.M.; Visser, W.; Steegers, E.A.; Saxena, P.R.; Vulto, A.G.; MaassenVanDenBrink, A. Functional reactivity of 5-HT receptors in human umbilical cord and maternal subcutaneous fat arteries after normotensive or pre-eclamptic pregnancy. *J Hypertens* **2006**, *24*, 1345-1353.

14. Bahado-Singh, R.; Poon, L.C.; Yilmaz, A.; Syngelaki, A.; Turkoglu, O.; Kumar, P.; Kirma, J.; Allos, M.; Accurti, V.; Li, J.; et al. Integrated Proteomic and Metabolomic prediction of Term Preeclampsia. *Sci Rep* **2017**, *7*, 16189.

15. Kuo, I.Y.; Wolfle, S.E.; Hill, C.E. T-type calcium channels and vascular function: the new kid on the block? *J Physiol* **2011**, *589*, 783-795.

16. Sonkusare, S.; Palade, P.T.; Marsh, J.D.; Telemaque, S.; Pesic, A.; Rusch, N.J. Vascular calcium channels and high blood pressure: pathophysiology and therapeutic implications. *Vascul Pharmacol* **2006**, *44*, 131-142.

17. Pinterova, M.; Kunes, J.; Zicha, J. Altered neural and vascular mechanisms in hypertension. *Physiol Res* **2011**, *60*, 381-402.

18. Rusch, N.J.; Liu, Y. Potassium channels in hypertension: homeostatic pathways to buffer arterial contraction. *Journal of Laboratory and Clinical Medicine* **1997**, *130*, 245-251.

19. Eichhorn, B.; Dobrev, D. Vascular large conductance calcium-activated potassium channels: functional role and therapeutic potential. *Naunyn Schmiedebergs Arch Pharmacol* **2007**, *376*, 145-155.

20. Lucas, K.A.; Pitari, G.M.; Kazerounian, S.; Ruiz-Stewart, I.; Park, J.; Schulz, S.; Chepenik, K.P.; Waldman, S.A. Guanylyl Cyclases and Signaling by Cyclic GMP. **2000**, *52*, 375-414.

21. Krumenacker, J.S.; Hanafy, K.A.; Murad, F. Regulation of nitric oxide and soluble guanylyl cyclase. *Brain Research Bulletin* **2004**, *62*, 505-515.

22. Mergia, E.; Friebe, A.; Dangel, O.; Russwurm, M.; Koesling, D. Spare guanylyl cyclase NO receptors ensure high NO sensitivity in the vascular system. *J Clin Invest* **2006**, *116*, 1731-1737.

23. Derbyshire, E.R.; Marletta, M.A. Structure and regulation of soluble guanylate cyclase. *Annu Rev Biochem* **2012**, *81*, 533-559.

24. Ruetten, H.; Zabel, U.; Linz, W.; Schmidt, H.H. Downregulation of soluble guanylyl cyclase in young and aging spontaneously hypertensive rats. *Circ Res* **1999**, *85*, 534-541.

25. Lorigo, M.; Oliveira, N.; Cairrao, E. PDE-Mediated Cyclic Nucleotide Compartmentation in Vascular Smooth Muscle Cells: From Basic to a Clinical Perspective. *J Cardiovasc Dev Dis* **2021**, *9*.